Black hole microstates : through and beyond supersymmetry

Anthony Houppe

université PARIS-SACLAY

Black Hole Microstates: through and beyond supersymmetry

Les Micro-états de trous noirs: à travers et au-delà de la supersymétrie

Thèse de doctorat de l'université Paris-Saclay

École doctorale n°564 : physique en Île-de-France (PIF)
Spécialité de doctorat: Physique
Graduate School : Physique. Référent : Faculté des Sciences d'Orsay

Thèse préparée à l'**Institut de Physique Théorique** (Université Paris-Saclay, CNRS, CEA), sous la direction de **Iosif BENA**, Directeur de recherche, et le co-encadrement de **Nicholas WARNER**, Professeur.

Thèse soutenue à Paris-Saclay, le 13 juin 2023, par

Anthony HOUPPE

Composition du jury

Membres du jury avec voix délibérative

Michela PETRINI Professeure des universités, LPTHE, Sorbonne Université	Présidente
Emil MARTINEC Professeur, Directeur, Kadanoff Center for Theoretical Physics, University of Chicago	Rapporteur & Examinateur
Masaki SHIGEMORI Professeur, School of Science Department of Physics, Nagoya University	Rapporteur & Examinateur
Oscar DIAS Professeur, University of Southampton	Examinateur
Chiara TOLDO Chercheuse post-doctorant, Harvard University	Examinatrice

THESE DE DOCTORAT
NNT : 2023UPASP054

université PARIS-SACLAY | ÉCOLE DOCTORALE Physique en Île-de-France (PIF)

Titre: Les micro-états de trous noirs: à travers et au-delà de la supersymétrie
Mots clés: Trous noirs, Théorie des cordes, AdS/CFT, Supergravité, Fuzzballs

Résumé: Près d'un siècle après avoir été théorisés, les trous noirs ont été observés dans la nature, d'abord indirectement par LIGO et VIRGO, puis directement par l'EHT. Selon la relativité générale, ils constituent l'état final de la matière suivant l'effondrement d'objets très massifs : toute leur masse est concentrée dans une singularité de l'espace-temps, qui est entourée d'un horizon dont rien ne peut s'échapper.

Les trous noirs se situent à la frontière entre la relativité générale et la mécanique quantique, et sont la source de nombreuses énigmes et paradoxes dont les réponses pourraient éclairer plusieurs aspects de la gravité quantique. Le principal d'entre eux est le paradoxe de l'information : les trous noirs peuvent s'évaporer sous l'effet du rayonnement de Hawking, et il semble que toutes l'information concernant les constituants du trou noir soit définitivement perdue à l'issue de ce processus.

La conjecture des *fuzzballs* est une tentative de résolution de ces paradoxes. Elle propose de remplacer les trous noirs tels que décrits par la relativité générale, par un ensemble de micro-états ayant une structure complexe, mais sans horizon. Ces solutions, qui sont construites à partir du grand nombre de degrés de liberté de la théorie des cordes, ressemblent et se comportent exactement comme des trous noirs à distance, mais diffèrent près de l'horizon. Parce qu'elles sont sans horizon, ces géométries ne sont pas sujettes aux mêmes paradoxes que le trou noir. En tant que théorie des champs effective, la relativité générale efface tous les détails complexes de ces micro-états, et ne peut capturer qu'une description moyenne : le trou noir avec un horizon.

Cette thèse a pour but de construire et d'étudier de tels micro-états dans le cadre de la supergravité, qui est la limite à basse énergie de la théorie des cordes. L'accent est mis sur la réponse à deux questions principales associées à la conjecture des *fuzzballs* : Peut-on construire des micro-états «typiques» qui imitent les comportements que l'on attend des trous noirs ? Peut-on trouver suffisamment de géométries de micro-états pour retrouver l'entropie totale des trous noirs ?

Title: Black Hole Microstates: through and beyond supersymmetry
Keywords: Black Holes, String Theory, AdS/CFT, Supergravity, Fuzzballs

Abstract: Almost a century after being theorized, Black Holes have now been observed in nature, first indirectly by LIGO and VIRGO, then directly by the EHT. According to General Relativity, they are the final state of matter after the collapse of very massive objects: all their mass is concentrated in a spacetime singularity, that is shrouded by a horizon from which nothing can escape.

Black Holes lie at the frontier between General Relativity and Quantum Mechanics, and are the source of many puzzles and paradoxes whose answers could shed light on several aspects of Quantum Gravity. Chief among them is the information paradox: black holes can evaporate through Hawking radiation, and it seems that all the information about the original constituents of the black hole is permanently lost at the end of this process.

The Fuzzball conjecture is an attempt to solve these paradoxes. It proposes to replace the standard black hole picture by an ensemble of fuzzy, horizonless microstates. These solutions, that are built out of the vast number of degrees of freedom of String Theory, look and behave exactly like black holes at a distance, but differ close to the horizon. Because they are horizonless, these geometries are not subject to the same paradoxes as the black hole. As an Effective Field Theory, General Relativity washes out all the intricate details of these microstates, and can only capture an average description: the black hole with a horizon.

This thesis aims to build and study such fuzzball microstates within the framework of Supergravity, the low-energy limit of String Theory. The focus is on addressing two main questions associated to the fuzzball conjecture: Can one construct "typical" microstates that mimic what is expected of black holes ? Can one find enough microstate geometries to recover the full entropy of black holes ?

Acknowledgements

First and foremost, I want to express my thanks to my supervisors, Nick Warner and Iosif Bena. I am deeply grateful to Nick, who was always patient and available for me. I cannot count the many hours we spent in his office, where he taught me so much about physics. His great explanations and analogies helped me develop a physical intuition and understanding of the complex concepts we manipulate. I am also thankful for his constant support and words of encouragement, which propelled me to overcome many obstacles throughout these years. I am also very grateful to Iosif, who taught me everything I needed to know about strings and branes. His enthusiasm was contagious, and he always pushed me to do better. His help and advice were also invaluable in the search for postdocs.

I would like to thank all the other people I have had the chance to work with: Bogdan Ganchev, for our long collaboration and for teaching me about numerics, and Rodolfo Russo and Stefano Giusto, for helping me to understand the subtleties of holography. Additional thanks go to Nejc Čeplak, Shaun Hampton, Yixuan Li and Dimitrios Toulikas, for our exciting conversations about the super-maze; and to Pierre Heidmann, for his rigor and efficiency.

I am thankful to Oscar Dias, Emil Martinec, Michela Petrini, Chiara Toldo and Masaki Shigemori for accepting to be part of my defense committee, and in particular to Emil Martinec and Masaki Shigemori for fulfilling the role of rapporteur.

I have been lucky to have been part of a very dynamic group at the IPhT, and I would like to thank all my colleagues – permanent members, postdocs and students, for creating this great atmosphere: Fabian Bautista, Iosif Bena, Antoine Bourget, Valentí Vall Camell, Nejc Ceplak, Soumangsu Chakraborty, Peng Cheng, Veronica Collazuol, Stefano De Angelis, Gabriele Di Ubaldo, Bernardo Fraiman, Bogdan Ganchev, Silvia Georgescu, Mariana Grana, Monica Guica, Bin Guo, Shaun Hampton, Pierre Heidmann, Alvaro Herraez, Nicolas Kovensky, Yixuan Li, Gabriele Lo Monaco, Daniel Mayerson, Ruben Minasian, Héctor Parra de Freitas, Hynek Paul, Eric Perlmutter, Himanshu Raj, Valentin Reys, Dimitrios Toulikas, Yiannis Tsiares, Robert Walker, and Nick Warner.

Finally, I would like to thank my family, for their love and support.

Publications

Published papers

- **Delaying the Inevitable: Tidal Disruption in Microstate Geometries**
  I. Bena, A. Houppe and N. P. Warner
  JHEP 02 (2021) 103 [*2006.13939*]

- **Supersymmetry and superstrata in three dimensions**
  A. Houppe and N. P. Warner
  JHEP 08 (2021) 133 [*2012.07850*]

- **Q-balls meet fuzzballs: non-BPS microstate geometries**
  B. Ganchev, A. Houppe and N. P. Warner
  JHEP 11 (2021) 028 [*2107.09677*]

- **New superstrata from three-dimensional supergravity**
  B. Ganchev, A. Houppe and N. P. Warner
  JHEP 04 (2022) 065 [*2110.02961*]

- **AdS3 holography for non-BPS geometries**
  B. Ganchev, S. Giusto, A. Houppe and R. Russo
  Eur.Phys.J.C 82 (2022) 3, 217 [*2112.03287*]

- **Elliptical and purely NS superstrata**
  B. Ganchev, A. Houppe and N. P. Warner
  JHEP 09 (2022) 067 [*2207.04060*]

- **The (amazing) Super-Maze**
  I. Bena, S. D. Hampton, A. Houppe, Y. Li and D. Toulikas
  JHEP 03 (2023) 237 [*2211.14326*]

Preprints

- **Solitonic Excitations in AdS2**
  P. Heidmann and A. Houppe
  [*2212.05065*]

- **Themelia: the irreducible microstructure of black holes**
  I. Bena, N. Čeplak, S. D. Hampton, A. Houppe, D. Toulikas and N. P. Warner
  [*2212.06158*]

Contents

Chapter 0

Introduction en Français

Le 20e siècle a vu l'émergence de deux théories de la nature extrêmement fécondes. D'un côté, la mécanique quantique, qui régit les interactions entre les particules à de très petites échelles. Son développement au fil des ans a conduit à l'établissement du modèle standard, qui unifie toutes les particules élémentaires connues et leurs trois interactions fondamentales dans un unique cadre. Ce modèle a été testé avec une précision étonnante et a permis de faire de puissantes prédictions, comme celle de l'existence du boson de Higgs quarante ans avant sa découverte au CERN. De son côté, la relativité générale a été développée par Einstein pour décrire les interactions gravitationnelles à longue portée entre les grands corps. La théorie a fait des prédictions qui ont depuis été rigoureusement testées, comme l'effet de retard de Shapiro ou la forme d'onde précise des signaux gravitationnels émis lors de la fusion de trous noirs, signaux qui ont été détectés pour la première fois par LIGO en 2016.

Poursuivant l'objectif qui a conduit à la construction du modèle standard, les physiciens ont tenté de construire une théorie de la gravité quantique, unifiant la physique des particules et la relativité générale. Ces deux théories sont cependant fondamentalement incompatibles : toute tentative directe de quantifier la gravité pour l'intégrer dans le modèle standard échoue inévitablement. Ce problème se pose dans deux cas majeurs, où les deux descriptions théoriques sont en échec : les premiers instants après le big bang, et l'intérieur des trous noirs. Dans les deux cas, la relativité générale ne parvient pas à décrire le comportement de la matière très dense à petite échelle et voit apparaître des singularités. Avec l'avènement de l'astronomie multi-messagers, les données expérimentales sur les trous noirs abondent aujourd'hui, faisant de ces derniers le laboratoire idéal pour tester de nouvelles physiques et théories de la gravité quantique.

Les trous noirs

Depuis Newton, on sait que les masses s'attirent, avec une force proportionnelle à leur masse et inversement proportionnelle au carré de la distance qui les sépare. La relativité générale, en tant que théorie de la gravitation, va plus loin : elle décrit comment les corps massifs déforment l'espace-temps. Ces déformations ont pour effet non seulement

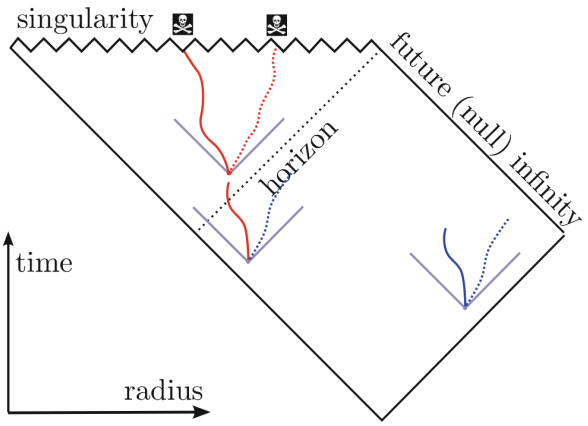

Figure 1: Diagramme de Penrose d'un trou noir de Schwarzschild. Le temps évolue de bas en haut, et les tranches horizontales sont spatiales. Les lignes bleues à 45° représentent les cônes de lumière en différents points : la causalité impose que les trajectoires de la matière et de la lumière restent toujours à l'intérieur de ces cônes. La singularité est représentée par une ligne en dents de scie, et l'horizon est en pointillés. Notez que lorsqu'une trajectoire traverse l'horizon, elle aboutit inévitablement à la singularité. Cette figure est tirée de [1].

d'attirer d'autres objets massifs, mais aussi de courber la trajectoire de la lumière dans leur voisinage. La situation extrême est celle d'un objet si massif et si compact que sa gravité est suffisamment forte pour piéger la lumière : ces objets sont appelés « trous noirs ».

La solution la plus simple de trou noir a été construite pour la première fois par Schwarzschild en 1916. Toute sa masse est concentrée dans une singularité spatio-temporelle, et celle-ci est enveloppée d'un horizon des événements sphérique, qui sert à délimiter l'intérieur et l'extérieur du trou noir. L'horizon des événements est une hypersurface nulle : c'est la limite à partir de laquelle la lumière ne peut plus s'échapper et tombe inévitablement dans la singularité. La figure 1 représente schématiquement la géométrie d'un espace-temps de trou noir. Il est important de comprendre que cette surface n'a aucune manifestation physique concrète ; une personne tombant dans un trou noir ne remarquerait pas qu'elle traverse l'horizon. Le rayon de l'horizon est proportionnel à la masse M du trou noir :

$$R_S = \frac{2GM}{c^2}. \tag{1}$$

Les trous noirs ont d'abord été considérés comme non physiques, mais leur existence dans la nature a maintenant été confirmée par des expériences sur les ondes gravitationnelles [2], et par des détections directes [3]. Ils sont entièrement caractérisés par très peu de paramètres : leur masse, leur charge et leur moment angulaire.

La thermodynamique des trous noirs

Les lois de la thermodynamique sont supposées régir tout système macroscopique dans l'univers. Pour préserver ces lois, les trous noirs doivent se comporter comme tout autre système thermodynamique ; ils doivent avoir une température et une entropie. En effet, la deuxième loi stipule qu'aucun processus physique ne peut diminuer l'entropie de l'univers. Le fait de jeter une masse dans un trou noir doit donc conduire à une augmentation de l'entropie du trou noir, pour compenser la perte d'entropie due à la disparition de cette masse.

Par un calcul classique, Bekenstein a réalisé dans les années 70 que l'entropie d'un trou noir est proportionnelle à la surface de son horizon des événements. Cela a été confirmé peu après, cette fois par un calcul quantique, lorsque Hawking a découvert qu'ils se comportent comme des corps noirs : ils émettent un rayonnement thermique qui émane de leur horizon. À partir de ce rayonnement, il est possible de calculer leur température T_H et, en utilisant la relation thermodynamique $T_H dS = dE$, leur entropie S :

$$T_H \;=\; \frac{\hbar\, c^3}{8\pi k_B G M}\,, \qquad S \;=\; \frac{k_B\, c^3\, A}{4G\hbar}\,, \tag{2}$$

où $A \equiv 4\pi R_S^2$ représente l'aire de l'horizon.

Ces formules font intervenir un nombre remarquable de constantes de la nature. Pour simplifier les calculs, il est habituel d'utiliser les unités dites naturelles, où $\hbar = c = k_B = G = 1$, mais nous faisons ici une exception, car la présence de ces constantes en dit long sur les mécanismes en jeu derrière ces formules :

- La constante gravitationnelle, G, apparaît dans la relativité générale, qui est partie intégrante de la description des trous noirs.
- La constante de Planck, $\hbar$, et la vitesse de la lumière, c, proviennent de la théorie quantique des champs, qui est utilisée pour décrire les particules et les champs entourant le trou noir et constituant le rayonnement.
- Enfin, la constante de Boltzmann, k_B, est issue de la thermodynamique, qui régit le comportement collectif de ces particules.

C'est par l'interaction entre ces théories que l'on peut découvrir l'existence du rayonnement et rendre compte de l'entropie. En effet, la dérivation de Hawking utilisait le fait que le vide des champs quantiques dans le fond courbé d'un trou noir n'est pas unique, il dépend de l'emplacement de l'observateur. Une manière plus simple de comprendre le phénomène est de le décrire en termes de particules. Le vide comporte toujours des créations et annihilations spontanées de particules et d'antiparticules. Cependant, lorsque cela se produit près de l'horizon, l'une de ces particules peut tomber et être piégée par le trou noir, tandis que l'autre s'échappe à l'infini. Ce processus se doit de conserver l'énergie, et c'est effectivement le cas : l'énergie de la particule piégée est strictement négative vue de l'infini, et la particule virtuelle qui s'échappe devient réelle, avec une énergie positive. Ainsi, par ce processus, la masse du trou noir se trouve amoindrie.

Le paradoxe de l'information

La dérivation du rayonnement de Hawking a soulevé deux interrogations.

La première énigme est la question de l'origine microscopique de l'entropie des trous noirs. L'entropie des trous noirs, donnée par (2), est énorme. Pour Sagittarius A*, le trou noir au centre de la Voie lactée, ce nombre est de 10^{90}. Cette entropie devrait correspondre à un grand nombre de micro-états, selon la formule de Boltzmann $N = \exp(S)$. Cependant, le théorème d'unicité du trou noir prouve qu'en relativité générale, il n'existe qu'une seule solution de trou noir. Où se trouvent donc tous ces micro-états ? Une théorie de la gravité quantique doit être capable de reproduire avec précision ce grand nombre.

La deuxième énigme survient lorsque l'on considère les conséquences à long terme du rayonnement de Hawking. Par ce processus, un trou noir perd lentement de sa masse et s'évapore, jusqu'à disparaître complètement – ou du moins jusqu'à ce que les approximations faites par Hawking dans le calcul cessent d'être valides, une fois que le trou noir est trop petit. Ce processus est toutefois radicalement différent de la combustion d'une feuille de papier, par exemple, et enfreint un principe fondamental de la mécanique quantique : *l'unitarité*.

Dans le cas d'un morceau de papier, le rayonnement se produit par le biais de réactions chimiques qui se produisent à la surface, et l'information sur les constituants du papier est emportée par le rayonnement lorsque celui-ci brûle : la transformation est unitaire. Cela signifie que si l'on rassemblait et mesurait toutes les particules émises lors de la combustion, on pourrait théoriquement simuler l'ensemble du processus et connaître l'état exact du papier avant qu'il ne brûle, jusqu'au texte qui y était écrit. Le rayonnement de Hawking, quant à lui, est émis à proximité de l'horizon du trou noir. À l'horizon, l'espace-temps est dans un vide parfait, car toute matière placée à cet endroit tomberait immédiatement dans le trou noir. En conjonction avec le théorème d'unicité du trou noir, cela signifie que le rayonnement est universel et ne peut pas emporter l'information des constituants originaux du trou noir. Une fois le trou noir évaporé, l'information et l'unité sont perdues (voir [4] pour une revue). C'est ce que l'on désigne parfois sous le nom de « paradoxe de l'information ».

Une théorie de la gravité quantique, qui unifie la mécanique quantique et la relativité générale, se doit d'apporter une solution à ces paradoxes. Le paradoxe de l'information, en particulier, est un problème très épineux, car le conflit existe à l'échelle de l'horizon, où l'espace est presque plat et où l'approximation semi-classique devrait s'appliquer. On ne peut donc pas le résoudre par une résolution de la singularité à l'échelle de Planck : il faut une nouvelle physique à l'échelle de l'horizon.

La conjecture des *Fuzzballs*

La théorie des cordes est un candidat à la gravité quantique. Elle postule que les constituants primitifs de la nature ne sont pas des particules mais des *cordes*, ainsi que des

objets étendus de dimension supérieure appelés *membranes*, sur lesquels les extrémités des cordes ouvertes peuvent se fixer. Ce que nous considérons comme des particules distinctes correspond alors à différents modes de vibration de ces cordes. Les interactions entre particules résultent de la division et de la fusion des cordes. Deux paramètres fondamentaux de la théorie des cordes apparaîtront dans la discussion : la *tension des cordes*, α', qui fixe une échelle d'énergie globale, et le *couplage des cordes*, g_s, qui contrôle la force de l'interaction entre les cordes.

La théorie des cordes intègre naturellement la supersymétrie et, pour être cohérente, elle requiert que le nombre de dimensions de l'espace-temps soit de 10 ou 11. Ces dimensions supplémentaires apparaissent dans un certain nombre d'extensions du modèle standard et sont considérées comme un ingrédient essentiel de toute théorie de la gravité quantique. Pour faire le lien avec notre espace-temps familier à quatre dimensions, ces dimensions supplémentaires doivent être compactes. Les cordes et les membranes peuvent alors les *envelopper*, de sorte que dans l'espace-temps à quatre dimensions, elles apparaissent comme des particules ponctuelles ou des objets de faible dimension.

À basse énergie, la plupart des modes de la corde ne peuvent être excités, et la théorie est décrite avec justesse par une théorie quantique des champs qui inclut la relativité générale. En effet, la quantification de la corde fermée révèle l'existence d'un boson de spin-2 sans masse, le graviton, qui est le médiateur de la force gravitationnelle. Avec les autres champs de basse énergie, ils forment une théorie de supergravité. La constante gravitationnelle, G, peut alors être exprimée en fonction des paramètres de la théorie :

$$G \sim g_s^2 l_s^{d-2}\,, \tag{3}$$

où d est le nombre de dimensions, et $l_s = \sqrt{2\pi\alpha'}$ est la longueur de corde.

Comme nous le verrons, il est possible de répondre aux énigmes des trous noirs grâce à la théorie des cordes. En effet, les cordes et les membranes peuvent se comporter très différemment de la matière normale. Une sphère de matière gravitante ordinaire suffisamment massive va nécessairement s'effondrer sur elle-même et, une fois enfermée dans un horizon des événements, le théorème de singularité de Penrose [5] stipule que l'état final de l'effondrement est une singularité, ou au moins un objet dont la taille est à l'échelle de Planck. Ce n'est pas le cas pour les membranes : une collection de N membranes peut former un état lié stable dont la taille croît avec une certaine puissance de N [6]. Plus important encore, cette taille croît également avec le couplage gravitationnel G [7]. Lorsque N est grand, l'échelle de l'état lié peut donc être du même ordre que le rayon de Schwarzschild : cet objet ne forme jamais d'horizon.

Ces configurations de la théorie des cordes sont appelées *fuzzballs* [6, 8], et sont des candidats de choix pour la description microscopique des trous noirs. Ces objets défient l'intuition issue de la théorie effective des champs : s'il s'agit de micro-états de trous noirs, la géométrie du trou noir est modifiée sur toute la distance entre le centre et l'horizon, où la courbure est faible et où la relativité générale est censée s'appliquer. Par construction, les fuzzballs ne sont pas sujets au paradoxe de l'information : ils rayonnent comme un corps normal, à partir de leur surface. Comme nous le verrons, ils évitent également le

problème de l'unicité : les fuzzballs ont un espace de configurations très riche, provenant des nombreuses façons dont les cordes et les membranes peuvent se plier.

Les dualités en théorie des cordes, et l'énumération des fuzzballs

Le nombre de micro-états des trous noirs est extrêmement élevé. Pour que les fuzzballs fournissent une description précise d'un micro-état de trou noir typique, il faut montrer qu'ils ont un nombre de configurations de l'ordre de e^S. Un premier pas dans cette direction a été accompli par Sen [9], puis par Strominger et Vafa en 1996 [10], en travaillant avec la supersymétrie et à couplage nul.

Ce dernier point mérite une explication. Dans notre univers, la valeur du couplage des cordes g_s doit être grande, nous sommes loin du régime où elle est nulle. Bien sûr, il est possible de discuter de scénarios hypothétiques où cette constante a des valeurs très différentes. Ces scénarios deviennent pertinents dans deux situations : les dualités de cordes et les supersymétries. Certaines quantités sont dites « protégées » par la supersymétrie, ce qui signifie que leur valeur ne change pas lorsque l'on fait varier la constante de couplage. Une quantité protégée peut être calculée dans n'importe quel régime, par exemple lorsque la constante de couplage est nulle, et le résultat est alors valable en général. L'indice supersymétrique est une telle quantité, et il fournit une bonne approximation, ainsi qu'une borne inférieure, pour le nombre de micro-états supersymétriques.

En présence d'un état lié de N D-branes, le couplage effectif des cordes ouvertes est g_sN. Nous distinguons deux régimes. Lorsque $g_sN \ll 1$, le secteur des cordes ouvertes se découple de la gravité, le système est décrit par l'interaction des cordes ouvertes dans un fond de membranes fixes. Lorsque $g_sN \gg 1$, les membranes rétroagissent, le secteur des cordes fermées domine et le système peut être décrit à l'aide de la supergravité, voir Figure 2.

Strominger et Vafa ont étudié le système supersymétrique D1-D5-P [10]. À faible couplage, il est décrit par les excitations de cordes par-dessus un état lié de branes D1 et D5. En utilisant la formule de Cardy, ils ont pu estimer l'entropie du système. Leur résultat correspond précisément à l'entropie du trou noir BTZ « à trois charges », obtenue dans la limite des grands couplages.

Les géométries de micro-état

Le succès de Strominger et Vafa montre que la théorie des cordes est capable de capturer les degrés de liberté des trous noirs, au moins dans le cas de la supersymétrie. Cependant, ces calculs sont effectués à faible couplage : ils montrent que les micro-états des trous noirs peuvent être décrits par la théorie des cordes, mais pas quelle forme ces micro-états prennent à fort couplage. Pour résoudre le paradoxe de l'information, il faut également comprendre les micro-états des trous noirs non supersymétriques.

Comme nous l'avons vu, ces micro-états sont conjecturés comme étant des géométries « crépues », sans horizon, connues sous le nom de fuzzballs. Par le mécanisme de fraction-

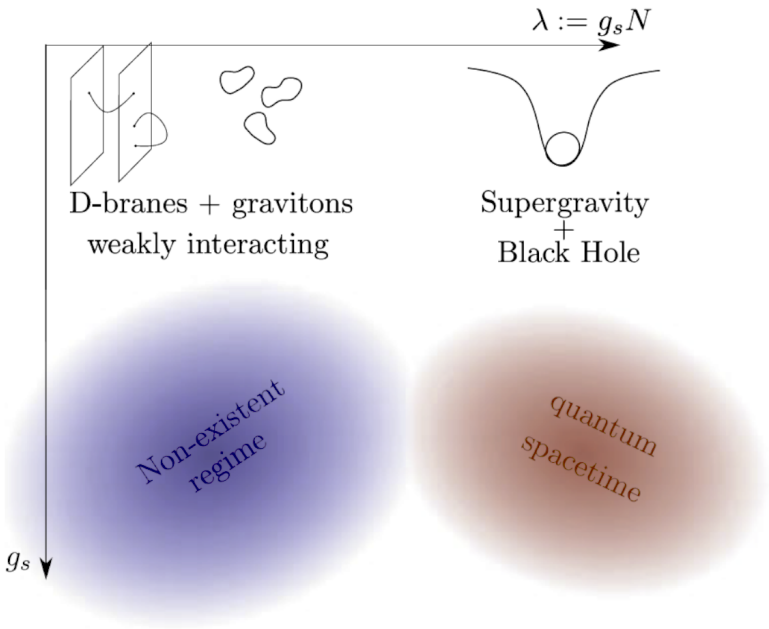

Figure 2: Représentation des différents régimes de la théorie, en fonction du couplage des cordes g_s. Lorsque $g_s N \ll 1$, la théorie est décrite efficacement par des cordes ouvertes dans un arrière-plan de D-branes, et la gravité est découplée. Lorsque $g_s N \gg 1$, tout en gardant $g_s \ll 1$, la gravité domine, le système est décrit par la supergravité. Notons que puisque N est un entier, il n'y a pas de régime de paramètres où $g_s > \lambda > 0$. La figure est extraite de [1].

nement, la taille d'un état lié de membranes croît avec la constante de couplage et peut atteindre l'échelle de l'horizon. Notez que la solution classique du trou noir de la relativité générale ne peut pas être un des micro-états, car les états purs ont nécessairement une entropie nulle. La solution classique du trou noir doit donc être interprétée comme une description moyennée de toutes ces solutions de fuzzballs, dans une théorie qui n'est pas assez riche pour en capturer les caractéristiques.

Une description complète et précise de ces fuzzballs est cependant hors de portée : on sait que les trous noirs sont des systèmes chaotiques, et on estime que leurs micro-états sont des systèmes quantiques très complexes. Au lieu de cela, on peut essayer de construire des superpositions cohérentes de ces états quantiques. Un état suffisamment cohérent peut être décrit classiquement, comme une solution de supergravité qui est nécessairement lisse et sans horizon, voir Figure 3. Le programme de géométrie des micro-états entreprend de construire de telles solutions classiques (voir [1, 11, 12] pour des revues récentes).

Ce programme a conduit à la construction de la totalité des géométries des micro-états du trou noir supersymétrique à deux charges. Ces géométries sont connues sous le nom de *supertubes* [14–17]. Cette construction a été étendue au trou noir à trois charges, conduisant en 2015 à une grande famille de géométries connues sous le nom de superstrata [18–20], qui ont été depuis largement étudiées [21–28, 28–36]. Cependant, le nombre d'états de cette famille est en deçà de l'entropie totale du trou noir à trois charges.

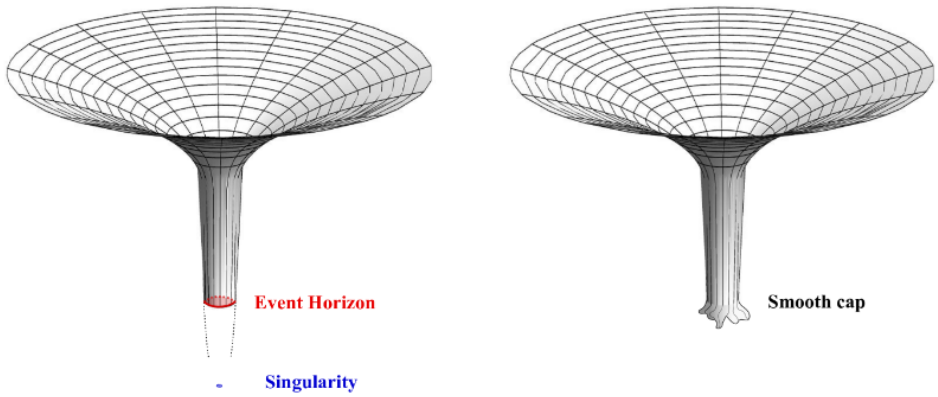

(a) Classical black hole. (b) Fuzzball.

Figure 3: Représentation schématique d'une géométrie de micro-état. À gauche, la géométrie classique du trou noir présente une longue « cavité » qui se termine par une singularité et qui est habillée par un horizon. Dans l'image de droite de la géométrie des micro-états, la cavité se referme avant l'horizon. La géométrie est partout lisse et sans horizon. Cette figure est tirée de [13].

Le défi actuel est donc double. Pour les trous noirs supersymétriques, il faut construire des familles de micro-états à trois charges plus vastes qui rendent compte de l'entropie totale du trou noir, prouvant ainsi que les micro-états typiques peuvent être décrits avec précision de manière classique. Mais les trous noirs qui existent dans notre univers ne sont pas supersymétriques, et on sait très peu de choses sur leurs micro-états. Une meilleure compréhension de ces micro-états est nécessaire pour résoudre complètement le paradoxe de l'information.

Contribution et organisation de ce manuscrit

Cette thèse propose des avancements sur le programme de géométrie des micro-états. Je présenterai et passerai en revue les travaux que mes collaborateurs et moi-même avons publiés dans [37–44]. L'accent est mis sur la construction et l'étude de nouvelles géométries de micro-états du système D1-D5-P à trois charges. En particulier, nous obtiendrons l'une des premières classes de géométries non-BPS dans le régime des trous noirs, ainsi que leur dictionnaire CFT. Nous explorerons également les possibilités de reproduire toute l'entropie d'un trou noir supersymétrique avec des géométries de micro-états, et nous proposerons des moyens de suivre les micro-états individuels depuis le régime du couplage nul jusqu'au régime du trou noir.

La première partie introduit les concepts de base et les résultats associés au système D1-D5. Le chapitre 2 sert d'introduction à la théorie des cordes et au système D1-D5 à petit couplage. En particulier, nous passons en revue la construction de Strominger-Vafa des micro-états à couplage nul. Le chapitre 3 décrit le même système D1-D5 dans le régime opposé : nous introduisons la supergravité et le trou noir à trois charges, et nous

vérifions que son entropie correspond au comptage des micro-états de cordes ouvertes.

Dans le chapitre 4, nous expliquons comment la situation précédente se présente dans le cadre plus général de la correspondance AdS/CFT. Nous décrivons ensuite la CFT D1-D5, qui constitue la limite à basse énergie du système de cordes ouvertes s'étirant entre les D-branes.

Dans la Partie II, nous présentons la construction de nouvelles géométries de micro-états dans le cadre d'une supergravité de jauge tridimensionnelle. Le chapitre 6 sert d'introduction.

Dans le chapitre 7, nous présentons la théorie de la supergravité tridimensionnelle qui sera utilisée. Après une brève introduction sur les notations et les conventions utilisées dans ce document, nous décrivons en détail la théorie et son contenu en champs, et nous dérivons les équations BPS. Le chapitre 8 examine ensuite comment une certaine classe de superstrata s'intègre dans la théorie 3D susmentionnée.

Dans le chapitre 9, nous construisons des ansätze spécifiques pour les champs de la théorie. Nous motivons ces choix en nous appuyant sur la théorie des Q-balls : les champs sont conçus pour avoir une dépendance temporelle très spécifique, de sorte que le tenseur énergie-impulsion, et en fin de compte les équations d'Einstein, sont indépendants du temps. Nous expliquons comment la théorie se décompose naturellement en deux secteurs ; le premier ansatz que nous construisons correspond à une troncation à un seul secteur, et nous montrons comment une sous-famille de superstrata s'y intègre. Le second ansatz est plus complexe et tire parti des deux secteurs ; il permet de décrire toute la famille des superstrata tridimensionnelles.

Dans le chapitre 10 nous dérivons les équations BPS en termes des champs des deux ansätze. Nous motivons le choix des projecteurs de supersymétrie en utilisant les superstrata comme guide. Le chapitre 11 est ensuite consacré à la résolution de ces équations. Nous construisons de nouvelles familles de solutions supersymétriques du système à trois charges. Nous nous concentrons d'abord sur une classe de solutions particulièrement simple : le « special locus ». Nous dérivons ensuite les solutions les plus générales des équations dans l'ansatz à un seul secteur, et nous étudions son élévation en six dimensions. Enfin, nous nous concentrons sur deux familles importantes de solutions : les superstrata « pure-NS » et les géométries qui sont asymptotiquement AdS_2.

Dans le chapitre 12 nous nous tournons vers la construction de géométries non-BPS. Nous présentons d'abord une méthode perturbative pour résoudre les équations du mouvement. Nous expliquons en détail le processus utilisé pour construire et identifier les solutions, à la fois dans les ansätze à un secteur et à deux secteurs, de manière perturbative au-dessus du vide AdS. L'ensemble des solutions se décompose en deux classes, que nous avons nommées « classe alpha » et « classe beta » ; ces solutions ont des porteurs de quantité de mouvement différents. Enfin, nous expliquons comment appliquer la théorie des perturbations à une géométrie de micro-état déjà profonde (supersymétrique), en utilisant l'approximation WKB.

Les chapitres 13 et 14 sont dédiés à l'interprétation CFT de ces solutions nouvellement construites. Nous commençons par une brève revue des opérateurs de la CFT D1-D5, puis

nous proposons une identification des solutions de supergravité en tant qu'états lourds de la théorie conforme. Nous utilisons ensuite l'holographie pour établir le dictionnaire entre la supergravité et la CFT. Cette tâche est compliquée par le fait que la plupart des observables ne sont pas protégées et sont sujettes à des variations au fur et à mesure que l'on se déplace dans l'espace des moduli. Pour les solutions dans l'ansatz à un seul mode, nous pouvons recourir à un test non trivial pour vérifier la validité du dictionnaire.

Le chapitre 15 aborde la question de la construction de solutions non-BPS sous l'angle des simulations numériques. Nous montrons que l'on peut construire des solutions numériques aux équations du mouvement, par deux méthodes différentes, et nous pouvons identifier et comparer ces solutions numériques avec le développement perturbatif du chapitre précédent. Nous terminerons cette partie par quelques commentaires finaux dans le chapitre 16.

Dans la Partie III, nous proposons une nouvelle voie pour reproduire l'entropie totale des trous noirs avec des géométries de micro-états. Dans le Chapitre 17, nous présentons l'idée du super-labyrinthe, une construction de membranes qui révèle l'origine de l'entropie des trous noirs d'une manière purement géométrique. Nous expliquons comment décrire un état lié de branes M2 et M5 avec impulsion dans la théorie M, et comment extraire sa géométrie à partir des projecteurs de supersymétrie. L'idée centrale est que ces configurations de branes préservent localement 16 supersymétries, et ne peuvent donc pas former d'horizon après la rétroaction. Enfin, le chapitre 18 introduit le concept de *themelia*, que nous conjecturons être l'élément fondamental des micro-états lisses des trous noirs. Nous décrivons une grande famille de ces themelia, y compris le super-labyrinthe, en utilisant des projecteurs de supersymétrie. Nous expliquons comment les themelia apparaissent naturellement dans plusieurs micro-états supersymétriques connus, tels que les « bubbling geometries » et les superstrata.

Chapter 1

Introduction

The 20th century has seen the emergence of two extremely successful theories of nature. On one side stands quantum mechanics, which governs the interactions between particles at very small scales. Its development throughout the years led to the establishment of the Standard Model, which unified all known elementary particles and their three fundamental interactions in a single framework. This model has been tested to amazing precision and made powerful predictions, such as predicting the existence of the Higgs boson forty years before its discovery at CERN. On the other side, General Relativity was developed by Einstein to describe the long-range gravitational interactions between large bodies. The theory has made predictions that have been since then been rigorously tested, such as the Shapiro time delay effect, or the precise waveform of the gravitational signals emitted during the merger of black holes, signals that have been first detected by LIGO in 2016.

Pursuing the goal behind the construction of the Standard Model, physicists have tried to build a theory of quantum gravity, unifying particle physics and General Relativity. These two theories are nevertheless fundamentally incompatible with each other: any direct attempt to quantize gravity to incorporate it in the Standard model inevitably fails. This issue arises in two major instances, where both theoretical descriptions break down: the first moments after the big bang, and the interior of black holes. In both instances, General Relativity fails to describe the behavior of very dense matter at small scales, and sees the appearance of singularities. With the advent of multi-messenger astronomy, experimental data on black holes now abound, making black holes the perfect laboratory to test new physics and theories of quantum gravity.

Black holes

Since Newton, it has been known that massive bodies attract each other, with a force that is proportional to their masses, and inversely proportional to the square of the distance separating them. General Relativity, as a theory of gravitation, goes further: it describes how massive bodies deform spacetime. These deformations not only causes other massive bodies to be attracted, but it also curves the path of light in its vicinity. The extreme

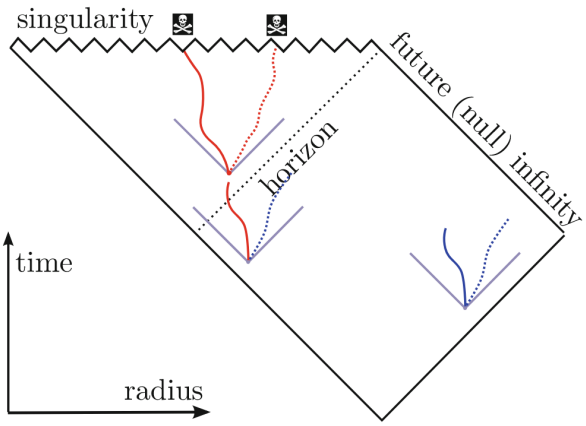

Figure 1.1: Penrose diagram of a Schwarzschild black hole. Time evolves from bottom to top, and horizontal slices are spatial. The blue lines at 45° represent the light-cones at various points: causality imposes that the trajectories of matter and light must always stay within these cones. The singularity is represented by a saw-tooth line, and the horizon is dotted. Note that when a trajectory crosses the horizon, it inevitably ends up at the singularity. This figure is taken from [1].

situation is that of an object so massive and compact that its gravity is strong enough to trap light: these objects are called *black holes*.

The simplest black hole solution was first constructed by Schwarzschild in 1916. All of its mass is concentrated in a spacetime singularity, and it is dressed by a spherical event horizon, which is used to delimit the interior and the exterior of the black hole. The event horizon is a *null hypersurface*: it is the limit from which light can no longer escape and must eventually fall to the singularity. Figure 1.1 represents schematically the geometry of a black-hole spacetime. It is important to understand that this surface has no concrete, physical manifestation ; a person falling into a black hole would not notice their crossing of the horizon. The radius of the horizon is proportional to the mass M of the black hole:

$$R_S = \frac{2GM}{c^2}. \tag{1.1}$$

Black holes were initially thought to be unphysical, but their existence in nature has now been confirmed via gravitational-waves experiments [2], and via direct detection [3]. They are completely characterized by very few parameters: their mass, their charge and their angular momentum.

Black-hole thermodynamics

The laws of thermodynamics are believed to govern any macroscopic system in the universe. To preserve these laws, black holes must behave as any other thermodynamic system; they must have a temperature and an entropy. Indeed, the second law states that through no physical process can the entropy of the universe decrease. Throwing a mass

into a black hole must lead to an increase of the black hole entropy, to compensate for the loss of entropy due to the disappearance of said mass.

By a classical computation, Bekenstein realized in the 70s that the black hole entropy is proportional to the area of its event horizon. This was confirmed shortly after, this time through a quantum calculation, when Hawking found that they behave as black bodies [45]: they emit a thermal radiation that originates from their horizon. From this radiation, it is possible to compute their temperature T_H, and, using the thermodynamical relation $T_H dS = dE$, their entropy S:

$$T_H = \frac{\hbar c^3}{8\pi k_B G M}, \qquad S = \frac{k_B c^3 A}{4G\hbar}, \tag{1.2}$$

where $A \equiv 4\pi R_S^2$ is the area of the horizon.

These formulas involve a remarkable number of different constants of nature. To simplify computations, it is usual to use the so-called natural units, where $\hbar = c = k_B = G = 1$, however we make an exception here, because the presence of these constants reveal a lot about the mechanisms at play behind these formulas:

- The gravitational constant, G, appears in General Relativity, which is integral to the description of black holes.
- The Planck constant, $\hbar$, and the speed of light, c, come from Quantum Field Theory, which is used to describe the particles and fields surrounding the black hole and constituting the radiation.
- Finally the Boltzmann constant, k_B, originates from thermodynamics, which governs the collective behavior of these particles.

This is through the interplay between these theories that one can find the existence of the radiation and account for the entropy. Indeed, Hawking's derivation used the fact that the vacuum of quantum fields in the curved background of a black hole is not unique, it depends on the location of the observer. A simpler way to understand the phenomenon is to describe it in terms of particles. The vacuum always contains spontaneous creation and annihilation of particle and anti-particle. When this happens close to the horizon, however, one of these particles can fall and be trapped by the black hole, while the other escapes at infinity. This process must, and does, conserve energy: the energy of the trapped particle is strictly negative as seen from infinity, and the escaping virtual particle becomes real, with a positive energy. Thus, through this process, the mass of the black hole is decreased.

The information paradox

The derivation of the Hawking radiation led to two mysteries.

The first puzzle is the question of the microscopic origin of the black hole entropy. The entropy of black holes, as given by (1.2), is enormous. For Sagittarius A*, the black hole at the center of Milky Way, this number is 10^{90}. This entropy should correspond to

a large number of microstates, following Boltzmann formula $N = \exp(S)$. However, the black-hole uniqueness theorem proves that in General Relativity, there exists only one black hole solution. Where, then, are all these microstates ? A theory of quantum gravity must be able to accurately reproduce this large number.

The second puzzle arises as one considers the long-term effects of the Hawking radiation. Through this process, a black hole slowly loses mass and evaporates, until it completely disappears – or at least until the approximations made by Hawking in the computation break down, once the black hole is too small. This process however is radically different from, for example, the burning of a piece of paper, and breaks a fundamental principle of quantum mechanics: *unitarity*.

For the piece of paper, the radiation happens through chemical reactions at the surface of the paper, and the information on the constituents of the paper is carried away by the radiation as the paper burns: the transformation is unitary. This means that if one were to gather and measure all the particles emitted through the burn, one could theoretically simulate the whole process and learn about the exact state of the paper before it burned, down to the text that was written on it. Hawking radiation, on the other hand, is emitted close to the horizon of the black hole. At the horizon, the spacetime is in a perfect vacuum, as any matter placed at this locus would fall immediately in the black hole. In conjunction with the black hole uniqueness theorem, it means that the radiation is universal and cannot carry away the information of the original constituents of the black hole. Once the black hole has evaporated, the information, and unitarity, is lost (see [4] for a review). This is sometimes called the *information paradox*.

A theory of quantum gravity, that unifies quantum mechanics and general relativity, must provide a resolution to these paradoxes. The information paradox, in particular, is a very sharp problem, because the conflict exists at the scale of the horizon, where space is almost flat and the semi-classical approximation should hold. Hence, one cannot solve it by a Planck-scale resolution of the singularity: there must be new physics at the scale of the horizon.

The Fuzzball Conjecture

String theory is a candidate for quantum gravity. It postulates that the primitive constituents of nature are not particles but *strings*, as well as higher-dimensional extended object called *branes*, on which open strings can end. What we think of as distinct particles then correspond to different modes of vibration of these strings. The interaction between particles happen because of the splitting and merging of strings. Two fundamental parameters of string theory will appear in the discussion: the *string tension*, α', which sets a global energy scale, and the *string coupling*, g_s, which controls the strength of the interaction between strings.

String theory naturally incorporates supersymmetry, and for its consistency, it requires that the number of spacetime dimensions is 10 or 11. Such extra dimensions appear in

a number of extensions of the Standard Model, and are conjectured to be an essential ingredient of any theory of quantum gravity. To connect to our familiar four-dimensional spacetime, these extra dimensions must be compact. Strings and branes can then *wrap* them, so that in the four-dimensional spacetime they appear as point particles or low-dimensional objects.

At low energy, most of the modes of the string cannot be excited, and the theory is accurately described by a quantum field theory that includes General Relativity. Indeed, quantizing the closed string reveal the existence of a massless spin-2 boson, the graviton, that mediates the gravitational force. With the other low-energy fields, they form a theory of supergravity. The gravitational constant, G, can then be expressed in terms of the parameters of the theory:

$$G \sim g_s^2 l_s^{d-2}\,, \tag{1.3}$$

where d is the number of dimensions, and $l_s = \sqrt{2\pi\alpha'}$ is called the string length.

As we will see, it is possible to answer the puzzles of black holes with string theory. Indeed, strings and branes can behave very differently from normal matter. A shell of sufficiently massive ordinary gravitating matter necessarily collapses, and, once enclosed by an event horizon, the Penrose singularity theorem [5] states that the final state of the collapse is a singularity, or at least to a Planck-sized object. This is not true for branes: a collection of N branes can form a stable bound state whose size grows with some power of N [6]. More importantly, this size also grows with the gravitational coupling G [7]. At large N, the scale of the bound state can thus be of the same order as the Schwarzschild radius: this object never forms a horizon.

These string theory configurations are termed *fuzzballs* [6,8], and are prime candidates for the microscopic description of black holes. These objects defy the intuition from effective field theory: if they are black-hole microstates, the geometry of the black hole is modified all the way from the center to the horizon, where the curvature is weak and general relativity is expected to hold. By construction, they are not subject to the information paradox: they radiate like a normal body, from their surface. As we will see, they also avoid the uniqueness problem: fuzzballs have a very rich phase space of configurations from the many ways that strings and branes can bend.

String dualities and fuzzball counting

The number of black-hole microstates is extremely large. For fuzzballs to provide an accurate description of a typical black-hole microstate, one must show that they have a number of configurations of order e^S. A first step in this direction was accomplished by Sen [9], then Strominger and Vafa in 1996 [10], working with supersymmetry and at vanishing coupling.

This last point deserves an explanation. In our universe, the value of the string coupling g_s must be large, we are far from the regime where it vanishes. Of course, it is possible to discuss hypothetical scenarios where this constant has very different values.

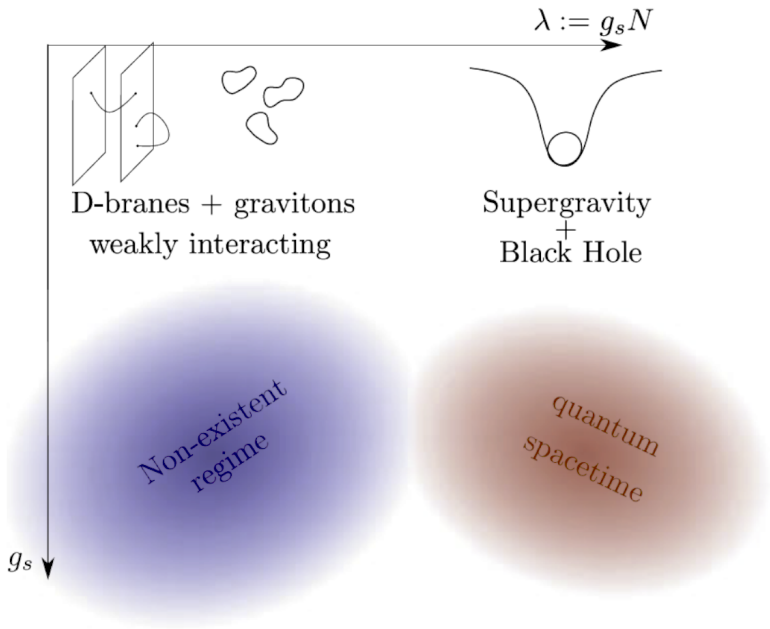

Figure 1.2: Representation of the different regimes of the theory, as one dials the string coupling g_s. At $g_s N \ll 1$, the theory is described effectively by open strings in a background of D-branes, and gravity is decoupled. At $g_s N \gg 1$, while keeping $g_s \ll 1$, gravity dominates, the system is described by supergravity. Note that since N is an integer, there is no regime of parameters where $g_s > \lambda > 0$. The figure is taken from [1].

These scenarios become significant in two instances: string dualities and supersymmetries. Some quantities are said to *protected* by supersymmetry, this means that their value does not change as one dial the coupling constant. A protected quantity can be computed in any regime, for example when the coupling constant vanishes, and the result then holds in generality. The supersymmetric index is such a quantity, and it provides a good approximation, and a lower bound, for the number of supersymmetric microstates.

In the presence of a bound state of N D-branes, the effective coupling of open strings is $g_s N$. We distinguish two regimes. When $g_s N \ll 1$, the open string sector decouples from gravity, the system is described by the interaction of open strings in the background of the branes. When $g_s N \gg 1$, the branes backreact, the closed-string sector dominates, and the system can be described using supergravity, see Figure 1.2.

Strominger and Vafa worked with the supersymmetric D1-D5-P system [10]. At low coupling, it is described by the stringy excitations on top of a bound state of D1 and D5 branes. Using Cardy's formula, they were able to estimate the entropy of the system. Their result matched precisely with the entropy of the "three-charge" BTZ black hole, that is obtained in the large coupling limit.

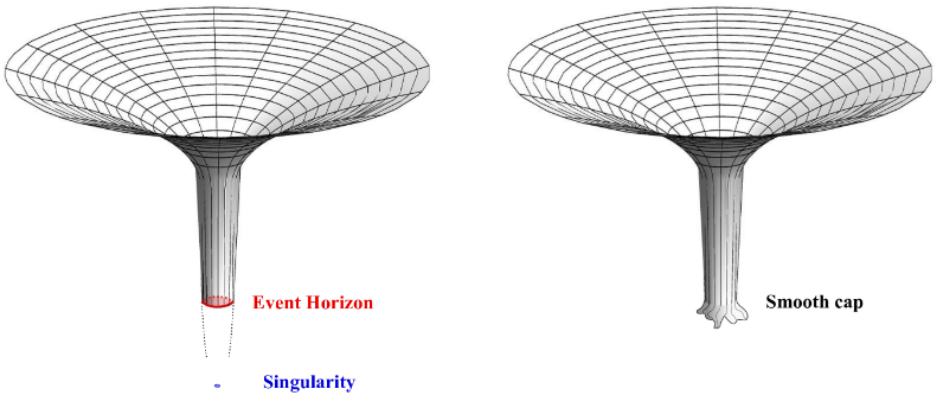

(a) Classical black hole. (b) Fuzzball.

Figure 1.3: Schematic representation of a microstate geometry. To the left, the classical black-hole geometry features a long throat that ends with a singularity, and is dressed by a horizon. In the microstate geometry picture to the right, the throat caps off before the horizon. The geometry is everywhere smooth and horizonless. This figure is taken from [13].

Microstate geometries

The success of Strominger and Vafa shows that string theory is able to capture the degrees of freedom of black holes, at least with supersymmetry. However, these computations are done at small coupling: they show that the black-hole microstates can be described by string theory, but not what form these microstates take at strong coupling. To solve the information paradox, one must also understand the microstates of non-supersymmetric black holes.

As we discussed, these microstates are conjectured to be horizonless "fuzzy" geometries known as fuzzballs. Through fractionation, the size of a bound state of branes grows with the coupling constant and can reach the scale of the horizon. Note that the classical black-hole solution of general relativity cannot be one of the microstates, as pure states have necessarily a null entropy. The classical black-hole solution must then be understood as an average description of all these fuzzball solutions, in a theory that is not rich enough to capture their features.

A complete, precise description of these fuzzballs is however out of reach: black holes are known to be chaotic systems, and their microstates are expected to be very complex, stringy quantum systems. Instead, one can try to build coherent superpositions of these quantum states. A sufficiently coherent state can be described classically, as a solution of supergravity that is necessarily smooth and horizonless, see Figure 1.3. The microstate geometry program endeavors to build such classical solutions (see [1, 11, 12] for recent reviews).

This programme led to the construction of the full set of microstate geometries of the two-charge supersymmetric black hole. These geometries are known as *supertubes* [14–17].

This construction has been extended to the three-charge black hole, leading in 2015 to a large family of geometries known as superstrata [18–20], that have been since extensively studied [21–28, 28–36]. However, the number of states in this family falls short to the total entropy of the three-charge black hole.

The challenge nowadays is two-fold. For supersymmetric black holes, one needs to build larger three-charge microstates families that account for the total entropy of the black, thus proving that typical microstates can be accurately described classically. But the black holes existing in our universe are not supersymmetric, and very little is known of their microstates. A better understanding of these microstates is necessary to fully resolve the information paradox.

Contribution and organization of the manuscript

This thesis proposes advances on the microstate geometry programme. I will introduce and review the works that my collaborators and I published in [37–44]. The focus is on the construction and study of new microstate geometries of the three-charge D1-D5-P system. In particular, we will derive one of the first class of non-BPS geometries deep in the black hole regime, along with their CFT dictionary. We will also explore the possibilities of reproducing the whole entropy of supersymmetric black hole with microstate geometries, and propose ways to track individual microstates from the regime of vanishing coupling all the way to the black hole regime.

The first part introduces the basic concepts and results associated to the D1-D5 system. Chapter 2 serves as an introduction to string theory and to the D1-D5 system at small coupling. In particular, we review the Strominger-Vafa construction of the microstates at vanishing coupling. Chapter 3 depicts the same D1-D5 system in the opposite regime: we introduce supergravity and the three-charge black hole, and check that its entropy matches with the counting of open-string microstates.

In Chapter 4, we explain how the previous situation takes place in the more general framework of the AdS/CFT correspondence. We then describe the D1-D5 CFT, that arises as the low-energy limit of the system of open strings stretching between the D-branes.

In Part II, we present the construction of new microstate geometries in the framework of a three-dimensional gauge supergravity. First, Chapter 6 serves as an introduction.

In Chapter 7 we introduce the three-dimensional supergravity theory that will be used. After a brief introduction on the notations and conventions used throughout this work, we describe in details the theory and its field content, and derive the BPS equations. Chapter 8 then reviews how a certain class of superstrata fits in the aforementioned 3D theory.

In Chapter 9 we construct specific ansätze for the fields of the theory. We motivate these choices from the theory of Q-balls: the fields are made to have a very specific time dependence, so that the energy-momentum tensor, and ultimately the Einstein equations, are time independent. We explain how the theory naturally decomposes into two "sectors";

the first ansatz that we construct corresponds to a single-sector truncation, and we show how a subfamily of superstrata fits inside it. The second ansatz is more involved and takes advantage of both sectors ; it can describe the full family of three-dimensional superstrata.

In Chapter 10 we derive the BPS equations in terms of the fields of both ansätze. We motivate the choice of supersymmetry projectors using superstrata as a guide. Chapter 11 is then dedicated to solving these equations. We construct new families of supersymmetric solutions of the three-charge system. We first focus on a particularly simple class of solution: the "special locus". We then derive the most general solutions of the equations in the single-sector ansatz, and study its uplift in six dimensions. Finally, we focus on two important families of solutions: the "pure-NS" superstrata and the geometries that are asymptotically AdS_2.

In Chapter 12 we turn to the construction of non-BPS geometries. We first present a perturbative method to solving the equations of motion. We explain in detail the process that is used to build and identify solutions, in both the single-sector and double-sector ansätze, perturbatively around the AdS vacuum. The set of solution decomposes into two classes, that we named "alpha-class" and "beta-class" ; these solutions have different momentum carriers. Finally, we explain how to do perturbation theory around an already deep (supersymmetric) microstate geometry, using a WKB approximation.

Chapter 13 and 14 are dedicated to the CFT interpretation of these newly-built solutions. We start with a brief review on the operator content of the D1-D5 CFT, we then propose an identification for the supergravity solutions as heavy states of the conformal theory. We then use holography to establish the dictionary between bulk and boundary. This task is complicated by the fact that most observables are not protected and subject to variations as one moves in the moduli space. For the solutions in the single-mode ansatz, we can use a non-trivial check to verify the validity of the dictionary.

Chapter 15 tackles the question of constructing non-BPS geometries through the lens of numerical simulations. We show that one can build numerical solutions to the equations of motion, through two different methods, and we can identify and compare those numerical solutions with the perturbative expansions. We will end this Part with some final comments in Chapter 16.

In Part III, we propose a new avenue to reproduce the full entropy of black holes with microstate geometries. In Chapter 17 we present the idea of the super-maze, an construct of branes that shows the origin of the black hole entropy in a purely geometric manner. We explain how to describe a bound states of M2 and M5 branes with momentum in M-theory, and how to extract its geometry from the supersymmetry projectors. The core idea is that these brane configurations locally preserve 16 supersymmetries, and therefore cannot form a horizon after backreaction. Finally, Chapter 18 introduces the concept of *themelia*, that we conjecture to be the fundamental building block of smooth black hole microstates. We describe a large family of these themelia, including the super-maze, using supersymmetry projectors. We explain how themelia naturally appears in several known supersymmetric microstates, such as the bubbling geometries and the superstrata.

Part I

The D1-D5 system

Chapter 2

A corner of string theory

String theory is one of the most prominent theories of gravity. While it is not fully defined and understood, many different "corners" (or limits) of the theory have been explored. While these corners were first mapped out independently, it has then been realized that can be related to each other through dualities. This is particularly useful: sometimes, a computation that is hard to do in a particular limit can be done in another limit, and using dualities the result can then be interpreted in the first.

The work presented in this thesis mainly takes place in one particular corner of the theory, or more precisely, in its low-energy limit, supergravity. The aim of this Chapter is to introduce this corner. After a brief general introduction to string theory, we describe a specific background of branes known as the D1-D5 system. We will then see how to reproduce the microstate counting of Strominger and Vafa.

2.1 A theory of strings and branes

String theory is a theory of strings, but also, as we will see, of other extended objects called branes. Usually, the first approach of students to string theory is through the worldsheet formalism. The string worldsheet, analogously to the worldline of particles, describes the behavior of a string in a fixed background. Because a string is a one-dimensional object, its worldsheet is two-dimensional. It is much richer than the analogy with the worldline formalism suggests, because the worldsheet can have many topologies, and can describe the interaction between several strings.

A fundamental ingredient of string theory is supersymmetry. Without it, the worldsheet theory only possesses bosonic degrees of freedom, and is furthermore unstable. The quantization of the theory also reveals that for consistency, the worldsheet must belong to a ten-dimensional spacetime.

Strings can be either open or closed. A closed string forms a loop, it is topologically a circle, and its worldsheet is represented by a surface with no boundaries. An open string on the other hand has free ends, and its worldsheet has two boundaries. One thus needs to impose boundary conditions, they can be either Dirichlet or Neumann, for each spatial direction. An open string with Dirichlet conditions, however, inevitably break

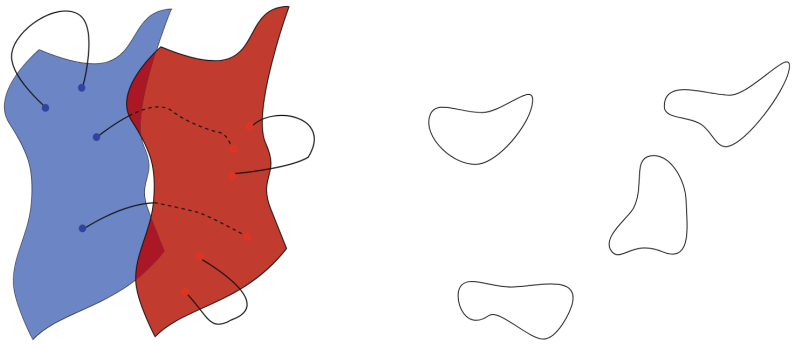

Figure 2.1: Strings can be open or closed, depending on boundary conditions. (a) shows open strings, they are one-dimensional objects whose endpoints are attached to D-branes. The two ends must not necessarily be attached to the same D-brane. (b) represents closed strings, they form loops and move freely in spacetime. The figure has been taken from [1].

Poincaré invariance. One can restore Poincaré invariance at the level of the theory if open strings are forced to end on some other dynamical objects. Then Poincaré invariance is only broken spontaneously. This is represented in Figure 2.1. These objects are called *D-branes*.

Note that D-branes can come in various dimensions, depending on how many of the string boundary conditions are Dirichlet versus Neumann. Branes with p spatial dimensions are named Dp-branes, where $0 \leq p \leq 9$. Not all dimensions can be present at once. In fact, we can distinguish two corners of string theory, called Type IIA and Type IIB, that differ by the way strings are quantized. In Type IIA, D-branes must have an odd number of spatial dimensions, while in Type IIB this number must be even. These two theories also include a different type of brane, called NS5 brane, that can be understood as the magnetic dual of the string. The content of each theory is summarized in the next Chapter in Table 3.1, where the coupling to the fields of supergravity is also explained. There also exist other corners of string theory (Type I, heterotic, etc.), that we will not detail here.

2.2 The D1-D5 system

D-branes are dynamical objects of string theory, but they are also solitons, and their dynamics cannot be captured by string perturbations. Indeed, their tension, and thus their mass, is proportional to the inverse string coupling:

$$T_p = \frac{1}{(2\pi)^p \alpha'^{(p+1)/2} g_s}, \tag{2.1}$$

where T_p is the tension of a Dp-brane. NS5 branes are even heavier, their tension scales like g_s^{-2}. We will always work in the limit $g_s \ll 1$, and thus consider string perturbations

in a fixed background of branes.

We focus on a very specific background in Type IIB string theory, called the D1-D5 system. The following description is valid in the limit of vanishing string coupling $g_s \to 0$, or in other words, in the top-left corner of the diagram in figure 1.2. Consider a spacetime with 5 compact dimensions, and 5 non-compact ones. One of the compact dimensions, that we name y, is taken to be much larger than the other four, and so we will single it out and write the spacetime as $\mathbb{R}^{1,4} \times S^1_y \times T^4$. In this spacetime we add a bound state made of many D1 and D5 branes: the D5 branes are wrapping both the four torus directions and the y-circle, while the D1 branes are only wrapping the y-circle, and are smeared along the torus. All branes are placed point-like in the non-compact spacetime. The configuration is summarized in Table 2.1.

	t	x_1	x_2	x_3	x_4	y	x_6	x_7	x_8	x_9
D1	—	•	•	•	•	—	⋯	⋯	⋯	⋯
D5	—	•	•	•	•	—	—	—	—	—

Table 2.1: Brane configuration of the D1-D5 system. The directions $x_1, \ldots, x_4$ denote the non-compact spacetime directions, while $x_6, \ldots, x_9$ are the torus directions, y is the special circle, and time is denoted by t. A dash — indicates that the branes are extended (wrapped) along the given direction, a point • indicates that the branes are point-like, and horizontal dots ⋯ indicate that the branes are smeared.

In general, each stack of identical D-branes preserves half of the 32 supersymmetries of string theory; the exact supersymmetry projectors for several types of branes are given in Appendix E. An arbitrary configuration of D-branes may not preserve any supersymmetry. In the current setup, however, the supersymmetric projector of the D1 and D5 branes are compatible, and the system preserves a quarter (8) of the supersymmetries.

One can furthermore excite this system by adding a momentum charge P along the y-circle. This corresponds to adding strings that are boosted along the compact direction, but do not wrap it. With this additional charge, the full system still preserves 4 supersymmetries.

Before moving on to the microscopic counting of string states in this configuration, note that the same system can be expressed in different duality frames. The use of different duality frames can let one make computations in a simple regime of parameters that would have been impossible in the original frame. A very commonly studied dual to our system is the NS5-F1-P system in Type IIA string theory – it is obtained from the D1-D5-P after taking an S duality, followed by a T duality along any of the torus directions. This frame has the advantage of enabling a simpler worldsheet description, since there are no longer any D-branes. In Part III we will also use the uplift in M-theory, which is made of M2, M5 branes and momentum P.

2.3 Microstate counting

We sketch here the results of [10, 46, 47] that provide a microscopic description of the entropy by counting the microstates of the D1-D5-P system. As in the original paper, we work in the regime of vanishing coupling $g_s \to 0$. It may seem restrictive, but because the system is supersymmetric, the entropy is protected, and so the computation must be valid in any regime of parameters.

In this regime, the D-branes are infinitely heavy, static objects, and gravity is decoupled. The momentum is carried (mainly) from free open strings stretching between the D-branes. We distinguish three types of open strings, the 1-1, 5-5 and 1-5 strings, whose endpoints are respectively on two D1-branes, on two D5-branes, or on one D1 and one D5 branes.

Our goal is to compute the number of open strings configurations stretching between N_1 D1 branes and N_5 D5 branes, with N_P units of momentum. We assume that the torus is much smaller than the y-direction, effectively reducing the problem to two-dimensions. We will see that the large entropy of the system arises thanks to the phenomenon of *momentum fractionation*.

As we said, the open strings are free, and because we look at supersymmetric configurations, we can restrict our attention to their zero-modes. Thus, the strings behave as point particles, whose wavefunctions can be identified with the momentum eigenstates of the y-circle.

Normally, such a wavefunction must be single-valued, $\Psi(y) = \Psi(y + 2\pi R)$, where R is the radius of the y-circle. It can then be decomposed as

$$\Psi(y) = \sum_n \alpha_n e^{\frac{2i\pi n}{R} y} . \tag{2.2}$$

After quantization, the constants α_n become creation and annihilation operators, that increase or decrease the momentum by n units. Thus, counting the number of states with momentum N_P corresponds to enumerating all the ways one can act with creation operators on the ground state, to reach momentum N_P.

The situation is different for open strings, however, as they also carry labels: the D-branes on which they end. For a 1-1 string stretching between D1 branes, the zero-modes can essentially be seen as particles belonging to the worldvolume of a D1 brane wrapping the circle N_1 times. This changes the periodicity of the wavefunction to $\Psi(y) = \Psi(y+2\pi N_1 R)$, and the momentum can now be distributed in units of $1/N_1$. This is what is called momentum fractionation. Similarly, for 5-5 strings, the momentum is fractionated in units of $1/N_5$.

The fractionation is even more important for 1-5 strings, because they inherit the periodicities of both the D1 and the D5 branes[1]: $\Psi(y) = \Psi(y+2\pi N_1 N_5 R)$. The momentum is fractionated in units of $1/(N_1 N_5)$.

[1]This is exact when N_1 and N_5 are coprime, which we suppose to be true. Otherwise, to find the dominant contribution to the entropy, one needs to consider a smaller number of branes n_1 and n_5 such

Because of this huge fractionation, the dominant contribution to the entropy of the system comes from 1-5 strings. Counting the number of microstates then comes down to enumerate the partitions of N_P in units of $1/(N_1 N_5)$, or equivalently counting the integer partitions of $N_1 N_5 N_P$. At leading order, we find that the entropy (which is the logarithm of the number of microstates) is

$$S_0 \;=\; 2\pi\sqrt{\frac{N_1 N_5 N_P}{6}}\,. \tag{2.3}$$

A more careful computation taking into account the possible polarizations of the string leads to

$$S \;=\; 2\pi\sqrt{N_1 N_5 N_P}\,, \tag{2.4}$$

which, as we will see in the next Chapter, matches with the Bekenstein-Hawking entropy computed in the supergravity regime.

that these numbers are coprime, and their product is maximal. When N_1 and N_5 are large, the results are asymptotically equivalent.

Chapter 3

The three-charge black hole in supergravity

In the previous chapter, we studied the regime where $g_s \to 0$, and N is large but finite. In this Chapter, we are interested in the opposite regime, where $\lambda = g_s N \gg 1$. The open strings are strongly coupled, and the perturbative description breaks down. This regime is however still classical if the string coupling is kept small[1], $g_s \ll 1$. As we will see, at low energies the theory can be described by supergravity.

Note that one can interpolate between the two regimes, $\lambda \to 0$ and $\lambda \gg 1$, by dialing the coupling constant g_s while keeping the number of branes fixed. This justifies why index theorems can apply, and we should be able to compute the same entropy in both theories.

3.1 The low-energy limit of string theory

The excitations of a string can be decomposed into its zero modes, and its oscillatory modes. As for a regular classical string, the oscillations have an energy cost, and their mass is a function of the tension of the string. Precisely, the mass of these modes is quantized in units of the inverse string length, l_s^{-1}. To have a good classical description, this mass scale has to be smaller than the Planck scale[2], but the gap between the Planck scale and the typical energies of the Standard Model is extremely large. Because stringy excitations have never been observed, the string scale must sit somewhere in between these two scales, and it generally assumed that it is close to the Planck scale.

When working with energies much smaller than l_s^{-1} (or equivalently at length scales much larger than the typical string size), the harmonics of the string can't be excited, they thus decouple and we are left with the zero modes. In this limit, strings look like point particles and are described by a number of quantum fields, corresponding to their

[1] Quantum effects come from loop diagrams that are suppressed by powers of g_s.

[2] Indeed, the ratio between these two mass scales is equal to the string coupling constant, g_s, that we assume to be very small.

Theories	**IIA**					**IIB**					
Potential	B_2	$C^{(1)}$	$C^{(3)}$	$C^{(5)}$	$C^{(7)}$	B_2	$C^{(0)}$	$C^{(2)}$	$C^{(4)}$	$C^{(6)}$	$C^{(8)}$
Electric	F1	D0	D2	D4	D6	F1	D(-1)	D1	D3	D5	D7
Magnetic	NS5	D6	D4	D2	D0	F1	D7	D5	D3	D1	D(-1)

Table 3.1: Coupling of branes to the gauge fields of Type IIA and Type IIB supergravity. The gauge fields can be be either sourced electrically or magnetically by the branes.

zero modes. Among these fields generated by the closed strings, there is a massless spin-2 field that mediates the gravitational interaction: the graviton.

The theories that are obtained through this procedure are supergravity theories: supersymmetric theories of gravity. From the different corners of string theory, one obtains different types of supergravities: Type IIA, Type IIB, eleven-dimensional supergravity, etc. They also all have branes as solitonic solutions of the equations of motion.

We focus on Type II supergravities. Type IIA has $\mathcal{N} = (1, 1)$ supersymmetries, while IIB has $\mathcal{N} = (2, 0)$ supersymmetries. The two theories share the same bosonic field content in the NS-NS sector:

- A spin-2 field g, giving rise to the metric;
- An antisymmetric two-form gauge field B_2;
- A scalar field field Φ, the dilaton.

The R-R sector of each theory is however different: Type IIA contains p-form gauge fields, $C^{(p)}$, where p is odd, while Type IIB contains similar gauge fields where p is even. As for standard electromagnetism, these gauge fields are sourced by objects of the theories. While for electromagnetism these sources are point particles (or magnetic monopoles), for the fields of supergravity the sources are branes. The couplings of branes to the gauge fields is summarized in Table 3.1.

The actions of both theories, that we will not detail here, decompose in three parts: the kinetic terms of the NS-NS fields, that are common for both theories, the kinetic terms of the R-R gauge fields, and a Chern-Simons interaction term. It contains a purely gravitational term of the form $\sqrt{-g}R$, similarly to the action of Einstein gravity.

3.2 A Dp-brane solution

Before delving into the D1-D5 system, it is instructive to construct the supergravity solution corresponding to a single stack of Dp-brane[3]. The branes source electrically the gauge field $C^{(p+1)}$, and magnetically the field $C^{(7-p)}$. We choose a set of Cartesian coordinates $(t, x_1, \ldots, x_{10})$ so that the branes are extended along the directions $x_1, \ldots, x_p$, and are located at $x_{p=1} = \cdots = x_{10} = 0$. The presence of the branes breaks the flat space

[3]The solutions have the same form whether we are in Type IIA (p even) or Type IIB (p odd) supergravity.

$SO(1,9)$ symmetry into $SO(1,p) \times SO(9-p)$. One must then construct an ansatz that respects these symmetries, and solve the equations of motion. The ansatz in the string frame is:

$$\begin{aligned} ds^2 &= Z_1^{1/2}\big(-dt^2 + dx_1^2 + \cdots + dx_p^2\big) + Z_2^{1/2}\big(dx_{p+1} + \cdots + dx_{10}^2\big)\,, \\ e^{2\Phi} &= Z_\Phi\,, \\ C^{(p+1)} &= Z_C\, dt \wedge dx_1 \wedge \cdots \wedge dx_p\,. \end{aligned} \tag{3.1}$$

where Z_1, Z_2, Z_Φ and Z_C are arbitrary functions, and all the fields but $C^{(7-p)}$ vanish, the latter can be obtained via dualities. Solving the equations of motion leads to

$$Z_1^{-1} = Z_2 = Z_\Phi^{2/(3-p)} = (1 - Z_C)^{-1} = H\,, \tag{3.2}$$

where H is harmonic in the transverse directions; and sourced by the branes at the origin:

$$H \;=\; 1 + \frac{Q_p}{r^{7-p}}\,, \tag{3.3}$$

and r is the radial coordinate on the transverse space. The charge Q_p is a constant, it can be related to the number of branes by integrating the Ramond gauge field:

$$Q_p \sim l_s^{7-p} g_s N_p\,, \tag{3.4}$$

with a constant of proportionality that can be written in terms of the volume of the transverse spheres. Note that as we approach the brane source, at $r \to 0$, the harmonic function diverges and the geometry is singular.

3.3 The D1-D5-P black hole

The D1-D5-P brane solution can also be constructed in supergravity, through the same procedure of building a suitable ansatz and solving the equations of motion. The resulting geometry is the commonly named three-charge black hole:

$$\begin{aligned} ds^2 &= \frac{2}{\sqrt{H_1 H_5}}\big[-dt^2 + dy^2 + (H_P - 1)(dy - dt)^2\big] + \sqrt{H_1 H_5}\, ds^2\big(\mathbb{R}^4\big) + \sqrt{\frac{H_1}{H_5}}\, ds^2\big(T^4\big)\,, \\ e^{2\Phi} &= \frac{H_1}{H_5}\,, \\ C_2 &= H_1^{-1} dt \wedge dy\,, \end{aligned} \tag{3.5}$$

where $ds^2(\mathbb{R}^4)$ and $ds^2(T^4)$ are the flat metrics on their respective spaces, and $H_{1,5,P}$ are harmonic functions on the $\mathbb{R}^4$, sourced by the branes at the origin:

$$H_{1,5,P} \;=\; 1 + \frac{Q_{1,5,P}}{r^2}\,. \tag{3.6}$$

The metric can also be understood as the uplift of a BMPV black hole with no angular momentum. A solution including angular momentum can be constructed in a similar way.

Once again, the supergravity charges can be expressed in terms of microscopic quantities: the number of branes and the units of momentum:

$$Q_1 \;=\; \frac{(2\pi)^4 g_s(\alpha')^3}{V_4} N_1\,, \qquad Q_5 \;=\; g_s\alpha' N_5\,, \qquad Q_P \;=\; \frac{(2\pi)^4 g_s^2(\alpha')^4}{V_4 R_y^2} N_P\,, \tag{3.7}$$

where V_4 is the volume of the four-torus and R_y is the radius of the y-circle.

Because of the 1's in the harmonic functions, the geometry is that of flat space at infinity. In the IR, the near-horizon geometry can be determined by "dropping the 1's". The resulting metric can be written as

$$ds^2 \;=\; \sqrt{Q_1Q_5}\left[\frac{d\hat{r}^2}{\hat{r}^2} - \hat{r}^2 dt^2 + \hat{r}^2 dy^2 + Q_P(dt-dy)^2\right] + \sqrt{Q_1Q_5}\, ds^2\big(S^3\big) + \sqrt{\frac{Q_1}{Q_5}}\, ds^2\big(T^4\big)\,, \tag{3.8}$$

where we can recognize an extremal BTZ black hole in AdS_3, trivially fibered with an S^3 and a T^4. The AdS radius is given by $l_{AdS} = \sqrt{Q_1Q_5}$. To summarize, the global geometry of the three-charge black hole is made of three parts: far away, the space is flat, asymptotic to $\mathbb{R}^{4,1} \times S^1$. As one gets closer to the black hole, the geometry changes and becomes locally $\mathrm{AdS}_3 \times S^3$. Decreasing the radius further, the AdS circle stabilizes, and a throat forms: the geometry is locally $\mathrm{AdS}_2 \times S^1 \times S^3$.

The horizon is given by the locus where $g^{rr} = 0$, it lies at $r = 0$ and its topology is $S^3 \times S^1_v \times T^4$ where $v = (t-y)/\sqrt{2}$ is a null direction. To compute its area, we need to integrate the Einstein metric, $g^E_{\mu\nu} \equiv e^{-\phi/2} g_{\mu\nu}$, on the horizon:

$$A_H \;\equiv\; \int_{S^3\times S^1_v\times T^4} \sqrt{g^E}|_{r=0} \;=\; e^{-2\phi|_{r=0}} \int_{S^3\times S^1_v\times T^4} \sqrt{g}|_{r=0}\,. \tag{3.9}$$

It is straightforward to integrate on each circle and the 3-sphere individually to obtain:

$$\begin{aligned} A_H \;&=\; \frac{Q_5}{Q_1}\cdot\big(2\pi^2(Q_1Q_5)^{3/4}\big)\cdot\left(2\pi R_y\sqrt{\frac{Q_P}{(Q_1Q_5)^{1/2}}}\right)\cdot\left(\frac{Q_1}{Q_5}V_4\right) \\ &=\; 4\pi^3 R_y V_4 \sqrt{Q_1Q_5Q_P}\,, \end{aligned} \tag{3.10}$$

then, using the Bekenstein-Hawking formula and the expression of the ten-dimensional gravitational constant $16\pi G = (2\pi)^7 g_s^2 \alpha'^4$, we obtain the entropy

$$S \;=\; \frac{A_H}{4G} \;=\; \frac{\pi^3 R_y V_4}{G}\sqrt{Q_1Q_5Q_P} \;=\; 2\pi\sqrt{N_1N_5N_P}\,. \tag{3.11}$$

This expression matches exactly with the one computed from the excitations of open strings (2.4). This is one of the great successes of string theory: the entropy of the supersymmetric black hole emerges as a microscopic counting of string states.

Chapter 4

D1-D5 CFT

4.1 The AdS/CFT correspondence

The AdS/CFT correspondence is the statement that a theory of quantum gravity in a $(D+1)$-dimensional AdS spacetime is *dual* to a conformal field theory (CFT) living *on the boundary* of the spacetime, which is D-dimensional. By duality, we mean that there is a one-to-one mapping between the states, operators and correlation functions of both theories. In effect, any calculation done in one theory has the same result in the other. The AdS/CFT correspondence is also a weak/strong duality, which means that the computations that are done in the perturbative regime of one side of the duality will be valid in the strongly-coupled regime on the other side.

The first realization of this concept was the idea of open-closed string duality: for example, the vacuum loop diagram of an open string stretching between two branes is exactly dual to the tree-level diagram of a closed string being emitted by one brane, and absorbed by the other. The low-energy limit of a theory of open strings at small coupling is a CFT, while the low-energy limit of a theory of closed strings at large effective coupling is supergravity.

Many manifestations of AdS/CFT emerged over the years. The most famous manifestation of the correspondence is the duality between string theory in $\mathrm{AdS}_5 \times S^5$, with the $\mathcal{N} = 4$ $SU(N)$ Super-Yang-Mills theory in four dimensions. This duality appears when one considers a stack of N coincident D3 branes in Type IIB string theory. For example, one can match the couplings of both theories:

$$2\pi g_s \leftrightarrow g^2_{\mathrm{YM}}\,, \qquad \left(\frac{R}{l_s}\right)^4 \leftrightarrow \lambda = g^2_{\mathrm{YM}} N\,, \tag{4.1}$$

where R is the AdS radius, g_{YM} is the Yang-Mills coupling and λ is the 't Hooft coupling. Note that the duality works in both ways: one can learn about quantum gravity by using CFT techniques, but one can also learn about the CFT in the non-perturbative regime by studying supergravity. This is especially relevant for the SYM theory, since it can act as a toy model for the strong interaction, and thus help explain phenomena such as confinement.

The duality can also be used to give a precise definition of quantum gravity. While string theory has only been defined perturbatively using worldsheet description, we know how to define a conformal field theory non-perturbatively. The AdS/CFT correspondence provides a clear non-perturbative formulation of quantum gravity in AdS backgrounds: one can simply *define* quantum gravity to be the bulk theory dual to the CFT.

4.2 A two-dimensional CFT

We now focus on the D1-D5 system described in Section 2.2. We already saw an example of the AdS/CFT duality in this system: we computed the entropy in two limits: $g_s N \ll 1$, where the system can be described by open strings stretching between the branes, and $g_s N \gg 1$, where the system is well approximated at low energies by supergravity in $\mathrm{AdS}_3 \times S^3$.

The aim of this Section is to introduce the CFT dual to the D1-D5 theory, Type IIB string theory in $\mathrm{AdS}_3 \times S^3 \times T^4$. This CFT lives on the boundary of $\mathrm{AdS}_3 \times S^3 \times T^4$, and so it must be a two-dimensional theory. It can be obtained by flowing to the IR fixed point of string theory in the D1-D5 background. Its simplest description is in terms of the gauge theory living on the branes, which results from the open-string zero modes. But there is another description, with a larger regime of validity, where the D1's are realized as instantons within the worldvolume theory of the D-branes. While we are not going to delve into the details of this derivation, we present the main results that are relevant for the work presented in this thesis. For a full review see for example [48].

The two-dimensional D1-D5 CFT is a $\mathcal{N} = (4,4)$ sigma model with target space $\mathcal{W}_{\mathrm{inst}}$, the moduli space of instantonic excitations living on the D5 branevolume. The central charge of the theory is $c = \bar{c} = 6N_1N_5$. The target space of the CFT depends on the string moduli, and it has be shown that on one point of the moduli space, the target space takes a simple form:

$$\mathrm{Sym}_{N_1N_5}(T^4) \;\equiv\; \left(T^4\right)^{N_1N_5}/\mathcal{S}_{N_1N_5}\,, \tag{4.2}$$

where $\mathcal{S}_n$ is the symmetric group of degree n. The theory with this symmetric product as moduli space is called the *orbifold theory*. It has been argued that, away from the orbifold point, the space of instantons should still be a smooth deformation of the symmetric product. Another remarkable point of the moduli space corresponds to the supergravity limit, it is far away from the orbifold point, in the strong coupling regime.

The CFT derives its symmetries from the symmetries of the supergravity background: an $SL(2,\mathbb{R})_L \times SL(2,\mathbb{R})_R$ from the isometries of AdS_3, an $SO(4)_E \approx SU(2)_L \times SU(2)_R$ from the isometries of S^3 and an $SO(4)_I \approx SU(2)_1 \times SU(2)_2$ from the rotations of the four-torus. In the CFT, the first group, $SL(2,\mathbb{R})_L \times SL(2,\mathbb{R})_R$, manifests itself as the group of symmetries generated by the sub-algebra of Virasoro operators $L_n, \bar{L}_n$, with $n = -1, 0, 1$. The second group, $SO(4)_E$ is identified with the R-symmetry of the superconformal algebra, while the third, $SO(4)_I$, is an internal global symmetry. The CFT also has two sectors, Neveu-Schwarz and Ramond, depending on the periodicities of

the fermions.

4.3 The orbifold model

Here we give a brief description of the orbifold model and outline the parts that will be relevant for the work of this thesis. For a more thorough introduction to this model, see [48]. We first describe the theory in the NS sector, then explain how to obtain the R sector from a spectral flow.

As we mentioned, the orbifold model is an $\mathcal{N} = (4,4)$ sigma model with target space $\mathrm{Sym}_{N_1N_5}(T^4)$. It thus consists of $N = N_1N_5$ copies of a base CFT, that are then symmetrized. The CFT is two-dimensional, the base space is $S^1_y \times R_t$, but it can be mapped to the complex plane, parametrized by $(z, \bar{z})$, through the exponential map. The theory has global symmetries $SO(4)_E \times SO(4)_I \approx SU(2)_L \times SU(2)_R \times SU(2)_1 \times SU(2)_2$, and the fields transform in representations of these symmetries. By convention, indices correspond to the following representations:

$$\begin{aligned} &\alpha, \beta \leftrightarrow \text{ doublet of } SU(2)_L\,, \qquad \dot{\alpha}, \dot{\beta} \leftrightarrow \text{ doublet of } SU(2)_R\,, \\ &A, B \leftrightarrow \text{ doublet of } SU(2)_1\,, \qquad \dot{A}, \dot{B} \leftrightarrow \text{ doublet of } SU(2)_2\,, \\ &\qquad\qquad i, j \leftrightarrow \text{ vector of } SO(4)_I\,. \end{aligned} \tag{4.3}$$

The field content of each copy consists consists of a vector of bosons, $X^i(z, \bar{z})$, and two fermionic spinors, $\psi^{\alpha\dot{A}}(z)$ and $\psi^{\dot{\alpha}\dot{A}}(\bar{z})$. From these fields one can build holomorphic currents, that form a closed OPE algebra: in the left-moving sector they are the $SU(2)_L$ current $J^a(z)$, the supersymmetry currents $G^{\alpha A}(z)$, and the stress-energy tensor $T(z)$. The currents can then be expanded in modes:

$$\mathcal{O}(z) \;=\; \sum_m \mathcal{O}_m z^{-(\Delta+m)} \tag{4.4}$$

where $\mathcal{O}$ is any operator and Δ is its weight. From the modes of the current algebra, we find an extension of the superconformal Virasoro algebra:

$$\begin{aligned} [J^a_m, J^b_n] &= \frac{c}{12} m \delta^{ab} \delta_{m+n,0} + i\epsilon^{ab}{}_c J^c_{m+n}\,, \\ [J^a_m, G^{\alpha A}_n] &= \frac{1}{2}(\sigma^{\star a})^\alpha{}_\beta G^{\beta A}_{m+n}\,, \\ \{G^{\alpha A}_m, G^{\beta B}_n\} &= -\frac{c}{6}\left(m^2 - \frac{1}{4}\right)\epsilon^{AB}\epsilon^{\alpha\beta}\delta_{m+n,0} + (m-n)\epsilon^{AB}\epsilon^{\beta\gamma}(\sigma^{\star a})^\alpha{}_\gamma J^a_{m+n} - \epsilon^{AB}\epsilon^{\alpha\beta}L_{m+n}\,, \\ [L_m, J^a_n] &= -nJ^a_{m+n}\,, \\ [L_m, G^{\alpha A}_n] &= \left(\frac{m}{2} - n\right)G^{\alpha A}_{m+n}\,, \\ [L_m, L_n] &= c\,\frac{m(m^2-1)}{12}\,\delta_{m+n,0} + (m-n)L_{m+n}\,, \end{aligned} \tag{4.5}$$

$\bar{h}=\bar{j}=\bar{m}$ \ $h=j=m$	0	1/2	1
0	(1) $\left\|\varnothing\right\rangle_{NS}$	(2) $\psi^{+\dot{A}}_{-1/2}\left\|\varnothing\right\rangle_{NS}$	(1) $J^{+}_{-1}\left\|\varnothing\right\rangle_{NS}$
1/2	(2) $\psi^{-\dot{A}}_{-1/2}\left\|\varnothing\right\rangle_{NS}$	(4) $\psi^{+\dot{A}}_{-1/2}\psi^{-\dot{B}}_{-1/2}\left\|\varnothing\right\rangle_{NS}$	(2) $J^{+}_{-1}\psi^{-\dot{A}}_{-1/2}\left\|\varnothing\right\rangle_{NS}$
1	(1) $J^{-}_{-1}\left\|\varnothing\right\rangle_{NS}$	(2) $\psi^{+\dot{A}}_{-1/2}J^{-}_{-1}\left\|\varnothing\right\rangle_{NS}$	(1) $J^{+}_{-1}J^{-}_{-1}\left\|\varnothing\right\rangle_{NS}$

Table 4.1: The 16 chiral primary operators in the singly twisted sector, classified by their dimensions. The indices $\dot{A}$ and $\dot{B}$ run from 1 to 2.

where σ^a are the Pauli matrices. There is an equivalent algebra in the right-moving sector. These generators exist in each copy of the CFT, but because the full theory is symmetrized over all the copies, only the diagonal sum survives as a symmetry. The algebra has a finite sub-algebra, spanned by $\left\{J^a_0, G^{\alpha A}_{\pm 1/2}, L_0, L_{\pm 1}\right\}$, they are the generators that annihilate the NS vacuum, and they correspond in AdS to the conformal transformations leaving the vacuum (global AdS_3) invariant. This sub-algebra plays an important role in the duality, it is usually named the "small algebra".

4.3.1 Representation theory

Because the algebra (4.5) represents the symmetries of the theory, all the states of the theory lie in different representations of this algebra. We will explain how to construct these representations. The Cartan sub-algebra, spanned by $\{L_0, J^3_0\}$ and $\{\bar{L}_0, \bar{J}^3_0\}$, is used to label the states. The eigenvalues of L_0 and $\bar{L}_0$ are the *conformal weights* of the states, often denoted by h and $\bar{h}$. The eigenvalues of J^3_0 and $\bar{J}^3_0$ are the spins, m and $\bar{m}$, of the state. Because these two operators are generators of $SU(2)$ groups, we can also use the usual $SU(2)$ representation theory and label states by their Casimir, j and $\bar{\jmath}$, and we have $-j \leq m \leq j$ and $-\bar{\jmath} \leq \bar{m} \leq \bar{\jmath}$. One can also check that physical states have necessarily $h \geq j$.

To construct a representation, one starts with a *chiral primary operator* (CPO) $|\phi\rangle$, this is a state that is annihilated by all the positive modes of the algebra, plus the fermionic generator $G^{+A}_{-1/2}$ (and the right moving equivalent). Such a state verifies $h = j = m$ and $\bar{h} = \bar{\jmath} = \bar{m}$. One then forms the *descendants* of $|\phi\rangle$ by acting on it with the negative modes[1].

The simplest CPO is the NS vacuum $\left|\varnothing\right\rangle_{NS}$, it is dual in the bulk to empty global AdS. From this, one can build a family of 16 CPOs, by acting either once or twice with each of the fermionic modes $\psi^{\pm\dot{A}}_{-1/2}$. Acting more than twice with the same mode annihilates the state. We summarize them in Table 4.1.

One can also find other chiral primaries in the *twist sectors* of the theory. Because we quotient out the N copies of the CFT by the symmetric group, the theory contain twist

[1]Note that the descendants formed by acting with $G^{-A}_{-1/2}$ are still primaries from the point of view of the Virasoro algebra, but they are not chiral.

operators, σ_{l+1}, whose action is to mix the boundary conditions on $l+1$ copies of the CFT. In effect, if we add an index (i) to the fields denoting their copy, the twist operator makes it so that, every time one circles the operator insertion, the fields get mapped to each other according to[2]

$$X^i_{(1)} \to X^i_{(2)} \to \cdots \to X^i_{(l+1)} \to X^i_{(1)} \,. \tag{4.6}$$

In each twist sector l, there is a specific chiral primary with dimensions

$$h = \bar{h} = \frac{l}{2} \,. \tag{4.7}$$

where $\hat{c} = 6$ is the central charge of a single copy of the CFT. Once again, acting with each of the fermionic modes $\psi^{\pm\dot{A}}_{-1/2}$, we construct 16 chiral primaries, in each twist sector l.

4.3.2 Spectral flow and R sector

So far we have discussed the states of the CFT in the NS sector, with periodic boundary conditions for the fermions in the complex plane. There is only one ground state, dual to empty global AdS. However, the states that are of interest for black hole physics are in the R sector, they are the states whose dual can be connected to flat space. Fortunately, a spectral flow can map the NS sector to the R sector.

A generic spectral flow depends on a parameter $\alpha \in \mathbb{R}$, it maps the charges of the states as[3]:

$$h' \;=\; h + \alpha j + \frac{\hat{c}\alpha^2}{24} \,, \qquad m' \;=\; m + \frac{\hat{c}\alpha}{12} \,. \tag{4.8}$$

Setting $\alpha = -1$ exchanges the NS and R sectors of the theory. The NS vacuum is mapped to a state with charges $h = \bar{h} = 1/4, m = \bar{m} = 1/2$. This is an R ground state, called $|\varnothing\rangle^{++}_R$. All Ramond ground states have dimensions 1/4.

Note that, following (4.8), all chiral primaries in the NS sector (with $h = j$) are mapped to Ramond ground states. In particular, the R sector has 16 vacua in the singly-twisted sector, in one-to-one mapping with the chiral primaries of the NS sector:

$$|\varnothing\rangle^{\alpha\dot{\alpha}}_R \;, \quad |\varnothing\rangle^{\dot{A}\dot{\alpha}}_R \;, \quad |\varnothing\rangle^{\alpha\dot{A}}_R \;, \quad |\varnothing\rangle^{\dot{A}\dot{B}}_R \;. \tag{4.9}$$

Of particular note are five ground states that are appearing in the construction of supertubes and superstrata, for which we give special names:

$$|\pm\pm\rangle \;=\; |\varnothing\rangle^{\pm\pm}_R \,, \qquad |00\rangle \;=\; \frac{1}{2}\epsilon_{\dot{A}\dot{B}}\,|\varnothing\rangle^{\dot{A}\dot{B}}_R \,. \tag{4.10}$$

We will denote the equivalent ground states in the twist sector k by $|\pm\pm\rangle_k$ and $|00\rangle_k$.

[2]The relation here is schematic, in practice one also has to symmetrize the action of the operator over all the copies.

[3]In the left sector, the right sector is similar, with a second parameter $\bar{\alpha}$.

Chapter 5

Supersymmetric microstates in six dimensions

In this Chapter we construct families of microstates of the three-charge black hole. This supersymmetric black hole has a large entropy that has been computed in 3.3, and we saw in Chapter 2 that this entropy could be reproduced by counting the microstates of the open strings at zero coupling. It is then natural to wonder what happens to these microstates at large coupling. As we will see, some of the microstates can be constructed within supergravity, as smooth and horizonless solutions of the BPS equations.

We focus on solutions with invariances in all the torus directions. The theory can be reduced on the T^4, and we get a six-dimensional theory of supergravity. We describe this theory in the next Section. We then present a family of microstates of the black hole with no momentum charge, called supertubes. In the last Section, we sketch how to add a momentum charge to supertubes, this leads to a family of solutions named superstrata.

5.1 Six-dimensional supergravity

The microstates we are building are solutions of $\mathcal{N} = (1, 0)$ supergravity in six-dimensions, coupled to n_T tensor multiplets. This theory can be obtained from the reduction of Type IIB theory on a four-torus or a $K3$, followed by a truncation that cuts all but one supersymmetry. Its field content comprises:

- A graviton multiplet, containing a gravitational field g, two left-handed spin-3/2 gravitini, and one self-dual tensor $B^+_{\mu\nu}$.
- n_T tensor multiplets, each containing one anti-self-dual tensor gauge field $B^-_{i\mu\nu}$, two right-handed spinors and one scalar.

The scalars can be regrouped in a coset:

$$\frac{SO(1, n_T)}{SO(n_T)} \,. \tag{5.1}$$

We can parametrize this coset by a vector v_I and a matrix x_I^A, $I = 0, \dots, n_T$, $A = 1, \dots, n_T$, subject to

$$\begin{aligned} \mathcal{S} \;&=\; \begin{pmatrix} v_I \\ x_I^A \end{pmatrix} \in \frac{SO(1,n_T)}{SO(n_T)} \\ v_I v^I \;&=\; 1\,, \qquad v_I v_J - x_I^A x_J^A \;=\; \eta_{IJ}\,, \qquad v^I x_I^A \;=\; 0\,, \end{aligned} \tag{5.2}$$

where the indices are raised and lowered by the following metric

$$\eta \;=\; \begin{pmatrix} 0 & 1 & 0 & \cdots & 0 \\ 1 & 0 & 0 & \cdots & 0 \\ 0 & 0 & -1 & \cdots & 0 \\ \vdots & \vdots & \vdots & \ddots & \vdots \\ 0 & 0 & 0 & \cdots & -1 \end{pmatrix}. \tag{5.3}$$

The field strength of the gauge potentials can be regrouped in a vector subject to a self-duality relation:

$$\mathcal{M}_{IJ} G^J \;=\; \eta_{IJ} \star_6 G^J \quad \text{where} \quad \mathcal{M} \;=\; \eta \mathcal{S}^T \mathcal{S} \eta\,. \tag{5.4}$$

5.1.1 BPS equations

The gravitini and tensorini variations lead to the following BPS equations:

$$\nabla_\mu \epsilon^i + \frac{1}{4} v_I G^I_{\mu\nu\rho} \Gamma^{\nu\rho} \epsilon^i \;=\; 0\,, \tag{5.5}$$

$$x_I^A \partial_\mu v^I \Gamma^\mu \epsilon^i + \frac{1}{6} x_I^A G^I_{\mu\nu\rho} \Gamma^{\mu\nu\rho} \epsilon^i \;=\; 0\,. \tag{5.6}$$

The BPS solutions have been classified in [49], and the system has been shown to have a linear structure: it can be rewritten as a "triangular system" of linear equations [50, 51].

The Killing vector $\mathcal{K}^\mu = \epsilon^i \Gamma^\mu \epsilon^i$ is shown to be null, and can be used to define a null coordinate u. The most general ansatz for the metric is

$$ds_6^2 \;=\; -\frac{2}{\sqrt{\mathcal{P}}}(dv + \beta)\left(du + \omega + \frac{1}{2}\mathcal{F}(dv+\beta)\right) + \sqrt{\mathcal{P}} ds_4^2\,, \tag{5.7}$$

where ds_4^2 is the metric on a four-dimensional hyper-Kähler base space, $\mathcal{P}$ and $\mathcal{F}$ are scalars, and ω and β are one-forms with legs on the base space. These quantites can *a priori* depend on all directions but u. The BPS equations can be rewritten in several layers of BPS equations. We are going to assume in the following that the base metric is flat, $ds_4^2 = \delta_{mn} dx^m dx^n$. For a general metric, the final system of equations is more complicated, but conserves a linear structure, except for the zeroth layer.

To express the equations in a linear structure, we introduce new notations. First, we define potentials as:

$$Z_I \;\equiv\; -\sqrt{2} \eta_{IJ} v^J \sqrt{\mathcal{P}}\,. \tag{5.8}$$

For historical reasons and compatibility with the five-dimensional BPS equations, we now relabel the index I so that it jumps index 3: $I = 1, 2, 4, \ldots, n_T + 2$. Note that the scalar constraint, $v_I v^I = 1$, leads to

$$\mathcal{P} \;=\; \frac{1}{2}\eta^{IJ} Z_I Z_J \;=\; Z_1 Z_2 - Z_4^2 - \cdots - Z_{n_T+2}^2. \tag{5.9}$$

Furthermore, the field strengths G^I can be encoded in a vector of magnetic two-forms Θ^I. We also define the following derivatives

$$\mathcal{D}\Phi \;\equiv\; d_4\Phi - \dot{\beta}\wedge\Phi\,, \qquad \dot{\Phi} \;\equiv\; \partial_v\Phi\,, \tag{5.10}$$

and d_4 is the exterior derivative on the four-dimensional base space.

The "zeroth layer" of BPS equations states that the base is hyper-Kähler, and that the two-form $\mathcal{D}\beta$ is self-dual: $\star_4\mathcal{D}\beta = \mathcal{D}\beta$. These equations are in general non-linear, however we chose the base space to be flat, and we can furthermore assume β to be v-independent, to make this layer linear[1].

The "first layer" of equations are linear equations on the potentials Z_I and the two-forms Θ^I, sourced by β:

$$\begin{aligned} \star_4\Theta^I \;&=\; \Theta^I\,, \\ \eta^{IJ}\mathcal{D}\star_4\Big(\mathcal{D}Z_J + Z_J\dot{\beta}\Big) \;&=\; -\,\Theta^I\wedge\mathcal{D}\beta\,, \\ \mathcal{D}\Theta^I - \dot{\beta}\wedge\Theta^I \;&=\; \eta^{IJ}\star_4\,\partial_v\Big(\mathcal{D}Z_J + Z_J\dot{\beta}\Big)\,. \end{aligned} \tag{5.11}$$

The last two equations constitute the "second layer", they are linear equations on ω and $\mathcal{F}$, sourced by all the other functions:

$$\begin{aligned} \mathcal{D}\omega + \star_4\mathcal{D}\omega + \mathcal{F}\mathcal{D}\beta &= \eta_I^J Z_J\Theta^I\,, \\ \star_4\mathcal{D}\star_4\Big(2\dot{\omega} + \mathcal{F}\dot{\beta} - \mathcal{D}\mathcal{F}\Big) \;&=\; -\,2\Big(2\dot{\omega} + \mathcal{F}\dot{\beta} - \mathcal{D}\mathcal{F}\Big)^m\partial_v\beta_m - \eta_{IJ}\star_4\big(\Theta^I\wedge\Theta^J\big) \\ &\quad + \eta^{IJ}\Big[\partial_v^2(Z_IZ_J) - \dot{Z}_I\dot{Z}_J\Big]\,. \end{aligned} \tag{5.12}$$

5.1.2 Uplifting to IIB supergravity

We now fix the number of tensor multiplets, $n_T = 2$, and we restrict to the case of a flat base space and of a v-independent one-form β. In Type IIB supergravity, the ansatz takes

[1]We present the rest of the BPS equations without assuming the v-independence, but the solutions that we study next will all verify it.

the form:

$$\begin{aligned}
ds_{10}^2 &= \sqrt{\frac{Z_1 Z_2}{\mathcal{P}}} ds_6^2 + \sqrt{\frac{Z_1}{Z_2}} ds^2(T^4)\,,\\
e^{2\Phi} &= \frac{Z_1^2}{\mathcal{P}}\,,\\
B_2 &= -\frac{Z_4}{\mathcal{P}}(du+\omega)(dv+\beta) + a_4 \wedge (dv+\beta) + \delta_4\,,\\
C^{(0)} &= \frac{Z_4}{Z_1}\,,\\
C^{(2)} &= -\frac{Z_2}{\mathcal{P}}(du+\omega)\wedge(dv+\beta) + a_1 \wedge (dv+\beta) + \delta_1\,,\\
C^{(4)} &= -\frac{Z_4}{Z_2}\mathrm{vol}(T^4) - \frac{Z_4}{\mathcal{P}}\delta_1 \wedge (du+\omega)\wedge(dv+\beta) + a_1 \wedge (dv+\beta) + x_3 \wedge (dv+\beta)\,,\\
C^{(6)} &= \mathrm{vol}(T^4) \wedge \left[-\frac{Z_1}{\mathcal{P}}(du+\omega)\wedge(dv+\beta) + a_2 \wedge (dv+\beta) + \delta_2\right],
\end{aligned} \tag{5.13}$$

where $\mathrm{vol}(T^4)$ is the volume form of the four-torus, and we have introduced forms on the base space: $a_{1,2,4}$ are one-forms, $\delta_{1,2,4}$ are two-forms and x_3 is a three-form. The forms a_I and δ_I are fixed such that the magnetic two-forms are expressed as

$$\Theta^I = \mathcal{D} a_I + \dot{\delta}_I\,, \tag{5.14}$$

and the three-form x_3 is fixed by the self-duality condition of $C^{(4)}$.

As a first example of solution, it is instructive to determine how the supersymmetric three-charge black hole described in Section 3.3 is embedded in this ansatz. Identifying (3.5) with (5.7) and (5.13) leads to

$$\begin{aligned}
Z_{1,5} &= H_{1,5} = 1 + \frac{Q_{1,5}}{r^2}\,, \qquad Z_4 = 0\,, \qquad \omega = \beta = 0\\
\mathcal{F} &= -2(H_P - 1) = -\frac{2Q_P}{r^2}\,, \qquad \Theta^I = 0\,.
\end{aligned} \tag{5.15}$$

Adding (left) angular momentum is also simple, by replacing

$$\omega = \frac{\sqrt{2} J_L}{r^2}\left(\sin^2\theta\, d\phi_1 + \cos^2\theta\, d\phi_2\right), \tag{5.16}$$

where the flat base space is expressed in spherical coordinates $(r, \theta, \phi_1, \phi_2)$.

5.2 The two-charge supertube

The two-charge geometries are best understood in a different duality frame, the F1-P system, which can be obtained from the D1-D5 by a chain of S and T dualities [52, 53]. In this frame, a stack of N_5 strings (or equivalently a long string with winding N_5) are

wrapping the y-circle, and there is N_1 units of left-moving momentum along the same circle. Each specific geometry is encoded by a curve $g_A(v')$ describing the profile of the string in spacetime, where the coordinate v' is the null direction $\sim t+y$, with enhanced periodicity: $v' \equiv v' + 2\pi\hat{R}$ with[2] $\hat{R} = Q_5/R_y$. The entropy is then recovered from all the possible ways the string can move.

To follow the dualities back to the D1-D5 frame, we are going to assume that the four-torus is rigid, which implies $g_i(v') = 0$ in all but one torus direction, that we name 5, so the string only moves in the four non-compact spacetime directions and in direction 5. The full solution can be expressed in the fields of the BPS ansatz in the following way:

$$\begin{aligned}
Z_1 &= 1 + \frac{Q_5}{2\pi\hat{R}}\int_0^{2\pi\hat{R}} \frac{|\dot{g}_m(v')|^2 + |\dot{g}_5(v')|^2}{|x_m - g_m(v')|^2} dv' \,, \quad Z_2 = 1 + \frac{Q_5}{2\pi\hat{R}}\int_0^{2\pi\hat{R}} \frac{1}{|x_m - g_m(v')|^2} dv' \,, \\
Z_4 &= -\frac{Q_5}{2\pi\hat{R}}\int_0^{2\pi\hat{R}} \frac{\dot{g}_m(v')}{|x_m - g_m(v')|^2} dv' \,, \quad d_4\gamma_2 = \star_4\, d_4 Z_2 \,, \quad d_4\delta_2 = \star_4\, d_4 Z_4 \,, \\
A &= -\frac{Q_5}{2\pi\hat{R}}\int_0^{2\pi\hat{R}} \frac{\dot{g}_n(v')dx^n}{|x_m - g_m(v')|^2} dv' \,, \quad d_4 B = -\star_4 d_4 A \,, \\
\beta &= \frac{-A+B}{\sqrt{2}} \,, \qquad \omega = \frac{-A-B}{\sqrt{2}} \,, \qquad \mathcal{F} = 0 \,, \qquad \Theta^I = 0 \,.
\end{aligned} \tag{5.17}$$

Note that the non-zero values of β and ω correspond to a deformation of the D1-D5 black hole with a KKm dipolar charge and angular momentum. This is a crucial ingredient to "puffing up" the branes and resolving the singularity. In Part III we explain what makes this resolution possible: the brane system along with the dipolar charges preserve locally 16 supersymmetries.

5.2.1 The round supertube

The round supertube is the simplest example of two-charge solutions. We consider a circular string profile in a plane (x_1, x_2) of the flat base space:

$$g_1(v') = a\cos\left(\frac{v'}{\hat{R}}\right) \,, \qquad g_2(v') = a\sin\left(\frac{v'}{\hat{R}}\right) \,, \tag{5.18}$$

where a is the radius of the supertube. This solution has a very simple expression in spherical bipolar coordinates. Define coordinates $(r, \theta, \phi_1, \phi_2)$ such that:

$$x_1 + ix_2 = \sqrt{r^2+a^2}\sin\theta e^{i\phi_1} \,, \qquad x_3 + ix_4 = r\cos\theta e^{i\phi_2} \,. \tag{5.19}$$

In these coordinates, the locus $r = 0$ describes a disk of radius a. The origin of space is at the center of this disk, $\theta = 0$, while the supertube is located on the edge, $\theta = \pi/2$. The flat metric is expressed as

$$ds_4^2 = \Sigma\left(\frac{dr^2}{r^2+a^2} + d\theta^2\right) + \left(r^2+a^2\right)\sin^2\theta d\phi_1^2 + r^2\cos^2\theta d\phi_2^2 \,, \tag{5.20}$$

[2] $\hat{R}$ is indeed proportional to $1/R_y$, this is because the chain of dualities between the F1-P frame and the D1-D5 frame involves a T-duality along y, inverting the radius.

where

$$\Sigma \;\equiv\; r^2 + a^2\cos^2\theta\,. \tag{5.21}$$

The fields of the ansatz are then given by:

$$\begin{aligned} Z_1 \;&=\; 1+\frac{Q_1}{\Sigma}\,, \qquad Z_2 \;=\; 1+\frac{Q_5}{\Sigma}\,, \qquad Z_4 \;=\; \mathcal{F} \;=\; 0\,, \qquad \Theta^I \;=\; 0\,, \\ \omega \;&=\; \omega_0 \;=\; \frac{R_y a^2}{\sqrt{2}\Sigma}\big(\sin^2\theta\, d\phi_1 + \cos^2\theta\, d\phi_2\big)\,, \quad \beta \;=\; \frac{R_y a^2}{\sqrt{2}\Sigma}\big(\sin^2\theta\, d\phi_1 - \cos^2\theta\, d\phi_2\big)\,. \end{aligned} \tag{5.22}$$

Note that $1/\Sigma$ is indeed a harmonic function, with a source that is smeared on the supertube locus. Imposing the regularity of the metric at the supertube locus leads to a relation between the radius of the y-circle, the charges and the radius of the supertube:

$$Q_1 Q_5 \;=\; R_y^2 a^2\,. \tag{5.23}$$

In the decoupling limit, when one drops the 1's in the harmonic functions, the metric is that of global $\mathrm{AdS}_3\times S^3$, with AdS radius $(l_{\mathrm{AdS}})^2 = \sqrt{Q_1Q_5}$. This solution is horizonless and smooth everywhere.:

$$\begin{aligned} ds_6^2 \;=\; \sqrt{Q_1Q_5}\Bigg[&-\frac{r^2+a^2}{a^2R_y}dt^2 + \frac{dr^2}{r^2+a^2} + \frac{r^2}{a^2R_y}dy^2 \\ &+ d\theta^2 + \sin^2\theta\big(d\phi_1 - R_y^{-1}dt\big)^2 + \cos^2\theta\big(d\phi_2 - R_y^{-1}dy\big)^2\Bigg]\,. \end{aligned} \tag{5.24}$$

One can also generalize the solution to a round supertube wrapping the circle k times:

$$g_1(v') \;=\; \frac{a}{k}\cos\left(\frac{kv'}{\hat{R}}\right)\,, \qquad g_2(v') \;=\; \frac{a}{k}\sin\left(\frac{kv'}{\hat{R}}\right)\,, \tag{5.25}$$

The decoupling limit of these solutions is an orbifolded global $\mathrm{AdS}_3\times S^3/\mathbb{Z}_k$ space.

5.2.2 The CFT description

In the decoupling limit, all the supertube solutions presented here possess $\mathrm{AdS}_3\times S^3$ asymptotics, with a rigid torus, and according to the AdS/CFT correspondence, they must be dual to states in the D1-D5 CFT. Since they do not have a momentum charge, they must be dual to R-R ground states. These ground states were described in Section 4.3.2, there are five such ground states in the seed T^4 theory of the orbifold: $|\pm,\pm\rangle$ and $|00\rangle$. The precise dictionary between these ground states and the harmonics of the string profile has been established in [18, 53, 54]:

$$\begin{aligned} g_1 + ig_2 \;&=\; \frac{a}{k}e^{\pm ikv'/\hat{R}} \qquad &\longleftrightarrow \qquad &\prod_{N_{\pm,\pm}} |\pm,\pm\rangle_k \\ g_3 + ig_4 \;&=\; \frac{a}{k}e^{\pm ikv'/\hat{R}} \qquad &\longleftrightarrow \qquad &\prod_{N_{\pm,\mp}} |\pm,\mp\rangle_k \\ g_5 \;&=\; \frac{b}{k}\sin\Big(k\,v'/\hat{R}\Big) \qquad &\longleftrightarrow \qquad &\prod_{N_k} |00\rangle_k \end{aligned} \tag{5.26}$$

where a and b are the amplitudes of the harmonics, k is the mode number, and $N_{\pm,\pm}, N_{\pm,\mp} \sim a^2$ and $N_k \sim b^2$ are respectively the number of strands of type $|\pm,\pm\rangle_k, |\pm,\mp\rangle_k$ and $|00\rangle_k$ in the complete state of the orbifold theory.

As an example, the dual of the round supertube (5.25) is

$$\prod_{N/k} |{+}{+}\rangle_k \ , \tag{5.27}$$

where $N = N_1 N_5$.

This dictionary has been tested extensively: on both sides of the correspondence, three-point and four-point correlators have been computed and shown to match.

5.3 Superstrata

Superstrata are are solutions of six-dimensional supergravity with three global charges, D1, D5, and P, preserving four supersymmetries [18–22]. They are constructed in an asymptotically AdS_3 space, their coupling to flat space will not be discussed here. Starting from a supertube seen as a "seed solution", one can construct superstrata by adding left-moving momentum waves to the solution. We will present the superstrata construction where the seed is a round supertube[3] This requires adding modes to the supertube shape, that have the phase dependence:

$$v_{k,m,n} \ = \ (m+n)\frac{\sqrt{2}v}{R_y} + (k-m)\phi_1 - m\phi_2 \, , \tag{5.28}$$

where (k, m, n) are non-negative integers, and $m \leq k$. To fully obtain the superstrata solution, one need to solve the three layers of BPS equations. The zeroth layer of BPS equations is trivially solved, as the four-dimensional base is kept flat, and the self-dual β is left unchanged:

$$\beta \ = \ \frac{R_y a^2}{\sqrt{2}\Sigma}\left(\sin^2\theta \, d\phi_1 - \cos^2\theta \, d\phi_2\right) . \tag{5.29}$$

5.3.1 First layer

To solve the first layer of equations (5.11), we make the following ansatz:

$$\begin{aligned} Z_1 \ &= \ \frac{Q_1}{\Sigma} + \sum_i b_1^{k_i,m_i,n_i} \tilde{z}_{k_i,m_i,n_i} \, , \qquad & Z_2 \ &= \ \frac{Q_5}{\Sigma} + \sum_i b_2^{k_i,m_i,n_i} \tilde{z}_{k_i,m_i,n_i} \, , \\ Z_4 \ &= \ -\sum_i b_4^{k_i,m_i,n_i} \tilde{z}_{k_i,m_i,n_i} \, , \qquad & \Theta^I \ &= \ \sum_i \eta^{IJ} b_J^{k_i,m_i,n_i} \tilde{\vartheta}_{k_i,m_i,n_i} \, , \end{aligned} \tag{5.30}$$

[3]The superstrata construction on generic supertube backgrounds is still an open problem. In Part II we construct a new family of superstrata, whose supertube base is ellipsoidal, but our method allows only for a very restricted set of modes, namely $(1, 0, n)$.

where the $b_I^{k,m,n}$ are Fourier coefficients, and $\tilde{z}_{k,m,n}$ and $\tilde{\vartheta}_{k,m,n}$ are functions with quantum numbers (k,m,n). The first layer of BPS equations then becomes:

$$\star_4\mathcal{D}\dot{\tilde{z}}_{k,m,n} \;=\; \mathcal{D}\tilde{\vartheta}_{k,m,n}\,, \quad \mathcal{D}\star_4\mathcal{D}\tilde{z}_{k,m,n} \;=\; -\,\tilde{\vartheta}_{k,m,n}\wedge d\beta\,, \quad \tilde{\vartheta}_{k,m,n} \;=\; \star_4\,\tilde{\vartheta}_{k,m,n}\,. \tag{5.31}$$

It is possible to solve these equations using a so-called momentum generating technique [18], that we will only sketch here. Besides providing us with explicit solutions to the BPS equations, these methods are very powerful because they let us readily construct the holographic dictionary of the geometries we are constructing.

First note that linearizing the generic supertube solution (5.17) around the round supertube leads to solutions with mode numbers $(k,k,0)$. Starting from these solutions, one can generate left-moving excitations by acting with some of the generators of the small algebra of the CFT (specifically L_{-1} and J_0^+ in the NS sector), whose action on the bulk geometry is known and corresponds to global coordinate transformations of $\mathrm{AdS}_3\times S^3$. This way, one obtains the original superstrata modes:

$$\begin{aligned}
\tilde{z}_{k,m,n} \;&=\; R_y\frac{\Delta_{k,m,n}}{\Sigma}\cos v_{k,m,n}\,,\\
\tilde{\vartheta}_{k,m,n} \;&=\; -\sqrt{2}\Delta_{k,m,n}\Bigg[\bigg((m+n)r\sin\theta+n\Big(\frac{m}{k}-1\Big)\frac{\Sigma}{r\sin\theta}\bigg)\Omega^{(1)}\sin v_{k,m,n}\\
&\qquad\qquad +\Big(m\Big(\frac{n}{k}+1\Big)\Omega^{(2)}+n\Big(\frac{m}{k}-1\Big)\Omega^{(3)}\Big)\cos v_{k,m,n}\Bigg]\,,
\end{aligned} \tag{5.32}$$

where we have defined a set of mode functions

$$\Delta_{k,m,n} \;=\; \left(\frac{a}{\sqrt{r^2+a^2}}\right)^k\left(\frac{r}{\sqrt{r^2+a^2}}\right)^n\sin^{k-m}\theta\cos^m\theta\,, \tag{5.33}$$

and where $\Omega^{(I)}$ are a basis of self-dual two-forms.

5.3.2 Second layer

Solving the second layer of BPS equations, (5.12), is much more involved. The sources of these equations are quadratic in Z_I and Θ^I and therefore mix the Fourier modes of the first-layer solutions. The question of whether the solutions constructed that way are smooth geometries is also non-trivial, and the task of finding the generic solutions for multi-mode superstrata is still in progress. For the purposes of this manuscript, we are going to put our focus on a subfamily of solutions for which these equations are simpler to solve: the multi-mode solutions with $k=1$. This means that only the Fourier modes $(1,0,n)$ and $(1,1,n)$ can be activated.

With this hypothesis, the first layer of solution can be rewritten in terms of holomorphic functions [26, 27]. Define the following complex coordinates:

$$\chi \;=\; \frac{a}{\sqrt{r^2+a^2}}\sin\theta e^{i\phi_1}\,, \quad \mu \;=\; \cot\theta e^{i\left(\sqrt{2}v/R_y-\phi_1-\phi_2\right)}\,, \quad \xi \;=\; \frac{r}{\sqrt{r^2+a^2}}e^{i\sqrt{2}v/R_y}\,. \tag{5.34}$$

We then introduce two holomorphic functions of ξ, $F_0(\xi)$ and $F_1(\xi)$, and define

$$F(\chi,\mu,\xi) \;=\; \chi[F_0(\xi)+\mu F_1(\xi)].$$

The holomorphic functions can be expanded at the origin

$$F_0(\xi) \;=\; \sum_n b_n\xi^n\,, \qquad F_1(\xi) \;=\; \sum_n d_n\xi^n\,, \tag{5.35}$$

and the coefficients b_n and d_n are respectively going to be the amplitudes of the Fourier modes $(1,0,n)$ and $(1,1,n)$. We also need to define auxiliary functions

$$A \;=\; \chi\mu(1+\xi\partial_\xi)F_1\,, \quad \text{and} \quad B \;=\; \chi\xi\partial_\xi F_0\,, \tag{5.36}$$

and self-dual forms

$$\Omega_y \;=\; \frac{1}{\sqrt{2}}\big(\Omega^{(2)}+ir\sin\theta\Omega^{(1)}\big)\,, \qquad \Omega_z \;=\; \frac{1}{\sqrt{2}}\left(\Omega^{(3)}+i\left(r\sin\theta-\frac{\Sigma}{r\sin\theta}\right)\Omega^{(1)}\right). \tag{5.37}$$

With these definitions, the fields of the first layer can be written as

$$\begin{aligned} Z_1 \;&=\; \frac{Q_1}{\Sigma}+\frac{R_y^2}{4Q_5\Sigma}\big(F^2+\bar F^2\big)\,, \quad Z_2 \;=\; \frac{Q_5}{\Sigma}\,, \quad Z_4 \;=\; \frac{R_y}{2\Sigma}\big(F+\bar F\big)\,,\\ \Theta^1 \;&=\; 0\,, \quad \Theta^2 \;=\; \frac{R_y}{Q_5}F(A\Omega_y+B\Omega_z)+\text{c.c.}\,, \quad \Theta^4 \;=\; -2(A\Omega_y+B\Omega_z)+\text{c.c.}\,. \end{aligned} \tag{5.38}$$

Note that, compared to (5.30), we did not merely restrict to the Fourier modes with $k=1$. We also suppressed the modes in Z_2, and fixed the relative amplitudes of the Fourier modes $b_1^{k,m,n}$ and $b_4^{k,m,n}$: the amplitudes appearing in Z_1 are the square of those in Z_4. This is because the quadratic sources of the equations of the second layer contain both non-oscillating "RMS" components and oscillating components, and the presence of RMS values generically lead to singularities in the final solution. These singularities can be eliminated by fixing the amplitudes as we did; this process is known as "coiffuring".

Having done these simplifications, the equations of the second layer can be solved, and the fields are given by

$$\begin{aligned} \mathcal{F} \;&=\; \frac{1}{a^2}\big(|F_0|^2+|\xi|^2|F_1|^2-c^2\big)\\ \omega \;&=\; \omega_0-\frac{R_y}{2\sqrt{2}a^2(1-|\chi|^2)}\Big[\big(\bar\chi\bar F_0F+\chi F_0\bar F-c^2|\chi|^2\big)d\phi_1\\ &\qquad +\big(\bar\chi\bar\mu\bar F_1F+\chi\mu F_1\bar F\big)d\phi_2\Big]-\frac{iR_y|\chi|^2}{\sqrt{2}a^2\sin(2\theta)}\big(\mu\bar F_0F_1-\bar\mu F_0\bar F_1\big)d\theta \end{aligned} \tag{5.39}$$

where c is a constant of integration, that is going to be fixed to ensure the regularity and the asymptotics of the solution. Note that we recover the round supertube solution by fixing all the amplitudes and the integration constant to zero, $F_0=F_1=c=0$.

5.3.3 Regularity and asymptotics

The coiffuring procedure that we applied on the first layer of fields already removed most of the singular behaviors of the solutions. One still need to ensure that the solutions are regular, and have the correct asymptotics.

The first condition the metric (5.7) must meet is to have the correct $\mathrm{AdS}_3 \times S^3$ asymptotics. This implies that both $\mathcal{F}$ and ω must decay at infinity, at least as quickly as r^{-2}. This can be achieved by fixing the integration constant c as:

$$c^2 \;=\; \sum_n \left(b_n^2 + d_n^2\right), \tag{5.40}$$

and by applying a large coordinate transformation, $u \to u + f(v)$, where f is suitably chosen[4] so as to have

$$\begin{aligned} \mathcal{F} \;&=\; -\frac{1}{r^2}\left(\sum_n d_n^2 + \sum_n n(b_n^2+d_n^2) + \text{oscillations}\right) + \dots\,, \\ \omega \;&=\; \omega_0 + \frac{R_y}{\sqrt{2}r^2}\left(\sum_n d_n^2\right)\left(\sin^2 d\phi_1 + \cos^2 d\phi_2 + \text{oscillations}\right) + \dots\,. \end{aligned} \tag{5.41}$$

The then need to impose the smoothness of the metric at the special locus. As for the supertube, it leads to a condition relating the charges with the radius of the y-circle, the radius of the supertube, and also the amplitude of the momentum wave:

$$Q_1 Q_5 \;=\; R_y^2\left(a^2 + \frac{c^2}{2}\right). \tag{5.42}$$

Once this is fixed, one can prove that the metric is smooth everywhere and has no closed time-like curves. A schematic depiction of the superstrata geometry is given in Figure 5.1.

5.3.4 Conserved charges

The superstrata solutions have five conserved charges. There is of course the three global charges of the D1-D5-P black hole, Q_1, Q_5, Q_P. But the solutions also have dipolar charges corresponding to the smeared KKm along the supertube locus. The charges are left and right angular momenta J_L, J_R.

From a given solution, the conserved charges can be read from the fall off of the fields at infinity. The D1 and D5 brane charges, Q_1, Q_5, are given by the r^{-2} term in the large r expansion of respectively Z_1, Z_2. The momentum charge is given by the RMS value of the expansion of $\mathcal{F}$:

$$\mathcal{F} \;=\; -\frac{1}{r^2}(2Q_P + \text{oscillations}) + \dots\,, \tag{5.43}$$

[4]It was necessary to fix the constant c first, to ensure that f is a periodic function of v.

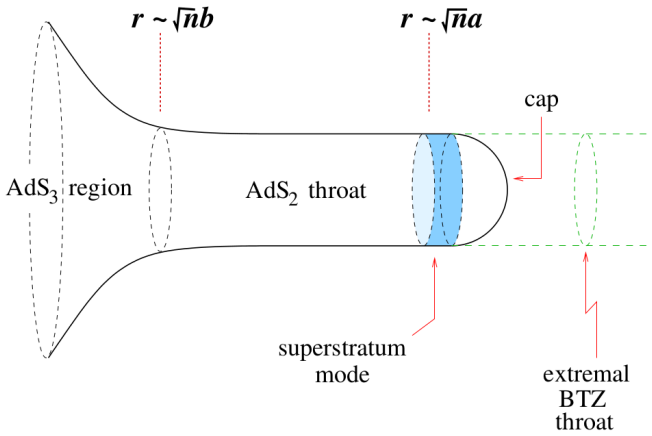

Figure 5.1: A depiction of the superstrata geometry. The geometry is like that of extremal BTZ, but contrary to the black hole solution, the geometry caps off at a finite redshift parametrized by a, the radius of the supertube. The scale that is named b in the figure is such that $Q_P \sim nb^2$. The figure was taken from [21].

and the angular momenta are obtained from the asymptotic expansion of ω and β:

$$\beta_{\phi_1} + \beta_{\phi_2} + \omega_{\phi_1} + \omega_{\phi_2} \;=\; \frac{\sqrt{2}}{r^2}[(J_R - J_L \cos 2\theta) + \text{oscillations}] + \dots \,. \tag{5.44}$$

For the $(1, m, n)$ superstrata solutions, these charges are given by

$$J_L \;=\; \frac{a^2 R_y}{2}\,, \quad J_R \;=\; \frac{R_y}{2}\left(a^2 + \sum_n d_n^2\right), \quad Q_P \;=\; \frac{1}{2}\left[\sum_n d_n^2 + \sum_n n(b_n^2 + d_n^2)\right]. \tag{5.45}$$

5.3.5 The CFT description

Once again, the superstrata constructed here must have a dual description as states within the D1-D5 CFT. The momentum-generating technique provides an invaluable guide to determine these states. Indeed, the original superstrata construction took the reverse path: the CFT state was first constructed and used as a guide for determining the bulk solution. To find the solutions to the first layer of BPS equations, the momentum-generating technique consists in using the $(k, k, 0)$ solution, corresponding to a supertube with $g_5 \neq 0$ linearized around the round supertube, and apply large gauge transformations to obtain the generic (k, m, n) solutions. These large gauge transformations correspond, in the CFT, to the application of specific operators of the small algebra. In the NS-NS sector, one has:

$$\begin{aligned}
L_0 \;&=\; \frac{iR_y}{2}(\partial_t + \partial_y)\,, \\
L_{\pm 1} \;&=\; ie^{\pm\frac{i}{R_y}(t+y)}\left[-\frac{R_y}{2}\left(\frac{r}{\sqrt{r^2+a^2}}\partial_t + \frac{\sqrt{r^2+a^2}}{r}\partial_y\right) \pm \frac{i}{2}\sqrt{r^2+a^2}\,\partial_r\right], \\
J_0^3 \;&=\; -\frac{i}{2}\left(\partial_{\tilde{\phi}_1} + \partial_{\tilde{\phi}_2}\right), \qquad J_0^{\pm} \;=\; \frac{i}{2}e^{\pm i(\tilde{\phi}_1 + \tilde{\phi}_2)}\left(\mp i\partial_\theta + \cot\theta\,\partial_{\tilde{\phi}_1} - \tan\theta\,\partial_{\tilde{\phi}_2}\right),
\end{aligned} \tag{5.46}$$

where the coordinates $\tilde{\phi}_1$ and $\tilde{\phi}_2$ are the result of the spectral flow that transforms the supertube metric to the global $\mathrm{AdS}_3 \times S^3$ metric (5.24):

$$\tilde{\phi}_1 \;=\; \phi_1 - \frac{t}{R_y}\,, \qquad \tilde{\phi}_2 \;=\; \phi_2 - \frac{y}{R_y}\,. \tag{5.47}$$

The superstrata construction uses the operators J_0^+ and L_1. To obtain the description in the R-R sector, one reverses the spectral flow, these two operators are then mapped respectively to J_{-1}^+ and $L_{-1} - J_{-1}^3$.

The momentum perturbations associated to the Fourier mode (k, m, n) are obtained by applying m times the operator J_{-1}^+, and n times $L_{-1} - J_{-1}^3$, on each supertube strand $|00\rangle_k$. The complete state dual to a multi-mode (k, m, n) superstrata is

$$\left(|{+}{+}\rangle_1\right)^{N_{++}} \prod_{k_i, m_i, n_i} \left[\frac{(J_{-1}^+)^{m_i}}{m_i!} \frac{\left(L_{-1} - J_{-1}^3\right)^{n_i}}{n_i!} |00\rangle_{k_i} \right]^{N_{k_i, m_i, n_i}}, \tag{5.48}$$

where the integers N_{++} and $N_{k,m,n}$ are functions of the amplitudes of each mode.

Part II

New microstate geometries of the D1-D5 system

Chapter 6

Introduction to Part II

The work that is presented in this Part is based on [37–42].

Superstrata have provided some of the most remarkable and broad families of microstate geometries. They approximate the exterior regions of black-holes to high precision, and yet cap off smoothly, at arbitrarily high red-shift, yielding smooth, BPS horizonless geometries. What makes superstrata all the more remarkable is that they have a precisely-known holographic dictionary in which the magnetic fluxes that support the superstrata can be directly related to coherent excitations in the dual conformal field theory. Indeed, this holographic dictionary has undergone highly non-trivial tests using precision holography in which the structure of the supergravity background has been checked against correlation functions in the CFT.

From the perspective of the black-hole information problem and for holography, it is very important to move beyond supersymmetry and construct non-extremal microstate geometries and map out the CFT states that they capture. *A priori,* this seems an impossible challenge. Superstrata are constructed in six-dimensional supergravity, and even the simplest of BPS superstrata depend on four variables, and the most general depend on five variables. It is, therefore, to be expected that non-trivial, non-extremal superstrata will be time-dependent and so will depend on, at least, five variables. At the technical level, one has to solve the full non-linear equations of the supergravity, and at the conceptual level, these states will no longer be "protected" by supersymmetry, and will be inherently more complicated and potentially unstable. Indeed, one ultimately expects to see them decay into some analog of Hawking radiation.

However, a new family of consistent truncations [27] has shown how to reduce a non-trivial "superstratum" sector of six-dimensional $(1,0)$ supergravity, to a family of gauged supergravities in three-dimensions. We use this as a new approach to the challenge of finding non-extremal superstrata.

There are many examples in which gauged supergravity in low dimensions represent consistent truncations of higher dimensional supergravity theories. A consistent truncation is much more than having a low-dimensional effective field theory: A consistent truncation means that solving the dynamics in the lower dimension provides an *exact* solution to the higher dimensional theory. This means that any dependence of a solution on the compactification manifold is handled through the machinery of the consistent

truncation and does not need to be solved directly. A consistent truncation can therefore dramatically simplify the BPS equations and, even more importantly, the equations of motion.

The significance of this consistent truncation is that it shows how particular families of BPS superstrata, depending on four variables in six dimensions, reduce to a three-dimensional solution that depends on only two variables. Moreover, we find that the three-dimensional theory can encode the collisions of BPS and anti-BPS superstratum waves, and thus can capture a whole range of non-extremal, non-BPS microstate geometries. Such non-extremal solutions can be described in terms of functions of, at most, three variables. To simplify further the problem we seek time-independent solutions with AdS_3 boundary conditions: this effectively puts the system in a box, and time-independence means that the open string collisions will be in equilibrium with the radiation they produce. We build ansätze inspired from the Q-ball solutions, that is often used for the construction of bose star solutions, to reduce the problem to only one dimension. Using these tools, we are able to build perturbatively non-BPS superstrata, or *microstrata*. Microstrata are the non-supersymmetric geometries created by combining left-moving superstrata excitations with right-moving "anti-superstrata" excitations. The truncation and ansätze also brings the problem within striking distance of numerical methods, and we use those to confirm the results of the pertubration theory, and probe the solutions in the very deep regime. As an added bonus, we also know the precise holographic dictionary for such solutions and can therefore study, and thoroughly test, such microstrata in the dual CFT.

Apart from the motivation of microstrata, we also analyse the BPS solutions in this particular three-dimensional gauged supergravity theory. Some supersymmetric solutions of this theory have already been found, they are the $(1, m, n)$ superstrata. As we will see, one can build other BPS solutions in this theory, using new momentum carriers. When uplifted in six-dimensions, these solutions correspond to superstrata with a non-flat base ; while standard superstrata are constructed on top of a round supertube, we find that these new solutions add elliptical deformations to the supertube.

Chapter 7

A three-dimensional gauge theory

The simplest way to construct of microstata is to work with a particular three-dimensional theory of gauged supergravity. This Chapter mostly reviews the work of [37], and aims to give a full and complete description of this theory, as well as an introduction to its supersymmetries. It serves as a basis for the next Chapters to build upon, and as an introduction to the various notations and conventions that are used throughout this manuscript.

We provide a translation between the supergravity theory in which the supersymmetries were analyzed [55,56] and the more recent discussions that involve the purely bosonic actions [27,57,58] for which the uplift formulae have been derived. All of these references use different conventions and, in testing the supersymmetry, a significant effort goes into making the translation between the various formulations. We therefore try to spell out many of the explicit details.

Initially, we will work with the $\mathcal{N}=8$ (16 supersymmetries) theory that was analyzed in [56]. The theory we ultimately seek to analyze is the $\mathcal{N}=4$ (8 supersymmetries) theory that underlies the D1-D5 system and that was used in [27,57,58].

7.1 A summary of notation and conventions

7.1.1 Group theory

We work with the group $G = SO(8,n)$, and its subgroup $H = SO(8) \times SO(n)$. Following [56], we use calligraphic indices as adjoint labels of $G = SO(8,n)$. We use barred, capital Latin indices, $\bar{I}, \bar{J}, \ldots$ to denote the vector of $SO(8,n)$, unbarred capital Latin indices, $I, J, \ldots$, to denote the vector of $SO(8)$, and small Latin indices, $r, s, \ldots$ to denote the vector of $SO(n)$. In the standard way, the adjoint indices of $G = SO(8,n)$, $SO(8)$ and $SO(n)$ can be written as skew pairs $\bar{I}\bar{J}$, IJ and rs. Such a labeling double counts the adjoint but when we use this notation we will always sum over all indices without any implicit factors of $\frac{1}{2}$. Later in the discussion we will restrict to $G = SO(4,n)$, and its subgroup $H = SO(4) \times SO(n)$, and this will result in the obvious restrictions on the index ranges.

We define the $G = SO(8,n)$ invariant matrix in its canonical form:

$$\eta^{\bar{I}\bar{J}} \;=\; \eta_{\bar{I}\bar{J}} \;\equiv\; \mathrm{diag}\big(1,1,\ldots,1,-1,-1,\cdots -1\big)\,, \qquad \eta^{IJ} \;=\; \eta_{IJ} \;=\; \delta^{IJ}\,, \qquad \eta^{rs} \;=\; \eta_{rs} \;=\; -\delta^{rs} \tag{7.1}$$

Later, when we restrict to $G = SO(4,n)$, we will introduce $\hat{\eta}^{\bar{I}\bar{J}} = \hat{\eta}_{\bar{I}\bar{J}}$, which will be adapted to the $GL(4,\mathbb{R})$ basis (see (7.37)).

The matrices, $t^{\mathcal{M}}$, will denote generators of the adjoint of G. In the obvious manner, it will be convenient to define

$$\Big\{t^{\mathcal{M}}\Big\} \;\equiv\; \Big\{X^{\bar{I}\bar{J}} = -X^{\bar{J}\bar{I}}\Big\} \;\equiv\; \Big\{X^{IJ} = -X^{JI}, X^{rs} = -X^{sr}, Y^{Ir} = -Y^{rI}\Big\} \tag{7.2}$$

The structure constants are defined, as usual, via $\big[\,t^{\mathcal{M}}\,,\,t^{\mathcal{N}}\,\big] = f^{\mathcal{M}\mathcal{N}}{}_{\mathcal{P}}\,t^{\mathcal{P}}$, which we write as

$$\begin{aligned}\Big[\,X^{\bar{I}\bar{J}}\,,\,X^{\bar{K}\bar{L}}\,\Big] \;&=\; f^{\bar{I}\bar{J}\,\bar{K}\bar{L}}{}_{\bar{M}\bar{N}}\,X^{\bar{M}\bar{N}} \\ &=\; -\,\eta^{\bar{I}\bar{K}}X^{\bar{J}\bar{L}} \;+\; \eta^{\bar{I}\bar{L}}X^{\bar{J}\bar{K}} \;+\; \eta^{\bar{J}\bar{K}}X^{\bar{I}\bar{L}} \;-\; \eta^{\bar{J}\bar{L}}X^{\bar{I}\bar{K}}\,.\end{aligned} \tag{7.3}$$

which leads to:

$$\begin{aligned}f^{\bar{I}\bar{J}\,\bar{K}\bar{L}}{}_{\bar{M}\bar{N}} \;=\; &-\frac{1}{2}\,\eta^{\bar{I}\bar{K}}\left(\delta^{\bar{J}}_{\bar{M}}\,\delta^{\bar{L}}_{\bar{N}} - \delta^{\bar{J}}_{\bar{N}}\,\delta^{\bar{L}}_{\bar{M}}\right) \;+\; \frac{1}{2}\,\eta^{\bar{I}\bar{L}}\left(\delta^{\bar{J}}_{\bar{M}}\,\delta^{\bar{K}}_{\bar{N}} - \delta^{\bar{J}}_{\bar{N}}\,\delta^{\bar{K}}_{\bar{M}}\right) \\ &+\; \frac{1}{2}\,\eta^{\bar{J}\bar{K}}\left(\delta^{\bar{I}}_{\bar{M}}\,\delta^{\bar{L}}_{\bar{N}} - \delta^{\bar{I}}_{\bar{N}}\,\delta^{\bar{L}}_{\bar{M}}\right) \;-\; \frac{1}{2}\,\eta^{\bar{J}\bar{L}}\left(\delta^{\bar{I}}_{\bar{M}}\,\delta^{\bar{K}}_{\bar{N}} - \delta^{\bar{I}}_{\bar{N}}\,\delta^{\bar{K}}_{\bar{M}}\right).\end{aligned} \tag{7.4}$$

Note that the factors of $\frac{1}{2}$ appear because we are summing over all values of $\bar{M}\bar{N}$ and so this leads to a double counting of the generators.

In terms of explicit matrix representations, (7.3) and (7.4) correspond to using the matrix generators:

$$\big(\,X^{\bar{I}\bar{J}}\,\big)_{\bar{K}}{}^{\bar{L}} \;=\; \delta^{\bar{I}}_{\bar{K}}\,\eta^{\bar{J}\bar{L}} \;-\; \delta^{\bar{J}}_{\bar{K}}\,\eta^{\bar{I}\bar{L}}\,. \tag{7.5}$$

One should note that these choices are the same as the conventions used in equation (A.3) of [59][1], and equation (2.4) in [58][2] but have the opposite signs to those of [27], equations (2.13) and (2.14). The conventions we use here appear to be the use used in [56], and match those of equation (3.9) of [60][3]. While the gauge matrices and structure constants that we use here have the opposite sign to those of [27], we will eventually arrive at the same formulation as [27] through the choice of the sign of a gauge coupling, or the ultimate sign of the embedding tensor. As we will see, the signs of these generators are crucial to showing that the supersymmetric solutions in [27] are indeed consistent with the supersymmetry variations of [56]. This provides many non-trivial tests of all the details we are cataloging here[4].

[1] However, in this reference, equation (A.3) is inconsistent with (A.1)!

[2] However, as noted in [27], there are inconsistencies in the gauge action of [58], and these suggest an inconsistent usage of the structure constants or gauge matrices. The gauge action in [27] is correct and consistent.

[3] This requires a small correction explained below.

[4] These results therefore provide detailed confirmation (and the occasional correction or clarification) of the conventions and results in the literature over the last 20 years.

While it is not directly relevant to our discussion here, to match our conventions to those of the commutators in equation (3.9) of [60] one must reverse the signs of the generators, X^{rs}. This sign reversal is natural because the metric (7.1) is negative definite on $SO(n)$ and this passes into (7.3) and (7.5): Reversing the signs of the X^{rs} give them commutators for a positive definite metric on $SO(n)$. Our computations are not sensitive to this sign and we will stay with the conventions above.

7.1.2 $SO(8)$ spinors

The $\mathcal{N}=8$ theory has an $SO(8)$ $\mathcal{R}$-symmetry, and the fermions transform in the spinor representations. Thus we will need 16×16, $SO(8)$ Γ-matrices that satisfy:

$$\left\{\,\Gamma^I\,,\,\Gamma^J\,\right\} \;=\; 2\,\delta^{IJ}\,\mathbb{1}_{16\times 16}\,. \tag{7.6}$$

We use capital Latin indices $I,J,K,\ldots$ to denote vector indices, capital Latin indices $A,B,C,\ldots$ to denote spinors in the 8^+ Weyl representation and dotted capital Latin indices $\dot{A},\dot{B},\dot{C},\ldots$ to denote spinors in the 8^- Weyl representation. We use a representation of the Γ-matrices where they are real and symmetric and in which the non-trivial, 8×8 blocks are the off-diagonal pieces: $\Gamma^J_{A\dot{A}}$ and $\Gamma^J_{\dot{A}A}$. The helicity projector is:

$$(\Gamma^{12345678})_{AB} \;=\; \delta_{AB}\,, \qquad (\Gamma^{12345678})_{\dot{A}\dot{B}} \;=\; -\,\delta_{\dot{A}\dot{B}}\,. \tag{7.7}$$

7.1.3 Space-time metric and spinors

Much of the literature on three-dimensional gauged supergravity uses the conventions set up in [61], and we will follow suit. This means that the metric has signature $(+--)$. The 2×2 space-time gamma matrices are:

$$\gamma^0 \;=\; \sigma_2 \;=\; \begin{pmatrix} 0 & -i \\ i & 0 \end{pmatrix}\,, \qquad \gamma^1 \;=\; i\,\sigma_3 \;=\; \begin{pmatrix} i & 0 \\ 0 & -i \end{pmatrix}\,, \qquad \gamma^3 \;=\; i\,\sigma_1 \;=\; \begin{pmatrix} 0 & i \\ i & 0 \end{pmatrix}\,. \tag{7.8}$$

and we have $\gamma^{012} = -i\mathbb{1}_{2\times 2}$.

The orientation is set by taking (in frames)[5]:

$$\epsilon^{012} \;=\; \epsilon_{012} \;=\; +1\,. \tag{7.9}$$

We will use ϵ^{abc} and ϵ_{abc} to denote the permutation signature that takes values $0,\pm 1$. The covariant ε-symbol will be denoted

$$\varepsilon_{\mu\nu\rho} \;=\; e\,\epsilon_{\mu\nu\rho}\,, \qquad \varepsilon^{\mu\nu\rho} \;=\; e^{-1}\,\epsilon^{\mu\nu\rho}\,, \tag{7.10}$$

where $e=\sqrt{|g|}$ is the frame determinant.

[5]Note that because the metric has signature $(+--)$, the sign of the ϵ tensor does not depend on whether the indices are up or down.

7.1.4 The three-dimensional metric

The most general, three-dimensional metric will depend on three arbitrary functions: six metric components minus three functions from coordinate transformations. One way to realize this is to fix two of the coordinate transformations to arrive at a conformally-flat spatial base. The time direction can also have its own scale factor, and there can also be two-component, angular-momentum vector, k. One can use the coordinate re-definition of t to gauge k so that it only has one spatial component. We therefore claim that, at least locally, the most general three-dimensional metric can be re-cast in the form:

$$\begin{aligned} ds_3^2 &= \hat{\Omega}_1^2 \, (dt + k_v \, dv)^2 \; - \; \hat{\Omega}_0^2 \, \frac{|d\zeta|^2}{(1-|\zeta|^2)^2} \\ &= \hat{\Omega}_1^2 \, (dt + k_v \, dv)^2 \; - \; \hat{\Omega}_0^2 \left(\frac{dr^2}{r^2+a^2} \; + \; \frac{2}{R_y^2 \, a^4} \, r^2 \, (r^2+a^2) \, dv^2 \right) , \end{aligned} \tag{7.11}$$

where

$$\zeta \; \equiv \; \xi \, e^{i \frac{\sqrt{2} v}{R_y}} , \quad \text{and} \quad \xi \; = \; \frac{r}{\sqrt{r^2+a^2}} \, . \tag{7.12}$$

The three arbitrary functions are $\hat{\Omega}_0$, $\hat{\Omega}_1$ and k_v. We are using here the coordinates (t, r, v) because they are well adapted to the discussion of asymptotically AdS_3 space, and superstrata. Indeed, the metric on global AdS_3 of radius R, can be written as:

$$ds_3^2 \; = \; R^2 \left(R_y^{-2} \left(dt + R_y \, \mathscr{A} \right)^2 \; - \; \frac{|d\zeta|^2}{\left(1-|\zeta|^2\right)^2} \right) , \tag{7.13}$$

where

$$\mathscr{A} \; \equiv \; \frac{i}{2} \left(\frac{\zeta \, d\bar{\zeta} - \bar{\zeta} \, d\zeta}{1-|\zeta|^2} \right) . \tag{7.14}$$

As usual on AdS_3, we interchange between (t, y) coordinates, and null coordinates (u, v) via:

$$u \; \equiv \; \frac{1}{\sqrt{2}} \, (t-y) \, , \qquad v \; \equiv \; \frac{1}{\sqrt{2}} \, (t+y) \, , \tag{7.15}$$

The parameter R_y, is the radius of the y-circle:

$$y \; \cong \; y \, + \, 2\pi R_y \, . \tag{7.16}$$

It is also convenient to write to write the metric using the compactified coordinate ξ, and use the scale-free coordinates

$$\tau \; = \; \frac{t}{R_y} \, , \qquad \psi \; = \; \frac{\sqrt{2} v}{R_y} \, , \tag{7.17}$$

where ψ inherits the periodicity $\psi \equiv \psi + 2\pi$. In these coordinates, we write

$$ds_3^2 \; = \; R_{\rm AdS}^2 \left[\Omega_1^2 \left(d\tau + \frac{k}{(1-\xi^2)} \, d\psi \right)^2 \; - \; \frac{\Omega_0^2}{(1-\xi^2)^2} \left(d\xi^2 \; + \; \xi^2 \, d\psi^2 \right) \right] , \tag{7.18}$$

for three arbitrary scale-free functions Ω_0, Ω_1 and k of the three coordinates, (τ, ξ, ψ). This is the parametrization we will mostly use throughout the rest of this manuscript.

We will return to these metrics later, but here we will fix our frame orientations. We will take frames with

$$e^0 \sim (dt + k_v\, dv)\,, \qquad e^1 \sim dr\,, \qquad e^2 \sim dv\,. \tag{7.19}$$

and use the ϵ-symbols defined in (7.9), or (7.10). This means that our volume form has the orientation:

$$vol_3 \sim dt \wedge dr \wedge dv \sim du \wedge dr \wedge dv\,. \tag{7.20}$$

The orientation in [27] was given as:

$$e^{-1}\varepsilon_{uvr} = -\varepsilon \qquad \Rightarrow \qquad vol_3 \sim -\varepsilon\, du \wedge dv \wedge dr = \varepsilon\, du \wedge dr \wedge dv\,, \tag{7.21}$$

where $\varepsilon = \pm 1$ is a parameter introduced in [27]. We will take $\varepsilon = -1$, and so, on the face of it, we seem to be using different orientations to that of [27]. However, one should remember that [27] uses the opposite of our metric signature and so raising all the indices to create $\varepsilon^{\mu\nu\rho}$ flips the sign in [27] but does not change the sign here. Thus the tensors, $\varepsilon^{\mu\nu\rho}$, have:

$$e\,\varepsilon^{urv} = \epsilon^{012} = -\varepsilon\,, \tag{7.22}$$

and are therefore the same as those of [27] (once we take $\varepsilon = -1$). This is the important convention because it is (7.22) that enters the expressions for the Chern-Simons terms and their kindred.

7.2 The $\mathcal{N}=8$ theory

Our presentation will closely follow that of [56]. Apart from the graviton, this theory has eight gravitini, ψ^A_μ, the gauge connections, $B_\mu{}^{\mathcal{M}}$, $8n$ fermions, $\chi^{\dot{A}r}$, and $8n$ bosons. The supersymmetries, ϵ^A, and the gravitini transform in the, 8^+, representation of $SO(8)$ and the fermions, $\chi^{\dot{A}r}$, transform in the opposite helicity, 8^-, representation of $SO(8)$.

As with most gauged supergravity theories, the starting point is the scalar manifold and its coupling to gauge fields. The scalar coset is

$$\frac{G}{H} \equiv \frac{SO(8,n)}{SO(8)\times SO(n)}\,. \tag{7.23}$$

The scalar fields are then parametrized by a coset representative, $L(x)$, that is viewed as transforming on the left under a global action of $g \in G$, and on the right under a composite, local symmetry $h(x) \in H$: $L(x) \to gL(x)h(x)^{-1}$. The gauge group, G_0, which we will specify later, is a subgroup of G and the gauging promotes G_0 to a local action on $L(x)$:

$$L(x) \longrightarrow g_0(x)\, L(x)\, h^{-1}(x)\,, \qquad g_0(x) \in G_0\,,\ h(x) \in H\,, \tag{7.24}$$

The gauge subgroup and its coupling are defined by an embedding tensor, $\Theta_{\mathcal{MN}}$:

$$\widehat{\mathcal{D}}_\mu \;\equiv\; \partial_\mu \;+\; g\,\Theta_{\mathcal{MN}}\,B_\mu{}^{\mathcal{M}} t^{\mathcal{N}}\,, \tag{7.25}$$

where $B_\mu{}^{\mathcal{M}}$ are the gauge connections.

The covariant derivative of $L(x)$ is then used to define various connection components via a Lie algebra decomposition[6]:

$$L^{-1}\left(\partial_\mu \;+\; g\,\Theta_{\mathcal{MN}}\,B_\mu{}^{\mathcal{M}} t^{\mathcal{N}}\right) L \;\equiv\; \frac{1}{2}\,\mathcal{Q}_\mu^{IJ}\,X^{IJ} + \frac{1}{2}\,\mathcal{Q}_\mu^{rs} X^{rs} + \mathcal{P}_\mu^{Ir}\,X^{Ir}\,, \tag{7.26}$$

The tensor $\mathcal{P}_\mu^{Ir}$ will define the bosonic kinetic term and the $\mathcal{Q}_\mu$'s are used to define covariant derivatives on fermions:

$$\begin{aligned}
D_\mu\,\psi_\nu^A \;&\equiv\; \partial_\mu\psi_\nu^A \;-\; \widehat{\Gamma}_{\mu\nu}^{\rho}\,\psi_\rho^A \;+\; \frac{1}{4}\,\omega_\mu{}^{ab}\,\gamma_{ab}\,\psi_\nu^A + \frac{1}{4}\,\mathcal{Q}_\mu^{IJ}\Gamma_{AB}^{IJ}\psi_\nu^B\,,\\
D_\mu\chi^{\dot{A}r} \;&\equiv\; \partial_\mu\chi^{\dot{A}r} \;+\; \frac{1}{4}\,\omega_\mu{}^{ab}\,\gamma_{ab}\,\chi^{\dot{A}r} \;+\; \frac{1}{4}\,\mathcal{Q}_\mu^{IJ}\Gamma_{\dot{A}\dot{B}}^{IJ}\,\chi^{\dot{B}r} \;+\; \mathcal{Q}_\mu^{rs}\,\chi^{\dot{A}s}\,.
\end{aligned}$$

Here $\widehat{\Gamma}_{\mu\nu}^{\rho}$ is the Christofflel connection and should not be confused with the Γ-matrices. This term is omitted in [56], but this omission is harmless because only the skew derivative $D_{[\mu}\,\psi_{\nu]}^A$ appears in the action and so the Christoffel connection disappears.

The scalar fields enter the action and supersymmetry variations in several non-trivial ways, and these are characterized by various A-tensors that are derived from the T-tensor. To define the latter one needs to decompose the adjoint action of the scalar matrix:

$$L^{-1}t^{\mathcal{M}}L \;\equiv\; \mathcal{V}^{\mathcal{M}}{}_{\mathcal{A}}\,t^{\mathcal{A}} \;=\; \frac{1}{2}\,\mathcal{V}^{\mathcal{M}}{}_{IJ}\,X^{IJ} \;+\; \frac{1}{2}\,\mathcal{V}^{\mathcal{M}}{}_{rs}\,X^{rs} \;+\; \mathcal{V}^{\mathcal{M}}{}_{Ir}\,X^{Ir}\,, \tag{7.27}$$

and then the T-tensor is defined by:

$$T_{\mathcal{A}|\mathcal{B}} \;\equiv\; \Theta_{\mathcal{MN}}\,\mathcal{V}^{\mathcal{M}}{}_{\mathcal{A}}\,\mathcal{V}^{\mathcal{N}}{}_{\mathcal{B}}\,. \tag{7.28}$$

The A-tensors are then constructed from various pieces of the T-tensor:

$$\begin{aligned}
A_1^{AB} \;&=\; -\,\delta^{AB}\,\theta - \frac{1}{48}\,\Gamma_{AB}^{IJKL}\,T_{IJ|KL}\,,\\
A_2^{A\dot{A}r} \;&=\; -\,\frac{1}{12}\,\Gamma_{A\dot{A}}^{IJK}\,T_{IJ|Kr}\,,\\
A_3^{\dot{A}r\,\dot{B}s} \;&=\; 2\delta^{\dot{A}\dot{B}}\delta^{rs}\,\theta + \frac{1}{48}\,\delta^{rs}\,\Gamma_{\dot{A}\dot{B}}^{IJKL}\,T_{IJ|KL} + \frac{1}{2}\,\Gamma_{\dot{A}\dot{B}}^{IJ}\,T_{IJ|rs}\,.
\end{aligned} \tag{7.29}$$

where $\theta \equiv \frac{2}{(8+n)(7+n)}\,\eta^{\mathcal{MN}}\Theta_{\mathcal{MN}}$, and $\eta^{\mathcal{MN}}$ is the Cartan-Killing form on G. For more details, see [56]. In the gauging we consider here, one has $\theta = 0$.

The Lagrangian is then given by:

[6]This is where the signs of the generators are critical.

$$\begin{aligned}\mathcal{L} \;=\; & -\frac{1}{4}\,e\,R \;+\; \frac{1}{2}\,\epsilon^{\mu\nu\rho}\,\overline{\psi}^{A}_{\mu}D_{\nu}\psi^{A}_{\rho} \;+\; \frac{1}{4}\,e\,\mathcal{P}^{Ir}_{\mu}\,\mathcal{P}^{\mu\,Ir} \;-\; \frac{1}{2}\,ie\,\overline{\chi}^{\dot{A}r}\gamma^{\mu}D_{\mu}\chi^{\dot{A}r}\\ & -\frac{1}{4}\,\epsilon^{\mu\nu\rho}\,g\,\Theta_{\mathcal{M}\mathcal{N}}\,B_{\mu}{}^{\mathcal{M}}\Big(\partial_{\nu}B_{\rho}{}^{\mathcal{N}} \;+\; \frac{1}{3}\,g\,\Theta_{\mathcal{K}\mathcal{L}}\,f^{\mathcal{N}\mathcal{K}}{}_{\mathcal{P}}\,B_{\nu}{}^{\mathcal{L}}B_{\rho}{}^{\mathcal{P}}\Big)\\ & -\frac{1}{2}\,e\,\mathcal{P}^{Ir}_{\mu}\,\overline{\chi}^{\dot{A}r}\,\Gamma^{I}_{A\dot{A}}\gamma^{\nu}\gamma^{\mu}\psi^{A}_{\nu} \;+\; \frac{1}{2}\,g\,e\,A_1^{AB}\,\overline{\psi}^{A}_{\mu}\gamma^{\mu\nu}\psi^{B}_{\nu}\\ & +\; i\,g\,e\,A_2^{A\dot{A}r}\,\overline{\chi}^{\dot{A}r}\gamma^{\mu}\psi^{A}_{\mu} \;+\; \frac{1}{2}\,g\,e\,A_3^{\dot{A}r\,\dot{B}s}\,\overline{\chi}^{\dot{A}r}\chi^{\dot{B}s} \;-\; e\,V\,,\end{aligned}$$

where the potential is defined by:

$$V \;=\; -\frac{1}{4}\,g^2\left(A_1^{AB}A_1^{AB} - \frac{1}{2}\,A_2^{A\dot{A}r}A_2^{A\dot{A}r}\right). \tag{7.30}$$

One should note that we have replaced the potential W of [56] by $-V$ as we wish to avoid confusion with the superpotential that will be defined later.

This action is then invariant under the supersymmetry transformations [56]:

$$L^{-1}\delta L \;=\; X^{Ir}\,\overline{\epsilon}^{A}\,\Gamma^{I}_{A\dot{A}}\,\chi^{\dot{A}r}\,, \qquad \delta\chi^{\dot{A}r} \;=\; \frac{1}{2}\,i\,\Gamma^{I}_{A\dot{A}}\gamma^{\mu}\epsilon^{A}\,\mathcal{P}^{Ir}_{\mu} \;+\; g\,A_2^{A\dot{A}r}\epsilon^{A}\,, \tag{7.31}$$

$$\delta e_{\mu}{}^{\alpha} \;=\; i\,\overline{\epsilon}^{A}\,\gamma^{\alpha}\psi^{A}_{\mu}\,, \qquad \delta\psi^{A}_{\mu} \;=\; D_{\mu}\epsilon^{A} \;+\; i\,g\,A_1^{AB}\gamma_{\mu}\epsilon^{B}\,, \tag{7.32}$$

$$\delta B_{\mu}{}^{\mathcal{M}} \;=\; -\frac{1}{2}\,\mathcal{V}^{\mathcal{M}}{}_{IJ}\,\overline{\epsilon}^{A}\,\Gamma^{IJ}_{AB}\,\psi^{B}_{\mu} \;+\; i\,\mathcal{V}^{\mathcal{M}}{}_{Ir}\,\overline{\epsilon}^{A}\,\Gamma^{I}_{A\dot{A}}\gamma_{\mu}\,\chi^{\dot{A}r}\,. \tag{7.33}$$

As usual there are also four-fermion terms in the action and higher fermion terms in the supersymmetry variations. According to the arguments in [56], these terms are the same as those given in [61]. Since we are interested in the BPS equations of supersymmetric bosonic backgrounds, we will not need any of these higher fermion terms.

7.3 Truncating to the $\mathcal{N}=4$ gauged supergravity

The $\mathcal{N}=4$ theory has half the supersymmetries and, at a minimum, this means removing half the gravitini and their superpartners. In six dimensions, the superpartners of the truncated gravitini are four of the self-dual tensors, whose removal translates, in three dimensions, to reducing the $SO(8,n)$ global symmetry of the ungauged theory to $SO(4,n)$. This reduction also reduces the number of scalars from $8n$ to $4n$, which means halving the number of fermions, $\chi^{\dot{A}r}$. The coset (7.23) is thus reduced to:

$$\frac{\hat{G}}{\hat{H}} \;\equiv\; \frac{SO(4,n)}{SO(4)\times SO(n)}\,. \tag{7.34}$$

The $SO(4,n)$ embeds in the obvious manner into $SO(8,n)$ and indeed, here we will simply view the $\mathcal{N}=4$ theory as embedded in the larger $\mathcal{N}=8$ theory. We will therefore consider the scalar matrix to be that of the $SO(8,n)$ theory but non-trivial only in the $SO(4,n)$ block defined by $I,J,\ldots=1,2,3,4$.

The corresponding truncation of the fermions is easily implemented: One must require

$$\left(\mathbb{1} \;-\; \Gamma^{5678}\right)\Phi \;=\; 0\,, \tag{7.35}$$

where Φ is any fermion, including the supersymmetries. Because the $SO(8)$ helicity projector is $\Gamma^{12345678}$, this condition translates to:

$$\left(\mathbb{1}-\Gamma^{1234}\right)_{AB}\epsilon^{B} \;=\; 0\,, \qquad \left(\mathbb{1}-\Gamma^{1234}\right)_{AB}\psi^{B}_{\mu} \;=\; 0\,, \qquad \left(\mathbb{1}+\Gamma^{1234}\right)_{\dot{A}\dot{B}}\chi^{\dot{B}r} \;=\; 0\,. \tag{7.36}$$

This cuts the supersymmetries, and all the fermionic degrees of freedom, in half.

It is easy to see that this truncation is consistent with the supersymmetry variations. Because of the restriction on the scalars, the Lie algebra matrices in (7.27) must live in $SO(4,n)$. This means that all the indices on the T-tensor and on $\mathcal{Q}^{IJ}_{\mu}$ and $\mathcal{P}^{Ir}_{\mu}$ must lie in the Lie algebra of $SO(4,n)$. It follows that $\mathcal{Q}^{IJ}_{\mu}\Gamma^{IJ}$, $\mathcal{P}^{Ir}_{\mu}\Gamma^{I}$, and all the A-tensors commute with Γ^{5678}. This implies that the supersymmetry variations of the fermions respect the projection (7.35). The variation $L^{-1}\delta L$ is easily seen to vanish along X^{Ir}, $I=5,\ldots,8$ as a consequence of (7.35). Finally, the fact that $\mathcal{V}^{\mathcal{M}}{}_{\mathcal{A}}$ lies in $SO(4,n)$ means that it is consistent with the supersymmetry variations to restrict the gauge fields, $B_{\mu}{}^{\mathcal{M}}$, to a sub-algebra of $SO(4,n)$.

There is a simple way to characterize this truncation in terms of a group invariant sector of the $\mathcal{N}=8$ theory. There is an $(SU(2))^4$ subgroup of $SO(8)$. One of these $SU(2)$ rotations is characterized as the self-dual rotations on the indices $5,6,7,8$. The projection condition (7.35) requires all the fermions to be singlets under this $SU(2)$. Moreover, the centralizer of this $SU(2)$ in $SO(8,n)$ is precisely $SO(4,n)$. Thus the truncation of the $\mathcal{N}=8$ theory to the $\mathcal{N}=4$ theory may be defined as reducing to the singlet sector of this $SU(2)$.

While the $\mathcal{N}=4$ theory was the starting point of [27], and can be directly related to superstrata, nothing prevents us from considering the three-dimensional solutions presented in [27] as being part of the larger $\mathcal{N}=8$ theory and analyzing the supersymmetry from that perspective. We will take this approach and find that the projection condition (7.36) emerges from the analysis of the supersymmetry of the solution.

7.4 The minimal couplings of $\mathcal{N}=4$ gauged supergravity

The three-dimensional theory that underlies the superstrata is the $SO(4,5)$ theory described in [27]. Here we will summarize the essential features of that theory. Our presentation will differ slightly from [27] because of our conventions and because we will fix some of the parameters[7] that appeared in [27].

[7] This is not a restriction because these parameters were ultimately fixed in [27] by requiring that the superstratum data solved the equations of motion.

First, it is most convenient to express the embedding tensor details in terms of the $GL(4\,,\mathbb{R})$ basis of $SO(4,5)$ in which the invariant matrix takes the form:

$$\hat{\eta} \;\equiv\; \begin{pmatrix} 0_{4\times4} & \mathbb{1}_{4\times4} & 0 \\ \mathbb{1}_{4\times4} & 0_{4\times4} & 0 \\ 0 & 0 & -1 \end{pmatrix} . \tag{7.37}$$

Note that we have fixed the parameter ε of [27] by taking:

$$\varepsilon \;=\; -\,1\,. \tag{7.38}$$

This is merely a choice of convention. The change of basis matrices to go back to canonical $SO(4,5)$ conventions with η of the form (7.1) may be found in the Appendix.

Following [27], a vector of $SO(4,5)$ will be denoted by

$$\mathcal{X}_{\bar{M}} \;\equiv\; (\mathcal{X}_I, \mathcal{X}^I, \mathcal{X}_0)\,, \qquad \mathcal{X}^{\bar{M}} \;\equiv\; (\mathcal{X}^I, \mathcal{X}_I, \varepsilon\mathcal{X}_0)\,, \tag{7.39}$$

where the indices are raised and lowered using (7.37). The components, $\mathcal{X}_I$ and $\mathcal{X}^I$, transform, respectively, in the 4 and $\overline{4}$ of $GL(4,\mathbb{R})$.

The embedding tensor, Θ, is totally anti-symmetric[8]:

$$\Theta_{\bar{K}\bar{L},\bar{M}\bar{N}} \;=\; \theta_{\bar{K}\bar{L}\bar{M}\bar{N}} \;=\; \theta_{[\bar{K}\bar{L}\bar{M}\bar{N}]}\,, \tag{7.40}$$

and the only non-vanishing pieces are [27, 57, 58, 60]:

$$\theta_{IJKL} \;=\; -\,g_0\,\epsilon_{IJKL}\,, \qquad \theta_{IJK}{}^{L} \;=\; \frac{1}{2}\,g_0\,\epsilon_{IJKM}\,\delta^{LM}\,, \tag{7.41}$$

One should note that we have replaced the parameters α and γ_0 in [27] according to:

$$\alpha \;=\; \gamma_0 \;=\; \frac{1}{2}\,g_0 \tag{7.42}$$

These replacements follow from equations (3.7) and (4.5) of [27] with $\varepsilon = -1$, as in (7.38). We also note the g_0 is related to the supergravity charges of the D1-D5 compactification via:

$$g_0 \;\equiv\; (Q_1 Q_5)^{-\frac{1}{4}}\,. \tag{7.43}$$

(See equation (4.5) of [27].)

The gauge group is $SO(4) \ltimes \mathbb{T}^6$ and the connection $A_\mu{}^{\bar{K}\bar{L}}$ has the following 12 fields:

$$A_\mu{}^{IJ} \;=\; -\,A_\mu{}^{JI}\,, \qquad A_\mu{}^{J}{}_{I} \;=\; -\,A_\mu{}_{J}{}^{I}\,. \tag{7.44}$$

Because of the ϵ-symbols in the embedding tensor, it is convenient to define:

$$\widetilde{A}_\mu{}^{IJ} \;\equiv\; \frac{1}{2}\,\epsilon_{IJKL}\,A_\mu{}^{KL}\,, \qquad \widehat{A}_\mu{}^{IJ} \;\equiv\; \frac{1}{2}\,\epsilon_{IJKL}\,A_\mu{}^{K}{}_{L}\,, \tag{7.45}$$

[8] This is why θ in (7.29) vanishes.

As in [27], we introduce:

$$B_\mu{}^{IJ} \;\equiv\; 4\,g_0\,\big(\,\widetilde{A}_\mu{}^{IJ} - \widehat{A}_\mu{}^{IJ}\big)\,. \tag{7.46}$$

The gauge connection acts according to (7.25), which we now write as:

$$\begin{aligned}\widehat{\mathcal{D}}_\mu\,\mathcal{X}_{\bar{P}} \;&\equiv\; \partial_\mu\,\mathcal{X}_{\bar{P}} \;+\; g\,A_\mu{}^{\bar{K}\bar{L}}\,\Theta_{\bar{K}\bar{L},\bar{M}\bar{N}}\,\big(\,X^{\bar{M}\bar{N}}\,\big)_{\bar{P}}{}^{\bar{Q}}(\mathcal{X}_{\bar{Q}})\\ &=\; \partial_\mu\,\mathcal{X}_{\bar{P}} \;+\; g\,A_\mu{}^{\bar{K}\bar{L}}\,\big(\Theta_{\bar{K}\bar{L},\bar{P}\bar{N}}\,\hat{\eta}^{\bar{N}\bar{Q}}\,\mathcal{X}_{\bar{Q}} - \Theta_{\bar{K}\bar{L},\bar{M}\bar{P}}\,\hat{\eta}^{\bar{M}\bar{Q}}\,\mathcal{X}_{\bar{Q}}\big)\,,\end{aligned} \tag{7.47}$$

where we have used (7.5). There are several things to note at this point. Because we have replaced adjoint indices by doubled indices like, $\bar{K}\bar{L}$, we are double summing over the adjoint representation. One can take this to be part of the definition and normalization of the components of the embedding tensor, $\Theta_{\bar{K}\bar{L},\bar{M}\bar{N}}$. Indeed one can compensate for the double sums by sending $\Theta \to \frac{1}{4}\Theta$. Next, compared to [27], we have introduced another gauge coupling, g, (inherited from (7.25)) and we are using the opposite signs for the group generators and structure constants. In principle, this will change the signs of the gauge couplings throughout the action. However we are now going to choose

$$g \;=\; -\,1\,. \tag{7.48}$$

This will compensate for all the opposite signs compared to [27], and lead to precisely the same covariant derivatives and actions. Indeed, exactly as in [27], our covariant derivative on a $SO(4,5)$ vector, (7.39), in the $GL(4,\mathbb{R})$ basis becomes

$$\begin{aligned}\widehat{\mathcal{D}}_\mu\,\mathcal{X}_I \;&=\; \partial_\mu\,\mathcal{X}_I \;+\; B_\mu{}^{IJ}\,\mathcal{X}^J \;-\; 2\,g_0\,\widetilde{A}_\mu{}^{IJ}\,\mathcal{X}_J\,,\\ \widehat{\mathcal{D}}_\mu\,\mathcal{X}^I \;&=\; \partial_\mu\,\mathcal{X}^I \;-\; 2\,g_0\,\widetilde{A}_\mu{}^{IJ}\,\mathcal{X}^J\,, \qquad \widehat{\mathcal{D}}_\mu\,\mathcal{X}_0 \;=\; \partial_\mu\,\mathcal{X}_0\,.\end{aligned} \tag{7.49}$$

It may seem circuitous to have used the opposite-sign generators for $SO(4,5)$ only to undo this choice through (7.48). However, the signs of the generators are also crucial to the definition of all the tensors in Section 7.2 and so we have taken this apparently circuitous route so as to arrive at the action of [27] while respecting the conventions essential to [56].

The connections, $B_\mu{}^{IJ}$, lie in the upper triangular part of the $SO(4,5)$ matrices:

$$\mathcal{B}_\mu \;\equiv\; \begin{pmatrix} 0 & B_\mu{}^{IJ} & 0\\ 0 & 0 & 0\\ 0 & 0 & 0\end{pmatrix}\,. \tag{7.50}$$

These are the gauge fields of $\mathbb{T}^6$ and will ultimately be integrated out of the action. The vector fields $A_\mu{}^{IJ}$ are those of $SO(4)$ but they act with their duals, and with a gauge coupling of $-2g_0$. It is therefore useful to introduce the $SO(4)$ covariant derivatives:

$$\begin{aligned}\mathcal{D}_\mu\,\mathcal{X}_I \;&=\; \partial_\mu\,\mathcal{X}_I \;-\; 2\,g_0\,\widetilde{A}_\mu{}^{IJ}\,\mathcal{X}_J\,,\\ \mathcal{D}_\mu\,\mathcal{X}^I \;&=\; \partial_\mu\,\mathcal{X}^I \;-\; 2\,g_0\,\widetilde{A}_\mu{}^{IJ}\,\mathcal{X}^J\,, \qquad \mathcal{D}_\mu\,\mathcal{X}_0 \;=\; \partial_\mu\,\mathcal{X}_0\,.\end{aligned} \tag{7.51}$$

7.5 The Maxwell fields

The connections, (7.51), lead to the Maxwell fields

$$F_{\mu\nu}{}^{IJ} \;=\; \frac{1}{2}\,\epsilon_{IJKL}\,\widetilde{F}_{\mu\nu}{}^{KL} \;=\; \partial_\mu A_\nu{}^{IJ} \,-\, \partial_\nu A_\mu{}^{IJ} \,-\, 2\,g_0\left(A_\mu{}^{IL}\,\widetilde{A}_\nu{}^{LJ} \,-\, A_\mu{}^{JL}\,\widetilde{A}_\nu{}^{LI}\right). \quad (7.52)$$

The Chern-Simons action appearing in (7.30) is:

$$\begin{aligned} &-\frac{1}{4}\,\epsilon^{\mu\nu\rho}\,g\,\Theta_{\mathcal{MN}}\,B_\mu{}^{\mathcal{M}}\Big(\partial_\nu B_\rho{}^{\mathcal{N}} \;+\; \frac{1}{3}\,g\,\Theta_{\mathcal{KL}}\,f^{\mathcal{NK}}{}_{\mathcal{P}}\,B_\nu{}^{\mathcal{L}}B_\rho{}^{\mathcal{P}}\Big) \\ &=\; +\frac{1}{4}\,\epsilon^{\mu\nu\rho}\,\Theta_{\mathcal{MN}}\,B_\mu{}^{\mathcal{M}}\Big(\partial_\nu B_\rho{}^{\mathcal{N}} \;-\; \frac{1}{3}\,\Theta_{\mathcal{KL}}\,f^{\mathcal{NK}}{}_{\mathcal{P}}\,B_\nu{}^{\mathcal{L}}B_\rho{}^{\mathcal{P}}\Big), \end{aligned} \quad (7.53)$$

where we have set $g = -1$. Using the double sum conventions, this translates into:

$$\mathcal{L}_{CS} \;=\; \frac{1}{4}\,\varepsilon^{\mu\nu\rho}\,A_\mu{}^{\bar{K}\bar{L}}\,\Theta_{\bar{K}\bar{L},\bar{M}\bar{N}}\left(\partial_\nu A_\rho{}^{\bar{M}\bar{N}} \;-\; \frac{1}{3}\,f^{\bar{M}\bar{N},\bar{P}\bar{Q}}{}_{\bar{R}\bar{S}}\,\Theta_{\bar{P}\bar{Q},\bar{U}\bar{V}}\,A_\nu{}^{\bar{U}\bar{V}}\,A_\rho{}^{\bar{R}\bar{S}}\right). \quad (7.54)$$

To compensate for the double sums one can rescale $\Theta \to \frac{1}{4}\Theta$, as one does in going from (7.25) to (7.47). This leads to the correct normalization in the first term, however this introduces a factor of $\frac{1}{16}$ in the second term whereas there are five double sums. The extra factor of $\frac{1}{2}$ is, however, built in through our definition of the structure constants in (7.3) and the resulting factors of $\frac{1}{2}$ in (7.4). One should also note that the second term in (7.54) has the opposite sign to that of [27]. This is because our structure constants also have the opposite sign.

Using (7.4), (7.41) and (7.46) we arrive at

$$\mathcal{L}_{CS} \;=\; \frac{1}{2}\,\varepsilon^{\mu\nu\rho}\left[g_0\left(A_\mu{}^{IJ}\,\partial_\nu\widetilde{A}_\rho{}^{IJ} \;+\; \frac{4}{3}\,g_0\,A_\mu{}^{IJ}\,A_\nu{}^{JK}\,A_\rho{}^{KI}\right) \;-\; \frac{1}{4}\,B_\mu{}^{IJ}\,F^{IJ}_{\nu\rho}\right], \quad (7.55)$$

which exactly matches[9] (2.33) of [27].

7.6 The scalar fields

Following [27], our scalar matrix will be defined by:

$$L_{\bar{M}}{}^{\bar{K}} \;=\; \begin{pmatrix} P_I{}^J & \frac{1}{2}\,\chi_I\left((P^{-1})_J{}^K\,\chi_K\right) & \chi_I \\ 0 & (P^{-1})_J{}^I & 0 \\ 0 & (P^{-1})_J{}^K\,\chi_K & 1 \end{pmatrix}, \quad (7.56)$$

where $P = P^T$ is a symmetric $GL(4,\mathbb{R})$ matrix. The matrix, P, can be chosen to be symmetric because of the composite local symmetry, H, in (7.24). We also have a local $SO(4)$ gauge symmetry, this symmetry can be used to diagonalize P, or in some other form, as we will see later.

[9] We have re-ordered some of the indices relative to the expression in [27].

One should remember that the gauge symmetry only acts on the left of L in (7.24), and this translates into the purely left action of the gauge fields in (7.26), which, in turn, means that the covariant derivative, $\mathcal{D}_\mu$, only acts on the left of P.

It is also convenient to define the scalar matrix m_{IJ} and its inverse, m^{IJ}:

$$m_{IJ} \equiv \left(P\,P^T\right)_{IJ}, \qquad m^{IJ} = \left((P^{-1})^T\,P^{-1}\right)^{IJ}. \tag{7.57}$$

One should note that the covariant derivative of m is therefore given by:

$$\mathcal{D}_\mu m_{IJ} = \partial_\mu m_{IJ} - 2\,g_0\,\widetilde{A}_\mu{}^{IK} m_{KJ} - 2\,g_0\,\widetilde{A}_\mu{}^{JK} m_{IK}\,. \tag{7.58}$$

We will also define the following combinations of fields:

$$\begin{aligned} Y_{\mu\,IJ} &\equiv \chi_J\,\mathcal{D}_\mu\chi_I - \chi_I\,\mathcal{D}_\mu\chi_J\,, \\ C_\mu^{IJ} &\equiv B_\mu{}^{IJ} + \frac{1}{2}\,Y_{\mu\,IJ}\,, \qquad\qquad \mathscr{C}_\mu^{IJ} \equiv P^{-1}{}_I{}^K\,P^{-1}{}_J{}^L\,C_\mu^{KL}\,. \end{aligned} \tag{7.59}$$

Note that these objects break the $GL(4\,,\mathbb{R})$ covariance and are to be considered only as $SO(4)$ tensors. This means that we will not distinguish raised and lowered indices for such objects.

The various pieces of the Lie algebra element (7.26) are then given by:

$$\begin{aligned} \mathcal{Q}_\mu^{IJ} &= \frac{1}{2}\Big[\left(P^{-1}\mathcal{D}_\mu P\right)_I{}^J - \left(P^{-1}\mathcal{D}_\mu P\right)_J{}^I + \mathscr{C}_\mu^{IJ}\Big]\,, \\ \mathcal{P}_\mu^{Ir} &= \frac{1}{2}\Big[\left(P^{-1}\mathcal{D}_\mu P\right)_I{}^r + \left(P^{-1}\mathcal{D}_\mu P\right)_r{}^I - \mathscr{C}_\mu^{Ir}\Big]\,, \qquad 1\le r\le 4\,, \\ \mathcal{Q}_\mu^{rs} &= -\frac{1}{2}\Big[\left(P^{-1}\mathcal{D}_\mu P\right)_r{}^s - \left(P^{-1}\mathcal{D}_\mu P\right)_s{}^r + \mathscr{C}_\mu^{rs}\Big]\,, \qquad 1\le r,s\le 4\,, \\ \mathcal{Q}_\mu^{r5} &= \frac{1}{\sqrt{2}}\left(P^{-1}\right)_r{}^J\mathcal{D}_\mu\chi_J\,, \qquad \mathcal{P}_\mu^{I5} = -\frac{1}{\sqrt{2}}\left(P^{-1}\right)_I{}^J\mathcal{D}_\mu\chi_J\,, \qquad 1\le r\le 4\,. \end{aligned} \tag{7.60}$$

Note that in defining $\mathcal{Q}_\mu^{rs}$ we are using the generators, X^{rs}, defined by (7.3) or (7.5), and not those of [60].

Next, we need to define the A-tensors appearing in the supersymmetry variations (7.29). An explicit form can be computed in the gauge where the matrix P is diagonal:

$$P = \mathrm{diag}\big(e^{x_1}\,,\,e^{x_2}\,,\,e^{x_3}\,,\,e^{x_4}\big)\,. \tag{7.61}$$

We introduce the superpotential:

$$\begin{aligned} W &\equiv \frac{1}{4}\,g_0\,(\det(P))^{-1}\Big[2\left(1-\frac{1}{4}\,(\chi_A\chi_A)\right) - \mathrm{Tr}\big(P\,P^T\big)\Big] \\ &= \frac{1}{4}\,g_0\,e^{-x_1-x_2-x_3-x_4}\Big[2\left(1-\frac{1}{4}\,(\chi_A\chi_A)\right) - \left(e^{2\,x_1}+e^{2\,x_2}+e^{2\,x_3}+e^{2\,x_4}\right)\Big]\,, \end{aligned} \tag{7.62}$$

Then we find:

$$\begin{aligned} A_1^{AB} &= W\,(\Gamma^{1234})_{AB}\,, \qquad A_2^{A\dot{A}\,r} = \frac{\partial W}{\partial x_r}\,(\Gamma^{1234}\,\Gamma^r)_{A\dot{A}}\,, \quad 1\le r\le 4\,, \\ & \qquad\qquad A_2^{A\dot{A}\,5} = -\sqrt{2}\sum_{j=1}^{4} e^{x_j}\,\frac{\partial W}{\partial\chi_j}\,(\Gamma^{1234}\,\Gamma^j)_{A\dot{A}}\,, \end{aligned} \tag{7.63}$$

where there is no sum on r in the expression for $A_2^{A\dot{A}\,r}$. While we will not need it, we also find:

$$\begin{aligned}
A_3^{\dot{A}r\,\dot{B}s} &= -W\,\delta^{rs}\,(\Gamma^{1234})_{\dot{A}\dot{B}} - \epsilon_{IJrs}\,\frac{\partial^2 W}{\partial x_r\,\partial x_s}(\Gamma^{IJ})_{\dot{A}\dot{B}}\,, \qquad 1\le r,s\le 4\,,\\
A_3^{\dot{A}r\,\dot{B}5} &= \sqrt{2}\sum_{j=1}^{4} e^{x_j}\,(\Gamma^{IJ})_{\dot{A}\dot{B}}\,\epsilon_{IJrj}\,e^{x_j}\,\frac{\partial^2 W}{\partial x_r\,\partial\chi_j}\,, \qquad 1\le r\le 4\,,\\
A_3^{\dot{A}5\,\dot{B}5} &= -W\,(\Gamma^{1234})_{\dot{A}\dot{B}}\,.
\end{aligned} \tag{7.64}$$

where there is no sum on r or s.

Using these expressions we find that the potential (7.30) is given by:

$$V = \delta^{ij}\frac{\partial W}{\partial x_i}\frac{\partial W}{\partial x_j} + 2\,m^{IJ}\,\frac{\partial W}{\partial\chi_I}\frac{\partial W}{\partial\chi_J} - 2\,W^2\,. \tag{7.65}$$

Thus the scalar sector of the theory, and its role in the supersymmetries, are determined entirely by the superpotential (7.62).

Using the explicit forms of P, or m, and then restoring the $SO(4)$ gauge symmetry, we find

$$V = \frac{1}{4}\,g_0^2\,\det(m^{IJ})\,\Big[2\,\big(1-\frac{1}{4}\,(\chi_I\chi_I)\big)^2 + m_{IJ}m_{IJ} + \frac{1}{2}\,m_{IJ}\chi_I\chi_J - \frac{1}{2}\,m_{II}\,m_{JJ}\Big]\,. \tag{7.66}$$

Using (7.61) and (7.60), the scalar kinetic term can be written

$$\begin{aligned}
\mathcal{P}_\mu^{Ir}\,\mathcal{P}^{\mu\,Ir} = g^{\mu\nu}\Big[&\frac{1}{4}\,\big(m^{IK}\,\mathcal{D}_\mu\,m_{KJ}\big)\big(m^{JL}\,\mathcal{D}_\nu\,m_{LI}\big)\\
&+ \frac{1}{2}\,m^{IJ}\,(\mathcal{D}_\mu\,\chi_I)\,(\mathcal{D}_\nu\,\chi_J) + \frac{1}{4}\,\big(m^{IJ}\,m^{KL}\,C_\mu^{IK}\,C_\nu^{JL}\big)\Big]\,.
\end{aligned} \tag{7.67}$$

Thus the expressions (7.66) and (7.67) precisely match the corresponding quantities in [27, 58].

7.7 The three-dimensional supergravity action

Putting all the pieces together, the three-dimensional action (7.30) becomes:

$$\begin{aligned}
\mathcal{L} = &-\frac{1}{4}\,e\,R - \frac{1}{2}\,ie\,\overline{\chi}^{\dot{A}r}\gamma^\mu D_\mu\chi^{\dot{A}r} + \frac{1}{2}\,\epsilon^{\mu\nu\rho}\,\overline{\psi}_\mu^A D_\nu\psi_\rho^A + \frac{1}{8}\,e\,g^{\mu\nu}\,m^{IJ}\,(\mathcal{D}_\mu\,\chi_I)\,(\mathcal{D}_\nu\,\chi_J)\\
&+ \frac{1}{16}\,e\,g^{\mu\nu}\,\big(m^{IK}\,\mathcal{D}_\mu\,m_{KJ}\big)\big(m^{JL}\,\mathcal{D}_\nu\,m_{LI}\big) + \frac{1}{16}\,e\,g^{\mu\nu}\,\big(m^{IJ}\,m^{KL}\,C_\mu^{IK}\,C_\nu^{JL}\big)\\
&+ \frac{1}{2}\,e\,\varepsilon^{\mu\nu\rho}\Big[g_0\,\big(A_\mu{}^{IJ}\,\partial_\nu\widetilde{A}_\rho{}^{IJ} + \frac{4}{3}\,g_0\,A_\mu{}^{IJ}\,A_\nu{}^{JK}\,A_\rho{}^{KI}\big) - \frac{1}{4}\,B_\mu{}^{IJ}\,F_{\nu\rho}^{IJ}\Big]\\
&- \frac{1}{2}\,e\,\mathcal{P}_\mu^{Ir}\,\overline{\chi}^{\dot{A}r}\,\Gamma^I_{A\dot{A}}\gamma^\nu\gamma^\mu\psi_\nu^A + \frac{1}{2}\,g\,e\,A_1^{AB}\,\overline{\psi}_\mu^A\gamma^{\mu\nu}\psi_\nu^B\\
&+ i\,g\,e\,A_2^{A\dot{A}r}\,\overline{\chi}^{\dot{A}r}\gamma^\mu\psi_\mu^A + \frac{1}{2}\,g\,e\,A_3^{\dot{A}r\,\dot{B}s}\,\overline{\chi}^{\dot{A}r}\chi^{\dot{B}s} - e\,V\,.
\end{aligned} \tag{7.68}$$

One now completes the square in all the terms that involve $B_\mu{}^{IJ}$, to arrive at the action:

$$\begin{aligned}\mathcal{L} \;=\; & -\frac{1}{4}\,e\,R \;-\; \frac{1}{2}\,ie\,\overline{\chi}^{\dot{A}r}\gamma^\mu D_\mu\chi^{\dot{A}r} \;+\; \frac{1}{2}\,\epsilon^{\mu\nu\rho}\,\overline{\psi}^A_\mu D_\nu\psi^A_\rho \;+\; \frac{1}{8}\,e\,g^{\mu\nu}\,m^{IJ}\,(\mathcal{D}_\mu\chi_I)\,(\mathcal{D}_\nu\chi_J)\\ & +\; \frac{1}{16}\,e\,g^{\mu\nu}\,\big(m^{IK}\,\mathcal{D}_\mu\,m_{KJ}\big)\big(m^{JL}\,\mathcal{D}_\nu\,m_{LI}\big) \;-\; \frac{1}{8}\,e\,g^{\mu\rho}\,g^{\nu\sigma}\,m_{IK}\,m_{JL}\,F^{IJ}_{\mu\nu}\,F^{KL}_{\rho\sigma}\\ & +\; \frac{1}{2}\,e\,\varepsilon^{\mu\nu\rho}\Big[g_0\,\big(A_\mu{}^{IJ}\,\partial_\nu\widetilde{A}_\rho{}^{IJ} \;+\; \frac{4}{3}\,g_0\,A_\mu{}^{IJ}\,A_\nu{}^{JK}\,A_\rho{}^{KI}\big) \;+\; \frac{1}{8}\,Y_\mu{}^{IJ}\,F^{IJ}_{\nu\rho}\Big]\\ & -\; \frac{1}{2}\,e\,\mathcal{P}^{Ir}_\mu\,\overline{\chi}^{\dot{A}r}\,\Gamma^I_{A\dot{A}}\gamma^\nu\gamma^\mu\psi^A_\nu \;+\; \frac{1}{2}\,g\,e\,A_1^{AB}\,\overline{\psi}^A_\mu\gamma^{\mu\nu}\psi^B_\nu\\ & +\; i\,g\,e\,A_2^{A\dot{A}r}\,\overline{\chi}^{\dot{A}r}\gamma^\mu\psi^A_\mu \;+\; \frac{1}{2}\,g\,e\,A_3^{\dot{A}r\,\dot{B}s}\,\overline{\chi}^{\dot{A}r}\chi^{\dot{B}s} \;-\; e\,V \;+\; \mathcal{L}_{\rm B}\,,\end{aligned} \tag{7.69}$$

where

$$\begin{aligned}\mathcal{L}_{\rm B} \;\equiv\; & \frac{1}{16}\,e\,g^{\mu\nu}\,m^{IK}\,m^{JL}\,\Big(B_\mu{}^{IJ} + \frac{1}{2}\,Y_{\mu\,IJ} - g_{\mu\sigma_1}\,\varepsilon^{\sigma_1\rho_1\rho_2}\,m_{IP_1}m_{JP_2}\,F^{P_1P_2}_{\rho_1\rho_2}\Big)\\ & \times\Big(B_\nu{}^{KL} + \frac{1}{2}\,Y_{\nu\,KL} - g_{\nu\sigma_2}\,\varepsilon^{\sigma_2\rho_3\rho_4}\,m_{KP_3}\,m_{LP_4}\,F^{P_3P_4}_{\rho_3\rho_4}\Big)\,.\end{aligned} \tag{7.70}$$

The action for the B_ν leads to the constraint:

$$C_\mu{}^{IJ} \;\equiv\; B_\mu{}^{IJ} \;+\; \frac{1}{2}\,Y_{\mu\,IJ} \;=\; g_{\mu\rho}\,\varepsilon^{\rho\sigma\nu}\,m_{IK}m_{JL}\,F^{KL}_{\sigma\nu}\,. \tag{7.71}$$

These actions, and the constraint, are exactly consistent with the bosonic action given in [27]. One should note that here we are using a metric signature of $(+--)$, whereas [27] uses $(-++)$. One can convert from one convention to the other by mapping $g_{\mu\nu}\to -g_{\mu\nu}$. This reverses the sign of the Ricci scalar and, in (7.68) and (7.70), we have written the metric contractions explicitly so as to facilitate comparison. One should remember that $e\,\varepsilon^{\mu\nu\rho}$ is actually independent of the metric and so such terms remain unchanged under $g_{\mu\nu}\to -g_{\mu\nu}$.

7.8 An executive summary of the BPS equations

For supersymmetric backgrounds we must require $\delta\psi^A_\mu = \delta\chi^{\dot{A}r} = 0$. These are the "BPS equations":

$$\delta\psi^A_\mu \;=\; D_\mu\epsilon^A \;-\; i\,A_1^{AB}\gamma_\mu\epsilon^B \;=\; 0\,, \qquad \delta\chi^{\dot{A}r} \;=\; \frac{1}{2}\,i\,\Gamma^I_{A\dot{A}}\gamma^\mu\epsilon^A\,\mathcal{P}^{Ir}_\mu \;-\; A_2^{A\dot{A}r}\epsilon^A \;=\; 0\,. \tag{7.72}$$

where we have taken $g=-1$ in accordance with (7.48). Here we will simply summarize the pertinent details needed to set up and solve these equations.

First, the covariant derivative on ϵ^A is defined by:

$$D_\mu\,\epsilon^A \;=\; \partial_\mu\epsilon^A \;+\; \frac{1}{4}\,\omega_\mu{}^{ab}\,\gamma_{ab}\,\epsilon^A + \frac{1}{4}\,\mathcal{Q}^{IJ}_\mu\Gamma^{IJ}_{AB}\,\epsilon^B\,, \tag{7.73}$$

where

$$\mathcal{Q}^{IJ}_\mu \;=\; \frac{1}{2}\,\Big[\,\big(P^{-1}\mathcal{D}_\mu\,P\big)_I{}^J \;-\; \big(P^{-1}\mathcal{D}_\mu\,P\big)_J{}^I \;+\; \mathscr{C}^{IJ}_\mu\,\Big]\,. \tag{7.74}$$

and $P = P^T$ is a symmetric $GL(4,\mathbb{R})$ matrix. The gauge covariant derivative is:

$$\mathcal{D}_\mu \mathcal{X}_I \;=\; \partial_\mu \mathcal{X}_I \;-\; 2\, g_0\, \widetilde{A}_\mu{}^{IJ}\, \mathcal{X}_J \,. \tag{7.75}$$

and it acts only on the left-hand side of P. The Chern-Simons vector fields are determined by:

$$\mathscr{C}_\mu^{IJ} \;\equiv\; P^{-1}{}_I{}^K\, P^{-1}{}_J{}^L\, C_\mu^{KL} \,, \qquad C_\mu{}^{IJ} \;=\; g_{\mu\rho}\, \varepsilon^{\rho\sigma\nu}\, m_{IK} m_{JL}\, F_{\sigma\nu}^{KL} \,. \tag{7.76}$$

The scalar kinetic terms, $\mathcal{P}_\mu^{Ir}$, are given by:

$$\begin{aligned} \mathcal{P}_\mu^{Ir} \;&=\; \frac{1}{2}\Big[\, \big(P^{-1}\mathcal{D}_\mu P\big)_I{}^r \;+\; \big(P^{-1}\mathcal{D}_\mu P\big)_r{}^I \;-\; \mathscr{C}_\mu^{Ir} \,\Big] \,, \qquad 1 \le r \le 4 \,, \\ \mathcal{P}_\mu^{I5} \;&=\; -\,\frac{1}{\sqrt{2}}\, \big(P^{-1}\big)_I{}^A\, \mathcal{D}_\mu \chi_A \,, \qquad 1 \le r \le 4 \,. \end{aligned} \tag{7.77}$$

We take the scalar matrix to be diagonal:

$$P \;=\; \mathrm{diag}\big(\, e^{\kappa_1} \,,\, e^{\kappa_2} \,,\, e^{\kappa_3} \,,\, e^{\kappa_4} \,\big) \,. \tag{7.78}$$

The superpotential is defined by:

$$\begin{aligned} W \;&\equiv\; \frac{1}{4}\, g_0\, (\det(P))^{-1} \Big[\, 2\left(1 - \frac{1}{4}\,(\chi_A \chi_A)\right) \;-\; \mathrm{Tr}\big(P\, P^T\big) \,\Big] \\ &=\; \frac{1}{4}\, g_0\, e^{-\kappa_1 - \kappa_2 - \kappa_3 - \kappa_4} \Big[\, 2\left(1 - \frac{1}{4}\,(\chi_A \chi_A)\right) \;-\; \left(e^{2\,\kappa_1} + e^{2\,\kappa_2} + e^{2\,\kappa_3} + e^{2\,\kappa_4}\right) \Big] \,, \end{aligned} \tag{7.79}$$

and the A-tensors are given by:

$$\begin{aligned} A_1^{AB} \;&=\; W\, \big(\Gamma^{1234}\big)_{AB} \,, \qquad & A_2^{A\dot{A}\, r} \;&=\; \frac{\partial W}{\partial \kappa_r}\, \big(\Gamma^{1234}\, \Gamma^r\big)_{A\dot{A}} \,, \quad 1 \le r \le 4 \,, \\ & & A_2^{A\dot{A}\, 5} \;&=\; -\sqrt{2} \sum_{j=1}^{4} e^{\kappa_j}\, \frac{\partial W}{\partial \chi_j}\, \big(\Gamma^{1234}\, \Gamma^j\big)_{A\dot{A}} \,, \end{aligned} \tag{7.80}$$

where there is no sum on r in the expression for $A_2^{A\dot{A}\, r}$.

Chapter 8

Superstrata in three dimensions

In [27], it was shown how to reduce the $(1, m, n)$ family of superstrata to an entirely three-dimensional description. In this Chapter we will summarize these results and use them to compute all the individual terms that go into the three-dimensional BPS equations.

The content of this Chapter is based on the work of [37]. It aims to provide a foothold on the way to constructing non-BPS geometries, by understanding how the well-known superstrata solutions fit inside the three-dimensional theory. It also serves as an indirect check of the uplift formulae of [27], by providing the means to verify that the 3D embedding of superstrata is indeed supersymmetric. This check will be done in Chapter 11.

8.1 The metric

Following on from Section 7.1.4, and for the rest of this Chapter, we use the coordinates (u, v, r) and work with asymptotically AdS geometries and use ζ defined in (7.12). For the superstrata, the three dimensional metric has the form [27]:

$$ds_3^2 = \frac{a^4 R_y^2 g_0^6}{2}\left(\mathrm{d}u + \mathrm{d}v + \frac{\sqrt{2}}{a^2 R_y g_0^4}\,\mathcal{A}\right)^2 - \frac{\Lambda^2}{g_0^2}\,ds_2^2\,, \tag{8.1}$$

where

$$ds_2^2 = \frac{|\mathrm{d}\zeta|^2}{\left(1-|\zeta|^2\right)^2} \quad \text{and} \quad \mathcal{A} = \frac{i}{2}\frac{\zeta\mathrm{d}\bar{\zeta} - \bar{\zeta}\mathrm{d}\zeta}{1-|\zeta|^2} = \frac{\sqrt{2}\,r^2}{a^2 R_y}\,\mathrm{d}v\,. \tag{8.2}$$

Note that, compared to (7.11), there is only one arbitrary function, Λ, in this metric. In particular, the "time fibration" part of the metric is a scaled version of that of the AdS metric.

For future reference, we note that the metric, ds_2^2, has a Kähler potential

$$\mathscr{K} \equiv -\log\left(1-|\zeta|^2\right) \tag{8.3}$$

and that $\mathcal{A}$ is the potential for the Kähler form. Thus the three-dimensional metric has the form of a canonical time-like Kähler fibration.

As we will see, supersymmetry requires that this warp factor be fixed in terms of the scalars:

$$\Lambda^2 \;=\; 1 \;-\; \frac{1}{4}\left(\chi_1^2+\chi_2^2+\chi_3^2+\chi_4^2\right). \tag{8.4}$$

We will use the frames:

$$e^0 \;=\; \frac{a^2 R_y g_0^3}{\sqrt{2}}(\mathrm{d}u+\mathrm{d}v)+\frac{1}{g_0}\mathcal{A}\,, \qquad e^1 \;=\; \frac{\Lambda}{g_0}\,\frac{1}{\sqrt{r^2+a^2}}\,\mathrm{d}r\;, \qquad e^2 \;=\; \frac{\Lambda}{g_0}\,\frac{\sqrt{2}\;r\,\sqrt{r^2+a^2}}{a^2 R_y}\,\mathrm{d}v\;, \tag{8.5}$$

such that

$$ds_3^2 \;=\; \left(e^0\right)^2-\left(e^1\right)^2-\left(e^2\right)^2\,. \tag{8.6}$$

The spin connection is then given by

$$\begin{aligned}
\omega^0{}_1 \;&=\; \omega^1{}_0 \;=\; \frac{g_0}{\Lambda^2}\,e^2\,, \qquad \omega^0{}_2 \;=\; \omega^2{}_0 \;=\; -\,\frac{g_0}{\Lambda^2}\,e^1\,,\\
\omega^1{}_2 \;&=\; -\,\omega^2{}_1 \;=\; \frac{g_0}{\Lambda^2}\,e^0+\frac{\lambda_2}{2\Lambda^2}\,e^1-\frac{\lambda_1}{2\Lambda^2}\,e^2-\frac{g_0}{\Lambda}\,\frac{2\,r^2+a^2}{r\,\sqrt{r^2+a^2}}\,e^2\,,
\end{aligned} \tag{8.7}$$

where λ_1 and λ_2 are defined by:

$$\mathrm{d}\left(\Lambda^2\right) \;\equiv\; \lambda_1\,e^1+\lambda_2\,e^2\,. \tag{8.8}$$

8.2 The scalars

The fundamental scalars that determine the superstratum fluxes are parameterized by two holomorphic functions, F_0 and F_1, of ζ:

$$\begin{aligned}
\chi_1+i\chi_2 \;&=\; -\,\frac{2\sqrt{2}\,a\,R_y\,g_0}{\sqrt{r^2+a^2}}\;i\,F_0(\zeta) \;=\; -\,2\sqrt{2}\,aR_y g_0\,i\left(e^{-\frac{1}{2}\mathscr{K}}\;F_0(\zeta)\right),\\
\chi_3-i\chi_4 \;&=\; \frac{2\sqrt{2}\,a\,R_y\,g_0}{\sqrt{r^2+a^2}}\;i\,F_1(\zeta) \;=\; 2\sqrt{2}\,aR_y g_0\,i\left(e^{-\frac{1}{2}\mathscr{K}}F_1(\zeta)\right).
\end{aligned} \tag{8.9}$$

where we have written these scalars in a more canonical form using the Kähler potential (8.3).

One should note that our expression for $\chi_3-i\chi_4$ differs by a phase from that of [27]. We have performed a $U(1)$ gauge transformation so as to make $\chi_3-i\chi_4$ have the same form as $\chi_1+i\chi_2$. As we will see, this gauge transformation also makes slight modifications elsewhere. One should also note the difference of sign in the two left-hand sides of (8.9): this will play a crucial role in the supersymmetry.

For future reference we note that the $(1,0,n)$ family of superstrata is defined by taking $\chi_3-i\chi_4=0$ and the $(1,1,n)$ family is defined by taking $\chi_1+i\chi_2=0$.

To describe the scalar sector, it is convenient to introduce the shorthand:

$$\rho_1^2 \;=\; \chi_1^2+\chi_2^2\;, \quad \rho_2^2 \;=\; \chi_3^2+\chi_4^2\;, \quad \rho_0^2 \;=\; \rho_1^2+\rho_2^2 \quad\text{and}\quad \Lambda^2 \;=\; 1-\frac{1}{4}\,\rho_0^2\,. \tag{8.10}$$

The scalar matrix m, with components m_{IJ}, which descends from the shape modes on S^3, is given by:

$$m = \mathbb{1} - \frac{1}{4}\begin{pmatrix} \rho_1^2 & 0 & \chi_1\chi_3 - \chi_2\chi_4 & \chi_1\chi_4 + \chi_2\chi_3 \\ 0 & \rho_1^2 & \chi_1\chi_4 + \chi_2\chi_3 & -(\chi_1\chi_3 - \chi_2\chi_4) \\ \chi_1\chi_3 - \chi_2\chi_4 & \chi_1\chi_4 + \chi_2\chi_3 & \rho_2^2 & 0 \\ \chi_1\chi_4 + \chi_2\chi_3 & -(\chi_1\chi_3 - \chi_2\chi_4) & 0 & \rho_2^2 \end{pmatrix}. \quad (8.11)$$

Note that this matrix is diagonal for the $(1,0,n)$ and $(1,1,n)$ sub-families separately. We also note that, while this matrix has exactly the same functional form as that of [27], it is, in fact, different. This is because we have made a gauge transformation to remove a phase from $\chi_3 - i\chi_4$. This gauge transformation also acts on the matrix m and preserves its functional form despite the non-trivial change in $\chi_3 - i\chi_4$.

8.3 The gauge fields

The gauge fields live in an $SU(2) \times U(1)$ subgroup of $SO(4)$ and so we introduce the matrices:

$$\eta_1 \equiv \begin{pmatrix} 0 & 0 & 0 & 1 \\ 0 & 0 & 1 & 0 \\ 0 & -1 & 0 & 0 \\ -1 & 0 & 0 & 0 \end{pmatrix}, \quad \eta_2 \equiv \begin{pmatrix} 0 & 0 & -1 & 0 \\ 0 & 0 & 0 & 1 \\ 1 & 0 & 0 & 0 \\ 0 & -1 & 0 & 0 \end{pmatrix}, \quad \eta_3 \equiv \begin{pmatrix} 0 & 1 & 0 & 0 \\ -1 & 0 & 0 & 0 \\ 0 & 0 & 0 & 1 \\ 0 & 0 & -1 & 0 \end{pmatrix}, \quad (8.12)$$

$$\bar{\eta}_1 \equiv \begin{pmatrix} 0 & 0 & 0 & 1 \\ 0 & 0 & -1 & 0 \\ 0 & 1 & 0 & 0 \\ -1 & 0 & 0 & 0 \end{pmatrix}, \quad \bar{\eta}_2 \equiv \begin{pmatrix} 0 & 0 & -1 & 0 \\ 0 & 0 & 0 & -1 \\ 1 & 0 & 0 & 0 \\ 0 & 1 & 0 & 0 \end{pmatrix}, \quad \bar{\eta}_3 \equiv \begin{pmatrix} 0 & 1 & 0 & 0 \\ -1 & 0 & 0 & 0 \\ 0 & 0 & 0 & -1 \\ 0 & 0 & 1 & 0 \end{pmatrix}. \quad (8.13)$$

The triplet (η_1, η_2, η_3) generates one of $\mathfrak{su}(2)$ algebra, while the triplet $(\bar{\eta}_1, \bar{\eta}_2, \bar{\eta}_3)$ generates the other commuting $\mathfrak{su}(2)$ algebra.

The gauge fields are then given by:

$$\tilde{A}^{IJ} = \frac{1}{\sqrt{2}a^2 R_y g_0}\left(C_1\eta_1^{IJ} + C_2\eta_2^{IJ} + C_3\eta_3^{IJ} + \bar{C}_3\bar{\eta}_3^{IJ}\right) \quad (8.14)$$

where

$$C_1 = \frac{1}{4}\left(\chi_1\chi_3 - \chi_2\chi_4\right)\kappa \qquad C_2 = \frac{1}{4}\left(\chi_1\chi_4 + \chi_2\chi_3\right)\kappa \qquad C_3 = -\frac{1}{8}\left(\rho_1^2 - \rho_2^2\right)\kappa, \quad (8.15)$$

$$\bar{C}_3 = -r^2\,\mathrm{d}v + \left(1 - \frac{1}{8}\left(\rho_1^2 + \rho_2^2\right)\right)\kappa, \quad (8.16)$$

and

$$\kappa \equiv \frac{1}{\Lambda^2}\left(\frac{a^4 R_y^2\, g_0^4}{2}(\mathrm{d}u + \mathrm{d}v) + r^2\,\mathrm{d}v\right) = \frac{a^2 R_y\, g_0}{\sqrt{2}\,\Lambda^2}\, e^0. \quad (8.17)$$

Once again, these gauge fields are slightly different from those given in [27] because we have made a gauge transformation to remove a phase from $\chi_3 - i\chi_4$.

8.4 The fields for the $(1,0,n)$ superstratum

It is extremely instructive to consider the pure $(1,0,n)$ superstratum in which one has $\chi_3 = \chi_4 = 0$. The scalar matrix reduces to:

$$m = \begin{pmatrix} \Lambda^2 & & & \\ & \Lambda^2 & & \\ & & 1 & \\ & & & 1 \end{pmatrix} \quad \Rightarrow \quad P = \begin{pmatrix} \Lambda & & & \\ & \Lambda & & \\ & & 1 & \\ & & & 1 \end{pmatrix}, \tag{8.18}$$

and the gauge fields (8.14) become

$$\begin{aligned} \tilde{A}^{12} &= \frac{a^2 R_y\, g_0^3}{2\sqrt{2}}\,(\mathrm{d}u + \mathrm{d}v) = \frac{e^0}{2} - \frac{r}{\sqrt{r^2+a^2}}\frac{e^2}{2\Lambda}, \\ \tilde{A}^{34} &= -\frac{a^2 R_y\, g_0^3}{2\sqrt{2}\Lambda^2}\,(\mathrm{d}u + \mathrm{d}v) + \frac{\Lambda^2-1}{\Lambda^2}\frac{r^2}{\sqrt{2}a^2 R_y g_0}\,\mathrm{d}v = -\frac{e^0}{2\Lambda^2} + \frac{r}{\sqrt{r^2+a^2}}\frac{e^2}{2\Lambda}. \end{aligned} \tag{8.19}$$

Since this connection is abelian, the field strength is simply $F = \mathrm{d}A$ and its components are given by:

$$F^{12} = -\frac{1}{\Lambda^4}\Big[g_0\,(1-\Lambda^2)\,e^1\wedge e^2 + \frac{1}{2}\,e^0\wedge\big(\lambda_1 e^1 + \lambda_2 e^2\big)\Big], \qquad F^{34} = 0\,. \tag{8.20}$$

We then find that the components of the Chern-Simons terms, (7.59), are given by:

$$\mathscr{C}^{12} = -\frac{1}{\Lambda^2}\Big[2g_0\,(1-\Lambda^2)\,e^0 + \lambda_2\,e^1 - \lambda_1\,e^2\Big], \qquad \mathscr{C}^{34} = 0\,. \tag{8.21}$$

Finally, the scalar kinetic terms (7.77) are:

$$\begin{aligned} \mathcal{P}^{Ir} &= \frac{1}{2\Lambda^2}\big(\lambda_1\,e^1 + \lambda_2\,e^2\big)\,\delta^r_I - \frac{1}{2}\mathscr{C}^{Ir}, \qquad 1\le r\le 2, \\ \mathcal{P}^{I3}_\mu &= \mathcal{P}^{I4}_\mu = 0, \qquad \mathcal{P}^{I5}_\mu = -\frac{1}{\sqrt{2}\,\Lambda}\,(\mathcal{D}_\mu\chi)_I\,. \end{aligned} \tag{8.22}$$

and the connection $\mathcal{Q}^{IJ}_\mu$, defined in (7.74), becomes

$$\mathcal{Q}^{IJ}_\mu = -2\,g_0\,A^{IJ}_\mu + \frac{1}{2}\mathscr{C}^{IJ}_\mu\,. \tag{8.23}$$

8.5 A gauge transformation of the full $(1,m,n)$ superstratum

We have written the supersymmetry transformations in terms of the "diagonal gauge" for P, (7.78), however (8.11) is not in that gauge. One can either recast the supersymmetry transformations in a general gauge, or one can diagonalize m. We choose the latter option.

Define

$$\mathscr{U} \equiv \begin{pmatrix} \frac{\rho_1}{\rho_0} & 0 & \frac{1}{\rho_0\,\rho_1}(\chi_1\chi_3 - \chi_2\chi_4) & \frac{1}{\rho_0\,\rho_1}(\chi_1\chi_4 + \chi_2\chi_3) \\ 0 & \frac{\rho_1}{\rho_0} & \frac{1}{\rho_0\,\rho_1}(\chi_1\chi_4 + \chi_2\chi_3) & -\frac{1}{\rho_0\,\rho_1}(\chi_1\chi_3 - \chi_2\chi_4) \\ 0 & \frac{\rho_2}{\rho_0} & -\frac{1}{\rho_0\,\rho_2}(\chi_1\chi_4 + \chi_2\chi_3) & \frac{1}{\rho_0\,\rho_2}(\chi_1\chi_3 - \chi_2\chi_4) \\ \frac{\rho_2}{\rho_0} & 0 & -\frac{1}{\rho_0\,\rho_2}(\chi_1\chi_3 - \chi_2\chi_4) & -\frac{1}{\rho_0\,\rho_2}(\chi_1\chi_4 + \chi_2\chi_3) \end{pmatrix}, \tag{8.24}$$

This is an $SO(4)$ matrix. Indeed, it commutes with $\bar{\eta}_3^{AB}$, and so lies in the same $SU(2) \times U(1)$ as the gauge connection (8.14). By construction, one has:

$$\hat{m} \equiv \mathscr{U}\, m\, \mathscr{U}^{-1} = \begin{pmatrix} \Lambda^2 & & & \\ & \Lambda^2 & & \\ & & 1 & \\ & & & 1 \end{pmatrix} \quad \Rightarrow \quad \hat{P} = \begin{pmatrix} \Lambda & & & \\ & \Lambda & & \\ & & 1 & \\ & & & 1 \end{pmatrix}, \tag{8.25}$$

where Λ is defined by (8.4). One also finds that

$$(\hat{\chi}_1, \hat{\chi}_2, \hat{\chi}_3, \hat{\chi}_4) \equiv \mathscr{U}\,(\chi_1, \chi_2, \chi_3, \chi_4) = \frac{\rho_0}{\rho_1}(\chi_1, \chi_2, 0, 0)\,. \tag{8.26}$$

Observe that, up to an overall factor, $\hat{\chi}_i$ is the same as for of the $(1, 0, n)$ superstratum. For future analysis, it is useful to separate out this factor and define:

$$\tilde{\chi}_I \equiv \frac{\rho_1}{\rho_0}\hat{\chi}_I\,, \qquad \Rightarrow \qquad \tilde{\chi} = (\chi_1, \chi_2, 0, 0)\,. \tag{8.27}$$

One should also note that

$$\hat{\Lambda}^2 \equiv 1 - \frac{1}{4}\left(\hat{\chi}_1^2 + \hat{\chi}_2^2 + \hat{\chi}_3^2 + \hat{\chi}_4^2\right) = \Lambda^2\,, \tag{8.28}$$

is gauge invariant.

The gauge transformation also significantly simplifies the gauge field:

$$\mathscr{U}\,\tilde{A}\,\mathscr{U}^{-1} = \frac{1}{2\sqrt{2}\,R_y a^2 g_0}\left[\left(\Lambda^2\,(\eta_3 + \bar{\eta}_3) + (\bar{\eta}_3 - \eta_3)\right)\kappa - 2\,r^2\,\bar{\eta}_3\,\mathrm{d}v\right] \equiv \tilde{A}_{\text{Abelian}}\,. \tag{8.29}$$

In terms of components, this implies that the only non-zero components are:

$$\begin{aligned} \tilde{A}^{12}_{\text{Abelian}} &= \left(\mathscr{U}\,\tilde{A}\,\mathscr{U}^{-1}\right)^{12} = \frac{e^0}{2} - \frac{r}{\sqrt{r^2 + a^2}}\frac{e^2}{2\Lambda}\,, \\ \tilde{A}^{34}_{\text{Abelian}} &= \left(\mathscr{U}\,\tilde{A}\,\mathscr{U}^{-1}\right)^{34} = -\frac{e^0}{2\Lambda^2} + \frac{r}{\sqrt{r^2 + a^2}}\frac{e^2}{2\Lambda}\,, \end{aligned} \tag{8.30}$$

which exactly matches the gauge connection (8.19) for the $(1, 0, n)$ superstratum. We have thus almost mapped the complete superstratum back onto the $(1, 0, n)$ superstratum using the local $SU(2) \times U(1)$ gauge transformation defined by $\mathscr{U}$. There are, however, two important differences. First, the functional dependence of (8.26) is a little more complicated than that of (8.9), and second, the transformed gauge potential is, of course:

$$\hat{\tilde{A}} = \tilde{A}_{\text{Abelian}} + \frac{1}{2\,g_0}\left(\mathrm{d}\mathscr{U}\right)\mathscr{U}^{-1}\,. \tag{8.31}$$

To write the last term in (8.31), we define:

$$\begin{aligned} K_1 &\equiv \frac{1}{\rho_1^2}(\chi_2\,\mathrm{d}\chi_1 - \chi_1\,\mathrm{d}\chi_2) = \mathrm{d}\arctan\left(\frac{\chi_1}{\chi_2}\right), \\ K_2 &\equiv \frac{1}{\rho_2^2}(\chi_4\,\mathrm{d}\chi_3 - \chi_3\,\mathrm{d}\chi_4) = \mathrm{d}\arctan\left(\frac{\chi_3}{\chi_4}\right), \\ L_1 &\equiv \mathrm{d}\log(\rho_1), \qquad L_2 \equiv \mathrm{d}\log(\rho_2), \end{aligned} \tag{8.32}$$

and then one has

$$\big(\mathrm{d}\mathscr{U}\big)\,\mathscr{U}^{-1} = \frac{1}{2\,\rho_0^2}(K_1+K_2)\Big[(\rho_2^2-\rho_1^2)\,\eta_3+\rho_0^2\,\bar\eta_3 + 2\,\rho_1\rho_2\,\eta_2\Big] + \frac{\rho_1\rho_2}{\rho_0^2}\big(L_1-L_2\big)\,\eta_1\,. \tag{8.33}$$

The field strength is then given by:

$$\hat{\tilde F} = \tilde F_{\rm Abelian} + \frac{\rho_1\rho_2}{8\,\Lambda^2}\,e^0\wedge\big((K_1+K_2)\,\eta_1 - (L_1-L_2)\,\eta_2\big) \tag{8.34}$$

where $\tilde F_{\rm Abelian} = \mathrm{d}\tilde A_{\rm Abelian}$ and $\tilde A_{\rm Abelian}$ is defined in (8.29), or (8.19). After taking the $SO(4)$ dual, $F_{\rm Abelian}$ can be read off from (8.20).

To compute the Chern-Simons terms we need the frame components of the K's and L's, and so we write

$$(K_1+K_2) = \mathcal{K}_1\,e^1 + \mathcal{K}_2\,e^2\,, \qquad (L_1-L_2) = \mathcal{L}_1\,e^1 + \mathcal{L}_2\,e^2\,. \tag{8.35}$$

We then obtain:

$$\begin{aligned} \hat{\mathscr{C}} = &-\frac{1}{2\,\Lambda^2}\Big[2g_0\,(1-\Lambda^2)\,e^0 + \lambda_2\,e^1 - \lambda_1\,e^2\Big](\eta_3+\bar\eta_3) \\ &+\frac{\rho_1\rho_2}{4\,\Lambda}\Big[\big(\mathcal{K}_2\,e^1 - \mathcal{K}_1\,e^2\big)\,\eta_1 - \big(\mathcal{L}_2\,e^1 - \mathcal{L}_1\,e^2\big)\,\eta_2\Big]. \end{aligned} \tag{8.36}$$

It is convenient to define the "Abelian" piece of this connection:

$$\mathscr{C}_{\rm Abelian} \equiv -\frac{1}{2\,\Lambda^2}\Big[2g_0\,(1-\Lambda^2)\,e^0 + \lambda_2\,e^1 - \lambda_1\,e^2\Big](\eta_3+\bar\eta_3)\,, \tag{8.37}$$

and we note that this is exactly the Chern-Simons connection (8.21) for the $(1,0,n)$ superstratum.

Finally, the scalar kinetic terms are a little more complicated than those of (8.22). We must use $\hat P$, defined in (8.25), which is identical to P in (8.18), in (7.60). The difference now is that the gauge field, $\tilde A$, is no longer $U(1)\times U(1)$ invariant and so $\mathcal{P}^{Ir}$ and $\mathcal{Q}^{IJ}$ have new gauge terms. We find:

$$\begin{aligned} \mathcal{P}^{Ir} &= \mathrm{d}\log(\Lambda)\,\delta^r_I - \frac{\rho_1\rho_2}{8\,\Lambda}\Big[(L_1-L_2)\,\eta_1 + (K_1+K_2)\,\eta_2\Big] - \frac{1}{2}\mathscr{C}^{Ir}\,, \qquad 1\le r\le 2\,, \\ \mathcal{P}^{Ir} &= +\frac{\rho_1\rho_2}{8\,\Lambda}\Big[(L_1-L_2)\,\eta_1 + (K_1+K_2)\,\eta_2\Big] - \frac{1}{2}\mathscr{C}^{Ir}\,, \qquad 3\le r\le 4\,, \\ \mathcal{P}^{I5}_\mu &= -\frac{1}{\sqrt{2}\,\Lambda}\,(\mathcal{D}_\mu\chi)_I\,. \end{aligned} \tag{8.38}$$

and the connection $\mathcal{Q}_\mu^{IJ}$, defined in (7.74), becomes

$$\mathcal{Q}_\mu^{IJ} \;=\; \begin{cases} -2\,g_0\,\tilde{A}_\mu^{IJ} \;+\; \frac{1}{2}\,\mathscr{C}_\mu^{IJ} & I,J\in\{1,2\} \text{ or } I,J\in\{3,4\} \\ -2\,g_0\,\frac{1+\Lambda^2}{\Lambda}\,\tilde{A}_\mu^{IJ} \;+\; \frac{1}{2}\,\mathscr{C}_\mu^{IJ} & I\in\{1,2\}\,,J\in\{3,4\} \text{ or } I\in\{3,4\}\,,J\in\{1,2\} \end{cases}. \tag{8.39}$$

Observe how the signs in front of the η-matrix terms flip between the first and second line of (8.38). This happens because because the covariant derivatives of P are symmetrized in $\mathcal{P}^{Ir}$.

8.6 Holomorphy

There are many significant aspects to holomorphy in the structure of the superstrata, but for now we focus on how this influences the solution of the BPS equations. In particular, we first observe that all the scalar fields, χ_i, in (8.9) involve a common, non-holomorphic pre-factor of $(r^2+a^2)^{-\frac{1}{2}}$. (As we saw in (8.9), this factor has a natural interpretation in terms of the Kähler potential.) The derivatives of this factor cancel out in (K_1+K_2) and (L_1-L_2), leaving only the derivatives of the holomorphic functions, F_0 and F_1.

Since we are working in real coordinates, it is simplest to express the holomorphy properties in terms of the Cauchy-Riemann equations, which take a very simple form when expressed in terms of the frames, e^1 and e^2. In particular, because the χ_i's are holomorphic up to a common pre-factor, we find that the Cauchy-Riemann equations imply:

$$\mathcal{K}_1 \;=\; \mathcal{L}_2\,, \qquad \mathcal{K}_2 \;=\; -\,\mathcal{L}_1\,. \tag{8.40}$$

One consequence of this is that the Chern-Simons term (8.36) can be re-written as:

$$\hat{\mathscr{C}} \;=\; \mathscr{C}_{\text{Abelian}} \;-\; \frac{\rho_1\rho_2}{4\,\Lambda}\Big[\,(L_1-L_2)\,\eta_1 \;+\; (K_1+K_2)\,\eta_2\,\Big]\,, \tag{8.41}$$

where $\mathscr{C}_{\text{Abelian}}$ is defined in (8.37).

As a result, we find that various pieces of the gauge connection and the Chern-Simons connection either cancel, or reinforce, in the 4×4 block of the scalar kinetic term:

$$\mathcal{P}^{IJ} \;=\; \begin{cases} \mathrm{d}\log(\Lambda)\,\delta^{IJ} \;-\; \frac{1}{2}\,\mathscr{C}^{IJ} & I,J\in\{1,2\} \\ 0 & I\in\{1,2\}\,,J\in\{3,4\} \\ -\mathscr{C}^{IJ} & I\in\{3,4\}\,,J\in\{1,2\} \\ 0 & I,J\in\{3,4\} \end{cases}, \tag{8.42}$$

and $\mathcal{P}_\mu^{I5}$ is unmodified:

$$\mathcal{P}_\mu^{I5} \;=\; -\,\frac{1}{\sqrt{2}\,\Lambda}\,(\mathcal{D}_\mu\chi)_I\,. \tag{8.43}$$

Holomorphy thus plays a critical role in the cancellation that produces the second row of (8.42), and, as we will see, this is essential to the supersymmetry.

Holomorphy also leads to another important identity. Observe that if χ_1 and χ_2 have the form (8.9) then $(\mathrm{d}-i\mathcal{A})(\chi_1+i\chi_2)$ is a holomorphic differential, and thus proportional to e^1+ie^2. This follows because the anti-holomorphic differentials cancel between $\mathcal{A}$ and $\mathrm{d}\mathscr{K}$. If one writes the differentials in terms of the real frame components:

$$\begin{aligned} \mathrm{d}\chi_1+\mathcal{A}\,\chi_2 &\equiv (\mathrm{d}\chi_1+\mathcal{A}\,\chi_2)_1\, e^1 \;+\; (\mathrm{d}\chi_1+\mathcal{A}\,\chi_2)_2\, e^2\,, \\ \mathrm{d}\chi_2-\mathcal{A}\,\chi_1 &\equiv (\mathrm{d}\chi_2-\mathcal{A}\,\chi_1)_1\, e^1 \;+\; (\mathrm{d}\chi_2-\mathcal{A}\,\chi_1)_2\, e^2\,, \end{aligned} \tag{8.44}$$

then holomorphy implies the Cauchy-Riemann conditions:

$$(\mathrm{d}\chi_1+\mathcal{A}\,\chi_2)_1 \;=\; (\mathrm{d}\chi_2-\mathcal{A}\,\chi_1)_2\,, \qquad (\mathrm{d}\chi_1+\mathcal{A}\,\chi_2)_2 \;=\; -\,(\mathrm{d}\chi_2-\mathcal{A}\,\chi_1)_1\,. \tag{8.45}$$

Note that (8.5) and (8.30) imply

$$\tilde{A}^{12}_{\text{Abelian}} \;=\; \frac{e^0}{2} \;-\; \frac{r}{\sqrt{r^2+a^2}}\frac{e^2}{2\Lambda} \;=\; \frac{1}{2}\,e^0 \;-\; \frac{1}{2\,g_0}\mathcal{A}\,, \tag{8.46}$$

which means that the covariant derivatives of χ_1 and χ_2 contain precisely the terms that are related by (8.45).

There is a parallel story for $\chi_3-i\chi_4$ if this also has the form given in (8.9).

Finally, we note that while the scalar matrix, m, generically lies in $GL(4,\mathbb{R})$, we have seen that we can use an $SU(2)\times U(1)$ gauge transformation to write it in terms of a simpler matrix, $\hat{m}$, in (8.25). This means that m actually lies in $GL(2,\mathbb{C})$. Similarly, the gauge fields are those of $SU(2)\times U(1)$ and the scalars, χ_I, should be thought of as a complex doublet, $(\chi_1+i\chi_2, \chi_3-i\chi_4)$, transforming under these global and local symmetries. Indeed, it might be natural to recast all the scalars in terms an element of $GL(3,\mathbb{C})$, or perhaps $SU(2,1)$. Either way, the BPS sector that we are studying can be recast in terms of the unitary gauge group acting on complex fields with precise holomorphy properties.

Chapter 9

Q-ball Ansätze

We now turn to the construction of new microstate geometries using the power of the three-dimensional consistent truncation. The first step, and the aim of the present Chapter, is to introduce ansätze for the fields of the theory that are generic enough to capture interesting new solutions, while being simple enough to be amenable to computations. In particular, we will show how these ansätze include the standard superstrata discussed in the previous Chapter.

This Chapter is based on the works of [38, 39] for the first two Sections, and on [42] for the last Section. We make use of a mechanism previously utilized for the construction of Q-balls, as well as for Bose stars. The core of the "Q-ball trick" is to isolate one or several complex scalar fields and give them a phase dependence of the form $e^{i\omega t}$, while arranging that these phases cancel in the currents and in the energy-momentum tensor. The result is to produce a background in which some of the scalars oscillate in time while the gauge fields and the metric are completely independent of t. The important effect of such time-dependent scalars is that they produce an effective shift in the scalar potential, changing the energetics.

9.1 A first ansatz with explicit time-dependence

There are several sectors of the three-dimensional supergravity in which the "Q-ball trick" can be implemented. In this Section, we start by describing a simple ansatz preserving the same $U(1)$ global symmetry as the $(1,0,n)$ superstrata. We aim to generalize these superstrata, so we will replace the expression for the scalar $\chi_1 + i\chi_2$ in (8.9) by

$$\chi_1 + i\chi_2 \;=\; \frac{a}{\sqrt{r^2+a^2}}\; F(\zeta,\bar{\zeta})\, e^{i\omega t}\,, \tag{9.1}$$

where we allow for the fact that a general non-supersymmetric solution will not necessarily lead to holomorphy. As for the $(1,0,n)$ superstrata, we put the other complex scalar field to zero, $\chi_3 + i\chi_4 = 0$ to preserve a global $U(1)$ invariance. The potential only depends on $|\chi|^2$ and so the time-dependence cancels there. However, the time-dependence does

not cancel in the equations for m_{IJ} and some of these scalars must also be made time dependent in a specific way.

This leads to an ansatz involving arbitrary functions of the coordinates r (or ξ) and ψ, and while there might be rich families of solutions, finding them is still too much of a challenge at this point. We further restrict the ansatz to "single-mode solutions", by electing to generalize only the single-mode superstratum, and thus fixing the dependence of the fields to the AdS circle ψ:

$$\chi_1 + i\chi_2 \;=\; \frac{a}{\sqrt{r^2+a^2}}\,\nu_1(\xi)\,e^{i(n\psi+\omega t)} \;=\; \sqrt{1-\xi^2}\,\nu_1(\xi)\,e^{i(n\psi+\omega t)}\,, \tag{9.2}$$

$$m_{IJ} \;=\; \begin{pmatrix} e^{\mu_1(\xi)}\,S_{2\times 2} & 0_{2\times 2} \\ 0_{2\times 2} & e^{\mu_2(\xi)}\,\mathbb{1}_{2\times 2} \end{pmatrix}\,, \tag{9.3}$$

where

$$S \;=\; \mathcal{O}^T \begin{pmatrix} e^{\lambda_1(\xi)} & 0 \\ 0 & e^{-\lambda_1(\xi)} \end{pmatrix} \mathcal{O}\,, \qquad \mathcal{O} \;=\; \begin{pmatrix} \cos(n\psi+\omega t) & \sin(n\psi+\omega t) \\ -\sin(n\psi+\omega t) & \cos(n\psi+\omega t) \end{pmatrix}\,, \tag{9.4}$$

for some scalar fields, ν_1, λ_1, μ_1 and μ_2, that depend only on the coordinate ξ. The mode numbers ω and n are fixed, and n must be an integer.

We also make an ansatz for the gauge fields:

$$\tilde{A}^{12} \;=\; \frac{1}{g_0}\,\big[\,\Phi_1(\xi)\,d\tau \;+\; \Psi_1(\xi)\,d\psi\,\big]\,, \qquad \tilde{A}^{34} \;=\; \frac{1}{g_0}\,\big[\,\Phi_2(\xi)\,d\tau \;+\; \Psi_2(\xi)\,d\psi\,\big]\,, \tag{9.5}$$

where we have introduced explicit factors of g_0^{-1} so as to cancel the g_0's in the minimal coupling and thus render the fields and interactions scale independent.

The metric is kept in the form (7.18), and we also assume that the fields Ω_0, Ω_1 and k are functions of ξ only.

The full ansatz thus involves eleven arbitrary functions of one variables, ξ, which can be assembled into a list:

$$\mathcal{F}_{\text{s.m.}} \;\equiv\; \{\,\nu_1\,,\;\lambda_1\,,\;\mu_1\,,\;\mu_2\,,\;\Phi_1\,,\;\Psi_1\,,\;\Phi_2\,,\;\Psi_2\,,\;\Omega_0\,,\;\Omega_1\,,\;k\,\}\,. \tag{9.6}$$

where the subscript s.m. stand for "single-mode". At this point, it is not clear that this ansatz, that we obtained in a very roundabout way, is consistent with the equations of motion. One way to prove it is to see that it corresponds to the more generic truncation of the theory that is invariant under the following four global symmetries:

(i) The internal $U(1)$ that rotates the indices $(3,4)$.

(ii) A time translation by $\tau \to \tau - \alpha$, accompanied by internal $U(1)$ rotation by $\alpha\,\omega$ in the $(1,2)$-direction, for an arbitrary parameter, α, and some frequency, ω.

(iii) A ψ-translation by $\psi \to \psi - \alpha$, accompanied by internal $U(1)$ rotation by $\alpha\,n$ in the $(1,2)$-direction, for an arbitrary parameter, α, and for some mode number, n.

(iv) Reflection invariance under $\psi \to -\psi$, $t \to -t$, accompanied by a discrete internal $SO(4)$ rotation, $2 \to -2$, $4 \to -4$.

9.1.1 The reduced action

The easiest way to express the equations of motion for this truncated system is to give the action from which they can be derived. The Lagrangian was given in (7.69), and here we simply specialize it to the ansatz.

The Lagrangian can be decomposed into pieces:

$$\mathcal{L} \;=\; \mathcal{L}_{\rm gravity} + \mathcal{L}_\chi + \mathcal{L}_m + \mathcal{L}_A + \mathcal{L}_{CS} + \mathcal{L}_Y - \sqrt{g}\,V \;, \tag{9.7}$$

and the explicit expressions are:

$$\begin{aligned}
\mathcal{L}_{\rm gravity} &\equiv -\frac{1}{4}\sqrt{g}\;R \\
&= \frac{\Omega_1}{8\,g_0\,\xi}\left[\frac{\Omega_1^2}{\Omega_0^2}\left(k' + \frac{2\,\xi}{1-\xi^2}\,k\right)^2 - 4\,\xi\left(\partial_\xi\Big(\xi\,\frac{\Omega_0'}{\Omega_0}\Big) + \frac{1}{\Omega_1}\,\partial_\xi\Big(\xi\,\Omega_1'\Big)\right) - \frac{16\,\xi^2}{(1-\xi^2)^2}\right]
\end{aligned} \tag{9.8}$$

$$\begin{aligned}
\mathcal{L}_\chi &\equiv \frac{1}{8}\sqrt{g}\,g^{\mu\nu}\,(\mathcal{D}_\mu\chi_I)\,m^{IJ}\,(\mathcal{D}_\nu\chi_J) \\
&= \frac{e^{\lambda_1-\mu_1}}{8\,g_0\,\xi\,(1-\xi^2)\,\Omega_1}\left[\Gamma\,\nu_1^2 \;-\; \xi^2\,(1-\xi^2)\,\Omega_1^2\,e^{-2\lambda_1}\left(\partial_\xi\Big(\sqrt{1-\xi^2}\,\nu_1\Big)\right)^2\right]
\end{aligned} \tag{9.9}$$

$$\begin{aligned}
\mathcal{L}_m &\equiv \frac{1}{16}\sqrt{g}\,g^{\mu\nu}\;\mathrm{Tr}\big(m^{-1}(\mathcal{D}_\mu m)m^{-1}(\mathcal{D}_\nu m)\big) \\
&= \frac{1}{2\,g_0\,\xi\,(1-\xi^2)^2\,\Omega_1}\left[\Gamma\,\sinh^2\lambda_1 \;-\; \frac{1}{4}\xi^2\,(1-\xi^2)^2\,\Omega_1^2\,\big((\lambda_1')^2 + (\mu_1')^2 + (\mu_2')^2\big)\right]
\end{aligned} \tag{9.10}$$

$$\begin{aligned}
\mathcal{L}_A &\equiv -\frac{1}{8}\,e\,g^{\mu\rho}\,g^{\nu\sigma}\,m_{IK}\,m_{JL}\,F_{\mu\nu}^{IJ}\,F_{\rho\sigma}^{KL} \\
&= \frac{1}{2g_0\,\xi\,\Omega_1}\Big[\xi^2\left(e^{2\mu_2}\;\Phi_1'^2 \;+\; e^{2\mu_1}\;\Phi_2'^2\right) \\
&\qquad\qquad - \frac{\Omega_1^2}{\Omega_0^2}\left(e^{2\mu_2}\left((1-\xi^2)\,\Psi_1' - k\,\Phi_1'\right)^2 + e^{2\mu_1}\left((1-\xi^2)\,\Psi_2' - k\,\Phi_2'\right)^2\right)\Big]
\end{aligned} \tag{9.11}$$

$$\begin{aligned}
\mathcal{L}_{CS} &\equiv \frac{1}{2}\,g_0\,e\,\varepsilon^{\mu\nu\rho}\left(A_\mu{}^{IJ}\,\partial_\nu\widetilde{A}_\rho{}^{IJ} \;+\; \frac{4}{3}\,g_0\,A_\mu{}^{IJ}\,A_\nu{}^{JK}\,A_\rho{}^{KI}\right) \\
&= \frac{1}{g_0}(\Phi_1\Psi_2' - \Psi_2\Phi_1' + \Phi_2\Psi_1' - \Psi_1\Phi_2')
\end{aligned} \tag{9.12}$$

$$\begin{aligned}
\mathcal{L}_Y &\equiv \frac{1}{16}\,e\,\varepsilon^{\mu\nu\rho}\,Y_\mu{}^{IJ}\,F_{\nu\rho}^{IJ} \\
&= \frac{1}{4g_0}\big(1-\xi^2\big)\,\nu_1^2\,\big((2\Psi_1+n)\,\Phi_2' \;-\; (2\Phi_1+\omega)\,\Psi_2'\big)
\end{aligned} \tag{9.13}$$

$$\begin{aligned}
V &= \frac{g_0^2}{2}\,e^{-2(\mu_1+\mu_2)}\Big[1 - 2\,e^{\mu_1+\mu_2}\cosh(\lambda_1) + e^{2\mu_1}\sinh^2\lambda_1 \\
&\qquad\qquad + \frac{1}{16}\nu_1^2\,\big(1-\xi^2\big)\big((1-\xi^2)\,\nu_1^2 + 4\,e^{\lambda_1+\mu_1} - 8\big)\Big]\,,
\end{aligned} \tag{9.14}$$

where, $'$ indicates a differentiation with respect to ξ. We are also using the convenient

shorthand that captures the mode dependence and minimal couplings:

$$\Gamma \;=\; \xi^2\Omega_0^2\left[\omega+2\,\Phi_1\right]^2 \;-\; \Omega_1^2\left[(1-\xi^2)\left(n+2\,\Psi_1\right) \;-\; k\left(\omega+2\,\Phi_1\right)\right]^2. \tag{9.15}$$

In particular, we note that the mode number, n, and the frequency, ω, can be absorbed into constant terms in Ψ_1 and Φ_1, respectively.

There are also three integrals of the motion:

$$\begin{aligned} H \;\equiv\; \frac{\xi^2\,(1-\xi^2)}{k}\Bigg[\frac{1}{\xi\,\Omega_1}\left(\widehat{\mathcal{L}}_{\rm gravity}+\mathcal{L}_A+\sqrt{g}\,V-\mathcal{L}_\chi-\mathcal{L}_m\right) \\ -\frac{1}{4g_0}\left((\lambda_1')^2+(\mu_1')^2+(\mu_2')^2 \;+\; e^{-(\lambda_1+\mu_1)}\left(\partial_\xi\left(\sqrt{1-\xi^2}\,\nu_1\right)\right)^2\right)\Bigg]. \end{aligned} \tag{9.16}$$

and

$$\mathcal{I}_1 \;\equiv\; \frac{e^{2\,\mu_1}\,(1-\xi^2)\,\Omega_1}{\xi\,\Omega_0^2}\left((1-\xi^2)\,\Psi_2'-k\,\Phi_2'\right) \;-\; \left(\omega+2\,\Phi_1\right)\left(1-\frac{1}{4}\,(1-\xi^2)\,\nu_1^2\right), \tag{9.17}$$

$$\mathcal{I}_2 \;\equiv\; \frac{e^{2\,\mu_1}\,k\,\Omega_1}{\xi\,\Omega_0^2}\left((1-\xi^2)\,\Psi_2'-k\,\Phi_2'\right) \;+\; \frac{e^{2\,\mu_1}\,\xi\,\Phi_2'}{\Omega_1} \;-\; \left(p+2\,\Psi_1\right)\left(1-\frac{1}{4}\,(1-\xi^2)\,\nu_1^2\right). \tag{9.18}$$

9.2 A time-independent single-sector ansatz

We have obtained in the previous Section a family of ansätze, parameterized by two mode numbers n and ω. We remarked that in the equations of motion, these two parameters can be reabsorbed into constant terms in Ψ_1 and Φ_1. As we will now explain, this is a consequence of the fact that all these ansätze are connected by gauge transformations.

In Section 7.6, we mentioned that three-dimensional theory has a residual $SO(4)$ gauge symmetry, that can be fixed by for example diagonalizing m_{IJ}. Consider the following $SO(4)$ matrix:

$$U=\begin{pmatrix}\cos(\Delta\omega\,t+\Delta n\,\psi) & -\sin(\Delta\omega\,t+\Delta n\,\psi) & 0 & 0\\ \sin(\Delta\omega\,t+\Delta n\,\psi) & \cos(\Delta\omega\,t+\Delta n\,\psi) & 0 & 0\\ 0 & 0 & 1 & 0\\ 0 & 0 & 0 & 1\end{pmatrix}. \tag{9.19}$$

where $\Delta\omega$ is a real number and Δn is an integer. The scalars χ_I transform in the vector representation, the matrix m_{IJ} transforms in the symmetric matrix representation, and the gauge fields transform as:

$$\tilde{A}\to U\,\tilde{A}\,U^{-1}+\frac{1}{2\,g_0}\,(d\,U)\,U^{-1}. \tag{9.20}$$

When acting on the fields on the ansatz, it leads to:

$$\omega\to\omega+\Delta\omega\,,\qquad n\to n+\Delta n\,,\qquad \Phi_1\to\Phi_1-\Delta\omega/2\,,\qquad \Psi_1\to\Psi_1-\Delta n/2\,. \tag{9.21}$$

This transformation thus shifts the mode numbers, and lets us rewrite solutions from one ansatz to another. In other words, all the ansätze in the family are equivalent.

This means that one can decide to focus uniquely on the ansatz where $\omega = n = 0$. Note that in this specific ansatz, the matrix m_{IJ} is diagonal, and all the scalars are time-independent, which makes the computation of the supersymmetry equations much easier. Because the mode numbers only appear as boundary values of the gauge fields, it also greatly simplifies the numerics.

Because of the importance of this ansatz, which we be used in many computations in the following Chapters, we make a recap of the field content. Starting from first principles, the ansatz can be obtained from the same symmetries as in the previous Section, replacing (ii) and (iii) by:

(ii') Invariance under time translation $\tau \to \tau - \alpha$.

(iii') Invariance under ψ-translation $\psi \to \psi - \beta$.

For the scalars, χ_I, the symmetries imply that

$$\chi_2 \;=\; \chi_3 \;=\; \chi_4 \;=\; 0\,, \tag{9.22}$$

and that the remaining field, χ_1, is only a function of ξ. Similarly, the scalar matrix must be diagonal, and the entries are only functions of ξ. Also note that the symmetry requirement (i) means that the last two eigenvalues of m must be equal. We therefore have

$$\chi_1 \;=\; \sqrt{1-\xi^2}\,\nu_1(\xi)\,, \quad \chi_2 = \chi_3 = \chi_4 \;=\; 0\,, \qquad m \;=\; \mathrm{diag}\left(\, e^{\mu_1+\lambda_1}\,,\, e^{\mu_1-\lambda_1}\,,\, e^{\mu_2}\,,\, e^{\mu_2}\,\right), \tag{9.23}$$

where we have introduced the factor of $\sqrt{1-\xi^2}$ into χ_1 for convenience later to define the perturbation theory and holography.

The symmetry (i) also reduces the gauge fields to $\tilde{A}^{12}$ and $\tilde{A}^{34}$, while remaining symmetries mean that these fields can only depend on ξ, and have no $d\xi$ components. The gauge fields can therefore be reduced to:

$$\tilde{A}^{12} \;=\; \frac{1}{g_0}\left[\,\Phi_1(\xi)\,d\tau \;+\; \Psi_1(\xi)\,d\psi\,\right], \qquad \tilde{A}^{34} \;=\; \frac{1}{g_0}\left[\,\Phi_2(\xi)\,d\tau \;+\; \Psi_2(\xi)\,d\psi\,\right], \tag{9.24}$$

where, as previously, we have introduced explicit factors of g_0^{-1} so as to cancel the g_0's in the minimal coupling and thus render the fields and interactions scale independent.

Finally, the time-translation and ψ-translational invariance means that Ω_0, Ω_1 and k, can only depend on ξ.

9.2.1 Remark on the physical meaning of the mode numbers

We explained how the mode numbers ω and n are artifacts that can be removed through a gauge transformation. Why, then, introduce them in the first place ?

The first thing to notice is that n is indeed a physical parameter, it corresponds to the periodicity of the scalars around the y-circle. It is indeed possible to choose a gauge where $n = 0$ to simplify the computation, but the solutions in this gauge are not smooth: Ψ_1 limits to a constant at the origin, which can be seen as a Dirac string singularity. The solutions are only really smooth when one comes back to the correct gauge where Ψ_1 limits to zero at the origin, and $n \neq 0$.

The standing of the parameter ω is more subtle. The gauge rotation (9.19), while perfectly valid in classical supergravity, is actually anomalous in the quantum theory. This means that, from the point of view of the quantum theory, there is really only one correct gauge in which the solution can live. The parameter ω in that gauge is thus the "physical" frequency. At the level of classical supergravity, this frequency cannot be determined. However, using the tools of holography and AdS/CFT, it is possible to compute this frequency. This point will be discussed in more details in Chapter 14 on holography.

9.2.2 Superstratum in the single-mode ansatz

For completeness, we summarize here how the $(1, 0, n)$ single-mode superstratum is written inside the ansatz. Note that the gauge invariances have not yet been completely fixed, and Ω_1 is at this point an arbitrary constant. We discuss how to gauge fix the solutions in Section 12.1.

$$\begin{aligned}
\nu_1 &= \alpha\xi^n\,, \qquad e^{\mu_1} = 1 - \frac{1}{4}\alpha^2(1-\xi^2)\xi^{2n}\,, \qquad e^{\lambda_1} = e^{\mu_2} = 1 \\
\Phi_1 &= \frac{\Omega_1}{2}\,, \qquad \Phi_2 = \frac{\Omega_1}{2}\left(1 - \frac{1}{1-\frac{1}{4}\alpha^2(1-\xi^2)\xi^{2n}}\right) \\
\Psi_1 &= n/2\,, \qquad \Psi_2 = \frac{1}{2}\frac{\xi^2}{1-\xi^2}\left(1 - \frac{1}{1-\frac{1}{4}\alpha^2(1-\xi^2)\xi^{2n}}\right) \\
\Omega_0^2 &= 1 - \frac{1}{4}\alpha^2(1-\xi^2)\xi^{2n}\,, \qquad k = \Omega_1^{-1}\xi^2\,.
\end{aligned} \tag{9.25}$$

The solution is parameterized by a real number $-2 < \alpha < 2$, which is related to the more standard superstrata parameters a and b through:

$$\frac{b}{a} = \sqrt{\frac{2\alpha^2}{4-\alpha^2}}\,. \tag{9.26}$$

9.3 Double-sector ansatz

We now build a more general truncation, that includes the full $(1, m, n)$ superstratum, and that allows for two independent pair of mode numbers (ω_1, n_1) and (ω_2, n_2). As explained in the previous Section, the single-mode ansätze with different mode numbers can be related through gauge transformations, and this remains true for the double-mode truncation that we define here. Thus, for simplicity we will write this ansatz directly in

a time-independent gauge, where the mode numbers appear only as boundary conditions for the gauge fields.

To obtain the truncation, we start with the same invariances as the single-sector ansatz, but we forgo the constraint (i). In other words, we no longer require that the truncation be invariant under a global $U(1)$ that rotates the indices $(3,4)$. The other constraints are kept identical:

(ii') Invariance under time translation $\tau \to \tau - \alpha$.

(iii') Invariance under ψ-translation $\psi \to \psi - \beta$.

(iv) Reflection invariance under $\psi \to -\psi$, $t \to -t$, accompanied by a discrete internal $SO(4)$ rotation, $2 \to -2$, $4 \to -4$.

The first immediate consequence is that χ_3 is no longer forced to be zero by the symmetry, and it appears as a new scalar field. We parameterize the χ_I scalars as

$$\chi_1 \;=\; \sqrt{1-\xi^2}\nu_1(\xi)\,, \qquad \chi_3 \;=\; \sqrt{1-\xi^2}\nu_2(\xi)\,, \qquad \chi_2 \;=\; \chi_4 \;=\; 0\,. \tag{9.27}$$

New degrees of freedom also appears in the scalar matrix m, that we can parameterize as:

$$m \;=\; \begin{pmatrix} e^{\mu_1+\lambda_1} & 0 & m_5 & 0 \\ 0 & e^{\mu_1-\lambda_1} & 0 & m_6 \\ m_5 & 0 & e^{\mu_2+\lambda_2} & 0 \\ 0 & m_6 & 0 & e^{\mu_2-\lambda_2} \end{pmatrix}, \tag{9.28}$$

and all these fields can only be functions of ξ.

The gauge fields, $\tilde{A}^{IJ}$, are classified as to whether they are even or odd under $2 \to -2$, $4 \to -4$: if they are odd, they can only have components along $d\tau$ or $d\psi$, and if they are even then they can only have $d\xi$ components. We therefore have:

$$\begin{aligned} \tilde{A}^{12} \;&=\; \frac{1}{g_0}\left[\,\Phi_1(\xi)\,d\tau \;+\; \Psi_1(\xi)\,d\psi\,\right], & \tilde{A}^{34} \;&=\; \frac{1}{g_0}\left[\,\Phi_2(\xi)\,d\tau \;+\; \Psi_2(\xi)\,d\psi\,\right], \\ \tilde{A}^{23} \;&=\; \frac{1}{g_0}\left[\,\Phi_3(\xi)\,d\tau \;+\; \Psi_3(\xi)\,d\psi\,\right], & \tilde{A}^{14} \;&=\; \frac{1}{g_0}\left[\,\Phi_4(\xi)\,d\tau \;+\; \Psi_4(\xi)\,d\psi\,\right], \\ \tilde{A}^{13} \;&=\; \frac{1}{g_0}\,\Psi_5(\xi)\,d\xi\,, & \tilde{A}^{24} \;&=\; \frac{1}{g_0}\,\Psi_6(\xi)\,d\xi\,. \end{aligned} \tag{9.29}$$

As for the metric functions, the symmetries imply once again that Ω_0, Ω_1 and k be functions of ξ only.

This truncation obviously contains the previous time-independent ansatz, but it also contains new fields and will allow for new solutions.

There are residual gauge invariances that allow one to make ξ-dependent $U(1)$ rotations in both the $(1,3)$ and $(2,4)$ directions. There are two natural ways to fix the gauge, that we explore in the following two subSections.

9.3.1 Diagonal gauge

Here one fixes the gauge by setting $m_5 = m_6 = 0$ in (9.28). We will find it useful to parametrize the matrix P, in this gauge according to

$$P \;=\; \mathrm{diag}\big(\, e^{\frac{1}{2}(\mu_1+\lambda_1)}\,,\, e^{\frac{1}{2}(\mu_1-\lambda_1)}\,,\, e^{\frac{1}{2}(\mu_2+\lambda_2)}\,,\, e^{\frac{1}{2}(\mu_2-\lambda_2)}\big) \quad \text{with} \quad m \;=\; P\,P^T\,, \tag{9.30}$$

as in (7.57). The gauge with diagonal P is more convenient for the analysis of the supersymmetry. In this gauge, the Ansatz involves the following nineteen arbitrary functions of one variable, ξ:

$$\mathcal{F}_{\text{d.m.d}} \;\equiv\; \big\{\, \nu_1\ ,\nu_2\,,\ \mu_1\,,\ \mu_2\,,\ \lambda_1\,,\ \lambda_2\,,\ \Phi_1\,,\ldots,\Phi_4\,,\ \Psi_1\,,\ldots\,,\Psi_6\,,\ \Omega_0\,,\ \Omega_1\,,\ k\,\big\}\,, \tag{9.31}$$

and the subscript d.m.d stands for "double-mode in diagonal gauge".

9.3.2 Axial gauge

Here one fixes the residual gauge invariance by setting $\Psi_5 = \Psi_6 = 0$ in (9.29). Note that if $m_5 = m_6 = 0$, then this parametrization matches (9.30).

As we will see, this gauge is more convenient for the perturbative solutions to the equations of motion. The Ansatz now involves the following nineteen arbitrary functions of one variable, ξ:

$$\mathcal{F}_{\text{d.m.a}} \;\equiv\; \big\{\, \nu_1\ ,\nu_2\,,\ \mu_1\,,\ \mu_2\,,\ \lambda_1\,,\ \lambda_2\,,\ m_5\,,\ m_6\,,\ \Phi_1\,,\ldots,\Phi_4\,,\ \Psi_1\,,\ldots\,,\Psi_4\,,\ \Omega_0\,,\ \Omega_1\,,\ k\,\big\}\,, \tag{9.32}$$

and the subscript d.m.a stands for "double-mode in axial gauge".

9.3.3 The double superstratum

As explained in Chapter 8, the double superstratum was obtained in [26] and recast in three-dimensional supergravity in [27]. The fundamental scalars that create this solution involve setting

$$\chi_1 + i\chi_2 \;=\; \sqrt{1-\xi^2}\,G_0(\zeta)\,, \qquad \chi_3 - i\chi_4 \;=\; \sqrt{1-\xi^2}\,G_1(\zeta)\,, \tag{9.33}$$

where $\zeta \equiv \xi e^{i\psi}$ and G_0 and G_1 are any holomorphic functions. The remaining fields are then determined in terms of the G_j.

To fit within the double-mode ansatz, one must first once again restrict to the solutions by taking $G_0(\zeta) = \alpha_1\zeta^{n_1}$ and $G_1(\zeta) = \alpha_1\zeta^{n_2}$, for some positive integers n_1, n_2 and some arbitrary constants α_1 and α_2. One must them make a gauge transformation so as to remove the ψ-dependence. This introduces n_1 and n_2 as constants in Ψ_1 and Ψ_2. One therefore starts from (9.27) with:

$$\nu_1 \;=\; \alpha_1\,\xi^{n_1}\,, \qquad \nu_2 \;=\; \alpha_2\,\xi^{n_2}\,, \qquad \Psi_1(0) \;=\; \frac{1}{2}\,n_1\,, \qquad \Psi_2(0) \;=\; -\,\frac{1}{2}\,n_2\,. \tag{9.34}$$

It will be easiest to verify the supersymmetries with the projectors (10.1) if one makes a further $SO(4)$ rotation in the $(1,3)$ plane so as to write the double superstratum in the diagonal gauge and obtain:

$$\nu_1 \;=\; \sqrt{\alpha_1^2\,\xi^{2\,n_1} \;+\; \alpha_2^2\,\xi^{2\,n_2}}\,, \qquad \nu_2 \;=\; 0\,. \tag{9.35}$$

As we will check, the full BPS solution is given by:

$$\begin{aligned}
&\lambda_1 \;=\; 0\,, \qquad \lambda_2 \;=\; 0\,, \qquad \mu_1 \;=\; \log\big(1 \;-\; \frac{1}{4}\,(1-\xi^2)\,\nu_1^2\big)\,, \qquad \mu_2 \;=\; 0\,,\\
&\nu_1 \;=\; \sqrt{\alpha_1^2\,\xi^{2\,n_1} \;+\; \alpha_2^2\,\xi^{2\,n_2}}\,, \qquad \nu_2 \;=\; 0\,,\\
&\Phi_1 \;=\; \frac{\Omega_1}{2}\,e^{-\mu_2} \;=\; \frac{1}{2}\,, \qquad \Phi_2 \;=\; -\,\frac{\Omega_1}{2}\,e^{-\mu_1}\,, \qquad \Phi_3 \;=\; \Phi_4 \;=\; 0\,,\\
&\Psi_1 \;=\; \frac{1}{2}\,n_2 \;+\; \frac{1}{2}(n_1-n_2)\frac{\alpha_1^2\,\xi^{2n_1}}{\nu_1^2}\,,\\
&\Psi_2 \;=\; -\,\frac{1}{2}\,n_1 \;+\; \frac{1}{2}(n_1-n_2)\frac{\alpha_1^2\,\xi^{2n_1}}{\nu_1^2} \;+\; \frac{\xi^2}{2(1-\xi^2)}\,\big(1-e^{-\mu_1}\big)\,,\\
&\Psi_3 \;=\; \Psi_4 \;=-\xi\,\Psi_5 \;=\; \xi\,\Psi_6 \;=\; \frac{1}{2}\,(n_1-n_2)\,\frac{\alpha_1\alpha_2\,\xi^{n_1+n_2}}{\nu_1^2}\,,\\
&\Omega_0 \;=\; \sqrt{1-\frac{1}{4}(1-\xi^2)\nu_1^2}\,, \qquad \Omega_1 \;=\; 1-\frac{1}{4}\big(\alpha_1^2+\alpha_2^2\big)\,, \qquad k \;=\; \Omega_1^{-1}\xi^2\,.
\end{aligned} \tag{9.36}$$

The standard single superstratum is obtained by setting $\alpha_1 = 0$ or $\alpha_2 = 0$. To recover (9.25) one also needs to reverse the $SO(4)$ that was used previously to obtain the solution in the diagonal gauge.

An important aspect of the double superstratum is that a non-trivial value of η_ψ is essential to its smoothness. Setting $\eta_\psi = 0$ gives $n_2 = -(n_1+1)$, which produces a smooth solution if and only $\alpha_1 = 0$ or $\alpha_2 = 0$.

Chapter 10

The BPS equations

In this Chapter, we derive the BPS equations of the three-dimensional theory, given in Section 7.8 for the specific ansätze described in Chapter 9. We will first focus on the single-mode truncation, for which we will derive the full set of BPS equations in details. The last Section will be devoted to the generalization to the double-mode ansatz. This Chapter is based on the work of [37, 41] for the results in the single-mode truncation, and on [42] for the last Section on the double-mode truncation.

The starting point of the BPS analysis is to decide which of the supersymmetries are to be preserved, and a standard way to do this is to use projectors. Indeed, we will require that any residual supersymmetries obey:

$$\left(\mathbb{1} \, - \, \gamma^{12}\,\Gamma^{12}\right)\epsilon \, = \, 0\,, \qquad \left(\mathbb{1} \, + \, \gamma^{12}\,\Gamma^{34}\right)\epsilon \, = \, 0\,, \tag{10.1}$$

which implies:

$$\left(\mathbb{1} \, - \, \Gamma^{1234}\right)\epsilon \, = \, 0\,. \tag{10.2}$$

We refer to the Section 7.1 for an explanation on the notations for the projectors. Any two of the projectors from (10.1) and (10.2) imply the third. These projectors are the ones that are preserved by superstrata: choosing them will let us find new BPS solutions that generalize the superstrata construction.

We also need to allow phase dependencies in the supersymmetries:

$$\mathrm{d}\epsilon \, = \, \Gamma^{12}\,(\eta_\tau \mathrm{d}\tau + \eta_\psi \mathrm{d}\psi)\,\epsilon\,, \tag{10.3}$$

for some constants η_τ and η_ψ. Note that this phase dependence is consistent with the discrete symmetries (ii') and (iii') defined in Section 9.2.

It is important to note that the projectors (10.1) and phase dependencies *are not invariant* under internal $SO(4)$ rotations, and, in particular, not invariant under the $1 \leftrightarrow 3$ and $2 \leftrightarrow 4$ rotations. None of these rotations preserve the single-mode truncation, but there are some rotations preserving the double-mode truncation, such as the rotation that transposes between the axial and diagonal gauges. Thus the projectors and phase dependencies that we are imposing are not the most general possibilities allowed in the double-mode truncation, and so, for this truncation, we will only derive a subsystem of all the BPS solutions.

10.1 Preparing the computation

We will set up the BPS equations in a manner that will cover both the single-mode Q-ball truncation and the Coulomb branch of the theory, that is not discussed in this manuscript, but can be found in [40]. In particular, this means that we will initially allow many of the fields to depend on ξ and ψ.

The field, ν_1, vanishes in the Coulomb branch flows and only depends on ξ in the Q-ball truncation, and so we will also restrict ν_1 to being a function of ξ alone throughout this analysis. Ω_1 is taken to be constant. The remaining fields, Ω_0, λ_1, μ_1, μ_2, Φ_j, Ψ_j will, initially, be allowed to be functions of both ξ and ψ. We will specialize them later to the two classes of truncation.

With these assumptions, we now catalog all the terms that go into the supersymmetry variations and thus define the BPS equations.

10.1.1 The frames and connection

We use the frames that are best adapted to the supersymmetry:

$$e^0 = g_0^{-1}\Omega_1\left(d\tau + \frac{k}{(1-\xi^2)}\,d\psi\right), \qquad e^1 = g_0^{-1}\frac{\Omega_0}{1-\xi^2}\,d\xi\,, \qquad e^2 = g_0^{-1}\frac{\Omega_0}{1-\xi^2}\,\xi\,d\psi \tag{10.4}$$

The spin connections, defined as $de^a + \omega^a_{\ b}\wedge e^b = 0$, are given by:

$$\omega_{01} = s_0 e^2\,, \quad \omega_{02} = -s_0 e^1 \quad \text{and} \quad \omega_{12} = -s_0 e^0 + s_1 e^1 + s_2 e^2 \tag{10.5}$$

where

$$\begin{aligned} s_0 &= g_0\Omega_1\frac{2\xi k + (1-\xi^2)\partial_\xi k}{2\xi\Omega_0^2}\,, \qquad & s_1 &= -g_0\frac{(1-\xi^2)\partial_\psi\Omega_0}{\xi\Omega_0^2}\\ s_2 &= g_0\frac{(1+\xi^2)\Omega_0 + \xi(1-\xi^2)\partial_\xi\Omega_0}{\xi\Omega_0^2}\,. \end{aligned} \tag{10.6}$$

10.1.2 The scalar terms

The scalar kinetic terms, $\mathcal{P}$, defined in (7.60), are given by:

$$\begin{aligned} \mathcal{P}^{IJ} = {}& 2g_0\sinh(\lambda_1)\left(\Omega_1^{-1}\Phi_1 e^0 + \frac{(1-\xi^2)\Psi_1 - k\Phi_1}{\xi\Omega_0}e^2\right)\mathcal{O}_1^{IJ}\\ &+ (d\lambda_1)\mathcal{O}_2^{IJ} + \frac{1}{2}\,\mathrm{diag}(d\mu_1, d\mu_1, d\mu_2, d\mu_2) - \frac{1}{2}\mathscr{C}^{IJ} \end{aligned} \tag{10.7}$$

$$\begin{aligned} g_0^{-1}\mathcal{P}^{I5} = {}& -2e^{\frac{1}{2}(\lambda_1-\mu_1)}\sqrt{\frac{1-\xi^2}{2}}\nu_1\left(\Omega_1^{-1}\Phi_1 e^0 + \frac{(1-\xi^2)\Psi_1 - k\Phi_1}{\xi\Omega_0}e^2\right)\mathcal{O}_1^{I1}\\ &+ e^{-\frac{1}{2}(\lambda_1+\mu_1)}\frac{1}{\sqrt{2}}\,d\Big(\sqrt{1-\xi^2}\nu_1\Big)\mathcal{O}_2^{I1} \end{aligned} \tag{10.8}$$

where

$$\mathcal{O}_1 \;=\; \begin{pmatrix} 0 & 1 & 0 & 0 \\ 1 & 0 & 0 & 0 \\ 0 & 0 & 0 & 0 \\ 0 & 0 & 0 & 0 \end{pmatrix} \quad \text{and} \quad \mathcal{O}_2 \;=\; \begin{pmatrix} 1 & 0 & 0 & 0 \\ 0 & -1 & 0 & 0 \\ 0 & 0 & 0 & 0 \\ 0 & 0 & 0 & 0 \end{pmatrix} \tag{10.9}$$

The composite connection, $\mathcal{Q}$, is also defined in (7.60) and is given by:

$$\mathcal{Q}^{12} \;=\; -2g_0\cosh(\lambda_1)\left(\Omega_1^{-1}\Phi_1 e^0 + \frac{(1-\xi^2)\Psi_1 - k\Phi_1}{\xi\Omega_0}e^2\right) \tag{10.10}$$

$$+\,\frac{1}{2}\mathscr{C}^{12} \tag{10.11}$$

$$\mathcal{Q}^{34} \;=\; -2g_0\left(\Omega_1^{-1}\Phi_2 e^0 + \frac{(1-\xi^2)\Psi_2 - k\Phi_2}{\xi\Omega_0}e^2\right) + \frac{1}{2}\mathscr{C}^{34} \tag{10.12}$$

The non-zero components of the Chern-Simons term (7.59) are given by:

$$\mathscr{C}^{12} \;=\; \frac{2g_0 e^{\mu_1}(1-\xi^2)}{\Omega_0}\left(\frac{(1-\xi^2)\partial_\xi\Psi_2 - k\partial_\xi\Phi_2}{\xi\Omega_0}e^0 \;-\; \frac{\Omega_1^{-1}}{\xi}(\partial_\psi\Phi_2)e^1 \;+\; \Omega_1^{-1}(\partial_\xi\Phi_2)e^2\right) \tag{10.13}$$

$$\mathscr{C}^{34} \;=\; \frac{2g_0 e^{\mu_2}(1-\xi^2)}{\Omega_0}\left(\frac{(1-\xi^2)\partial_\xi\Psi_1 - k\partial_\xi\Phi_1}{\xi\Omega_0}e^0 \;-\; \frac{\Omega_1^{-1}}{\xi}(\partial_\psi\Phi_1)e^1 \;+\; \Omega_1^{-1}(\partial_\xi\Phi_1)e^2\right) \tag{10.14}$$

10.1.3 The A-tensors

The A-tensors were defined in (7.80) for a diagonal matrix of scalars, P. The superpotential (10.15) is:

$$W \;=\; \frac{1}{2}g_0\, e^{-\mu_1-\mu_2}\left(1 \;-\; \frac{1}{4}(1-\xi^2)\nu_1^2 \;-\; e^{\mu_1}\cosh(\lambda_1) \;-\; e^{\mu_2}\right). \tag{10.15}$$

The tensors are then given by:

$$A_1^{AB} \;=\; W\big(\Gamma^{1234}\big)_{AB}\,, \quad A_2^{A\dot{A}5} \;=\; -\sqrt{2}P_I{}^J\frac{\partial W}{\partial\chi_J}\big(\Gamma^{1234}\Gamma^I\big)_{A\dot{A}} \tag{10.16}$$

and

$$\begin{aligned} A_2^{A\dot{A}1} &= (\partial_{\mu_1}W + \partial_{\lambda_1}W)\big(\Gamma^{1234}\Gamma^1\big)_{A\dot{A}} \\ A_2^{A\dot{A}2} &= (\partial_{\mu_1}W - \partial_{\lambda_1}W)\big(\Gamma^{1234}\Gamma^2\big)_{A\dot{A}} \\ A_2^{A\dot{A}3} &= \partial_{\mu_2}W\big(\Gamma^{1234}\Gamma^3\big)_{A\dot{A}} \\ A_2^{A\dot{A}4} &= \partial_{\mu_2}W\big(\Gamma^{1234}\Gamma^4\big)_{A\dot{A}} \end{aligned} \tag{10.17}$$

10.2 Deriving the BPS equations

As stated in the introduction of this Chapter, our purpose here is not an exhaustive classification of BPS solutions, but to get to the generalized superstrata, and so we will

occasionally take a short cut that could potentially omit some solutions but will get us efficiently to our target.

From here on, when the indices on the various matrices are omitted, it is to be understood that there is implicit left-multiplication.

10.2.1 The first set of equations

Using (10.16), the equation for the fifth component of the fermion variation (7.72) is:

$$\frac{1}{2}i\,\Gamma^I_{A\dot{A}}\gamma^\mu\epsilon^A\,\mathcal{P}^{I5}_\mu \;-\; \sqrt{2}(P\,\partial_\chi W)_I\,(\Gamma^{1234}\,\Gamma^I)_{A\dot{A}}\epsilon^A \;=\; 0\,, \tag{10.18}$$

The sum over I runs from 1 to 2, since the elements 3 and 4 are trivial.

We can multiply (10.18) by γ^1 to the left, and $\Gamma^2_{\dot{A}B}$ to obtain:

$$\begin{aligned}&\frac{1}{2}i\big(\Gamma^{12}\mathcal{P}^{15}_1-\Gamma^{12}\gamma^{12}\mathcal{P}^{15}_2-\mathcal{P}^{25}_1+\gamma^{12}\mathcal{P}^{25}_2\big)\epsilon\\&+\frac{1}{2}\gamma^{12}\big(\Gamma^{12}\mathcal{P}^{15}_0-\mathcal{P}^{25}_0\big)\epsilon+\Big(\sqrt{2}(P\partial_\chi W)_1\Gamma^{12}\Gamma^{1234}-\sqrt{2}(P\partial_\chi W)_2\Gamma^{1234}\Big)\epsilon \;=\; 0\,.\end{aligned} \tag{10.19}$$

One can rewrite this as:

$$\begin{aligned}&\frac{1}{2}i\big(\Gamma^{12}\mathcal{P}^{15}_1+\gamma^{12}\mathcal{P}^{25}_2\big)\epsilon-\frac{1}{2}i\big(\mathcal{P}^{25}_1+\Gamma^{12}\gamma^{12}\mathcal{P}^{15}_2\big)\epsilon\\&+\Big(\frac{1}{2}\gamma^{12}\Gamma^{12}\mathcal{P}^{15}_0-\sqrt{2}(P\partial_\chi W)_2\Gamma^{1234}\Big)\epsilon-\Big(\frac{1}{2}\gamma^{12}\mathcal{P}^{25}_0-\sqrt{2}(P\partial_\chi W)_1\Gamma^{12}\Gamma^{1234}\Big)\epsilon \;=\; 0\,.\end{aligned} \tag{10.20}$$

After applying the projection conditions (10.1), one sees that this equation is solved if one requires:

$$\mathcal{P}^{15}_0 \;=\; 2\sqrt{2}(P\partial_\chi W)_2\,, \qquad \mathcal{P}^{25}_0 \;=\; -\,2\sqrt{2}(P\partial_\chi W)_1\,, \tag{10.21}$$

$$\mathcal{P}^{15}_1 \;=\; \mathcal{P}^{25}_2\,, \qquad \mathcal{P}^{15}_2 \;=\; -\,\mathcal{P}^{25}_1\,, \tag{10.22}$$

where the lower indices are frame indices.

For the configurations we consider, the first two conditions are identical, as are the last two; and this is actually the only way to solve theses equations given the projection conditions. Using (10.8) and (10.15), the first two conditions lead to the equation:

$$\nu_1\left(\Phi_1-\frac{\Omega_1}{2}e^{-\mu_2}\right) \;=\; 0\,, \tag{10.23}$$

while the last two lead to:

$$\frac{1}{\sqrt{1-\xi^2}}\,\xi\partial_\xi(\sqrt{1-\xi^2}\nu_1) \;=\; 2e^{\lambda_1}\left(\Psi_1-\frac{k}{1-\xi^2}\Phi_1\right)\nu_1\,. \tag{10.24}$$

10.2.2 The second set of equations

The equations for the other fermion variations (7.72) are:

$$\frac{1}{2}i\,\Gamma^{I}_{A\dot{A}}\gamma^{\mu}\epsilon^{A}\,\mathcal{P}^{Ir}_{\mu} \;-\; A_2^{A\dot{A}r}\epsilon^{A} \;=\; 0\,, \tag{10.25}$$

where r runs from 1 to 4.

We will see that the equations for $r = 1, 2$ are equivalent, as are the equations for $r = 3, 4$.

Equations from $r = 3, 4$

We start with $r = 3$, and use (10.17). After multiplying by Γ^4 on the right, and γ^2 on the left, and rearranging the terms, we find:

$$\frac{1}{2}i\big(\Gamma^{34}\mathcal{P}_1^{33} - \gamma^{12}\mathcal{P}_2^{34}\big)\epsilon + \frac{1}{2}i\big(\mathcal{P}_1^{34} - \Gamma^{34}\gamma^{34}\mathcal{P}_2^{33}\big)\epsilon + \frac{1}{2}\big(\gamma^{12}\mathcal{P}_0^{34} + (\partial_{\mu_2}W)\Gamma^{34}\Gamma^{1234}\big)\epsilon \;=\; 0\,. \tag{10.26}$$

An obvious way to solve this equation is to require that the three terms in parentheses vanish independently. Applying the projection conditions (10.1) these three equations lead to:

$$\mathcal{P}_1^{33} \;=\; \mathcal{P}_2^{34}\,, \quad \mathcal{P}_1^{34} \;=\; -\mathcal{P}_2^{33} \quad \text{and} \quad \mathcal{P}_0^{34} \;=\; -2\partial_{\mu_2}W\,. \tag{10.27}$$

Using (10.7), the first equation leads to

$$\partial_{\xi}\left(\Phi_1 - \frac{\Omega_1}{2}e^{-\mu_2}\right) \;=\; 0 \tag{10.28}$$

while the second leads to

$$\partial_{\psi}\left(\Phi_1 - \frac{\Omega_1}{2}e^{-\mu_2}\right) \;=\; 0 \tag{10.29}$$

If $\nu_1 \neq 0$ then these two equations are redundant by virtue of (10.23). Thus, at least for $\nu_1 \neq 0$, the only non-trivial term in (10.26) is the last parenthesis, and, using (10.15), this leads to: .

$$\frac{1-\xi^2}{\xi}\frac{e^{\mu_1+2\mu_2}}{\Omega_0^2}\big(k\partial_{\xi}\Phi_1 - (1-\xi^2)\partial_{\xi}\Psi_1\big) \;=\; 1 - e^{\mu_1}\cosh(\lambda_1) - \frac{1-\xi^2}{4}\nu_1^2 \tag{10.30}$$

As we noted earlier, the equation for with $r = 4$ leads to the same set of equations.

Equations from $r = 1, 2$

For $r = 1$, we use (10.17) and multiply to the right by Γ^2 and on the left by γ^2. Rearranging the result then leads to:

$$\begin{aligned}&\frac{1}{2}i\big(\Gamma^{12}\mathcal{P}_1^{11} - \gamma^{12}\mathcal{P}_2^{12}\big)\epsilon + \frac{1}{2}i\big(\mathcal{P}_1^{12} - \Gamma^{12}\gamma^{12}\mathcal{P}_2^{11}\big)\epsilon + \frac{1}{2}\big(\gamma^{12}\Gamma^{12}\mathcal{P}_0^{11}\big)\epsilon \\ &+ \frac{1}{2}\big(\gamma^{12}\mathcal{P}_0^{12} + ((2\partial_{\mu_1}W) + (2\partial_{\lambda_1}W))\Gamma^{12}\Gamma^{1234}\big)\epsilon = 0\end{aligned} \tag{10.31}$$

Once again we ask for each term to vanish independently. We apply the projection conditions (10.1) and arrive at:

$$\mathcal{P}_1^{11} \;=\; -\,\mathcal{P}_2^{12}\,, \qquad\qquad \mathcal{P}_1^{12} \;=\; \mathcal{P}_2^{11} \tag{10.32}$$

$$\mathcal{P}_0^{11} \;=\; 0\,, \qquad \mathcal{P}_0^{12} \;=\; -\,2(\partial_{\lambda_1} W + \partial_{\mu_1} W) \tag{10.33}$$

The first and second equations lead to the simple constraints

$$\partial_\xi\left(\Phi_2 + \frac{\Omega_1}{2} e^{-\mu_1}\right) \;=\; 0\,, \qquad \partial_\psi\left(\Phi_2 + \frac{\Omega_1}{2} e^{-\mu_1}\right) \;=\; 0\,, \qquad \partial_\psi \lambda_1 \;=\; 0 \tag{10.34}$$

along with the more interesting equation

$$(1-\xi^2)\xi\partial_\xi\lambda_1 \;=\; -\,4\sinh(\lambda_1)\big[k\Phi_1 - (1-\xi^2)\Psi_1\big] \tag{10.35}$$

The third and fourth equations lead to the simple constraint

$$\sinh\left(\frac{1}{2}\lambda_1\right)\left(\Phi_1 - \frac{\Omega_1}{2} e^{-\mu_2}\right) \;=\; 0 \tag{10.36}$$

which is redundant with (10.23) if $\nu_1 \neq 0$ and $\lambda_1 \neq 0$; along with the interesting equation:

$$-\frac{1-\xi^2}{\xi}\frac{e^{2\mu_1+\mu_2}}{\Omega_0^2}\big(k\partial_\xi\Phi_2 - (1-\xi^2)\partial_\xi\Psi_2\big) \;=\; 1 - e^{\mu_2} - \frac{1-\xi^2}{4}\nu_1^2\,. \tag{10.37}$$

Again, the equation for with $r = 2$ leads to the same result.

10.2.3 The third set of equations

The equation for the gravitino variation (7.72) is

$$\mathrm{d}\epsilon^A \;+\; \frac{1}{4}\,\omega_{ab}\,\gamma^{ab}\,\epsilon^A + \frac{1}{4}\,\mathcal{Q}^{IJ}\Gamma^{IJ}_{AB}\,\epsilon^B \;-\; iW\,(\Gamma^{1234})_{AB}\,\gamma_c\,e^c\,\epsilon^B \;=\; 0\,. \tag{10.38}$$

Using (10.5), we obtain

$$\begin{aligned}\mathrm{d}\epsilon \;+\; \frac{1}{2}s_0\big(\gamma^{01}e^2 - \gamma^{02}e^1 - \gamma^{12}e^0\big)\,\epsilon \;+\; \frac{1}{2}(s_1e^1 + s_2e^2)\gamma^{12}\,\epsilon \\ + \frac{1}{4}\,\mathcal{Q}^{IJ}\Gamma^{IJ}\,\epsilon \;-\; W(i\gamma_c e^c)\Gamma^{1234}\,\epsilon \;=\; 0\,,\end{aligned} \tag{10.39}$$

which we can rewrite as:

$$\begin{aligned}\mathrm{d}\epsilon \;=\; &\left(\frac{1}{2}s_0 + W\Gamma^{1234}\right)(\gamma^{02}e^1 - \gamma^{01}e^2)\epsilon \\ &- e^0\left(\frac{1}{2}\mathcal{Q}_0^{12}\Gamma^{12} + \frac{1}{2}\mathcal{Q}_0^{34}\Gamma^{34} - \frac{1}{2}s_0\gamma^{12} + W\gamma^{12}\Gamma^{1234}\right)\epsilon \\ &- e^1\left(\frac{1}{2}\mathcal{Q}_1^{12}\Gamma^{12} + \frac{1}{2}s_1\gamma^{12}\right)\epsilon \\ &- e^2\left(\frac{1}{2}\mathcal{Q}_2^{12}\,\Gamma^{12} + \frac{1}{2}\mathcal{Q}_2^{34}\,\Gamma^{34} + \frac{1}{2}s_2\gamma^{12}\right)\epsilon\,,\end{aligned} \tag{10.40}$$

where s_0 is defined in (10.6).

We can now replace the derivative of the spinor using (10.3). Note that, because of the projection condition (10.2), the gauge rotation $(1,2)$ direction also implicitly rotates ϵ in the $(3,4)$ directions, and so η_τ and η_ψ will depend on all the $U(1)$ gauge choices.

We now distribute the terms η_τ and η_ψ to their logical place in equation (10.40), and ask that each term vanishes independently. After applying the projection conditions (10.1), we get

$$
\begin{aligned}
W &= -\frac{1}{2}s_0 && (10.41)\\
\frac{1}{2}\big(\mathcal{Q}_0^{12}-\mathcal{Q}_0^{34}\big) &= -g_0\Omega_1^{-1}\eta_\tau + W - \frac{1}{2}s_0 \;=\; -g_0\Omega_1^{-1}\eta_\tau + 2W && (10.42)\\
\frac{1}{2}\big(\mathcal{Q}_1^{12}-\mathcal{Q}_1^{34}\big) &= \frac{1}{2}s_1 && (10.43)\\
\frac{1}{2}\big(\mathcal{Q}_2^{12}-\mathcal{Q}_2^{34}\big) &= -\frac{g_0}{\xi\Omega_0}\big((1-\xi^2)\eta_\psi - k\eta_\tau\big) + \frac{1}{2}s_2 && (10.44)
\end{aligned}
$$

We now use (10.12), (10.6) and (10.15). The first equation leads to

$$
\frac{\Omega_1 e^{\mu_1+\mu_2}}{2\xi\Omega_0^2}\big((1-\xi^2)\partial_\xi k + 2\xi k\big) \;=\; -1 + e^{\mu_1}\cosh(\lambda_1) + e^{\mu_2} + \frac{1-\xi^2}{4}\nu_1^2\,. \tag{10.45}
$$

The second equation leads to

$$
\begin{aligned}
&\frac{1-\xi^2}{2\xi\Omega_0^2}\big[e^{\mu_1}(k\partial_\xi\Phi_2 - (1-\xi^2)\partial_\xi\Psi_2) - e^{2\mu_2}(k\partial_\xi\Phi_1 - (1-\xi^2)\partial_\xi\Psi_1))\big] \;=\\
&\Omega_1^{-1}(\eta_\tau + \Phi_2 - \cosh(\lambda_1)\Phi_1) + e^{-(\mu_1+\mu_2)}\left(-1 + e^{\mu_1}\cosh(\lambda_1) + e^{\mu_2} + \frac{1}{4}(1-\xi^2)\nu_1^2\right).
\end{aligned} \tag{10.46}
$$

The third equation leads to

$$
\Omega_1\frac{\partial_\psi\Omega_0}{\Omega_0} \;+\; e^{\mu_2}\partial_\psi\Phi_1 - e^{\mu_1}\partial_\psi\Phi_2 \;=\; 0\,. \tag{10.47}
$$

And the fourth equation leads to

$$
\begin{aligned}
\xi\left(\frac{\partial_\xi\Omega_0}{\Omega_0} + \Omega_1^{-1}e^{\mu_2}\partial_\xi\Phi_1 - \Omega_1^{-1}e^{\mu_1}\partial_\xi\Phi_2\right) \;&=\; 2\frac{\cosh(\lambda_1)}{1-\xi^2}\big(k\Phi_1 - (1-\xi^2)\Psi_1\big) + 1\\
&\quad - \frac{2}{1-\xi^2}\big(k(\eta_\tau+\Phi_2) - (1-\xi^2)(\eta_\psi+\Psi_2) + 1\big)\,.
\end{aligned} \tag{10.48}
$$

The gauge invariant combinations of the η_τ and η_ψ parameters are:

$$
\eta_\tau \;+\; \Phi_2 \;-\; \Phi_1 \quad\text{and}\quad \eta_\psi \;+\; \Psi_2 \;-\; \Psi_1\,. \tag{10.49}
$$

The precise value of η_τ and η_ψ can be derived from the asymptotics of the fields, at the origin and at the AdS boundary. In Section 12.1 we detail how to fix these asymptotics by

imposing regularity and other conditions. Here we will only use the following conditions: $\lambda_1, \mu_1, \mu_2 \to 0$ and $k \to 1$ as $\xi \to 1$, and $\lambda_1(0) = k(0) = 0$. Using these conditions in (10.48) leads to

$$\eta_\tau \;=\; \Phi_1(1) - \Phi_2(1) - 1 \qquad \text{and} \qquad \eta_\psi \;=\; \Psi_1(0) - \Psi_2(0) + \frac{1}{2}\,. \tag{10.50}$$

10.3 Summary of the BPS equations in the single-mode truncation

We now summarize and rewrite the equations obtained in the previous Section. For convenience, we are going to ignore the BPS solutions on the Coulomb branch, when $\nu = \lambda_1 = 0$. This assumption for example simplifies the equations (10.23), (10.36). We will also assume that the fields only depend on the variable, as stated originally in the ansatz.

After simplifications, we find a number of algebraic and first-order equations. The simplest of the differential equations is $\Omega_1' = 0$, and so Ω_1 is constant. This reflects the freedom to rescale the time coordinate, τ, and in some of the earlier papers on three-dimensional superstrata and microstrata, Ω_1 was simply set to 1. However, as was pointed out in [39], this is not the correct choice for holography, and so we will keep Ω_1 as an arbitrary constant for now.

The algebraic equations connect the scalars and the gauge fields ; they are[1]:

$$\Phi_1 \;=\; \frac{\Omega_1}{2} e^{-\mu_2}\,, \qquad \Phi_2 \;=\; -\,\frac{\Omega_1}{2} e^{-\mu_1}\,. \tag{10.51}$$

To write the first order equations, it is convenient to define:

$$\begin{aligned} H_0 \;&\equiv\; \frac{\xi^2 \Omega_0^2}{(1-\xi^2)^2 \Omega_1^2}\,, \qquad H \;\equiv\; H_0\, \Omega_1^2\, e^{-(\mu_1+\mu_2)} = -4\, H_0\, \Phi_1 \Phi_2\,, \\ F_j \;&\equiv\; \Psi_j - \frac{k}{1-\xi^2}\, \Phi_j\,, \quad j = 1, 2\,. \end{aligned} \tag{10.52}$$

Then one has the scalar equations:

$$\begin{aligned} &\xi \partial_\xi \lambda_1 - 4 \sinh(\lambda_1) F_1 \;=\; 0\,, \\ &\xi \partial_\xi \Big(\sqrt{1-\xi^2}\, \nu_1 \Big) - 2 e^{\lambda_1} F_1 \Big(\sqrt{1-\xi^2}\, \nu_1 \Big) \;=\; 0\,, \end{aligned} \tag{10.53}$$

that can be combined into an additional algebraic equation:

$$(1-\xi^2) \nu_1^2 \;=\; \sigma \big(1 - e^{2\lambda_1} \big)\,, \tag{10.54}$$

[1]The equations allow for an additional arbitrary constant in Φ_2. This constant is pure gauge in the single-mode truncation, and does not exist in the double-mode truncation. We thus choose to fix it to zero.

for some real integration constant σ. The electromagnetic equations are:

$$\begin{aligned} \xi\partial_\xi F_1 + H &= 0\,, \\ \xi\partial_\xi F_2 - H\cosh(\lambda_1) &= 0\,, \end{aligned} \tag{10.55}$$

and metric equations:

$$\begin{aligned} &\xi\partial_\xi \Omega_1 = 0\,, \\ &\xi\partial_\xi\left(\frac{k}{1-\xi^2}\right) - \frac{2H}{\Omega_1}\left(e^{\mu_1}\cosh(\lambda_1) + e^{\mu_2} - (1-(1-\xi^2)\nu_1^2/4)\right) = 0\,, \\ &\xi\partial_\xi \log(H) - 4\left(\eta_\psi - \cosh(\lambda_1)F_1 + F_2\right) = 0\,. \end{aligned} \tag{10.56}$$

Note that, using the condition that the scalar fields vanish at infinity and (10.51), we find that the phase parameter in time vanishes, $\eta_\tau = 0$. The other phase parameter, η_ψ, only appears in the last equation. It is important to keep in mind while solving this equation that this parameter is bound to the values of magnetic gauge fields through (10.50).

There are eleven functions in (9.6) to be determined. The BPS equations provide eight algebraic or first-order constraints. They are not enough to find solutions, as they do not fix the deformations of the Coulomb branch, and the complete solution of the system requires that we use two of the equations of motion to determine μ_1 and μ_2. They can be written as:

$$\begin{aligned} \xi\partial_\xi\left(\xi\partial_\xi e^{\mu_1} - 2\frac{\Omega_1 k}{(1-\xi^2)} - 4F_1\left(1-(1-\xi^2)\frac{\nu_1^2}{4}\right)\right) &= 0\,, \\ \xi\partial_\xi(\xi\partial_\xi e^{\mu_2}) - 4H\left(e^{\mu_1} - e^{\lambda_1} + e^{\mu_2}\cosh(\lambda_1) - e^{-\lambda_1}\left(1-(1-\xi^2)\frac{\nu_1^2}{4}\right)\right) &= 0\,. \end{aligned} \tag{10.57}$$

10.4 The BPS equations of the double-mode truncation

This Chapter developed the tools to derive the BPS equations in the single-mode truncation. The same analysis can be performed for the more general double-mode truncation, in the diagonal gauge. This computation only adds technical difficulties, and for this reason we will simply present here the resulting BPS equations.

The BPS equations lead once again to a set of algebraic constraints and first-order differential equations. The algebraic BPS equations become:

$$\begin{aligned} &\Phi_1 = \frac{\Omega_1}{2}\,e^{-\mu_2}\,, \qquad \Phi_2 = -\frac{\Omega_1}{2}\,e^{-\mu_1}\,, \qquad \Phi_3 = \Phi_4 = 0\,, \\ &\Psi_5 = -\frac{\sinh(\lambda_2)\,\Psi_3 + \sinh(\lambda_1)\,\Psi_4}{\xi\sinh(\lambda_1-\lambda_2)}\,, \qquad \Psi_6 = \frac{\sinh(\lambda_1)\,\Psi_3 + \sinh(\lambda_2)\,\Psi_4}{\xi\sinh(\lambda_1-\lambda_2)} \end{aligned} \tag{10.58}$$

To write the first order equations, it is again convenient to define:

$$\begin{aligned} H_0 &\equiv \frac{\xi^2\Omega_0^2}{(1-\xi^2)^2\Omega_1^2}\,, \qquad H \equiv H_0\,\Omega_1^2\,e^{-(\mu_1+\mu_2)} = -4\,H_0\,\Phi_1\Phi_2\,, \\ F_j &\equiv \Psi_j - \frac{k}{1-\xi^2}\,\Phi_j\,, \quad j=1,2,3,4\,. \end{aligned} \tag{10.59}$$

Then one has the scalar equations:

$$\begin{aligned}
&\xi\,\partial_\xi\lambda_1 \;-\; 4\,\sinh(\lambda_1)\,F_1 \;=\; 0\,, \qquad \xi\,\partial_\xi\lambda_2 \;+\; 4\,\sinh(\lambda_2)\,F_2 \;=\; 0\,,\\
&\frac{1}{\sqrt{1-\xi^2}}\,\xi\,\partial_\xi\Big(\sqrt{1-\xi^2}\nu_1\Big) \;-\; 2\,e^{\lambda_1}F_1\,\nu_1 \;+\; \frac{2\,e^{-\lambda_2}\,\sinh(\lambda_1)}{\sinh(\lambda_1-\lambda_2)}\,(e^{\lambda_1}F_3+e^{\lambda_2}F_4)\,\nu_2 \;=\; 0\,,\\
&\frac{1}{\sqrt{1-\xi^2}}\,\xi\,\partial_\xi\Big(\sqrt{1-\xi^2}\nu_2\Big) \;+\; 2\,e^{\lambda_2}F_2\,\nu_2 \;-\; \frac{2\,e^{-\lambda_1}\,\sinh(\lambda_2)}{\sinh(\lambda_1-\lambda_2)}\,(e^{\lambda_1}F_3+e^{\lambda_2}F_4)\,\nu_1 \;=\; 0\,;
\end{aligned} \tag{10.60}$$

the electromagnetic equations:

$$\begin{aligned}
&\xi\,\partial_\xi F_1 \;+\; 2\,(F_3\Psi_5 - F_4\Psi_6) \;+\; H\,\cosh(\lambda_2) \;=\; 0\,,\\
&\xi\,\partial_\xi F_2 \;+\; 2\,(F_4\Psi_5 - F_3\Psi_6) \;-\; H\,\cosh(\lambda_1) \;=\; 0\,,\\
&\xi\,\partial_\xi F_3 \;-\; 2\,(F_1\Psi_5 - F_2\Psi_6) \;=\; 0\,,\\
&\xi\,\partial_\xi F_4 \;-\; 2\,(F_2\Psi_5 - F_1\Psi_6) \;=\; 0\,,
\end{aligned} \tag{10.61}$$

and metric equations:

$$\begin{aligned}
&\xi\,\partial_\xi\Omega_1 \;=\; 0\,,\\
&\xi\,\partial_\xi\left(\frac{k}{1-\xi^2}\right) \;-\; \frac{2}{\Omega_1}\left(e^{\mu_1}\cosh(\lambda_1)+e^{\mu_2}\cosh(\lambda_2)-\left(1-\frac{1-\xi^2}{4}(\nu_1^2+\nu_2^2)\right)\right)H \;=\; 0\,,\\
&\xi\,\partial_\xi\log(H) \;-\; 4\Big(\eta_\psi-\cosh(\lambda_1)\,F_1+\cosh(\lambda_2)\,F_2\Big) \;=\; 0\,.
\end{aligned} \tag{10.62}$$

The phase parameter, η_ψ, only appears in the last equation and is determined by the boundary conditions for F_1, F_2 and H.

There is also an elementary first integral of these equations

$$H\,\sinh(\lambda_1)\,\sinh(\lambda_2) \;=\; c_0\,\xi^{4\eta_\psi}\,, \tag{10.63}$$

for some constant, c_0.

Once again, the BPS equations are not enough to find the solutions, and the complete solution of the system requires to use two additional equations of motion.

Chapter 11

Supersymmetric solutions

Having derived the BPS equations, one can try to construct new supersymmetric solutions. Perhaps surprisingly, we find that even in the single-mode truncation, the common $(1, 0, n)$ superstrata are not the only scaling solutions. Indeed, we are able to construct new 3-charge solutions using a different momentum carrier: the shape mode of the 3-sphere, rather than the Ramond fields.

This Chapter reviews the work of [40,41]. As stated, the simplest class of the solutions of the BPS equations are the single-mode and double-mode superstrata, (9.25) and (9.36). One of the purposes of the work of [37] was to check that these solutions verify all the BPS equations of Chapter 10. These solutions were already known to be supersymmetric ; this can be seen as a check of the derivation of the superstrata truncation or of the BPS equations.

A second, simple class of solution that one can build is the BPS "special locus". Its existence was conjectured in [38], but the full solution was derived in [40], and this was the first analytic BPS solution that was discovered after the superstrata. The reason for its name will be developed in further Chapters, it comes from the specific relation between the amplitudes of the momentum carriers. Its construction is developed in Section 11.1.

More recently, [41], it has been possible to construct the full space of solutions to the BPS equations of the single-mode truncation given in Section 10.3. This is the subject of Section 11.2. We will take a particular care in studying these solutions and their uplift in six dimensions. Finally, the last Section is devoted to the study of two particular limits of the space of solutions: the "pure-NS" superstrata, and the asymptotically $\mathrm{AdS}_2 \times S^1$ geometries.

11.1 The special locus

The "special locus" BPS solution is a very specific family of solutions of the single-mode BPS equations. We start by making some assumptions to simplify the BPS equations:

$$\lambda_1 \equiv \mu_1 \,, \qquad \mu_2 \equiv 0 \,. \tag{11.1}$$

The equation of motion for μ_2 (10.57) leads to a algebraic constraint:

$$\sigma \equiv 2 \qquad \text{or equivalently} \qquad (1-\xi^2)\nu_1^2 \;=\; 2\big(1-e^{2\lambda_1}\big) \tag{11.2}$$

where σ was defined in (10.54). The BPS equations for the gauge fields (10.51) and (10.55) then imply

$$\Phi_1 \;=\; \frac{1}{2} \quad \text{and} \quad \partial_\xi \Psi_1 \;=\; 0\,. \tag{11.3}$$

The absence of Dirac string would normally imply that regular solutions have $\Psi_1 = 0$, but we are working here in the time-independent gauge, which was obtained by a gauge rotation that shifted the gauge fields. As was discussed in Section 9.2, the magnetic gauge fields can be half-integers at the origin. Thus we have

$$\Psi_1 \equiv \frac{n}{2}\,, \qquad n \in \mathbb{N}. \tag{11.4}$$

The non-trivial dynamics is now reduced to four equations for four functions, $\lambda_1, \Psi_2, \Omega_0$ and k:

$$\xi\partial_\xi\lambda_1 + 2\sinh(\lambda_1)\left(\frac{k}{1-\xi^2} - n\right) \;=\; 0\,, \tag{11.5}$$

$$\xi\partial_\xi F_2 - H\cosh(\lambda_1) \;=\; 0\,, \tag{11.6}$$

$$\xi\partial_\xi \log(H) - 4\left(\eta_\psi - \frac{1}{2}\cosh(\lambda_1)\left(n - \frac{k}{1-\xi^2}\right) + F_2\right), \tag{11.7}$$

$$\xi\partial_\xi\left(\frac{k}{1-\xi^2}\right) \;=\; 2H\,. \tag{11.8}$$

There are several things to note. First, on the special branch (11.1), the first-order BPS system is enough to determine the solution: there is no need for the second order equations of motion. This is because the special branch corresponds to a fixed locus on the Coulomb branch.

Secondly, while the equations (11.5)-(11.8) appear rather complicated, there seems to be a natural geometric underpinning that remains to be fully fleshed out. To see this, define

$$h \;\equiv\; \log\tanh\left(-\frac{1}{2}\lambda_1\right), \tag{11.9}$$

then the equations for λ_1 and k become

$$\begin{aligned} \xi\partial_\xi h \;&=\; 2\left(n - \frac{k}{1-\xi^2}\right), \\ \xi\partial_\xi\left(\frac{k}{1-\xi^2}\right) \;&=\; 2H\,. \end{aligned} \tag{11.10}$$

Now observe that, apart from the factor of $e^{-\lambda_1}$ in H, the right-hand side of the latter equation defines the scale of the spatial base metric. Indeed, were it not for the factor of $e^{-\lambda_1}$, these two equations would imply that the three-dimensional metric is a Kähler

fibration as in [27,37]. For want of a better term, we will refer to this form of the metric as a *conformal Kähler fibration*.

Now one can differentiate (11.7) and eliminate $\partial_\xi F_2$ using (11.6). Writing the result in terms of h leads to a differential equation for h:

$$\partial_x^2 \log\left(\partial_x^2 h\right) \;+\; \frac{2\,(1+e^{2h})}{(1-e^{2h})}\,\partial_x^2 h \;+\; \frac{4\,e^{2h}(\partial_x h)^2}{(1-e^{2h})^2} \;=\; 0\,, \tag{11.11}$$

where $x \equiv -\log\xi$. One can also write this equation as:

$$\partial_x^2 \log\left(\frac{\partial_x^2 h}{\sinh(h(x))}\right) \;-\; \coth(h(x))\,\partial_x^2 h \;=\; 0\,. \tag{11.12}$$

At first sight, (11.11) equation appears moderately terrifying, but for a Kähler base, the first term is simply the Ricci tensor and the other terms are related to the metric and to the fibration vector, k. We have managed to find a complete, analytic solution to the system.

11.1.1 An analytic solution to the system

The system of equations (11.5)-(11.8) admits an analytic family of solutions, parametrized by a real constant γ. If one defines

$$\Lambda_1^2 \;\equiv\; 1-\gamma^4\,\xi^{4p+2}\,, \quad \Lambda_2^2 \;\equiv\; (2n+1)\,\gamma^2\,\xi^{2p}\,(1-\xi^2) \tag{11.13}$$

the solutions are then given by

$$\begin{aligned}
&\nu_1 \;=\; \frac{2\sqrt{2}}{\sqrt{1-\xi^2}}\frac{\Lambda_1\Lambda_2}{\Lambda_1^2+\Lambda_2^2}\,, \qquad \lambda_1 \;=\; \mu_1 \;=\; -\,2\,\mathrm{arctanh}\left(\frac{\Lambda_2^2}{\Lambda_1^2}\right), \qquad \mu_2 \;=\; 0\,,\\
&\Phi_1 \;=\; \frac{1}{2}\,, \qquad \Psi_1 \;=\; \frac{n}{2}\,,\\
&\Phi_2 \;=\; -\,\frac{\Lambda_2^2}{\Lambda_1^2-\Lambda_2^2}\,, \qquad \Psi_2 \;=\; -\,\frac{\xi^2}{1-\xi^2}\frac{\Lambda_2^2}{\Lambda_1^2-\Lambda_2^2}\left(1-\gamma^2\xi^{2p}\right),\\
&k \;=\; \xi^2\left(1\;-\;\gamma^2\,\xi^{2p}\,\frac{\Lambda_2^2}{\Lambda_1^2}\right), \qquad \Omega_0 \;=\; 1-\frac{\Lambda_2^2}{\Lambda_1^2}\,, \qquad \Omega_1 \;=\; 1\,.
\end{aligned} \tag{11.14}$$

for general n.

One can then define

$$\alpha \;\equiv\; \sqrt{8(2n+1)}\,\gamma\,, \tag{11.15}$$

to obtain $\nu \sim \alpha\,\xi^n$ as $\xi \to 0$.

Using the form of the metric (7.18) and the analytic solution, one can compute explicitly the coefficient of $d\psi^2$ in the metric, and find the range of parameters for which the solution is CTC-free. We find that the solutions are CTC-free when

$$\gamma^2 \;\le\; \frac{1}{4n+1} \quad \text{or equivalently} \quad \alpha^2 \;\le\; 4\cdot\frac{4n+2}{4n+1}\,. \tag{11.16}$$

11.2 The generalized single-mode superstrata

11.2.1 The BPS layers

In this Section we aim to construct the most general solutions to the system of BPS equations in the single-mode truncation. We start by focusing on the equations for λ_1, F_1, F_2 and H, that we recall here:

$$\begin{aligned}
&\xi\partial_\xi\lambda_1 - 4\sinh(\lambda_1)F_1 \;=\; 0\,,\\
&\xi\partial_\xi F_1 + H \;=\; 0\,,\\
&\xi\partial_\xi F_2 - H\cosh(\lambda_1) \;=\; 0\,,\\
&\xi\partial_\xi\log(H) - 4\left(\eta_\psi - \cosh(\lambda_1)F_1 + F_2\right) \;=\; 0\,.
\end{aligned} \tag{11.17}$$

Observe that this is a "base-layer" - a system of four first-order, non-linear equations for the four functions. This system has been decoupled from the other BPS equations and from the equations of motion. It plays the same role as the "zeroth layer" of six-dimensional BPS equations did for superstrata, that we described in Section 5.3. This non-linear system determines the geometry of the base in six dimensions.

Now observe that if one uses (10.56) to eliminate the derivatives of k in (10.57) and then takes the sums and differences of these two equations, one finds:

$$\begin{aligned}
&\frac{1}{4}\,\xi\,\partial_\xi\left[\xi\,\partial_\xi\left(e^{\mu_1}+e^{\mu_2}\right)\right] \;-\; 2\,H\,\cosh^2\!\left(\frac{1}{2}\lambda_1\right)\left(e^{\mu_1}+e^{\mu_2}\right)\\
&\qquad=\; -\,H\,e^{\lambda_1} \;-\; H\left(1+e^{-\lambda_1}\right)\left(1-\frac{1}{4}\left(1-\xi^2\right)\nu_1^2\right) \;+\; \xi\,\partial_\xi\left[F_1\left(1-\frac{1}{4}\left(1-\xi^2\right)\nu_1^2\right)\right],\\
&\frac{1}{4}\,\xi\,\partial_\xi\left[\xi\,\partial_\xi\left(e^{\mu_1}-e^{\mu_2}\right)\right] \;-\; 2\,H\,\sinh^2\!\left(\frac{1}{2}\lambda_1\right)\left(e^{\mu_1}-e^{\mu_2}\right)\\
&\qquad=\; H\,e^{\lambda_1} \;-\; H\left(1-e^{-\lambda_1}\right)\left(1-\frac{1}{4}\left(1-\xi^2\right)\nu_1^2\right) \;+\; \xi\,\partial_\xi\left[F_1\left(1-\frac{1}{4}\left(1-\xi^2\right)\nu_1^2\right)\right],
\end{aligned} \tag{11.18}$$

Since F_1, H and λ_1 are known from solving the base-layer equations, (11.17), the functions appearing in (11.18) are known, with ν_1 being determined by (10.54). Therefore the equations in this "first layer," (11.18), are *linear* equations in $(e^{\mu_1}+e^{\mu_2})$ and $(e^{\mu_1}-e^{\mu_2})$. The solutions to the base layer determine the sources and coefficients of this linear system, and the functions determined by these equations are precisely the electrostatic potentials (10.51).

Once this linear system is solved, one finally determines k from the first-order equation in (10.56), which is considered as a linear "second-layer" equation, where the sources are entirely determined by the previous layers:

$$\xi\partial_\xi\left(\frac{k}{1-\xi^2}\right) - \frac{2H}{\Omega_1}\left(e^{\mu_1}\cosh(\lambda_1) + e^{\mu_2} - \left(1-(1-\xi^2)\nu_1^2/4\right)\right) \;=\; 0\,. \tag{11.19}$$

These BPS equations thus have precisely the "linear structure" discovered in the earlier BPS systems that underpin microstate geometries [18, 50, 62]. Note also that the base

geometry, which is determined by F_1, F_2, H and λ_1 , is entirely independent of ν_1, or σ, and hence independent of the amplitude of the standard superstratum excitation.

11.2.2 Solving the base layer

The base-layer system, (11.17), has a remarkable structure that enables us to solve the system completely. Indeed, one can easily verify that these equations imply:

$$\xi\partial_\xi\Big[\xi\partial_\xi(F_1{+}F_2) - 2(F_1{+}F_2)^2\Big] \;=\; 0\,, \qquad \xi\partial_\xi\Big[\xi\partial_\xi(F_1{-}F_2) + 2(F_1{-}F_2)^2\Big] \;=\; 0\,. \tag{11.20}$$

These equations are trivially solved to give:

$$F_1 \;=\; \frac{1}{4}\left[q_1\frac{1+\gamma_1\,\xi^{2q_1}}{1-\gamma_1\,\xi^{2q_1}} \;-\; q_2\frac{1+\gamma_2\,\xi^{2q_2}}{1-\gamma_2\,\xi^{2q_2}}\right], \qquad F_2 \;=\; \frac{1}{4}\left[q_1\frac{1+\gamma_1\,\xi^{2q_1}}{1-\gamma_1\,\xi^{2q_1}} \;+\; q_2\frac{1+\gamma_2\,\xi^{2q_2}}{1-\gamma_2\,\xi^{2q_2}}\right], \tag{11.21}$$

where the four constants of integration in (11.20) are q_1, q_2, γ_1 and γ_2

One should note that with these choices one has

$$\xi\partial_\xi(F_1{+}F_2) - 2(F_1{+}F_2)^2 \;=\; -\frac{1}{2}q_1^2\,, \qquad \xi\,\partial_\xi\,(F_1{-}F_2) + 2(F_1{-}F_2)^2 \;=\; +\frac{1}{2}q_2^2\,. \tag{11.22}$$

Note that we have implicitly chosen the signs of the constants of integration in these equations. One can choose the opposite sign, and this leads to imaginary exponents and solutions with singular behavior at $\xi = 0$. Our choice leads to rational functions, and one must have $2q_1,\, 2q_2 \in \mathbb{Z}$ if one wishes to avoid branch cuts.

From the first equation in (11.17) one obtains:

$$\lambda_1 \;=\; -\log\left[\frac{\xi^{q_2}\,(1-\gamma_1\,\xi^{2q_1}) \;-\; \beta\,\xi^{q_1}\,(1-\gamma_2\,\xi^{2q_2})}{\xi^{q_2}\,(1-\gamma_1\,\xi^{2q_1}) \;+\; \beta\,\xi^{q_1}\,(1-\gamma_2\,\xi^{2q_2})}\right]. \tag{11.23}$$

where β is yet another constant of integration.

Substituting these back into (11.17) one finds that the first order system yields:

$$H \;=\; \frac{q_2^2\,\gamma_2}{(1-\gamma_1\,\xi^{2q_1})^2\,(1-\gamma_2\,\xi^{2q_2})^2}\Big(\xi^{2q_2}\,(1-\gamma_1\,\xi^{2q_1})^2 \;-\; \beta^2\,\xi^{2q_1}\,(1-\gamma_2\,\xi^{2q_2})^2\Big)\,. \tag{11.24}$$

along with a constraint on the constants of integration:

$$q_1^2\gamma_1 \;-\; \beta^2\,q_2^2\,\gamma_2 \;=\; 0\,, \tag{11.25}$$

which, in particular, means that γ_1 and γ_2 must have the same sign.

We later constrain some of these parameters through re-parametrizations and regularity. For the present we construct the rest of the solution in full generality.

11.2.3 Solving the remaining layers of BPS equations

One can actually solve the linear system of the first layer, (11.18), by quadrature. Indeed, it follows from (11.20) that for any function, P, one has:

$$\xi\,\partial_\xi\left[(F_1\pm F_2)^2\,\xi\,\partial_\xi\left((F_1\pm F_2)^{-1}\,P\right)\right] \;=\; (F_1\pm F_2)\left[\xi\,\partial_\xi\left(\xi\,\partial_\xi\,P\right) \;\mp\; 4\left(\xi\,\partial_\xi(F_1\pm F_2)\right)P\right]. \tag{11.26}$$

Now observe that

$$\xi\,\partial_\xi(F_1+F_2) \;=\; 2H\,\sinh^2\!\left(\frac{1}{2}\lambda_1\right), \qquad \xi\,\partial_\xi(F_1-F_2) \;=\; 2H\,\cosh^2\!\left(\frac{1}{2}\lambda_1\right), \tag{11.27}$$

which means that the differential operators on the left-hand sides of (11.18) can be rewritten using (11.26), to give the following form of the first layer:

$$\begin{aligned}
&\xi\,\partial_\xi\left[(F_1-F_2)^2\,\xi\,\partial_\xi\left((F_1-F_2)^{-1}\left(e^{\mu_1}+e^{\mu_2}\right)\right)\right]\\
&\qquad=\; 4(F_1-F_2)\left[-\,H\,e^{\lambda_1}\;+\;\xi\,\partial_\xi\left[F_1\,\left(1-\frac{1}{4}\,(1-\xi^2)\,\nu_1^2\right)\right]\right],\\
&\xi\,\partial_\xi\left[(F_1+F_2)^2\,\xi\,\partial_\xi\left((F_1+F_2)^{-1}\left(e^{\mu_1}-e^{\mu_2}\right)\right)\right]\\
&\qquad=\; 4(F_1+F_2)\left[H\,e^{\lambda_1}\;-\;2H\left(1-\frac{1}{4}\,(1-\xi^2)\,\nu_1^2\right)\;+\;\xi\,\partial_\xi\left[F_1\left(1-\frac{1}{4}\,(1-\xi^2)\,\nu_1^2\right)\right]\right],
\end{aligned} \tag{11.28}$$

The important point is that the sources on the right-hand side of these expressions consist of known functions. One can therefore solve these equations by integrating and we find:

$$\begin{aligned}
\left(e^{\mu_1}+e^{\mu_2}\right) \;&=\; \sigma\,\frac{\beta\,\xi^{q_1}\,(1-\gamma_2\,\xi^{2q_2})}{\xi^{q_2}\,(1-\gamma_1\,\xi^{2q_1})\;-\;\beta\,\xi^{q_1}\,(1-\gamma_2\,\xi^{2q_2})}\;-\;\frac{2\,c_4}{1-\gamma_2\,\xi^{2q_2}}\\
&\quad-\;\frac{1+\gamma_2\,\xi^{2q_2}}{1-\gamma_2\,\xi^{2q_2}}\big((c_4+2)\,q_2\,\log\xi\;+\;c_6\big)\,,\\
\left(e^{\mu_1}-e^{\mu_2}\right) \;&=\; \sigma\,\frac{\xi^{q_2}\,(1-\gamma_1\,\xi^{2q_1})}{\xi^{q_2}\,(1-\gamma_1\,\xi^{2q_1})\;-\;\beta\,\xi^{q_1}\,(1-\gamma_2\,\xi^{2q_2})}\;-\;\frac{2\,c_5}{1-\gamma_1\,\xi^{2q_1}}\\
&\quad-\;\frac{1+\gamma_1\,\xi^{2q_1}}{1-\gamma_1\,\xi^{2q_1}}\big((c_5-2)\,q_1\,\log\xi+c_7\big)\,,
\end{aligned} \tag{11.29}$$

where c_4, c_5, c_6 and c_7 are constants of integration.

Exponentiating (11.23) yields:

$$e^{\lambda_1} \;=\; \frac{\xi^{q_2}\,(1-\gamma_1\,\xi^{2q_1})\;+\;\beta\,\xi^{q_1}\,(1-\gamma_2\,\xi^{2q_2})}{\xi^{q_2}\,(1-\gamma_1\,\xi^{2q_1})\;-\;\beta\,\xi^{q_1}\,(1-\gamma_2\,\xi^{2q_2})}\,, \tag{11.30}$$

and hence

$$\begin{aligned}
\left(\frac{1}{2}\,\sigma\,e^{\lambda_1}-e^{\mu_1}\right) \;&=\; \frac{1}{2}\,\frac{1+\gamma_2\,\xi^{2q_2}}{1-\gamma_2\,\xi^{2q_2}}\big((c_4+2)\,q_2\,\log\xi+c_6\big)\;+\;\frac{c_4}{1-\gamma_2\,\xi^{2q_2}}\\
&\quad+\;\frac{1}{2}\,\frac{1+\gamma_1\,\xi^{2q_1}}{1-\gamma_1\,\xi^{2q_1}}\big((c_5-2)\,q_1\,\log\xi+c_7\big)\;+\;\frac{c_5}{1-\gamma_1\,\xi^{2q_1}}\,,\\
e^{\mu_2} \;&=\; -\,\frac{1}{2}\,\sigma\;-\;\frac{1}{2}\,\frac{1+\gamma_2\,\xi^{2q_2}}{1-\gamma_2\,\xi^{2q_2}}\big((c_4+2)\,q_2\,\log\xi+c_6\big)\;-\;\frac{c_4}{1-\gamma_2\,\xi^{2q_2}}\\
&\quad+\;\frac{1}{2}\,\frac{1+\gamma_1\,\xi^{2q_1}}{1-\gamma_1\,\xi^{2q_1}}\big((c_5-2)\,q_1\,\log\xi+c_7\big)\;+\;\frac{c_5}{1-\gamma_1\,\xi^{2q_1}}\,.
\end{aligned} \tag{11.31}$$

One can now integrate the last layer, (11.19), to arrive at:

$$k = -(1-\xi^2)\left[\left((c_4+2)\,q_2\,\log\xi + c_4 + c_6\right)\frac{q_2\,\gamma_2\,\xi^{2q_2}}{(1-\gamma_2\,\xi^{2q_2})^2} + \frac{1}{2}\frac{c_4\,q_2}{1-\gamma_2\,\xi^{2q_2}} + \left((c_5-2)\,q_1\,\log\xi + c_5 + c_7\right)\frac{q_1\,\gamma_1\,\xi^{2q_1}}{(1-\gamma_1\,\xi^{2q_1})^2} + \frac{1}{2}\frac{c_5\,q_1}{1-\gamma_1\,\xi^{2q_1}} + c_8\right], \tag{11.32}$$

where c_8 is a constant of integration.

The rest of the fields can now be easily determined algebraically using (10.51), (10.54) and (11.17). For completeness, the expressions are given in Appendix A.

11.2.4 Gauge fixing, regularity and asymptotic behavior

We start by removing redundancies from the parametrization of the solution and ensuring the regularity of the base-layer functions F_1, F_2, H and λ_1 for $0 \le \xi < 1$.

The base system

Note that:

- The solution to the base-layer, first-order BPS system is invariant under both $(q_1 \to -q_1, \gamma_1 \to 1/\gamma_1, \beta \to -\beta/\gamma_1)$ and $(q_2 \to -q_2, \gamma_2 \to 1/\gamma_2, \beta \to -\beta/\gamma_2)$, which means that we can choose $q_1 \ge 0$ and $q_2 \ge 0$.
- The regularity of λ_1 as $\xi \to 0$ implies $q_1 \ge q_2$.
- The absence of any singularity in F_1 and F_2 (except possibly at $\xi = 1$, due to the finiteness of k at infinity and the form of (10.52)) implies $\gamma_1, \gamma_2 \le 1$.
- If $\sigma \neq 0$, then regularity of ν_1 at infinity ($\xi = 1$) means that $\lambda_1 \to 0$ as $\xi \to 1$. This means either $\gamma_1 = 1$ or $\gamma_2 = 1$ or $\beta = 0$. The choice $\beta = 0$ will be examined later. When choosing between the gammas, positivity of $e^{-\lambda_1}$ implies one must take $\gamma_2 = 1$. We therefore have either $\sigma = 0$ or $\gamma_2 = 1$, for $\beta \neq 0$.

Next, we observe that there is an unfixed coordinate choice: $\xi \to \xi^\lambda$, with $\lambda > 0$. This leaves $\xi = 0, 1$ unchanged. Moreover, the BPS equations (11.17) , (11.18) and (11.19) only involve the differential operator $\xi\partial_\xi$, and this scales by λ^{-1}. The system is therefore invariant under this re-definition, as long as one leaves λ_1, μ_1, μ_2 unchanged but replaces:

$$F_1\,,\,F_2 \;\to\; \lambda^{-1}F_1\,,\,\lambda^{-1}F_2\,,\quad H \;\to\; \lambda^{-2}H\,,\quad \frac{k}{1-\xi^2} \;\to\; \lambda^{-1}\frac{k}{1-\xi^2}\,, \tag{11.33}$$

We therefore fix the rescaling of ξ by setting $q_2 = 1$ in (11.22).

To summarize: for $\sigma \neq 0$, and using (11.25), we arrive at:

$$\sigma \neq 0\,,\qquad q_2 = 1\,,\qquad 0 \le \gamma_1 \le 1\,,\qquad \gamma_2 = 1\,,\qquad \beta^2 = q_1^2\gamma_1\,; \tag{11.34}$$

while for $\sigma = 0$, one simply has $\gamma_1, \gamma_2 \leq 1$ and

$$\sigma \;=\; 0\,, \qquad q_2 \;=\; 1\,, \qquad q_1^2 \gamma_1 \;=\; \beta^2\, \gamma_2\,. \tag{11.35}$$

We discuss this solution in more detail in Section 11.4.1. Its significance lies in the fact that the momentum carrier of the standard superstrata vanishes, $\nu_1 \equiv 0$, and yet it still produces a scaling solution. This can then be S-dualized to a scaling, pure NS superstratum.

Smoothness of the complete solution

To obtain a smooth solution one must remove the log terms in the solutions for μ_1, μ_2 and k and require $k \to 0$ as $\xi \to 0$. We will do this without implementing the constraints from the previous Section and comment on how they combine at the end. This means one must take:

$$c_4 \;=\; -\,2\,, \qquad c_5 \;=\; 2\,, \qquad c_8 \;=\; q_2 - q_1\,, \tag{11.36}$$

With these choices one has:

$$\begin{aligned} \frac{1}{2}\,\sigma\, e^{\lambda_1} - e^{\mu_1} \;&=\; -\,\frac{1}{2}\,(c_6 + c_7) \;+\; \frac{c_6 - 2}{1 - \gamma_2\,\xi^{2q_2}} \;+\; \frac{c_7 + 2}{1 - \gamma_1\,\xi^{2q_1}}\,, \\ e^{\mu_2} \;&=\; -\,\frac{1}{2}\,(\sigma - c_6 + c_7) \;-\; \frac{c_6 - 2}{1 - \gamma_2\,\xi^{2q_2}} \;+\; \frac{c_7 + 2}{1 - \gamma_1\,\xi^{2q_1}}\,. \end{aligned} \tag{11.37}$$

and

$$\frac{k}{1-\xi^2} \;=\; -\,(c_6 - 2)\,\frac{q_2\,\gamma_2\,\xi^{2q_2}}{(1 - \gamma_2\,\xi^{2q_2})^2} \;+\; \frac{q_2\,\gamma_2\,\xi^{2q_2}}{1 - \gamma_2\,\xi^{2q_2}} \;-\; (c_7 + 2)\,\frac{q_1\,\gamma_1\,\xi^{2q_1}}{(1 - \gamma_1\,\xi^{2q_1})^2} \;-\; \frac{q_1\,\gamma_1\,\xi^{2q_1}}{1 - \gamma_1\,\xi^{2q_1}}\,. \tag{11.38}$$

The parameters γ_2, c_6 and c_7 determine the values of the scalars at infinity ($\xi = 1$). If one requires that the solution goes to the supersymmetric critical point at infinity, where all the μ_j and λ_1 vanish, one must take:

$$\gamma_2 \;=\; 1\,, \qquad c_6 \;=\; 2\,, \qquad c_7 \;=\; \frac{(1 - \gamma_1)\,\sigma - 4}{1 + \gamma_1}\,. \tag{11.39}$$

This leads to:

$$e^{\lambda_1} \;=\; \frac{\xi^{q_2}\,(1 - \gamma_1\,\xi^{2q_1}) \;+\; \beta\,\xi^{q_1}\,(1 - \xi^{2q_2})}{\xi^{q_2}\,(1 - \gamma_1\,\xi^{2q_1}) \;-\; \beta\,\xi^{q_1}\,(1 - \xi^{2q_2})}\,. \tag{11.40}$$

$$\begin{aligned} \Big(e^{\mu_1} \;-\; \frac{1}{2}\,\sigma\, e^{\lambda_1}\Big) \;&=\; -\,\frac{1}{2}\,(\sigma - 2)\,\frac{(1 - \gamma_1)}{(1 + \gamma_1)}\,\frac{(1 + \gamma_1\,\xi^{2q_1})}{(1 - \gamma_1\,\xi^{2q_1})}\,, \\ e^{\mu_2} - 1 \;&=\; -\,(\sigma - 2)\,\frac{\gamma_1}{1 + \gamma_1}\,\frac{1 - \xi^{2q_1}}{1 - \gamma_1\,\xi^{2q_1}}\,, \end{aligned} \tag{11.41}$$

$$\frac{k}{1-\xi^2} \;=\; \frac{q_2\,\xi^{2q_2}}{1 - \xi^{2q_2}} \;-\; \frac{q_1\,\gamma_1\,\xi^{2q_1}}{1 - \gamma_1\,\xi^{2q_1}} \;-\; (\sigma - 2)\,\frac{(1 - \gamma_1)}{(1 + \gamma_1)}\,\frac{q_1\,\gamma_1\,\xi^{2q_1}}{(1 - \gamma_1\,\xi^{2q_1})^2}\,. \tag{11.42}$$

In particular, this implies

$$\Big(e^{\mu_1} \;-1\Big) \;+\; \Big(e^{\mu_2} \;-1\Big) \;-\; \frac{1}{2}\,\sigma\,\Big(e^{\lambda_1} \;-1\Big) \;=\; 0\,. \tag{11.43}$$

One should also recall that there is the constraint (11.25), which now becomes

$$q_1^2\gamma_1 \;-\; \beta^2\, q_2^2 \;=\; 0\,. \tag{11.44}$$

To summarize how the results from this and the previous Section combine. Demanding that the scalars, μ_j and λ_1, vanish at infinity, we have the same constraints, irrespective of the value of σ:

$$q_2 = 1, \quad 0 \le \gamma_1 \le 1, \quad \gamma_2 = 1, \quad q_1^2\gamma_1 = \beta^2, \quad c_4 = -2, \quad c_5 = 2, \quad c_8 = 1 - q_1,$$
$$c_6 = 2, \quad c_7 = \frac{(1-\gamma_1)\,\sigma - 4}{1+\gamma_1}. \tag{11.45}$$

On the other hand, if the μ_j and λ_1 scalars are not required to vanish at infinity, then we have 2 cases:

$$\sigma \neq 0, \quad q_2 = 1, \quad 0 \le \gamma_1 \le 1, \quad \gamma_2 = 1, \quad q_1^2\gamma_1 = \beta^2, \quad c_4 = -2, \quad c_5 = 2, \quad c_8 = 1 - q_1, \tag{11.46}$$

and

$$\sigma = 0, \quad q_2 = 1, \quad \gamma_1, \gamma_2 \le 1, \quad q_1^2\gamma_1 = \gamma_2\,\beta^2, \quad c_4 = -2, \quad c_5 = 2, \quad c_8 = 1 - q_1. \tag{11.47}$$

Each of (11.45), (11.46) and (11.47) leads to all the rest of the functions, given in Appendix A, being regular as well.

Note that the special locus solution described in Section 11.1 is also contained within this family of solutions: one must take (11.45) and

$$\sigma \;=\; 2\,, \qquad q_1 \;=\; (2n+1)\,, \qquad \beta \;=\; -\,(2n+1)\,\gamma^2\,, \qquad \gamma_1 \;=\; \gamma^4\,. \tag{11.48}$$

The standard $(1,0,n)$ superstratum solution, given in Section 9.2.2, is obtained in the same case, (11.45), by setting $q_1 = 2n+1$, $q_2 = 1$, $\gamma_1 = 0$ and taking the limit $\sigma \to \infty$, $\beta \to 0$, with $\sigma\beta = -\frac{1}{2}\alpha^2$ finite.

11.3 Features of the six-dimensional uplift

The complete uplift formulae are given in [27], however we will focus on a subset of the fields, and especially upon the metric. To write the Ansatz for the uplift one defines the S^3 by introducing four Cartesian coordinates, x^I, on $\mathbb{R}^4$, obeying the constraint $x^I x^I = 1$. One also defines

$$\Delta \;=\; m_{IJ}x^I x^J\,. \tag{11.49}$$

where m_{IJ} is the matrix of scalars, (7.57), in three dimensions. The six-dimensional metric ansatz is then given by:

$$ds_6^2 \;=\; -\,(\det m_{IJ})^{-1/2}\Delta^{1/2}\,ds_3^2 \;+\; g_0^{-2}(\det m_{IJ})^{1/2}\Delta^{-1/2}m^{IJ}\mathcal{D}x^I\mathcal{D}x^J, \tag{11.50}$$

where ds_3^2 is the three-dimensional metric, (7.18), and $\mathcal{D}$ is the covariant derivative defined in (7.51). The $-$ sign in front of ds_3^2 is to convert the metric into "mostly plus" signature.

The six-dimensional scalars, the dilaton and axion, are given by:

$$e^{-\sqrt{2}\varphi} \;=\; \Delta, \qquad X \;=\; \chi_I x^I \,. \tag{11.51}$$

The standard BPS form of the six-dimensional metric is:

$$ds_6^2 \;=\; -\frac{2}{\sqrt{\mathcal{P}}}\,(dv+\hat\beta)\big(du+\omega+\tfrac{1}{2}\,\mathcal{F}\,(dv+\hat\beta)\big) \;+\; \sqrt{\mathcal{P}}\,ds_4^2\,, \tag{11.52}$$

where ds_4^2 is a metric on a base manifold, $\mathcal{B}$. (We have relabeled the fibration vector as $\hat\beta$ so as to avoid confusion with the parameter, β, in our solutions.) Our primary goal is to use (11.50) to determine the various pieces of this metric. Indeed, supersymmetry requires the base metric, ds_4^2, to be hyper-Kähler and $d\hat\beta$ to be self dual on $\mathcal{B}$. As we will see, the result is a new family of elliptically deformed, two centered ambi-polar hyper-Kähler metrics.

We should note, at this point, that one might have expected to get a standard superstratum in which the base metric is $\mathbb{R}^4$ and the fields depend on the v-coordinate in six dimensions. However, at the outset, we chose a gauge in which the fields are independent of ψ, and hence v. This gauge choice is equivalent to a spectral flow that converts the canonical $\mathbb{R}^4$ base into a two centered ambi-polar hyper-Kähler metric.

While we are not going to compute the detailed uplifts of the tensor gauge fields, we note that the tensor gauge field components, usually denoted by $\Theta^{(4)}$, are proportional to the components, B^4_{ij}, in the uplift formula given in [27]:

$$B^4_{ij} \;=\; \left(-\frac{\sqrt{2}}{g_0^2}\right)\,\frac{1}{2}\,\mathring\omega_{ijk}\,\mathring g^{kl}\,\Delta^{1/2}\,\partial_l\left(\Delta^{-1/2}X\right)\,. \tag{11.53}$$

Note that the scalar, X, is the axion, whose uplift is given in (11.51), and this is the field that one calls Z_4 in six dimensions.

It is important to note here that if $\sigma = 0$, then $\nu_1 \equiv 0$, which means that $X \equiv 0$ and hence $(Z_4, \Theta^{(4)})$ vanish identically. In the standard superstratum, the pair, $(Z_4, \Theta^{(4)})$, are the momentum-carrying "seeds" of the solution. However, in our work, the field λ_1 can also carry momentum charge.

11.3.1 The four-dimensional base metric

A straightforward but somewhat involved computation leads to the metric, ds_4^2, on the base manifold, $\mathcal{B}$. One finds that this metric only depends on the four functions, λ_1, F_1, F_2 and H that appear in the lowest layer of the BPS equations described in Section 11.2.1. We parametrize the $S^3 \subset \mathbb{R}^4$ using polar coordinates by taking:

$$x^1 \;=\; \sin\theta\,\sin\varphi\,, \qquad x^2 \;=\; \sin\theta\,\cos\varphi\,, \qquad x^3 \;=\; \cos\theta\,\sin\chi\,, \qquad x^4 \;=\; \cos\theta\,\cos\chi\,. \tag{11.54}$$

As we will describe in detail below, we obtain a new family of ambi-polar, hyper-Kähler geometries, parametrized by γ_1, γ_2, q_1 and q_2. Indeed, the first-order system, (11.17), is precisely what defines the hyper-Kähler structure. We will also see that, for $\gamma_2 = 1$, these geometries are asymptotically locally-Euclidean (ALE) [63] in that they are asymptotic to the flat metric on $\mathbb{R}^4/\mathbb{Z}_{q_2}$ at infinity ($\xi \to 1$). Thus, the choice $q_2 = 1$ makes the base geometries asymptotically Euclidean, and the coordinate reparametrization $\xi \to \xi^\lambda$ used in Section 11.2.4 to set $q_2 = 1$ may be viewed as "undoing" the $\mathbb{Z}_{q_2}$ orbifold. The ambi-polar structure of the metric then emerges through individual geometric charges, $\frac{1}{2}(q_2 + q_1)$ and $\frac{1}{2}(q_2 - q_1)$, in the interior.

It should be stressed that these geometries are not the canonical Gibbons-Hawking ALE metrics because they only have one $U(1)$ isometry and, as we will see in Section 11.3.1, this isometry is *not* tri-holomorphic. These metrics are expressed in terms of rational functions of ξ, and are therefore not some variant of the Atiyah-Hitchin metric. They are thus completely new ambi-polar, hyper-Kähler geometries.

The base metric

The metric, ds_4^2, may be written as the sum of the squares of the frames:

$$ds_4^2 = a^2 \sum_{i=1}^{4} \big(e^i\big)^2, \tag{11.55}$$

$$\begin{aligned}
e^1 &= \sqrt{H(\xi)\,\Gamma}\,\frac{d\xi}{\xi}\,,\\
e^2 &= \sqrt{\frac{H(\xi)}{\Gamma}}\,\Big[\sinh(\lambda_1)\,\sin\theta\cos\theta\sin 2\varphi\,d\theta\\
&\qquad\qquad -\big(\cosh(\lambda_1) - \sinh(\lambda_1)\,\cos 2\varphi\big)\sin^2\theta\,d\varphi \;+\; \cos^2\theta\,d\chi\Big]\,,\\
e^3 &= \frac{2}{\sqrt{\Gamma}}\,\Big[\big(F_1(\xi)\,e^{-\frac{1}{2}\lambda_1}\sin^2\theta \;-\; F_2(\xi)\,e^{\frac{1}{2}\lambda_1}\cos^2\theta\big)\,\cos\varphi\,d\theta\\
&\qquad\qquad - e^{\frac{1}{2}\lambda_1}\sin\theta\cos\theta\,\sin\varphi\,\big(F_1(\xi)\,d\chi - F_2(\xi)\,d\varphi\big)\Big]\,,\\
e^4 &= \frac{2}{\sqrt{\Gamma}}\,\Big[\big(F_1(\xi)\,e^{\frac{1}{2}\lambda_1}\sin^2\theta \;-\; F_2(\xi)\,e^{-\frac{1}{2}\lambda_1}\cos^2\theta\big)\,\sin\varphi\,d\theta\\
&\qquad\qquad + e^{-\frac{1}{2}\lambda_1}\sin\theta\cos\theta\,\cos\varphi\,\big(F_1(\xi)\,d\chi - F_2(\xi)\,d\varphi\big)\Big]\,,
\end{aligned} \tag{11.56}$$

where

$$\Gamma \;\equiv\; 2F_2(\xi)\,\cos^2\theta \;-\; 2F_1(\xi)\,\big(\cosh(\lambda_1) - \sinh(\lambda_1)\,\cos 2\varphi\big)\,\sin^2\theta\,. \tag{11.57}$$

This metric is positive definite for $q_1 = q_2$ and ambi-polar for $q_1 > q_2$. The latter is easily seen by taking $\xi \to 0$, where $\lambda_1 \to 0$ and $F_1 \to \frac{1}{4}(q_1 - q_2)$, $F_2 \to \frac{1}{4}(q_1 + q_2)$, whence:

$$\lim_{\xi\to 0}\Gamma \;=\; \frac{1}{2}\,\big(q_2 \;+\; q_1\cos 2\theta\big)\,. \tag{11.58}$$

Since one has $0 < \theta < \frac{\pi}{2}$, this changes sign for $q_1 > q_2$. The general expression for $\lambda_1 = 0$ is:

$$\Gamma \;=\; (F_2(\xi){-}F_1(\xi)) + (F_2(\xi){+}F_1(\xi))\,\cos 2\theta \;=\; \frac{q_2}{2}\,\frac{(1+\gamma_2\,\xi^{2q_2})}{(1-\gamma_2\,\xi^{2q_2})} + \frac{q_1}{2}\,\frac{(1+\gamma_1\,\xi^{2q_1})}{(1-\gamma_1\,\xi^{2q_1})}\,\cos 2\theta\,. \tag{11.59}$$

We have computed the curvature of ds_4^2 and it is, as one should expect, non-trivial and self-dual for $q_1 > q_2$ and that of flat $\mathbb{R}^4$ for $q_1 = q_2$.

The complex structures

There is an obvious candidate for a Kähler form:

$$J \;\equiv\; e^1\wedge e^2 \;-\; e^3\wedge e^4\,. \tag{11.60}$$

This is manifestly anti-self-dual, and one can easily verify that it is closed as a result of the differential identities (11.17). The other two complex structures, K and L, are almost as simple, and are defined by:

$$\begin{aligned} K \;&\equiv\; (e^1\wedge e^3 \;+\; e^2\wedge e^4)\,\cos\chi \;+\; (e^1\wedge e^4 \;-\; e^2\wedge e^3)\,\sin\chi\,,\\ L \;&\equiv\; -\,(e^1\wedge e^3 \;+\; e^2\wedge e^4)\,\sin\chi \;+\; (e^1\wedge e^4 \;-\; e^2\wedge e^3)\,\cos\chi\,. \end{aligned} \tag{11.61}$$

These are again manifestly anti-self-dual and are closed by virtue of the differential identities (11.17).

One should note that $\frac{\partial}{\partial\chi}$ is a Killing vector of the metric ds_4^2, but it is not tri-holomorphic because of the χ-dependence in (11.61).

It is elementary to obtain potentials for these Kähler forms:

$$\begin{aligned} J \;&=\; dA\,, \qquad K + i\,L \;=\; dB\,,\\ A \;&=\; -\left[\frac{1}{2\,\xi}\,H(\xi)\,\sinh(\lambda_1)\,\sin^2\theta\,\sin 2\varphi\,d\xi \;+\; F_2(\xi)\,\sin^2\theta\,d\varphi \;+\; F_1(\xi)\,\cos^2\theta\,d\chi\right],\\ B \;&=\; e^{-i\,\chi}\left(e^{\frac{1}{2}\lambda_1}\cos\varphi + i\,e^{-\frac{1}{2}\lambda_1}\sin\varphi\right)\sqrt{H(\xi)}\,\left[\frac{2F_2(\xi)}{\xi}\,\sin\theta\,\cos\theta\,d\xi - \sin^2\theta\,d\theta - i\,\sin\theta\,\cos\theta\,d\chi\right]. \end{aligned} \tag{11.62}$$

While one can choose any linear combination of J, K and L to define a complex structure, we will use $J^\mu{}_\nu$ as the complex structure henceforth.

Some complex coordinates and the hermitian form of the metric

Using $J^\mu{}_\nu$ as the complex structure, one can define holomorphic coordinates:

$$z_1 \;\equiv\; \frac{\left(e^{\frac{1}{2}\lambda_1}\cos\varphi - i\,e^{-\frac{1}{2}\lambda_1}\sin\varphi\right)}{\sqrt{\sinh\lambda_1}}\,\sin\theta\,, \qquad z_2 \;\equiv\; e^{i\,\chi}\,\sqrt{2H(\xi)\,\sinh\lambda_1}\,\cos\theta\,. \tag{11.63}$$

The metric, ds_4^2 can then be written in hermitian form:

$$ds_4^2 \;=\; A_1\left|dz_1\right|^2 \;+\; A_2\left|dz_2\right|^2 \;+\; A_3\left(\frac{dz_1}{z_1}\,\frac{d\bar z_2}{\bar z_2} + \frac{d\bar z_1}{\bar z_1}\,\frac{dz_2}{z_2}\right) \;-\; i\,A_4\left(\frac{dz_1}{z_1}\,\frac{d\bar z_2}{\bar z_2} - \frac{d\bar z_1}{\bar z_1}\,\frac{dz_2}{z_2}\right). \tag{11.64}$$

We then find:

$$\begin{aligned} A_1 &= 2\,\sinh(\lambda_1)\left[2F_2(\xi) \;+\; \mathcal{Q}\left(\cosh(\lambda_1) - \sinh(\lambda_1)\,\cos 2\varphi\right)\,\sin^2\theta\right], \\ A_2 &= \frac{1}{H(\xi)\,\sinh(\lambda_1)}\left[-2F_1(\xi) \;+\; \mathcal{Q}\,\cos^2\theta\right], \\ A_3 &= \mathcal{Q}\,\sin^2\theta\,\cos^2\theta\,, \qquad A_4 \;=\; -\,\mathcal{Q}\,\sinh(\lambda_1)\,\sin^2\theta\,\cos^2\theta\,\sin 2\varphi\,. \end{aligned} \tag{11.65}$$

where

$$\mathcal{Q} \;\equiv\; \frac{1}{\Gamma}\left(4F_1(\xi)\,F_2(\xi) + \,H(\xi)\right) \;=\; \frac{1}{4\,\Gamma}\,(q_1^2 - q_2^2)\,. \tag{11.66}$$

It is interesting to note that for $q_1 = q_2$ one has $\mathcal{Q} \equiv 0$, which means $H(\xi) = -4F_1(\xi)\,F_2(\xi)$. Moreover, one has:

$$F_2\,\sinh(\lambda_1) \;=\; \frac{q_1\,\beta}{1-\beta^2}\,. \tag{11.67}$$

As a result, the metric defined by (11.64) and (11.65) becomes

$$ds_4^2 \;=\; A_1\left|dz_1\right|^2 \;+\; A_2\left|dz_2\right|^2 \;=\; \frac{4\,q_1\beta}{(1-\beta^2)}\left|dz_1\right|^2 \;+\; \frac{(1-\beta^2)}{2\,q_1\beta}\,\left|dz_2\right|^2. \tag{11.68}$$

This is manifestly a flat metric in (scaled) Cartesian coordinates.

A Kähler potential

One can write the standard expression for the Kähler potential, $\mathcal{K}$, in terms of real variables implicitly as

$$A_\mu \;=\; \partial_\mu \mathcal{U} \;+\; J_\mu{}^\nu\,\partial_\nu\,\mathcal{K}\,. \tag{11.69}$$

where the potential, A_μ, is given in (11.62) and J is the complex structure defined by (11.60). The function, $\mathcal{U}$, is simply a gauge transformation reflecting an implicit gauge choice in (11.62).

A straightforward computation leads to a solution:

$$\begin{aligned} \mathcal{U} \;&=\; \frac{\beta}{8}\,(q_1+q_2)\,\frac{\xi^{q_1-q_2}(1-\gamma_2\,\xi^{2q_2})}{(1-\gamma_1\,\xi^{2q_1})} \;-\; \frac{1}{4}\left(\frac{q_1}{\beta\,\xi^{q_1-q_2}(1-\gamma_2\,\xi^{2q_2})} \;+\; \frac{q_2\,\beta\,\xi^{q_1-q_2}}{(1-\gamma_1\,\xi^{2q_1})}\right), \\ \mathcal{K} \;&=\; \frac{1}{4}\left[\frac{q_1}{(1-\gamma_1\,\xi^{2q_1})} \;-\; \frac{q_2}{(1-\gamma_2\,\xi^{2q_2})} \;+\; \frac{1}{2}\,(q_1^2-q_2^2)\,\log\xi \;-\; q_1\,\cos^2\theta\right. \\ &\qquad + \left(\frac{q_1}{\beta\,\xi^{q_1-q_2}(1-\gamma_2\,\xi^{2q_2})} \;-\; \frac{q_2\,\beta\,\xi^{q_1-q_2}}{(1-\gamma_1\,\xi^{2q_1})}\right. \\ &\qquad\qquad \left.\left. +\; \frac{\beta}{2}\,(q_1+q_2)\,\xi^{q_1-q_2}\,\frac{(1-\gamma_2\,\xi^{2q_2})}{(1-\gamma_1\,\xi^{2q_1})}\right)\sin^2\theta\,\cos 2\varphi\right]. \end{aligned} \tag{11.70}$$

11.3.2 The other parts of the six-dimensional metric

The warp factor

The warp factor, $\mathcal{P}$, is relatively straightforward. One finds that

$$\mathcal{P} \;=\; \frac{\Delta}{g_0^4\, a^4\, \Gamma^2}\,, \tag{11.71}$$

where

$$\Delta \;\equiv\; m_{AB}x^A x^B \;=\; e^{\mu_2}\cos^2\theta \;+\; e^{\mu_1}\big(\cosh(\lambda_1) - \sinh(\lambda_1)\,\cos 2\varphi\big)\,\sin^2\theta\,. \tag{11.72}$$

The fibration vector

The connection, $\hat{\beta}$, of the v-fibration is given by:

$$\begin{aligned}\hat{\beta} \;&=\; -\frac{R_y}{\sqrt{2H(\xi)\,\Gamma}}\,e^2\\ &=\; -\frac{R_y}{\sqrt{2}\,\Gamma}\Big[\sinh(\lambda_1)\,\sin\theta\cos\theta\sin 2\varphi\, d\theta\\ &\qquad\qquad -\big(\cosh(\lambda_1) - \sinh(\lambda_1)\,\cos 2\varphi\big)\sin^2\theta\, d\varphi \;+\; \cos^2\theta\, d\chi\Big]\,.\end{aligned} \tag{11.73}$$

where e^2 is one of the frames in (11.56).

One can then verify that one has:

$$\begin{aligned}\Theta_3 \;&=\; d\hat{\beta}\\ &=\; \frac{\sqrt{2}\,R_y}{\Gamma^2}\,\big(\cosh(\lambda_1) - \sinh(\lambda_1)\,\sin^2\theta\cos 2\varphi\big)(e^1\wedge e^2 \;+\; e^3\wedge e^4)\\ &\quad + \frac{4\,R_y\,F_1(\xi)}{\sqrt{2H(\xi)}\,\Gamma^2}\,\sinh(\lambda_1)\,\sin\theta\cos\theta\,\Big(e^{\frac{1}{2}\lambda_1}\sin\varphi\,(e^1\wedge e^3 \;-\; e^2\wedge e^4)\\ &\qquad\qquad +\; e^{-\frac{1}{2}\lambda_1}\cos\varphi\,(e^1\wedge e^4 \;+\; e^2\wedge e^3)\Big)\,.\end{aligned} \tag{11.74}$$

This is manifestly a self-dual flux.

The momentum function and angular momentum vector

The momentum function, $\mathcal{F}$, is given by:

$$\begin{aligned}\mathcal{F} \;=\; 2 - \frac{2}{R_y^2 a^2 g_0^4}\Big[&\frac{1}{\Gamma}\big(4e^{\mu_2}\,F_1(\xi)^2 + e^{\mu_1}\,H(\xi)\big)\big(\cosh(\lambda_1) - \sinh(\lambda_1)\,\cos 2\varphi\big)\sin^2\theta\\ &+\frac{1}{\Gamma}\big(4e^{\mu_1}\,F_2(\xi)^2 + e^{\mu_2}\,H(\xi)\big)\cos^2\theta \;-\; \frac{2k}{1-\xi^2}\Big]\,.\end{aligned} \tag{11.75}$$

The non-trivial components of the angular momentum vector are:

$$\omega \;\equiv\; \omega_\theta\, d\theta \;+\; \omega_\varphi\, d\varphi \;+\; \omega_\chi\, d\chi\,, \tag{11.76}$$

with

$$\begin{aligned}
\omega_\theta &= -\frac{\sqrt{2}}{R_y\, a^2 g_0^4\, \Gamma}\, \sinh(\lambda_1)\, \sin\theta\cos\theta\, \sin 2\varphi\, \left(2e^{\mu_1} F_2(\xi) + \omega_0\right), \\
\omega_\varphi &= \frac{\sqrt{2}}{R_y\, a^2 g_0^4\, \Gamma}\, \big(\cosh(\lambda_1) - \sinh(\lambda_1)\, \cos 2\varphi\big)\, \sin^2\theta\, \left(2e^{\mu_1} F_2(\xi) + \omega_0\right), \\
\omega_\chi &= \frac{\sqrt{2}}{R_y\, a^2 g_0^4\, \Gamma}\, \cos^2\theta\, \left(2e^{\mu_2} F_1(\xi) - \omega_0\right)
\end{aligned} \tag{11.77}$$

where $\mathcal{Q}$ is defined in (11.66) and

$$\omega_0 \equiv -\frac{k}{1-\xi^2} - \frac{1}{2}\, R_y^2\, a^2 g_0^4 + \mathcal{Q}\,\Delta\,. \tag{11.78}$$

11.3.3 Asymptotics and conserved charges

We can extract the conserved charges of the geometries according to the methods of [18].

At large r, the momentum function limits to a constant value:

$$\lim_{r\to\infty} \mathcal{F} = 2 + \frac{2}{R_y^2\, a^2 g_0^4}\left(2q_1 - q_2 - \frac{q_1\sigma}{1-\sqrt{\gamma_1}} + \frac{q_1(\sigma-2)}{1+\gamma_1}\right). \tag{11.79}$$

In order to get the correct $AdS_3 \times S^3$ asymptotics, this constant must vanish [18, 27]. This leads to the following constraint, which is akin to what is often called the "regularity condition" of superstrata:

$$R_y^2\, a^2 g_0^4 = q_2 - 2q_1 + \frac{q_1\sigma}{1-\sqrt{\gamma_1}} - \frac{q_1(\sigma-2)}{1+\gamma_1}\,. \tag{11.80}$$

As we will discuss below, the positivity of the left-hand side places bounds on σ and γ_1.

Upon applying the constraint, the momentum function then decays at infinity as

$$\mathcal{F} = -\frac{q_1^2 - q_2^2}{2R_y^2\, g_0^4\, r^2} + O\Big(\frac{a}{r}\Big)^4. \tag{11.81}$$

The fibration and angular momentum vectors, $\hat{\beta}$ and ω, also decreases as $1/r^2$ at infinity:

$$\begin{aligned}
\hat{\beta} &= \frac{R_y}{\sqrt{2}}\big(\sin^2\theta\, d\varphi - \cos^2\theta\, d\chi\big)\frac{a^2}{r^2} + O\Big(\frac{a}{r}\Big)^4, \\
\omega &= \frac{R_y}{\sqrt{2}}\left[1 + \frac{q_1 - q_2}{R_y^2\, a^2 g_0^4}\right]\big(\sin^2\theta\, d\varphi + \cos^2\theta\, d\chi\big)\frac{a^2}{r^2} + O\Big(\frac{a}{r}\Big)^4.
\end{aligned} \tag{11.82}$$

Using these results, one can then follow the procedure described in [18] to read-off the

conserved charges[1]:

$$\begin{aligned} \hat{\beta}_\phi + \hat{\beta}_\chi + \omega_\phi + \omega_\chi &= \frac{\sqrt{2}}{r^2}(J_L - J_R \cos 2\theta) + \mathcal{O}(r^{-4})\,, \\ \mathcal{F} &= -\frac{2Q_P}{r^2} + \mathcal{O}(r^{-4})\,, \end{aligned} \tag{11.83}$$

leading to:

$$J_L = \frac{R_y}{2}\left(a^2 + \frac{q_1 - q_2}{R_y^2 g_0^4}\right), \qquad J_R = \frac{a^2 R_y}{2}\,, \qquad Q_P = \frac{q_1^2 - q_2^2}{4R_y^2\, g_0^4}\,. \tag{11.84}$$

11.3.4 Inverting the spectral flow

Because of the gauge choices described in Section 9.2, our six-dimensional solution is v-independent even though it carries momentum charge. The more canonical formulation as a superstratum would involve a topologically trivial $\mathbb{R}^4$ base and would have explicit v-dependence in the fluctuating modes, and trivial constant terms in the magnetic potentials. To convert the canonical superstratum into the solution presented here one needs to do a spectral flow of the form:

$$\varphi \;\to\; \varphi \;-\; \frac{1}{2}\,(q_1 - q_2)\,\psi\,, \qquad \chi \;\to\; \chi \;-\; \frac{1}{2}\,(q_1 - q_2)\,\psi\,, \tag{11.85}$$

which means the Hopf fiber of the Gibbons-Hawking space is shifted by:

$$(\varphi + \chi) \;\to\; (\varphi + \chi) \;-\; (q_1 - q_2)\,\psi\,. \tag{11.86}$$

This flow takes the trivial base to a base with GH charges $\frac{1}{2}(q_1 + q_2)$ and $\frac{1}{2}(q_1 - q_2)$. It also shifts the quantized CFT charges according to [64–68]:

$$j_L \;\to\; j_L \;+\; \frac{c}{12}(q_1 - q_2)\,, \qquad h \;\to\; h \;+\; (q_1 - q_2) j_L \;+\; \frac{c}{24}(q_1 - q_2)^2\,. \tag{11.87}$$

where $c = 6N_1N_5$ is the central charge of the D1-D5 CFT. This translates into the following shift of the supergravity charges[2]:

$$J_L \;\to\; J_L + \frac{q_1 - q_2}{2R_y g_0^4}\,, \qquad Q_P \;\to\; Q_P + (q_1 - q_2)\frac{J_L}{R_y} + \frac{(q_1 - q_2)^2}{4\,R_y^2\, g_0^4}\,. \tag{11.88}$$

This means that the canonical form of our new superstratum solution on an $\mathbb{R}^4$ base with v-dependent modes must have

$$J_L \;=\; J_R \;=\; \frac{a^2 R_y}{2}\,, \qquad Q_P \;= \frac{q_1 - q_2}{2R_y^2 g_0^4}\big(q_2 - a^2 R_y^2 g_0^4\big)\,. \tag{11.89}$$

[1] We are using the standard conventions in which the excitations of the supertube are in the left-moving sector. Section D.5 of [27] uses the opposition conventions, swapping J_L and J_R.

[2] The translation between quantized and supergravity charges can be found in many places, see, for example, [18, 21].

These charges are determined by the fact that the spectral flow (11.88) applied to them results in the charges (11.84). The canonical superstratum therefore has $J_L = J_R \sim a^2$. The momentum charge determines the AdS_3 radius, $g_0^{-1} \equiv (Q_1 Q_5)^{1/4}$, and is related to the mode numbers and the amplitudes through the constraint (11.80). It is interesting to note that the expression for Q_P may be rewritten as:

$$\frac{2\,Q_P}{(q_1 - q_2)} \;+\; a^2 \;=\; \frac{q_2}{R_y^2 g_0^4} \;=\; \frac{q_2\,Q_1 Q_5}{R_y^2}\,, \tag{11.90}$$

which is the analogue of the usual superstratum regularity condition.

11.4 Two Important Examples

11.4.1 Pure-NS superstrata

The solution with $\sigma = 0$ may seem a rather degenerate limit of the solutions we have presented here, but it is very significant. As we noted at the beginning of Section 11.3, setting $\sigma = 0$ removes the standard momentum carriers of the original superstratum. On the other hand, this solution can still have momentum charge carried by λ_1. We will therefore examine this solution in more detail.

What makes it important is that the six-dimensional uplift only has excitations in the metric, the gauge fields $(Z_1, \Theta^{(2)})$ and $(Z_2, \Theta^{(1)})$, and the dilaton. The axion and flux, $(Z_4, \Theta^{(4)})$, are identically zero. If one takes the S-dual of such a D1-D5 superstratum, then it becomes a *pure F1-NS5 superstratum whose excitations lie only in the NS-NS sector of the theory*: there are no R-R excitations. This means one has the possibility of using exact world-sheet methods for exploring these geometries.

While such solutions exist for arbitrary $\gamma_1, \gamma_2 \leq 1$, we will focus on smooth solutions that limit to the supersymmetric critical point at infinity. That is, we impose (11.45), with $\sigma = 0$, and use the general solution given in (11.30), (11.31), (11.32) and Appendix A:

$$\begin{aligned} &\nu_1 \;\equiv\; 0\,, \qquad e^{\lambda_1} \;=\; \frac{(1-\lambda^2\,\xi^{2q_1}) \;+\; \lambda\,q_1\,\xi^{q_1-1}\,(1-\xi^2)}{(1-\lambda^2\,\xi^{2q_1}) \;-\; \lambda\,q_1\,\xi^{q_1-1}\,(1-\xi^2)}\,, \\ &e^{\mu_1} \;=\; 1 \;-\; \frac{2\,\lambda^2\,(1-\xi^{2q_1})}{(1+\lambda^2)(1-\lambda^2\,\xi^{2q_1})}\,, \qquad e^{\mu_2} \;=\; 1 \;+\; \frac{2\,\lambda^2\,(1-\xi^{2q_1})}{(1+\lambda^2)(1-\lambda^2\,\xi^{2q_1})}\,, \end{aligned} \tag{11.91}$$

where we have solved the constraint in (11.35) by introducing a new parameter, λ:

$$\beta \;\equiv\; \lambda\,q_1\,, \qquad \gamma_1 \;\equiv\; \lambda^2\,. \tag{11.92}$$

The metric functions are[3]:

$$\Omega_0^2 \;=\; \frac{(1-\lambda^2)(1+\lambda^2\,\xi^{2q_1})}{(1+\lambda^2)(1-\lambda^2\,\xi^{2q_1})}\left(1\;+\;\frac{2\,\lambda^2\,(1-\xi^{2q_1})}{(1+\lambda^2)(1-\lambda^2\,\xi^{2q_1})}\right)\left(1\;-\;\lambda^2\,q_1^2\,\xi^{2q_1-2}\,\frac{(1-\xi^2)^2}{(1-\lambda^2\,\xi^{2q_1})^2}\right), \tag{11.93}$$

$$\frac{k}{1-\xi^2} \;=\; \Omega_1^{-1}\left(\frac{\xi^2}{1-\xi^2}+\frac{q_1\,\lambda^2\,\xi^{2\,q_1}\Big(1-\lambda^2\big(3-\xi^{2\,q_1}(1+\lambda^2)\big)\Big)}{(1+\lambda^2)(1-\lambda^2\,\xi^{2\,q_1})^2}\right). \tag{11.94}$$

For completeness, we re-state the gauge fields in terms of the other fields and the functions F_1 and F_2, (11.21), with parameters fixed by (11.45), which provides the easiest way of obtaining expressions for them:

$$\begin{aligned}
\Phi_1 \;&=\; \frac{\Omega_1}{2}e^{-\mu_2}\,, \qquad \Psi_1 \;=\; \left(F_1(\xi)\;+\;\frac{\Omega_1 k}{2(1-\xi^2)}\,e^{-\mu_2}\right),\\
\Phi_2 \;&=\; -\,\frac{\Omega_1}{2}e^{-\mu_1}\,, \qquad \Psi_2 \;=\; \left(F_2(\xi)\;-\;\frac{\Omega_1 k}{2(1-\xi^2)}\,e^{-\mu_1}\right),\\
F_1 \;&=\; \frac{1}{4}\left[q_1\frac{1+\lambda^2\,\xi^{2q_1}}{1-\lambda^2\,\xi^{2q_1}}\;-\;\frac{1+\xi^2}{1-\xi^2}\right], \qquad F_2 \;=\; \frac{1}{4}\left[q_1\frac{1+\lambda^2\,\xi^{2q_1}}{1-\lambda^2\,\xi^{2q_1}}\;+\;\frac{1+\xi^2}{1-\xi^2}\right].
\end{aligned} \tag{11.95}$$

11.4.2 Asymptotically $AdS_2 \times S^1$ geometries

We now return to superstrata with generic values of σ and to obtain a better understanding these solutions, it is useful to track the evolution of the length of the ψ-circle in the 3-dimensional geometry (7.18):

$$L_\psi(\xi) \;\equiv\; \frac{2\pi}{R_{AdS}}\sqrt{g_{\psi\psi}}\,. \tag{11.96}$$

We can generally identify three distinct regions:

- Close to the origin of space, one has $L_\psi(r) \sim 2\pi r/a$, the solution caps off smoothly with no conical singularity.
- There is an intermediate regime where $L_\psi(\xi)$ remains constant, which means that the size of the circle is fixed, and the geometry is approximately $AdS_2 \times S^1$. We call this region the *throat*.
- Asymptotically, the size of the circle typically grows linearly with r, forming an AdS_3 region. It is given by

$$L_\psi(r) \;\sim_{r\to\infty}\; 2\pi C\Big(\frac{r}{a}\Big), \quad \text{or equivalently} \quad L_\psi(\xi) \;\sim_{\xi\to 1}\; \frac{2\pi C}{\sqrt{1-\xi^2}}\,, \tag{11.97}$$

[3] Ω_1 is a free constant that can be rescaled by a rescaling of the time coordinate. We do not fix it for now.

where C is a constant that depends on the exact solution we are looking at. We can compute it using (11.24) and (11.40)-(11.42). Its value depends on the parameters β and σ, and on the modes q_1 and q_2:

$$C^2 \;=\; q_2 \,-\, 2q_1 \,+\, \frac{\sigma\, q_1^2}{q_1 - q_2\,\beta} \,-\, \frac{(\sigma-2)\, q_1^3}{q_1^2 + q_2^2\,\beta^2}\,. \tag{11.98}$$

Note that using the regularity condition (11.80), one can write C simply in terms of the radii of the supertube locus and of the AdS space:

$$C^2 \;=\; R_y^2\, a^2\, g_0^4\,. \tag{11.99}$$

More precisely, when C^2 is positive, L_ψ grows linearly at infinity, and the geometry is asymptotically AdS_3. But at certain values of the parameters, when $C = 0$, the size of the circle is kept finite at infinity, the asymptotically AdS_3 region disappears, the throat becomes infinite, and the geometry is asymptotically $AdS_2 \times S^1$. If we keep on increasing the parameters, we reach a regime where C^2 is negative, the solution then develops closed time-like curves and is therefore unphysical.

To illustrate this behavior, we take $q_2 = 1$ and plot, in Fig. 11.1, the logarithm of the length of the circle, $\log L_\psi$, against x, defined through $\xi \equiv \frac{e^x}{\sqrt{e^{2x}+1}}$. This is done, as an example, on the special locus, (11.48). There we obtain

$$C^2 \;=\; \frac{1-(4\,n+1)\gamma^2}{1+\gamma^2} = \frac{1-(2\,q_1-1)\gamma^2}{1+\gamma^2}\,, \tag{11.100}$$

where $q_1 = 2n+1$ as in (11.48). Asking for C^2 to be positive, we find again the condition given in (11.16):

$$\gamma^2 \le \frac{1}{4\,n+1} = \frac{1}{2\,q_1-1}, \quad \text{or equivalently} \quad -\beta \le \frac{q_1}{2\,q_1-1}. \tag{11.101}$$

A choice of parameters for which this bound is respected is shown on the left graph of Fig. 11.1. The aforementioned three regions are identified as follows: the linear growth on the left corresponds to the cap; the plateau, in the middle, is the throat; and the growing part to the right signifies the AdS_3 region.

The bound is saturated when $C = 0$. The solutions saturating the bound are asymptotically $AdS_2 \times S^1$ geometries, as shown on the right graph of Fig. 11.1.

More generally, moving away from the special locus, one finds that the length of the ψ circle at infinity when $C = 0$ is:

$$L_\psi^{(\infty)} \;=\; \sqrt{2q_2\,(q_1-q_2)}\,\pi\,. \tag{11.102}$$

The solutions of the equation $C = 0$ describe a contour in the plane (σ, β), that separates it into two regions: the physical region, and the region with CTCs. This is represented on Fig. 11.2, for $q_1 = 5$ and $q_2 = 1$. Alternatively, one can replace σ by $\alpha^2 = -2\beta\sigma$ – a better parametrization in relation to the standard superstratum in our

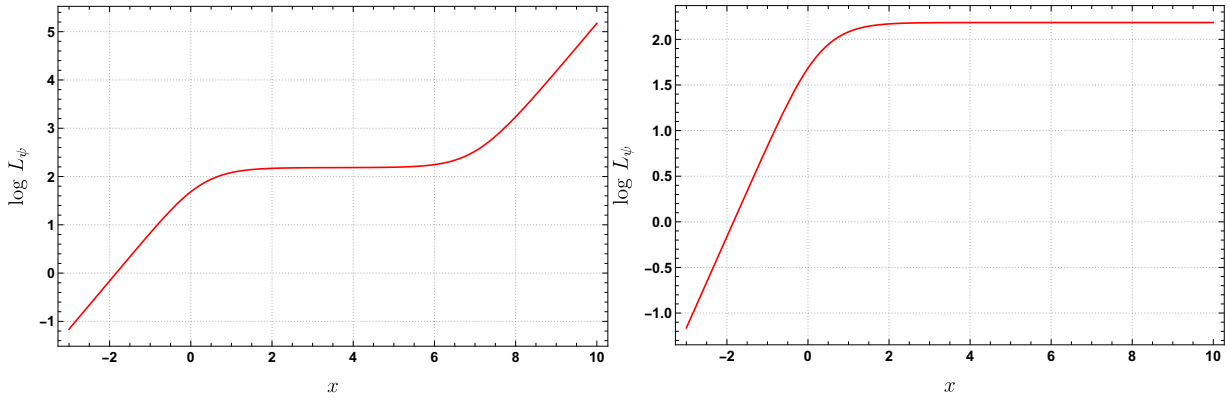

Figure 11.1: *Plots of* $\log L_\psi$ *against* x*, where* $\xi = \frac{e^x}{\sqrt{e^{2x}+1}}$*. In the first graph we have taken* $\sigma = 2$*,* $\beta = -\frac{q_1}{2q_1-1} + \frac{1}{10^6}$*,* $q_1 = 5$*. Here* C^2 *has a small positive value, and we identify the two* AdS_3 *regions of linear growth separated by a plateau, which is the throat. The second graph corresponds to* $\sigma = 2$*,* $\beta = -\frac{q_1}{2q_1-1}$*,* $q_1 = 5$*. For this solution,* C *is zero, and the asymptotic* AdS_3 *region is not present.*

three-dimensional notation, and plot the contour $C = 0$ in the (α, β) plane. This is done in Fig. 11.3, using once again $q_1 = 5$ and $q_2 = 1$. We recover a similar result to the one presented in figure 12 of [38].

Because of (11.99), the $C = 0$ locus can also be identified with the "$a \to 0$ limit" of superstrata geometries. In the standard construction of the latter, there are two ways of taking that limit. To see that, one needs to transform back to the original r coordinate, (7.12). Then, one possibility is to keep r finite and take $a \to 0$, this leads to an asymptotically AdS_3 geometry with an infinitely-deep throat at the origin and a metric approaching that of extremal BTZ. The other option is to take both $r \to 0$ and $a \to 0$, while keeping the ratio r/a fixed. This is a choice we have implicitly made by using the compactified radial variable, ξ. As we have seen, it produces an asymptotically $AdS_2 \times S^1$ spacetime, as the AdS_3 region is pushed to an infinite distance, with a smooth AdS_3 cap at the origin.

The significance of the $a \to 0$ limit for the standard superstratum and a resolution to the issue of whether a black hole solution can be obtained as a limit of such a horizonless geometry is discussed in [69].

We have therefore shown, and depicted in Fig. 11.1, that our new superstrata, including the family in Section 11.4 that can be S-dualized to a solution with only NS-fields, can exhibit the deep scaling behavior of the standard superstrata as the momentum charge is increased towards its maximum value. Intriguingly enough, one can see from (11.40) and (11.41) that the scalars λ_1, μ_1 and μ_2 remain smooth and bounded even in the deepest such superstrata[4], except when $q_1 = q_2$. See, for example, Fig. 11.4, which shows a plot of λ_1 on the special locus, (11.48), where $\lambda_1 = \mu_1$ and $\mu_2 = 0$. We use the same values of the parameters as in Fig. 11.1, and while that leads to different spacetime asymptotics,

[4]Here, we are only considering solutions where the scalars are taken to vanish at infinity.

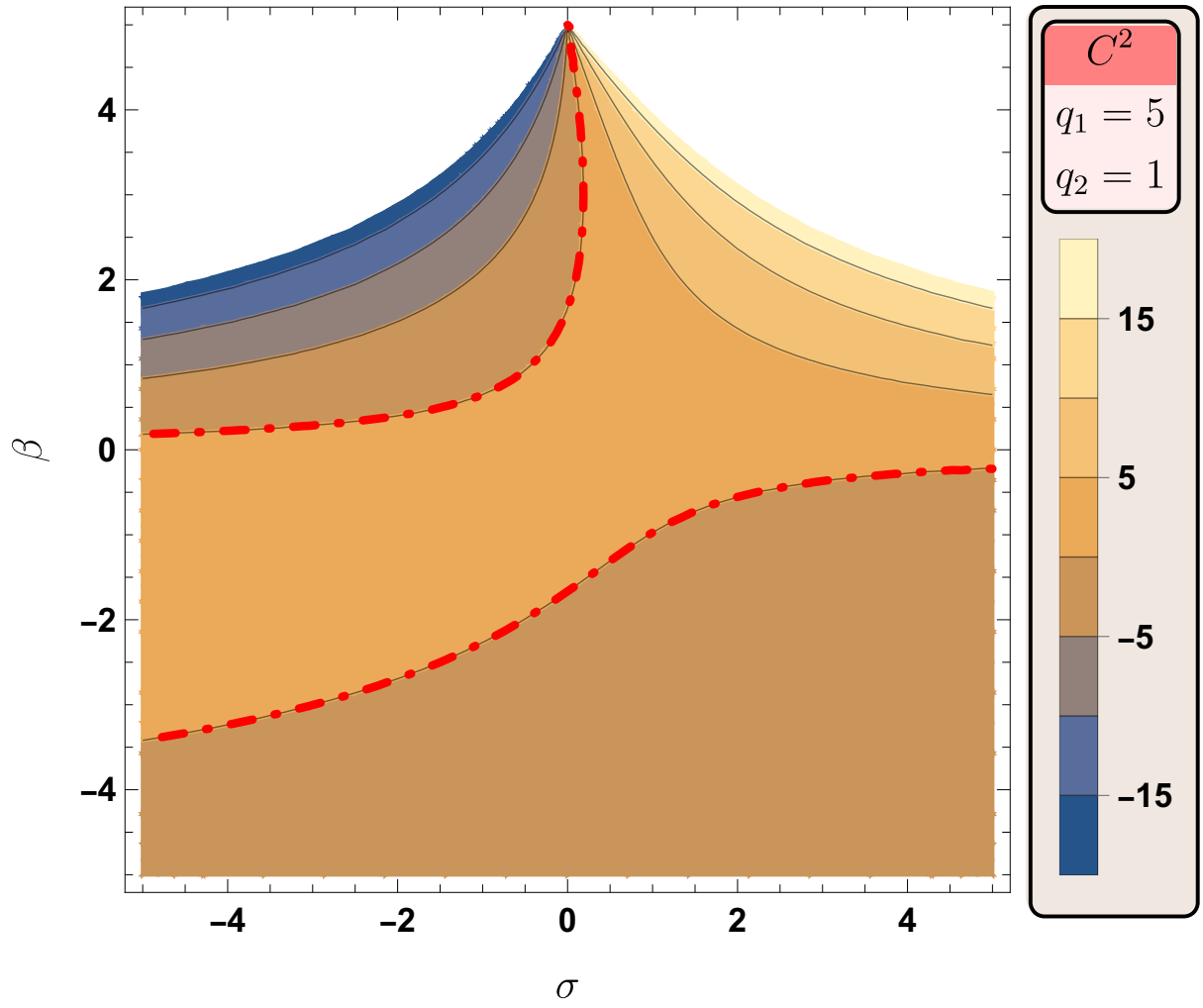

Figure 11.2: *Plot of* C^2, (11.98), *for* $q_1 = 5$, $q_2 = 1$, *as a function of* σ *and* β. *The red dashed-dotted lines indicates the* $C = 0$ *contour. In the region between them is where the values are positive.* C^2 *determines the size of the* ψ *circle at infinity, in the asymptotically* AdS_3 *region.*

λ_1 barely changes. This means that the elliptical deformation also remains bounded and goes nowhere near "flattening the ellipse."

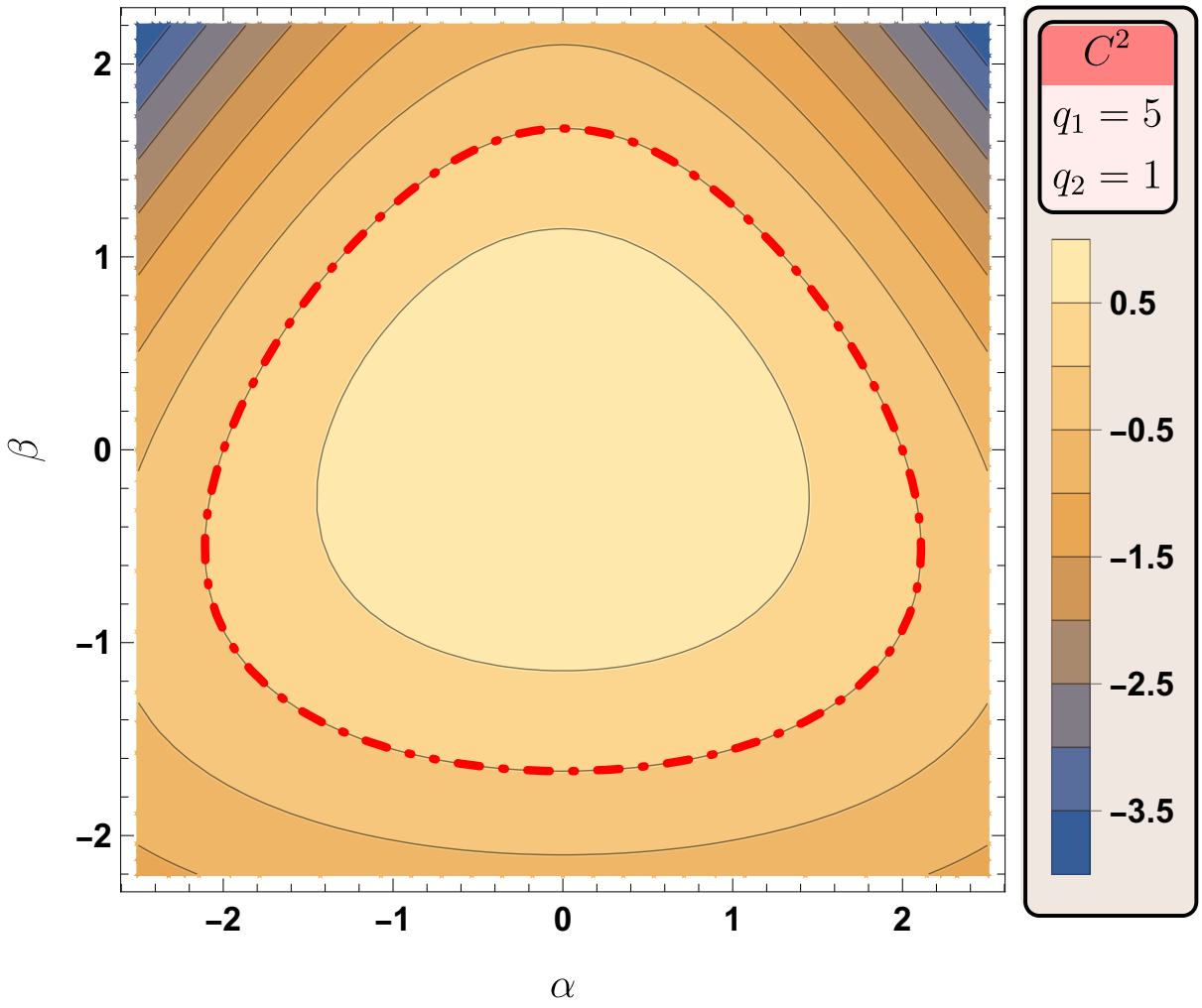

Figure 11.3: *Plot of* C^2, (11.98), *for* $q_1 = 5$, $q_2 = 1$, *as a function of* α *and* β. *The red dashed-dotted lines indicates the* $C = 0$ *contour, which encloses the region of positive values.* C^2 *determines the size of the* ψ *circle at infinity, in the asymptotically* AdS_3 *region.*

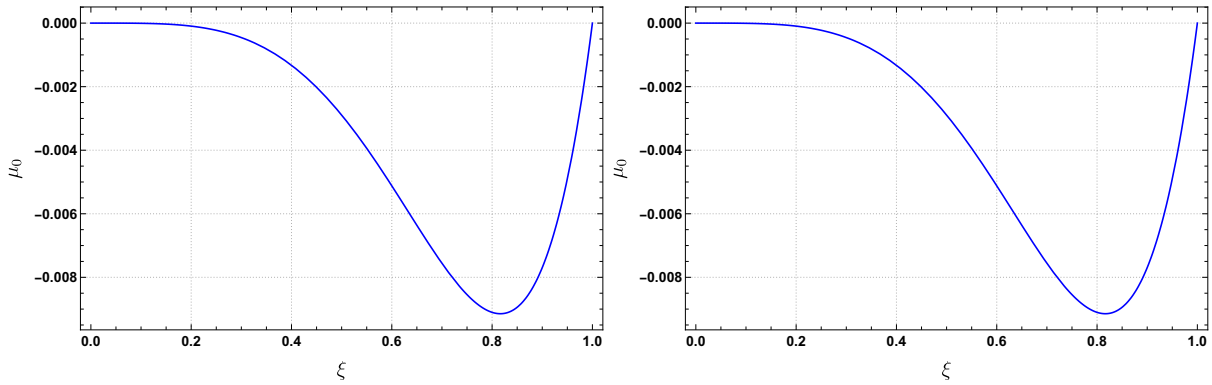

Figure 11.4: *Plots of* $\frac{1}{2}\lambda_1 \equiv \mu_0$ *against* ξ. *In the first graph we have taken* $\sigma = 2$, $\beta = -\frac{q_1}{(2q_1-1)^2} + \frac{1}{10^6}$, $q_1 = 5$. *The second graph corresponds to* $\sigma = 2$, $\beta = -\frac{q_1}{(2q_1-1)^2}$, $q_1 = 5$.

Chapter 12

Perturbative constructions of non-BPS geometries

Having explored the space of supersymmetric solutions, we now turn to the construction of non-BPS states. While the ansätze presented in Chapter 9 have drastically simplified the problem by making it one-dimensional, we are still left with the problem of finding solutions to the equations of motion: a system of many coupled non-linear differential equations. Finding analytical solutions to this system is out of reach. The main tool at our disposal is perturbation theory, but we also make use of numerical methods.

This Chapter is based on the work of [38,39,42]. In Section 12.1, we start by reviewing the technicalities of imposing physical constraints on the solutions, and gauge fixing the ansätze. In Section 12.2, we present the perturbative construction of solutions in the single-mode ansatz. This system consists of 11 second order ODEs for these functions plus 3 first-order constraints. We find two large classes of new non-BPS solutions whose properties we explore.

In Section 12.3, we then work in the Axial gauge of Section 9.3 with the functions (9.32). This system is a superset of the previous one, and in total consists of 19 second order ODEs for these functions plus 3 first-order constraints. We study this system and make use of the relative independence of the two sectors of the truncation to construct "almost-BPS" solutions.

Section 12.4 finally presents a radically different approach to the perturbative computation, taking as a base a deep superstratum solution rather than the vacuum. We construct solutions within the framework of the WKB approximation, and are able to compare some of the results with those of the previous perturbation theory.

The scope of this Chapter is limited to the presentation of the new non-BPS solutions, and the computations that lead to these solutions, within supergravity. The analysis and interpretation of these solutions using holography and the CFT will be the object of the Chapters 13 and 14.

12.1 Gauge fixing and boundary conditions

We start by determining as many of the boundary conditions as we can. Since the single-mode truncation is included in the double-mode truncation, we use the latter to fix the conditions, and it is straightforward to specialize the results to the single-mode truncation. First and foremost, we fix the geometry to be asymptotic to AdS_3. This means that the leading divergences in (7.18) must cancel as $\xi \to 1$, and this implies:

$$\Omega_1(1) \;=\; \frac{\Omega_0(1)}{k(1)}\,. \tag{12.1}$$

The metric now has divergences proportional to $(1-\xi)^{-1} \sim \rho^2$ that multiply the metric in the $(d\psi, d\tau)$-directions. This describes some, possibly boosted, asymptotically AdS geometry.

It is convenient to use the coordinate σ, defined in (7.12). The components of (7.18) then satisfy:

$$g_{\sigma\sigma} \;+\; g_{\tau\tau} \;-\; 2\,g_{\sigma\tau} \;=\; \Omega_1^2\,, \tag{12.2}$$

for all ξ. The fixed canonical periodicity of σ prevents it from being rescaled. On the other hand, we have not yet fixed the rescaling of the time coordinate, $\tau \to c\,\tau$ (along with the appropriate rescaling of the electric gauge fields and metric functions[1]). In previous work [38], this gauge was fixed by requiring $\Omega_1(\xi = 1) = 1$, however, as was pointed out in [39], holography suggests a more natural choice. We want the asymptotic geometry to be sectioned by canonically normalized (cylindrical) Minkowski slices with

$$ds_2^2 \;\sim\; \rho^2(d\tau^2 - d\sigma^2)\,. \tag{12.3}$$

We therefore fix the scaling of τ by requiring:

$$\lim_{\xi\to 1} \frac{g_{\sigma\sigma}}{g_{\tau\tau}} \;=\; -\,1\,. \tag{12.4}$$

However, combining this with (12.2), one sees that this condition also removes the ρ^2 divergent term in $g_{\sigma\tau}$, and so (12.4) sets the asymptotic metric to the *unboosted*, conically-normalized, Minkowski-sliced AdS_3 with (12.3).

We therefore use the boundary conditions (12.1) and (12.4) throughout this manuscipt.

From (7.18) we see that we can also absorb a scale of Ω_0 into the definition of R_{AdS}, and thus we can, without loss of generality take[2]:

$$\Omega_0(1) \;=\; 1\,. \tag{12.5}$$

In order for the solution to limit to the supersymmetric vacuum at infinity, the scalar fields must limit to the supersymmetric critical point of the potential. This means that

[1] Precisely, the change of coordinates $\tau \to c\,\tau$ leads to the redefinitions $\Omega_1 \to c\,\Omega_1$, $\Phi_{1,2} \to c\,\Phi_{1,2}$, $k \to c^{-1}k$.

[2] The overall scale, R_{AdS}, is fixed by the equations of motion. Since we will actually set $R_{AdS} = g_0^{-1}$, the condition $\Omega_0(1) \;=\; 1$ will then emerge from the equations of motion.

χ_I and m_{IJ} must vanish at infinity, which in terms of the fields of the ansatz translates to:

$$\nu_{1,2}(1) \;=\; \mathcal{O}(1)\,, \qquad \mu_{1,2}(1) \;=\; \lambda_{1,2}(1) \;=\; 0\,, \qquad m_{5,6}(1) \;=\; 0\,. \tag{12.6}$$

We are, of course, going to require that all the fields in (9.6) or (9.32) are smooth functions of ξ on the whole interval $[0,1]$, including at the boundaries. In particular, this imposes some conditions at the origin. Since we are working with τ and ψ independent solutions, the value at the origin of the potentials Ψ_1 and Ψ_2 fixes the "modes," or "magnetic quantum numbers," of our excitations. The other magnetic potentials must limit to 0 at the origin[3]:

$$\Psi_1(0) \;=\; \frac{1}{2}\,n_1\,, \qquad \Psi_2(0) \;=\; \frac{1}{2}\,n_2\,, \qquad \Psi_3(0) \;=\; \Psi_4(0) \;=\; 0\,. \tag{12.7}$$

The periodicity of the ψ-circle and smoothness requires[4] that $n_j \in \mathbb{Z}$. Note that the situation is only slightly different in the single-mode truncation. This ansatz contains a residual global $U(1)$ rotation, whose action is to shift the values of the potentials: Φ_2, Ψ_2. We thus need to impose additional conditions to uniquely fix a solution, we choose $\Phi_2(1) \;=\; 0$ and $n_2 = 0$.

Finally, ensuring the regularity of the metric at the origin also requires that Ω_0 and Ω_1 remain finite at $\xi = 0$ and that

$$k(\xi) = \mathcal{O}(\xi^2) \quad \text{as} \quad \xi \to 0\,. \tag{12.8}$$

We will show that the system has two classes of smooth "solitonic" solutions, which we refer to as α-class and β-class. Each solution is defined by a locus with parameters that depend on the truncation: $(n_1, \hat{\omega}_1, \zeta_1)$ for the single-mode truncation, and $(n_1, n_2, \hat{\omega}_1, \hat{\omega}_2, \zeta_1, \zeta_2)$ for the double-mode truncation, where $n_1, n_2 \in \mathbb{Z}$ are the "magnetic quantum numbers" defined in (12.7), $\hat{\omega}_1, \hat{\omega}_2$ are discrete "frequencies," or energies, of normal modes of oscillation and ζ_1 and ζ_2 are continuous parameters that determine the magnitudes of various component fields. As one would expect, all these parameters emerge from the choice of boundary conditions that result in smooth solutions. Pinning down the solution locus exactly can be done using perturbation theory, or numerics. These methods lead to different possible characterizations of the parameters ζ_1, and ζ_2. In Chapter 14, we will show how one extracts the energies, $\hat{\omega}_1, \hat{\omega}_2$, from the boundary data.

[3]We work here in the axial gauge. In the diagonal gauge, one also needs to impose $\Psi_5(0) = \Psi_6(0) = 0$.

[4]Combining (7.75) and (9.5), one sees that the minimal couplings of the gauge potentials inherit a factor of 2, and hence all the factors of $\frac{1}{2}$ in (12.7).

12.2 Perturbation theory in the single-mode truncation

In this Section we work in the single-mode truncation, described in Section 9.2, and with the fields (9.6). To construct the perturbative solutions, we expand each field as:

$$X(\xi) = X^{\rm AdS}(\xi) + \sum_{k=1}^{\infty} \epsilon^k \, \delta^{(k)} X(\xi), \tag{12.9}$$

where ϵ is a bookkeeping parameter. We will introduce parameters for the (small) amplitudes of the perturbations at linear order, and so in the end, we will be able to take $\epsilon = 1$. The superscript AdS denotes the AdS vacuum. Furthermore, we will sometimes work with a slightly different basis of fields that makes the computations easier, namely:

$$\mu_\pm = \frac{1}{2}\big(\mu_1 \pm \mu_2\big), \qquad \Phi_\pm = \frac{1}{2}(\Phi_1 \pm \Phi_2), \quad \Psi_\pm = \frac{1}{2}(\Psi_1 \pm \Psi_2). \tag{12.10}$$

The values of $X^{\rm AdS}$ are determined by the AdS_3 vacuum. For the scalars and the metric fields, this is simply:

$$\nu_1^{\rm AdS} = 0, \quad \mu_{1,2}^{\rm AdS} = 0, \quad \lambda_1^{\rm AdS} = 0, \quad \Omega_0^{\rm AdS} = 1, \quad \Omega_1^{\rm AdS} = 1, \quad k^{\rm AdS} = \xi^2 \,. \tag{12.11}$$

The gauge fields require more care, as the vacuum possesses many symmetries that individual solutions do not. The magnetic potentials must be fixed at the origin as in (12.7). In addition, as explained in the previous Section, the residual global $U(1)$ symmetry rotating the indices (34) can be fixed by choosing $\Phi_2(1) = 0$ and $n_2 = 0$. Remains the other electric potential, Φ_1. At this level, Φ_1 is unconstrained, and so we need to introduce a new mode number, ω_1, to parametrize the range of values it can take. The gauge fields are then:

$$\Phi_1^{\rm AdS} \;=\; \frac{\omega_1}{2} \,, \quad \Phi_2^{\rm AdS} \;=\; 0 \,, \quad \Psi_1^{\rm AdS} \;=\; \frac{n_1}{2} \,, \quad \Psi_2^{\rm AdS} \;=\; 0 \,. \tag{12.12}$$

We can now solve the system of second order, ordinary differential equations, order by order in ϵ. We will first compute the linearised equations of motion and determine their solutions. At higher orders, the equations one needs to solve are given by the linear piece plus additional sources coming from the previous orders.

12.2.1 Linear perturbations

We now turn to the linear perturbations. The linearized equations of motion around the vacuum can be derived from the action (9.7), they are:

$$\xi\,\partial_\xi\big(\xi\,(1-\xi^2)\,\delta^{(1)}\nu_1'\big) - \big(n_1^2 - (\omega_1+n_1+1)(\omega_1+n_1-1)\xi^2\,\big)\,\delta^{(1)}\nu_1 \;=\; 0\,, \tag{12.13}$$

$$\xi\,\partial_\xi\big(\xi\,\delta^{(1)}\lambda_1'\big) \;-\; \frac{4}{(1-\xi^2)}(n_1^2 - (\omega_1+n_1)^2\xi^2)\,\delta^{(1)}\lambda_1 \;=\; 0, \tag{12.14}$$

$$\xi\,\partial_\xi\big(\xi\,\delta^{(1)}\mu_+'\big) \;-\; \frac{8\xi^2}{(1-\xi^2)^2}\delta^{(1)}\mu_+ \;=\; 0\,, \qquad \xi\,\partial_\xi\big(\xi\,\delta^{(1)}\mu_-'\big) \;=\; 0, \tag{12.15}$$

$$\partial_\xi\big(\xi\delta^{(1)}\Phi'_+\big) \;=\; 0\,, \qquad \partial_\xi\left(\frac{1-\xi^2}{2\,\xi}\delta^{(1)}\Psi'_+ \,-\, \delta^{(1)}\Psi_+ \,-\, \delta^{(1)}\Phi_+\right) \;=\; 0 \tag{12.16}$$

$$\partial_\xi\left(\frac{1-\xi^2}{2\,\xi}\delta^{(1)}\Psi'_- \,+\, \delta^{(1)}\Psi_- \,+\, \delta^{(1)}\Phi_-\right) \;=\; 0\,, \tag{12.17}$$

$$\partial_\xi\big(\xi\delta^{(1)}\Phi'_-\big) \,+\, 4\,\delta^{(1)}\Psi'_- - 4\,\frac{\xi^2}{1-\xi^2}\,\delta^{(1)}\Phi'_- \;=\; 0, \tag{12.18}$$

$$\partial_\xi\big(\xi\,\big(1-\xi^2\big)\,\delta^{(1)}\Omega'_1 \,-\, 2\,\delta^{(1)}\Omega_1\big) \;=\; 0\,, \tag{12.19}$$

$$\partial_\xi\big(\xi\delta^{(1)}\Omega'_0\big) \,-\, 8\frac{\xi}{\big(1-\xi^2\big)^2}\,\delta^{(1)}\Omega_0 \;=\; -\,3\,\frac{1+\xi^2}{1-\xi^2}\,\delta^{(1)}\Omega'_1\,, \tag{12.20}$$

$$\partial_\xi\left(\frac{\delta^{(1)}k}{1-\xi^2}\right) + \frac{1+\xi^2}{1-\xi^2}\delta^{(1)}\Omega'_1 \;=\; \frac{2\xi}{(1-\xi^2)^2}(2\delta^{(1)}\Omega_0 - \delta^{(1)}\Omega_1)\,. \tag{12.21}$$

The only fields that admit regular and normalizable solutions to their linearised equations are ν_1 and λ_1:

$$\begin{aligned}\nu_1 =&\alpha_1\,\xi^{n_1}\,{}_2F_1\big((1-\omega_1)/2,\,n_1+(1+\omega_1)/2,\,1+n_1,\,\xi^2\big),\\ \lambda_1 =&\beta_1\,\xi^{2\,n_1}\,{}_2F_1\big(-\omega_1,\,2\,n_1+\omega_1,\,1+2\,n_1,\,\xi^2\big)\,,\end{aligned} \tag{12.22}$$

where α_1 and β_1 are the amplitudes of the scalar perturbations, they are real numbers. Depending on which of (12.22) we turn on, we can identify two main classes of solutions - the "alpha class" if ν_1 is excited at linear order and the "beta class" if λ_1 is switched on at linear order. For these perturbations to be regular, ω_1 must be an odd integer, $\omega_1 \in 2\mathbb{Z}+1$.

The linear perturbations play an important role in holography, since they allow the identification of the bulk fields with CFT operators. This identification, and the complementary field theory interpretation of the bulk gravitational results, is the subject of Chapter 13.

Linearizing the generalized superstrata solution described in Section 11.2 around the AdS vacuum, one finds a result that matches the expansion (12.22) with $\omega_1 = 1$. The amplitudes α_1 and β_1 are expressed in terms of the parameters of the superstrata as:

$$\alpha_1^2 \;=\; -\,2\sigma\beta\,, \quad \text{and} \quad \beta_1 \;=\; \beta. \tag{12.23}$$

This means that all solutions with $\omega_1 = 1$ are BPS. Since we are interested in building non-supersymmetric solutions, we turn to the next simplest value for the frequency, and for the rest of this section, *we fix* $\omega_1 = 3$. In the double-mode truncation, that will be investigated in the next section, it will be possible to build non-BPS solutions with $\omega_1 = 1$.

12.2.2 The α-class of non-BPS solutions

We will first focus solely on the α_1-deformation, setting $\beta_1 = 0$ in (12.22) to turn off λ_1 at linear order.

It is necessary to compute the expansion up to at least fourth order in α_1, for two reasons. The first is that this order will be needed to perform non-trivial checks in the CFT. The second reason is that the coiffuring condition appears at this order. This non-trivial result shows that, in order for the α-deformation to be normalizable, one needs to also excite the scalar λ_1 (at higher than linear order), corresponding to the β-deformation, in a precise relation to α_1.

First order

The linear perturbation has already been described in section 12.2.1. Only one scalar field is excited, ν_1, with $\omega_1 = 3$:

$$\delta^{(1)}\nu \;=\; \alpha_1 \xi^n \left(1 - \frac{n_1+2}{n_1+1}\xi^2\right), \tag{12.24}$$

and the other fields are set to zero. Note that α_1 is normalised so that $\nu_1 \sim \alpha_1\, \xi^n$ as $\xi \to 0$.

Second order

At order α_1^2, all fields but ν_1 receive normalizable corrections. One could argue that the scalar ν_1, as well as λ_1, have normalizable homogeneous solutions, which can always be added to the two scalars at each order. Indeed, as we will see, the homogeneous term in λ_1 will prove to be very important for assuring the normalizability of the solutions. On the other hand, this term in ν_1 would only lead to a redefinition of α_1, and therefore can be discarded.

For the scalars, we find

$$\begin{aligned}
\delta^{(2)}\lambda_1 \;=\; & \frac{(n_1+2)\alpha_1^2}{16(2n_1+1)(n_1+1)^2}\xi^{2+2n_1}(1-\xi^2)\big((2n_1+3)\xi^2 - 2(n_1+1)\big) \\
& + \beta_{(2)}\,\xi^{2n}(1-\xi^2)\left(1 - 4\frac{n_1+2}{2n_1+1}\xi^2 + \frac{(n_1+2)(2n_1+5)}{(n_1+1)(2n_1+1)}\xi^4\right), \qquad (12.25)\\
\delta^{(2)}\mu_1 \;=\; & -\frac{\alpha_1^2}{16}\xi^{2n}(1-\xi^2)\left(1 - \frac{n_1+2}{n_1+1}\xi^2\right)^2, \qquad (12.26)\\
\delta^{(2)}\mu_2 \;=\; & 0\,, \qquad (12.27)
\end{aligned}$$

where we named $\beta_{(2)}$ the constant of integration for the homogeneous solution in λ_1. We will find that it gets fixed at order α_1^4 by a coiffuring mechanism.

The corrections to the gauge fields are

$$\begin{aligned}
\delta^{(2)}\Phi_1 \;=\; & \gamma_{(2)} \qquad \delta^{(2)}\Psi_1 \;=\; 0 \qquad (12.28)\\
\delta^{(2)}\Phi_2 \;=\; & \frac{\alpha_1^2}{4(n_1+1)^2}\xi^{2n}\big(1 + n_1(n_1+2)(1-\xi^2)^2\big)\,, \qquad (12.29)\\
\delta^{(2)}\Psi_2 \;=\; & \frac{\alpha_1^2}{4(n_1+1)^2}\xi^{2n_1+2}\big((n_1+1)(n_1+3)(1-\xi^2)^2 + \xi^4\big)\,, \qquad (12.30)
\end{aligned}$$

where γ_2 is a constant, which will be fixed at the next order by demanding regularity of ν_1 at infinity. Again, the subscript denotes the order at which these constants are introduced.

The corrections to the metric are

$$\delta^{(2)}\Omega_0 = -\frac{\alpha_1^2}{8(n_1+1)^2}\xi^{2n_1}(1-\xi^2)\big[(n_1+1)^2-2(n_1^2+3n_1+1)\xi^2+(n_1+2)^2\xi^4\big], \tag{12.31}$$

$$\delta^{(2)}\Omega_1 = -\frac{3\alpha_1^2}{4(n_1+1)^2}+\frac{\alpha_1^2}{2(n_1+1)^2}\xi^{2n_1+2}(1-\xi^2), \tag{12.32}$$

$$\delta^{(2)}k = \frac{3\alpha_1^2}{4(n_1+1)^2}\xi^2+\frac{\alpha_1^2}{2(n_1+1)^2}\xi^{2n_1+2}(1-\xi^2)\big(n_1+1-(n_1+2)\xi^2\big). \tag{12.33}$$

Note that the constant factor of $3/4$ appearing in Ω_1 and k is a result of the normalization of time (12.4).

Third order

As we progress to higher orders, it becomes harder to solve the equations for a general mode number n_1, as the source terms become more complicated. Two methods can be used to determine the solutions. The first is based on the fact that all normalizable solutions appear to be polynomials in ξ. The differential equations thus become recurrence equations, that can sometimes be solved. The second method is to solve the equations for a large number of different values of n_1, and to try to extrapolate the general solution. The result can then be checked against the original equations. We use the latter method.

Akin to the linear order situation, at third order in α_1 only $\delta^{(3)}\nu_1$ receives a non-trivial correction (non-linearly sourced by lower order solutions). We again find a non-normalizable (log-divergent at infinity) piece, whose vanishing gives us an expression for one of the constants that was not fixed at the previous order, $\gamma_{(2)}$. This results in:

$$\gamma_{(2)} = \frac{9}{4(n_1+1)^2}-\frac{3}{32(n_1+1)^2}\left(\frac{1}{2n_1+1}+\frac{22}{2n_1+3}+\frac{1}{2n_1+5}\right). \tag{12.34}$$

Moreover, one can add homogeneous solutions in $\delta^{(3)}\lambda_1$ and $\delta^{(3)}\Phi_1$, by introducing respectively the constants $\beta_{(3)}$ and $\gamma_{(3)}$. We have:

$$\delta^{(3)}\nu = \frac{3(3n_1^2+9\,n_1+4)\,\xi^{2+n_1}}{2(8n_1^3+36n_1^2+46n_1+15)(n_1+1)^3}\left[\sum_{k=1}^{n_1-1}\frac{n_1+k+2}{k(k+1)}\xi^{2k}-(n_1+3)\right]-\xi^{3n_1}\mathcal{P}_{n_1}(\xi^2)\,, \tag{12.35}$$

$$\delta^{(3)}\lambda_1 = \beta_3\,\xi^{2n_1}(1-\xi^2)\left(1-2\frac{2n_1+4}{2n_1+1}\xi^2+\frac{(n_1+2)(2n_1+5)}{(n_1+1)(2n_1+1)}\xi^4\right), \tag{12.36}$$

$$\delta^{(3)}\Phi_1 = \gamma_{(3)}\,, \tag{12.37}$$

where $\mathcal{P}_{n_1}(\xi^2)$ is a family of polynomials of order 4 in ξ^2, whose terms are complicated rational functions of the mode n_1, and have a linear dependence on $\beta_{(2)}$.

The constant $\gamma_{(3)}$ will be fixed at next order, by the regularity of the scalars at infinity, and $\beta_{(3)}$ will get fixed two orders later (at α_1^5) to avoid non-normalizable solutions, as explained earlier.

Fourth and higher orders

At fourth order in the perturbative expansion, one finds that all fields but ν receive corrections, as was the case at order α_1^2. The scalar $\delta^{(4)}\lambda_1$ is normalizable (and polynomial) if and only if the following coiffuring constraint is satisfied

$$\beta_2 \;=\; -\frac{\alpha_1^2}{4} \quad \text{and} \quad \gamma_{(3)} \;=\; 0\,. \tag{12.38}$$

The expression for the other fields is also known, but of little interest here. They are all polynomial in ξ.

At higher orders, while the analysis becomes too involved when keeping n_1 general, it is possible to continue it at a fixed value of n_1. We did this up to tenth order, and for n_1 up to 10. We find patterns that we postulate are true for all modes, in particular

$$\delta^{(2\,k)}\nu = 0, \quad \text{and} \quad \delta^{(2\,k+1)}\lambda_1 = 0\,, \quad \text{for} \quad k \in \mathbb{N}\,, \tag{12.39}$$

$$\gamma_{(k)} \;=\; 0 \quad \text{and} \quad \beta_{(k)} \;=\; 0\,, \quad \text{for} \quad k \geq 3\,. \tag{12.40}$$

12.2.3 Properties of the special locus

We call *special locus* the precise relation (12.38), between the amplitudes of the alpha-perturbation and the beta-perturbation, found in the previous Section. The non-BPS alpha-class solutions that we can construct within the truncation are necessarily on this special locus. This locus also exists for BPS solutions, as we have seen in Section 11.1, however in this case more general solutions can be constructed, as we did in Section 11.2.

The special locus plays an essential role in the construction of smooth non-BPS solutions. We describe it first through its rather prosaic description in supergravity. The understanding of its significance only comes from its description in the dual CFT, which is the object of a following chapter.

However, the definition of the special locus in terms of equation (12.38) is very narrow, we want to give a broader definition that can be applicable to the other Q-ball truncations, and beyond perturbation theory. We will thus define it by the properties that the solutions at the special locus seem to enjoy.

Definition. A solution is said to be on the *special locus* if it satisfies two very specific algebraic relationship between the scalars χ_I, the scalars m_{IJ} and the Maxwell fields, ${F_{\mu\nu}}^{IJ}$:

- χ_I is an eigenvector of m_{IJ}, and the corresponding eigenvalue, m_0, is the only non-

trivial eigenvalue of m_{IJ}, with

$$m_0 = 1 - \frac{1}{2}\,\chi_I \chi_I\,. \tag{12.41}$$

All other eigenvalues of m_{IJ} are equal to 1.

- Furthermore, χ_I is a null vector of the dual field strengths.

$$\widetilde{F}_{\mu\nu}{}^{IJ}\,\chi_J \;=\; 0\,. \tag{12.42}$$

These properties are indeed satisfied by both the BPS solution at the special locus, and perturbatively by the non-BPS solutions constructed in the previous Section. Note that the first property means that the matrix m_{IJ} has an $SO(3)$ invariance in the directions orthogonal to χ_I. This matrix encodes the deformation of the S^3 on which the parent supergravity theory has been reduced from six to three dimensions. However, the $SO(3)$ is typically broken by the gauge fields, A_μ^{IJ}.

We should stress that these are "empirical" properties of the special locus that were found through the construction of smooth non-BPS solutions. The significance of the special locus in supergravity remains somewhat mysterious.

12.2.4 The β-class of perturbative non-BPS solutions

We now repeat the previous analysis with the solutions emerging from the second deformation in (12.22). That is, we turn off the ν_1 deformation by setting $\alpha_1 = 0$, and make a perturbative expansion of the solution in small β_1. The β-deformation does not require a coiffuring. While our results with general n_1 are limited to the third order, we will continue the analysis for a few fixed values of n_1, as done for the α-deformation.

First order

The linear solution has been described in section 12.2.1. The only excited 3D field is

$$\delta^{(1)}\lambda_1 \;=\; \beta_1\left(1-\xi^2\right)\xi^{2n_1}\left(1 - 2\frac{2n_1+4}{2n_1+1}\xi^2 + \frac{(n_1+2)(2n_1+5)}{(n_1+1)(2n_1+1)}\xi^4\right). \tag{12.43}$$

Second order

At second order, most of the fields receive a correction. The scalars are given by

$$\delta^{(2)}\nu_1 \;=\; \delta^{(2)}\lambda_1 \;=\; 0, \tag{12.44}$$

and

$$\delta^{(2)}\mu_1 \;=\; -\,\delta^{(2)}\mu_2 \;=\; \frac{1}{4}\beta_1^2\xi^{4n_1+2}\left(\frac{12(n_1+2)\left(4n_1^2+12n_1+7\right)\xi^4}{(n_1+1)(2n_1+1)^2(2n_1+3)^2} + \frac{2(n_1+2)^2\xi^8}{(n_1+1)^2(2n_1+1)^2}\right.$$
$$\left. - \frac{4(2n_1+5)\xi^6}{(n_1+1)(2n_1+1)^2} - \frac{4(n_1+2)\xi^2}{(n_1+1)^2(2n_1+1)} + \frac{2}{(2n_1+1)^2}\right) - \frac{3\beta_1^2}{2(n_1+1)^2(2n_1+1)^2(2n_1+3)^2}\,. \tag{12.45}$$

The gauge fields are more appropriately written in the basis described in (12.10). They are

$$\delta^{(2)}\Phi_+ = \frac{-3\beta_1^2}{2(2n_1+1)^2}\Bigg[\frac{(n_1+2)^2\xi^8}{(n_1+1)^2} - \frac{2(2n_1+5)\xi^6}{n_1+1} + \frac{6(n_1+2)\left(4n_1^2+12n_1+7\right)\xi^4}{(n_1+1)(2n_1+3)^2} - \frac{2(n_1+2)(2n_1+1)\xi^2}{(n_1+1)^2} + 1\Bigg]\xi^{4n_1+2} + \gamma_{(2)}. \tag{12.46}$$

$$\delta^{(2)}\Phi_- = \frac{-3\beta_1^2\left(1-\xi^2\right)^2\left((n_1^2+4n_1+4)\xi^4 - (2n_1^2+6n_1+3)\xi^2 + n_1^2+2n_1+1\right)\xi^{4n_1+2}}{2(n_1+1)^2(2n_1+1)^2} + \gamma_{(2)}. \tag{12.47}$$

$$\delta^{(2)}\Psi_- = \frac{1}{4}\beta_1^2\xi^{4n_1+2}\Bigg[-\frac{(n_1+2)^2\xi^8}{(n_1+1)^2(2n_1+1)} + \frac{2\left(4n_1^3+16n_1^2+17n_1+4\right)\xi^6}{(n_1+1)^2(2n_1+1)^2} - \frac{2\left(12n_1^4+60n_1^3+99n_1^2+59n_1+9\right)\xi^4}{(n_1+1)^2(2n_1+1)^2(2n_1+3)} + \frac{2\left(4n_1^2+8n_1+1\right)\xi^2}{(n_1+1)(2n_1+1)^2} - \frac{1}{2n_1+1}\Bigg]. \tag{12.48}$$

$$\begin{aligned}\delta^{(2)}\Psi_+ = \frac{-\beta_1^2\xi^2}{4(n_1+1)^2(2n_1+1)^2(2n_1+3)^2}\Bigg[\xi^{4n_1}\Big((n_1+2)^2(2n_1-1)(2n_1+3)^2\xi^8 \\ - 2(n_1+1)(2n_1+3)^2\left(4n_1^2+9n_1-4\right)\xi^6 \\ + 6(n_1+1)\left(8n_1^4+40n_1^3+58n_1^2+14n_1-9\right)\xi^4 \\ - 2(2n_1+1)\left(8n_1^4+42n_1^3+73n_1^2+39n_1-9\right)\xi^2 \\ + 8n_1^5+44n_1^4+94n_1^3+97n_1^2+48n_1-9\Big) - \frac{18\left(1-\xi^{4n_1}\right)}{1-\xi^2}\Bigg].\end{aligned} \tag{12.49}$$

Finally, the corrections to the metric functions are

$$\delta^{(2)}\Omega_1 = \frac{3\beta_1^2\Big(2(2n_1+3)\left(\xi^2-1\right)^2\xi^{4n_1+2}\left((n_1+2)^2\xi^4 - (2n_1(n_1+3)+3)\xi^2 + (n_1+1)^2\right) - 3\Big)}{2(n_1+1)^2(2n_1+1)^2(2n_1+3)}. \tag{12.50}$$

$$\delta^{(2)}\Omega_0 = \frac{1}{4}\beta_1^2\left(1-\xi^2\right)^2\xi^{4n_1}\Big(-\frac{(n_1+2)^2(2n_1+5)^2\xi^8}{2(n_1+1)^2(2n_1+1)^2} + \frac{2(n_1+2)^2\left(4n_1^2+14n_1+5\right)\xi^6}{(n_1+1)^2(2n_1+1)^2} - \frac{\left(12n_1^4+72n_1^3+133n_1^2+75n_1+9\right)\xi^4}{(n_1+1)^2(2n_1+1)^2} + \frac{2\left(4n_1^2+10n_1-1\right)\xi^2}{(2n_1+1)^2} - \frac{1}{2}\Big). \tag{12.51}$$

$$\begin{aligned}\delta^{(2)}k = -\frac{\beta_1^2\xi^2}{4(n_1+1)^2(2n_1+1)^2(2n_1+3)}\Bigg[\left(\xi^2-1\right)\xi^{4n_1}\Big(5(n_1+2)^2(2n_1+3)(2n_1+5)\xi^8 \\ - 4(n_1+2)(2n_1+3)(5n_1(2n_1+7)+23)\xi^6 + 2\Big(n_1(n_1+3)\Big(60n_1^2+180n_1+209\Big)+171\Big)\xi^4 \\ - 4(n_1+1)(2n_1+3)(10n_1^2+25n_1+8)\xi^2 + 5(n_1+1)^2(2n_1+1)(2n_1+3)\Big) - 18\Bigg].\end{aligned} \tag{12.52}$$

One could add a homogeneous term to the scalar $\delta^{(2)}\nu_1$, but we find at next order that it has to vanish. Here again, $\gamma_{(2)}$ is an integration constant that is fixed when requiring that the solution is normalizable at third order

Third order

At this order the only field that receives a non-trivial correction is λ_1:

$$\begin{aligned}\delta^{(3)}\lambda_1 = -\frac{1}{4}\beta_1^3(1-\xi^2)\xi^{2+2\,n}\Bigg[&\frac{48\,n_{1,2}\,B_1}{n_{1,1}^2\,n_{2,1}^3\,n_{2,3}^2\,n_{4,3}\,n_{4,5}\,n_{4,7}\,n_{4,9}} - \frac{B_2\,\xi^2}{n_{1,1}^3\,n_{2,1}^3\,n_{2,3}\,n_{4,3}\,n_{4,5}\,n_{4,7}\,n_{4,9}}\\ &+\frac{\xi^{4\,n}}{3}\Bigg(\frac{4\,n_{8,17}+47}{n_{2,1}^2} - \frac{1}{\xi^2} - \frac{B_3\,\xi^2}{n_{1,1}^2\,n_{2,1}^3} + \frac{B_4\,\xi^4}{n_{1,1}^3\,n_{2,1}^4\,n_{2,3}^2\,n_{4,7}\,n_{4,9}} - \frac{B_5\,\xi^6}{n_{1,1}^4\,n_{2,1}^3\,n_{2,3}^2\,n_{4,9}}\\ &\qquad + \frac{B_6\,\xi^8}{n_{1,1}^3 n_{2,1}^3} - \frac{B_7\,\xi^{10}}{n_{1,1}^3\,n_{2,1}^3} + \frac{n_{1,2}^3\,B_8\,\xi^{12}}{n_{1,1}^3\,n_{2,1}^3} - \frac{B_9\,\xi^{14}}{n_{1,1}^3\,n_{2,1}^3}\Bigg)\\ &+\frac{24\left(n_{4,3}\,n_{4,5}\,n_{4,7}\right)^{-1}}{n_{1,1}^3\,n_{2,1}^3\,n_{2,3}^3\,,n_{4,9}}\sum_{k=1}^{2n}\frac{\xi^{2k+2}}{k\,k_{1,1}\,k_{1,2}}\Bigg(C_1\,n^5 - C_2\,n^4 - C_3\,n^3 - C_4\,n^2 - C_5 n\\ &\qquad - 1260\left(k^3-15k^2-88k-120\right) + 7824(k+8)n^6 + 5216n^7\Bigg)\Bigg],\end{aligned} \tag{12.53}$$

where,

$$n_{a,b} = (a\,n+b), \tag{12.54}$$

and B_j an C_j are constants that are polynomial in n_1, an given in [39]. Moreover, the constant parts in the $\Phi_\pm$ fields are left undetermined until the next order:

$$\delta^{(3)}\Phi_+ = \gamma_{(3)} \quad \text{and} \quad \delta^{(3)}\Phi_- = \gamma_{(3)}. \tag{12.55}$$

Analogously to the α-class calculation, in the process of solving the equations, we need to discard a non-normalizable mode for the scalar field driving the solution, λ_1. This sets the constant $\gamma_{(2)}$ to

$$\gamma_{(2)} \;=\; 3\beta_1^2\,\frac{2304n_1^5+16360n_1^4+44880n_1^3+59330n_1^2+37671n_1+9135}{2(n_1+1)^2(2n_1+1)^2(2n_1+3)^2(4n_1+3)(4n_1+5)(4n_1+7)(4n_1+9)}\,. \tag{12.56}$$

As before, we could have added a homogeneous term to the scalar $\delta^{(3)}\nu$, but it vanishes at next order.

Fourth and higher orders

Once again, the solution at higher order becomes too complicated to determine for a general mode number, but it is possible to continue the computations with a fixed value

of n_1, and deduce some general properties of the solution. This has been done up to eighth order, and with n_1 up to 10.

We find at all orders a polynomial expression for all the fields. At order k, one can introduce a constant $\gamma_{(k)}$ in the gauge field Φ_1, and this constant is fixed at order $k+1$, whereby it is zero for odd values of k. Furthermore, we find that $\nu_1 = 0$ at every order we compute. We postulate that this is an exact result, and that it holds for all values of n_1.

12.3 Perturbation theory in the double-mode truncation

In this Section we work in the double-mode truncation, described in Section 9.3, and in the Axial gauge, with the fields (9.32). We aim to construct non-BPS solutions perturbatively, and once again, we start by expanding each field as

$$X(\xi) = X^{\rm AdS}(\xi) + \sum_{k=1}^{\infty} \epsilon^k \, \delta^{(k)} X(\xi), \tag{12.57}$$

where ϵ is a bookkeeping parameter, that will be taken to 1 at the end. We have to adapt the AdS vacuum of (12.11)-(12.12) to this new truncation, giving extra attention to the gauge fields. The new scalars are simply put to zero:

$$\nu_{1,2}^{\rm AdS} = 0, \quad \mu_{1,2}^{\rm AdS} = 0, \quad \lambda_{1,2}^{\rm AdS} = 0, \quad m_{5,6}^{\rm AdS} = 0, \quad \Omega_0^{\rm AdS} = 1, \quad \Omega_1^{\rm AdS} = 1, \quad k^{\rm AdS} = \xi^2 \,. \tag{12.58}$$

The magnetic gauge fields at zeroth order are fixed by the boundary conditions (12.7). The electric potentials however, are not. We introduce two new parameters, ω_1 and ω_2, and choose:

$$\Phi_{1,2}^{\rm AdS} = \frac{1}{2}\,\omega_{1,2}, \quad \Phi_{3,4}^{\rm AdS} = 0, \quad \Psi_{1,2}^{\rm AdS} = \frac{1}{2}\,n_{1,2}, \quad \Psi_{3,4}^{\rm AdS} = 0\,, \tag{12.59}$$

We will now solve the system of equations order by order in ϵ, starting with the linearised equations of motion. The equations at each order split in five sub-sectors: 1) the three metric functions $\Omega_{0,1}$ and k; 2) the χ^I scalars $\nu_{1,2}$; 3) the m_{IJ} scalars $\mu_{1,2}$, $\lambda_{1,2}$ and $m_{5,6}$; 4) the four gauge fields $\Phi_{1,2}$ and $\Psi_{1,2}$; and 5) the other four gauge fields $\Phi_{3,4}$ and $\Psi_{3,4}$. These are easier to solve using the redefinitions:

$$\begin{aligned} \mu_\pm = \mu_1 \pm \mu_2, \quad m_\pm =& m_5 \pm m_6, \quad \Phi_\pm^{(1,2)} = \Phi_1 \pm \Phi_2, \quad \Psi_\pm^{(1,2)} = \Psi_1 \pm \Psi_2, \\ \Phi_\pm^{(3,4)} =& \Phi_3 \pm \Phi_4, \quad \Psi_\pm^{(3,4)} = \Psi_3 \pm \Psi_4. \end{aligned} \tag{12.60}$$

12.3.1 Linear perturbations

The linearised equations of motion can be derived from the action, as was done in Section 12.2.1. For brevity we will not give the equations here. A few more fields admit regular

and normalizable solutions to their linearised equations around the vacuum, they are $\nu_{1,2}$, $\lambda_{1,2}$ and $m_\pm = m_5 \pm m_6$:

$$\begin{aligned}
\nu_{1,2} =& \alpha_{1,2}\, \xi^{n_{1,2}}\, {}_2F_1\big((1-\omega_{1,2})/2,\, n_{1,2}+(1+\omega_{1,2})/2,\, 1+n_{1,2},\, \xi^2\big),\\
\lambda_{1,2} =& \beta_{1,2}\, \xi^{2\,n_{1,2}}\, {}_2F_1\big(-\omega_{1,2},\, 2\,n_{1,2}+\omega_{1,2},\, 1+2\,n_{1,2},\, \xi^2\big),\\
m_+ =& \gamma_+\, \xi^{|n_1-n_2|}\, {}_2F_1\Big(-\text{sign}(n_1-n_2)\frac{\omega_1-\omega_2}{2},\, |\,n_1-n_2|+\text{sign}(n_1-n_2)\frac{\omega_1-\omega_2}{2},\, 1+|n_1-n_2|,\, \xi^2\Big),\\
m_- =& \gamma_-\, \xi^{n_1+n_2}\, {}_2F_1\big(-(\omega_1+\omega_2)/2,\, n_1+n_2+(\omega_1+\omega_2)/2,\, 1+n_1+n_2,\, \xi^2\big). \qquad (12.61)
\end{aligned}$$

where we have several amplitudes of the scalar perturbations, $\alpha_{1,2}, \beta_{1,2}$ and $\gamma_{+,-}$. Note that they are fixed so that $\nu_{1,2} \sim \alpha_{1,2}\xi^{n_{1,2}}$ and $\lambda_{1,2} \sim \beta_{1,2}\xi^{2n_{1,2}}$ at the origin.

As we did for the single-mode truncation, depending on which of (12.61) we turn on, we can identify two main classes of solutions in each of the two sectors $(1,0,n_1)$ and $(1,1,n_2)$ - the alpha class if only one of $\nu_{1,2}$ are excited at linear order and the beta class if one of $\lambda_{1,2}$ are switched on at linear order. These were already investigated in detail in Section 12.2 for the $(1,0,n_1)$ solutions and their features in the $(1,1,n_2)$ sector are exactly the same, so we will only briefly go over them below. The scalars $m_\pm$ also lead to a class of solutions, but our ansatz does not seem to be well suited for analyzing them. Activating only m_- at linear order produces an easy-to-handle perturbative BPS solution. However, the same does not hold for m_+ and we cannot find a solution within our ansatz. Turning both $m_\pm$ on simultaneously should produce a non-BPS geometry, but the expressions become quickly very cumbersome to work with and we have not been able to explore the system in any significant detail. Therefore, from here onward we will mostly focus on the alpha and beta classes of solutions.

We find that there need not be a correlation between the classes in each sector. That is, one can choose to keep the perturbations associated with α_1 and β_2, for example. In this Section, however, we make the choice to present two of the four allowed combinations of classes: We first present the "alpha-alpha" class, then the "beta-beta" class, and will not discuss the "alpha-beta" and "beta-alpha" classes.

Note that once again, these perturbations are regular only if $\omega_{1,2}$ are odd integers, $\omega_{1,2} \in 2\mathbb{Z}+1$. In the single-mode truncation, we found that solutions with $\omega_1 = 1$ were BPS, and this led us to choose $\omega_1 = 3$. However, this is no longer true in the double-mode truncation: solutions with $\omega_1 = \omega_2 = 1$ are generally not BPS, provided that at least one scalar perturbation is activated in each sector. Indeed, while the double superstratum solution detailed in Section 9.3.3 does match with the form of the linearized perturbations[5], it does so with different mode numbers: $\omega_1 = -\omega_2 = 1$.

For the rest of this Section, we will then make the choice $\omega_1 = \omega_2 = 1$. We emphasize again that in this work, if only *one* of the sectors is activated, then the solution is BPS. Only when excitations in *both sectors* are turned on is the resulting geometry non-BPS. There is one rather interesting exception: $n_1 = n_2$, $\alpha_{1,2} \neq 0$ and $\beta_{1,2} = 0$ at linear order.

[5]The double superstratum was presented in the Diagonal gauge, it needs first to be rotated to the Axial gauge before linearizing and comparing with the perturbations (12.61)

The resulting geometry can be generated with a finite $SU(2)_R$ gauge rotation[6] of the single sector *supersymmetric* solution with $\alpha_2 = \beta_1 = \beta_2 = 0$ at linear order.

Solving the perturbative system for general $n_{1,2}$ is challenging as the equations very quickly grow to unmanageable size, and we have only managed to reach fourth order for the alpha class of solutions on the special locus. Some of the expressions are given in the next section.

We also have perturbative solutions to sixth order for various specific values of n_1 and n_2 for both classes of solutions.

12.3.2 Alpha class and special locus

Taking α_i, $i \in \{1, 2\}$, non-zero and setting $\beta_{1,2} = 0$ in (12.61) at linear order gives us the alpha class of solutions, in both sectors. One can now solve the linearized equations order by order, with progressively more complicated source terms.

The main result of this analysis is that, as we have found for the single-mode truncation, the regular solutions of this expansion all sit on the *special locus*, defined in Section 12.2.3. Indeed, at second order in perturbation theory it is necessary to turn on the $\lambda_{1,2}$ fields, in order to have a normalizable solution to the equations of motion. At fourth order regularity requires

$$\beta_i = -\frac{\alpha_i^2}{4}. \tag{12.62}$$

This relation is a generalization of the same constraint in the single-mode truncation, (12.38), and all the specific properties described in Section 12.2.3 are clearly verifiable with the perturbative expansion.

These properties of m_{IJ} on the *special locus* allow us to easily solve for the scalar fields in the perturbative expansion. In fact, the perturbative solution suggests certain relations between some of the scalar fields:

$$\begin{aligned} \mu_{1,2}(\xi) = \lambda_{1,2}(\xi) &= \frac{1}{2}\log\left(1 - \frac{1-\xi^2}{2}\nu_{1,2}(\xi)^2\right), \\ m_5(\xi) &= -\frac{1}{2}(1-\xi^2)\,\nu_1(\xi)\,\nu_2(\xi), \quad m_6(\xi) = 0, \end{aligned} \tag{12.63}$$

with the only non-trivial eigenvalue of the m_{IJ} given by (12.41). Remarkably, one can check that these relations are indeed consistent with the full non-linear system of equations, by substituting them in and then reducing the equations to a consistent set. What is more, within that set all the gauge fields, as well as the metric function $k(\xi)$, satisfy first-order, linear ordinary differential equations. One can, furthermore, derive a first-order equation for a linear combination of $\Omega_0(\xi)$ and $\Omega_1(\xi)$, in addition to a "Wronskian-like" constraint that relates the first derivatives of $\nu_1(\xi)$ and $\nu_2(\xi)$. The equations are given in Appendix B. We have checked that solutions to this reduced system of equations also

[6] This finite rotation does not respect the form of the projectors (10.1) and so the rotated solution does not appear amongst the BPS solutions considered in Chapter 11. The supersymmetries of the unrotated "single sector" solution do respect the projectors (10.1).

verify all the second-order, non-linear equations of motion. We will make some comments about this below.

Therefore, we only need to determine $\nu_{1,2}$, Φ_i, Ψ_i and the metric functions $\Omega_{0,1}$ and k on the *special locus* in order to satisfy the equations of motion. We will now give the first three orders of the solution for general n_1, n_2.

At first order only the ν fields are non-zero:

$$\begin{aligned}\delta^{(1)}\nu_1 = \alpha_1\,\xi^{n_1}, \quad \delta^{(1)}\nu_2 = \alpha_2\,\xi^{n_2},\\ \delta^{(1)}\Phi_i = \delta^{(1)}\Psi_i = \delta^{(1)}\Omega_{0,1} = \delta^{(1)}k = 0.\end{aligned} \tag{12.64}$$

At second order the $\nu_{1,2}$ fields vanish, but all the others are excited:

$$\begin{aligned}
\delta^{(2)}\nu_{1,2} =& 0,\\
\delta^{(2)}\Phi_1 =& \frac{1}{8}\Bigg[-\alpha_1^2+\alpha_2^2\bigg(-1+\frac{2\,(n_1-n_2)^2}{(n_1+n_2)\,(n_1+n_2+1)\,(n_1+n_2+2)}-\xi^{2\,n_2}(1-\xi^2)\bigg)\Bigg],\\
\delta^{(2)}\Phi_2 =& \frac{1}{8}\Bigg[-\alpha_2^2+\alpha_1^2\bigg(-1+\frac{2\,(n_1-n_2)^2}{(n_1+n_2)\,(n_1+n_2+1)\,(n_1+n_2+2)}-\xi^{2\,n_1}(1-\xi^2)\bigg)\Bigg],\\
\delta^{(2)}\Phi_3 =& \frac{1}{4}\,\alpha_1\,\alpha_2\,\xi^{n_1+n_2}\bigg(\frac{\xi^2\,(n_2+1)}{n_1+n_2+2}-\frac{n_2}{n_1+n_2}\bigg),\\
\delta^{(2)}\Phi_4 =& -\frac{1}{4}\,\alpha_1\,\alpha_2\,\xi^{n_1+n_2}\bigg(\frac{\xi^2\,(n_1+1)}{n_1+n_2+2}-\frac{n_1}{n_1+n_2}\bigg),\\
\delta^{(2)}\Psi_1 =& -\frac{1}{8}\,\alpha_2^2\,\xi^{2+2\,n_2}, \quad \delta^{(2)}\Psi_2 = -\frac{1}{8}\,\alpha_1^2\,\xi^{2+2\,n_1},\\
\delta^{(2)}\Psi_3 =& -\frac{\alpha_1\,\alpha_2\,(n_2+1)\,\xi^{n_1+n_2+2}}{4\,(n_1+n_2+2)}, \quad \delta^{(2)}\Psi_4 = \frac{\alpha_1\,\alpha_2\,(n_1+1)\,\xi^{n_1+n_2+2}}{4\,(n_1+n_2+2)},\\
\delta^{(2)}\Omega_0 =& -\frac{1}{8}\,(1-\xi^2)\,\big(\alpha_1^2\,\xi^{2\,n_1}+\alpha_2^2\,\xi^{2\,n_2}\big), \quad \delta^{(2)}\Omega_1 = -\frac{1}{4}\big(\alpha_1^2+\alpha_2^2\big), \quad \delta^{(2)}k = \frac{\xi^2}{4}\big(\alpha_1^2+\alpha_2^2\big).
\end{aligned} \tag{12.65}$$

Then at third order again only the ν fields are non-trivial:

$$\begin{aligned}
\delta^{(3)}\,\nu_{1,2} = \frac{\alpha_{1,2}\,\xi^{n_{1,2}}}{8}\Bigg[&-\alpha_{1,2}^2\,\xi^{2\,n_{1,2}}\,(1-\xi^2)+2\,\alpha_{2,1}^2\bigg(\xi^{2\,n_{2,1}}\bigg(-\frac{n_{1,2}}{n_1+n_2}+\frac{(1+n_{1,2})\,\xi^2}{2+n_1+n_2}\bigg)\\
&+\frac{(n_1-n_2)^2\big(-\xi^{2\,n_{2,1}}+n_{2,1}\,\xi^{2\,n_{2,1}}\,\Phi(\xi^2,\,1,\,n_{2,1})+n_{2,1}\,\log(1-\xi^2)\big)}{n_{2,1}\,(n_1+n_2)\,(1+n_1+n_2)\,(2+n_1+n_2)}\bigg)\\
&+\frac{2\,(n_1-n_2)^2\,\alpha_{2,1}^2\Big(n_1+n_2+\frac{n_{1,2}}{n_{2,1}}+(n_1-n_2)\,\big(\gamma+\psi^{(0)}(n_{2,1})\big)\Big)}{(n_1+n_2)\,(1+n_1+n_2)\,(2+n_1+n_2)}\Bigg],
\end{aligned} \tag{12.66}$$

$$\delta^{(3)}\Phi_i = \delta^{(3)}\Psi_i = \delta^{(3)}\Omega_{0,1} = \delta^{(3)}k = 0, \tag{12.67}$$

where $\Phi(z,\,s,\,a)$ is the Lerch transcendent, γ is the Euler-Mascheroni constant and $\psi^{(m)}(z)$ is the polygamma function of order m. The function $\psi^{(0)}(z)$ is also known as the digamma function.

The solution is smooth - in particular, the log gets cancelled with a log part of the Lerch transcendent, $\Phi(\xi^2,\, 1,\, n_{2,1})$, and the entire expression is a polynomial in ξ. Moreover, the coefficients are all rational despite the appearance of γ and $\psi^{(0)}(z)$. We see no issues, in principle, to continuing this to arbitrarily high orders. We also have gone to 8^{th} order for specific values of n_1 and n_2 and have encountered no problems.

In constructing these solutions we find that the asymptotic values at infinity of the metric coefficient, Ω_1, and the electromagnetic potentials, Φ_j and Ψ_j, get corrected in terms of $\alpha_{1,2}$ at every order in perturbation theory. As we will discuss in Chapter 14, this results in an energy shift of the normal modes away from their AdS values, $\omega_{1,2}$, to new, lower energies represented by $\hat{\omega}_{1,2}$.

12.3.3 Almost-BPS solutions

Before describing more non-BPS solutions to our three-dimensional system, it is worth stepping back and commenting on the somewhat surprising result summarized in Appendix B: some the equations of motion of some of the non-BPS solutions described here can be reduced to first-order, linear ordinary differential equations.

This phenomenon has already played a significant role in the construction of special families non-BPS solutions in higher dimensions. It was observed in [70–77] that one could construct non-supersymmetric solutions by assembling "locally supersymmetric components" whose individual supersymmetries are incompatible with one another and so the solution preserves no supersymmetry when considered globally. At a computational level, this could be implemented by solving some first-order BPS equations in backgrounds that satisfied incompatible BPS conditions, or backgrounds that break supersymmetry altogether. For example, one can find non-BPS solutions by solving BPS equations for electromagnetic fields in a gravitational background that has non-trivial, supersymmetry-breaking holonomy. The non-trivial result of such an approach is to show that, despite the mismatched supersymmetry conditions, the background one creates is still a solution to the complete set of equations of motion.

Thus the construction of such "Almost-BPS solutions" typically involves solving a combination of first-order BPS-like equations and second-order equations of motion. The results of Section 12.3.2 are highly reminiscent of this process, especially because a few of the equations in Appendix B display a close parallel to some of the BPS equations.

We will not pursue this issue here, but it would be very interesting to revisit the Almost-BPS approach in three dimensions and see, to what extent, the solutions described here can be characterized as being Almost-BPS. Intuitively, the success of the Almost-BPS procedure requires a "decoupling" between the distinct, but incompatible, supersymmetric elements. While we do not expect our general non-BPS solutions to behave in such a manner, it is possible that the special locus might be characterized through such behavior in supergravity.

12.3.4 Beta class

This sector starts, at linear order, with $\alpha_{1,2} = 0$ in (12.61) and non-zero β_i, $i \in \{1, 2\}$. There is no need of a *special locus*, and one finds $\nu_{1,2} = 0$ at all orders in perturbation theory. One also finds that $m_{5,6}$, $\Phi_{3,4}$, $\Psi_{3,4}$ vanish to all orders we have checked. When both $\beta_{1,2}$ are turned on, the CFT representation of the resulting non-BPS state is given in (13.29).

As with the α-class, the individual solutions with $\beta_1 = 0$ or $\beta_2 = 0$ are separately supersymmetric, but the combined excitation breaks all the supersymmetry. Unlike the α-class, there is no accidental supersymmetry for $n_1 = n_2$: global $SO(4)$ rotations of $\alpha_1 = \alpha_2 = \beta_2 = 0$ create additional background fields that move outside our Ansatz. We have computed the perturbative solution for general $\beta_{1,2}$ and $n_{1,2}$ up to 3^{th} order:

$$\begin{aligned}
&\delta^{(1)}\lambda_1 = \beta_1\, \xi^{2\,n_1}\,(1-\xi^2), \quad \delta^{(1)}\lambda_2 = \beta_2\, \xi^{2\,n_2}\,(1-\xi^2),\\
&\delta^{(1)}\mu_{1,2} = \delta^{(1)}\Phi_i = \delta^{(1)}\Psi_i = \delta^{(1)}\Omega_{0,1} = \delta^{(1)}k = 0.
\end{aligned} \tag{12.68}$$

$$\begin{aligned}
\delta^{(2)}\lambda_{1,2} =& 0,\\
\delta^{(2)}\mu_1 =& \beta_2^2\,\frac{1-\xi^{2\,(1+2\,n_2)}}{2\,(1+2\,n_2)^2} - \beta_1^2\,\frac{1-\xi^{2\,(1+2\,n_1)}}{2\,(1+2\,n_1)^2},\\
\delta^{(2)}\mu_2 =& \beta_1^2\,\frac{1-\xi^{2\,(1+2\,n_1)}}{2\,(1+2\,n_1)^2} - \beta_2^2\,\frac{1-\xi^{2\,(1+2\,n_2)}}{2\,(1+2\,n_2)^2},\\
\delta^{(2)}\Phi_1 =& \beta_1^2\,\frac{\xi^{2\,(1+2\,n_1)} - 2\,(1+2\,n_1)}{4\,(1+2\,n_1)^2} + \beta_2^2\,\frac{(1+n_1+n_2)\,\xi^{2\,(1+2n_2)} - 2\,(n_1+n_1\,n_2+n_2^2)}{4\,(1+n_1+n_2)\,(1+2\,n_2)^2},\\
\delta^{(2)}\Phi_2 =& \beta_2^2\,\frac{\xi^{2\,(1+2\,n_2)} - 2\,(1+2\,n_2)}{4\,(1+2\,n_2)^2} + \beta_1^2\,\frac{(1+n_1+n_2)\,\xi^{2\,(1+2n_1)} - 2\,(n_2+n_1\,n_2+n_1^2)}{4\,(1+n_1+n_2)\,(1+2\,n_1)^2},\\
\delta^{(2)}\Psi_1 =& -\beta_2^2\,\frac{\xi^2\left(1-\xi^{2\,(1+2\,n_2)}\right)}{4\,(1+2\,n_2)^2\,(1-\xi^2)} - \beta_1^2\,\frac{\xi^2\left(1-\xi^{4\,n_1}\left(1+2\,n_1\,(1-\xi^2)\right)\right)}{4\,(1+2\,n_1)^2\,(1-\xi^2)},\\
\delta^{(2)}\Psi_2 =& -\beta_1^2\,\frac{\xi^2\left(1-\xi^{2\,(1+2\,n_1)}\right)}{4\,(1+2\,n_1)^2\,(1-\xi^2)} - \beta_2^2\,\frac{\xi^2\left(1-\xi^{4\,n_2}\left(1+2\,n_2\,(1-\xi^2)\right)\right)}{4\,(1+2\,n_2)^2\,(1-\xi^2)}.
\end{aligned} \tag{12.69}$$

$$\delta^{(3)}\mu_{1,2} = \delta^{(3)}\Phi_i = \delta^{(3)}\Psi_i = \delta^{(3)}\Omega_{0,1} = \delta^{(3)}k = 0, \tag{12.70}$$

$$
\begin{aligned}
\delta^{(3)}\lambda_{1,2} =& \frac{\beta_{1,2}\,\beta_{2,1}^2\,\xi^{2\,n_{1,2}}}{4\,(1+n_1+n_2)\,(1+2\,n_{2,1})^2}\Big[4\,(1-\xi^2)\,(1+2\,n_{2,1})\,\big(\log(4)+2\,H_{4\,n_{2,1}-1}-H_{2\,n_{2,1}-\frac{1}{2}}\big)\\
&+\frac{1}{n_{2,1}\,(1+4\,n_{2,1})}\Big[2\,(1-\xi^2)\,\xi^{4\,n_{2,1}}\,(8\,n_{2,1}^2+6\,n_{2,1}+1)\,{}_2F_1\big(1,\,4\,n_{2,1};\,1+4\,n_{2,1};\,\xi\big)\\
&-8\,(1-\xi^2)\,\xi^{1+4\,n_{2,1}}\,n_{2,1}\,(1+2\,n_{2,1})\,{}_2F_1\Big(1,\,\frac{1}{2}+2\,n_{2,1};\,\frac{3}{2}+2\,n_{2,1};\,\xi^2\Big)\\
&+(1+4\,n_{2,1})\,\Big(n_{2,1}\,\big(5+n_{1,2}-\xi^2(1-n_{1,2})-\big(4+\xi^2\,(1-\xi^2)(1+n_{1,2})\big)\,\xi^{4\,n_{2,1}}\big)\\
&-n_{2,1}^2\,(1-\xi^2)(\xi^{2\,(1+2\,n_2)}+7)+2\,(1-\xi^2)\,(1-\xi^{4\,n_{2,1}})\Big)\Big]\\
&+4\,(1-\xi^2)(1+2\,n_{2,1})\,\log\big(1-\xi^2\big)\Big]\\
&+\frac{\beta_{1,2}^3\,(1-\xi^2)\,\xi^{2\,n_{1,2}}}{12\,(1+2\,n_{1,2})^2}\,\Big[(1+2\,n_{1,2})^2\,\xi^{4\,n_{1,2}}+\big(1-8\,n_{1,2}\,(1+n_{1,2})\big)\xi^{2\,(1+2\,n_{1,2})}\\
&+(1+2\,n_{1,2})^2\,\xi^{4\,(1+n_{1,2})}-3\Big],
\end{aligned}
\tag{12.71}
$$

where H_n is a harmonic number. We again find a smooth solution, and as for the α class, despite appearances, this is a polynomial in ξ with rational coefficients. Hence, there should be no issues, in principle, to continuing this to arbitrarily high orders. As before, we also have examples for specific values of n_1 and n_2 that we have taken to 8^{th} order with no complications.

Like the α-class solutions, the β-class solutions also develop non-trivial perturbative corrections to the asymptotic values, at infinity, of the metric coefficient, Ω_1, and the electromagnetic potentials, Φ_j and Ψ_j. This also results in an energy shift of the normal modes away from their AdS values, $\omega_{1,2}$, to new, lower energies represented by $\hat{\omega}_{1,2}$.

12.4 Perturbation theory around the pure-NS superstrata solutions

The previous Sections explored the construction of microstrata using perturbation theory around the vacuum. However, having at our disposal various BPS microstate geometries corresponding to finite excitations, it is natural to ask whether one can build similar microstrata as perturbations on top of these known geometries.

This kind of analysis is in general difficult to achieve, as one is lead to find solutions to systems of complicated, coupled differential equations. However, this work is facilitated in many ways by our truncation. A first, trivial reason is that the Q-ball ansätze reduces the problem to solving equations involving functions of only one variable. This alone is not sufficient, as the resulting equations can be arbitrarily complex and highly-coupled. The remarkable property of the double-mode truncation is the existence of two sets of mostly independent, mutually incompatible, BPS sectors. This lets one build an analytic BPS solution in one sector, and add supersymmetry-breaking excitations through the second sector.

The first step is thus to choose the BPS geometry that will be used as a base for the perturbation. Because it is very simple and already well-studied, it would be tempting to use the standard single-sector superstratum geometry, (9.25). However, the results of the perturbation theory around the vacuum show that such solutions cannot be described within the ansatz, as they ultimately lead to divergences.

The consequence is that only two families of superstrata solutions can be used as the base: the "special locus" solution in (11.14), and the "pure-NS" solution described in Section 11.4.1. The former can be used as a base to construct non-BPS linear excitations of the scalar ν_2, and using the set of reduced equations on the special locus in Appendix B, one finds that at first order, the problem reduces to a system of first-order differential equations for the fields $\nu_2, \Phi_{3/4}, \Psi_{3/4}$.

It is however more interesting to use the "pure-NS" solution as a base. Indeed, at first order in the perturbation, one finds that only one field receives a contribution: the scalar λ_2.

12.4.1 The linearized perturbation

We start with the pure-NS solution given in Section 11.4.1. This is a single-mode solution, and as such there is still a gauge transformation that shifts the fields Φ_2 and Ψ_2. In accordance with the discussion on boundary conditions in Section 12.1, we first need to introduce the mode numbers of the $(1, 1, n_2)$ sector by applying shifts to the gauge fields:

$$\Phi_2 \to \Phi_2 + c_{\phi_2}\,, \qquad \Psi_2 \to \Psi_2 + n_2\,. \tag{12.72}$$

As will be explained in Chapters 13 and 14 on holography, the constant c_{ϕ_2} is related, up to a shift, to the physical frequency of the solution: $c_{\phi_2} = 1/2 + \Omega_1\,\hat{\omega}_2$. Note that this frequency is generally not equal to the parameter ω_2 that we have introduced in the perturbation theory, and in particular it is not an integer.

We now use the action to derive the linearized equations of motion. Concentrating on the normalizable perturbations, the problem reduces to solving a single linear differential equation:

$$\xi\partial_\xi(\xi\partial_\xi\lambda_2) + V_0(\xi)\lambda_2 \;=\; 0\,, \tag{12.73}$$

where the function V_0 is defined in terms of the fields of the "pure-NS" BPS solution:

$$V_0(\xi) \;=\; 16(F_2^2 + H_0\Phi_2^2) - 4H_0\big(e^{-2\mu_1} - e^{-\mu_1-\mu_2}\cosh\lambda_1\big)\,. \tag{12.74}$$

where we used the notations introduced in (10.59).

We wish to find bound states of the scalar λ_2, where the excitation lives entirely in the throat of the geometry, and compute the normal modes of these excitations. These normal modes, once fully-backreacted, translate to shifts in the energy of the microstratum. Thus, solving the problem defined by the equation (12.73) with suitable boundary conditions on the scalar λ_2 (which will be precised in the following), one can have access to the first-order corrections to the energy of these non-BPS microstates, and on the CFT side to the anomalous dimension of the constituent operators of the microstratum.

12.4.2 The WKB approximation

It is not possible to solve the equation (12.73) exactly, so one has to resort to approximations. We will use the WKB method, which is well-suited to dispersive or dissipative problems with large separation of scales: the potential must vary slowly with respect to the oscillations of the scalar. This method has often been used to compute normal or quasi-normal modes, and has recently been applied successfully to the computation of the quasi-normal modes of superstrata in [29, 35]. Here we will review the basics of the approximation. Its application to the problem at hand will be explained in the next section.

The WKB method has been originally developed for equations in the Schrödinger form, for which it is well understood:

$$\frac{\mathrm{d}^2 f}{\mathrm{d}x^2} + V(x) f \;=\; 0\,. \tag{12.75}$$

One can easily transform any second-order linear equation, such as (12.73), into the Schrödinger form, by making change of variables of the form

$$\xi \;\to\; x(\xi)\,, \qquad \lambda_2(\xi) \;\to\; \Lambda(x(\xi))\, f(x(\xi))\,, \tag{12.76}$$

for suitably chosen functions x and Λ.

The WKB method consists in approximating the solutions of (12.75) by

$$f^{\pm}_{\mathrm{WKB}}(x) \;=\; C_{\pm}\, |V(x)|^{-1/4} \exp\left(\pm \int^x V(y)^{1/2} dy \right) \tag{12.77}$$

where $C_{\pm}$ are integration constants. Formal estimations of the quality of this approximation can be done (see [78] for a detailed review). For the approximation to be close to the exact solution, the potential must obey

$$\left| V(x)^{-3/2} V'(x) \right| \;\ll\; 1\,, \quad \text{and} \quad \int^x \left| \frac{V''(y)}{V(y)^{3/2}} - \frac{5V'(y)^2}{4V(y)^{5/2}} \right| dy \;\ll\; 1\,. \tag{12.78}$$

The first condition ensures the separation of scales between the oscillations of the solution and the variation of the potential. The second condition is a technical necessity that is usually satisfied when the first condition is.

Notice that if $V(x) > 0$, the solutions (12.77) are exponentially growing or decaying, while if $V(x) < 0$, they are oscillating. The solutions break down at the *turning points* of the potential, when $V(x) = 0$. It is also easy to see that the conditions (12.78) cannot be satisfied in the neighborhood of the turning points. It does not mean however that one must give up on using the WKB approximation: one can use a different approximation to construct the solutions in the problematic regions, then match with the WKB solution at the edges of these domains.

Assuming that the first derivative of the potential does not vanish, one can approximate the potential around a turning point $x_\star$ by a linear function $V(x) \sim V'(x_\star)(x - x_\star)$.

The solutions to the Schrödinger equation for a linear potential are well known and can be expressed in terms of the Airy functions

$$f_\star(x) \;=\; C_1\,\mathrm{Ai}\big(V'(x_\star)^{1/3}(x-x_\star)\big) \;+\; C_2\,\mathrm{Bi}\big(V'(x_\star)^{1/3}(x-x_\star)\big)\,. \tag{12.79}$$

One can then construct the full solutions to the problem in patches. Away from the turning points, the solution is well-described by (12.77). Around each turning point, one uses the solution (12.79). It is then necessary to ensure that the solutions are regular, by relating the integration constants of neighboring patches to each other. These conditions are called *connection formulas*.

For any matching to be possible, it is of course necessary that the domains of validity of the solutions (12.77) and (12.79) overlap. This leads to another condition on the potential, relating its slope at the turning points to its curvature:

$$V'(x_\star)^{-4/3}V''(x_\star) \;\ll\; 1\,. \tag{12.80}$$

12.4.3 Quantization condition

We now explain how to use the WKB approximation to derive the solutions of the wave equation for λ_2, and find a quantization condition on the frequency $\hat{\omega}_2$. The first step is to rewrite the equation in the Schrödinger form, using a change of variable of the form (12.76). Many choices are possible: the particular choice of variable $x(\xi)$ can affect the precision of the WKB method as well as the simplicity of the treatment of boundary conditions. We make the same choice as in [29, 35], as it makes the boundary conditions relatively simple:

$$x(\xi) \;\equiv\; \log\left(\frac{\xi}{\sqrt{1-\xi^2}}\right) \;=\; \log\left(\frac{r}{a}\right). \tag{12.81}$$

After this change of variable, the function f, defined by

$$\lambda_2(\xi) \;\equiv\; \sqrt{1-\xi^2}\,f(x(\xi))\,, \tag{12.82}$$

satisfies the Schrödinger equation (12.75) with potential

$$V(x) \;=\; 1-\frac{1}{(1+e^{2x})^2}(1+V_0(x))\,, \tag{12.83}$$

where V_0 is given by (12.74). This potential depends on several parameters: the initial BPS superstrata parameters β_1, n_1, and the parameters of the excitation n_2, c_{ϕ_2} (or equivalently $\hat{\omega}_2$). Figure 12.1 depicts the typical shape of the potential. It has two turning points x_1, x_2 ; it limits to 1 at positive infinity, and to $4\,n_2^2$ at negative infinity. The minimum of the potential is negative and scales as

$$|\min V(x)| \;\sim\; \mathcal{O}(n_2^2,\, c_{\phi_2}^2) \quad \text{as} \quad n_2 \gg 1 \text{ or } c_{\phi_2} \gg 1\,. \tag{12.84}$$

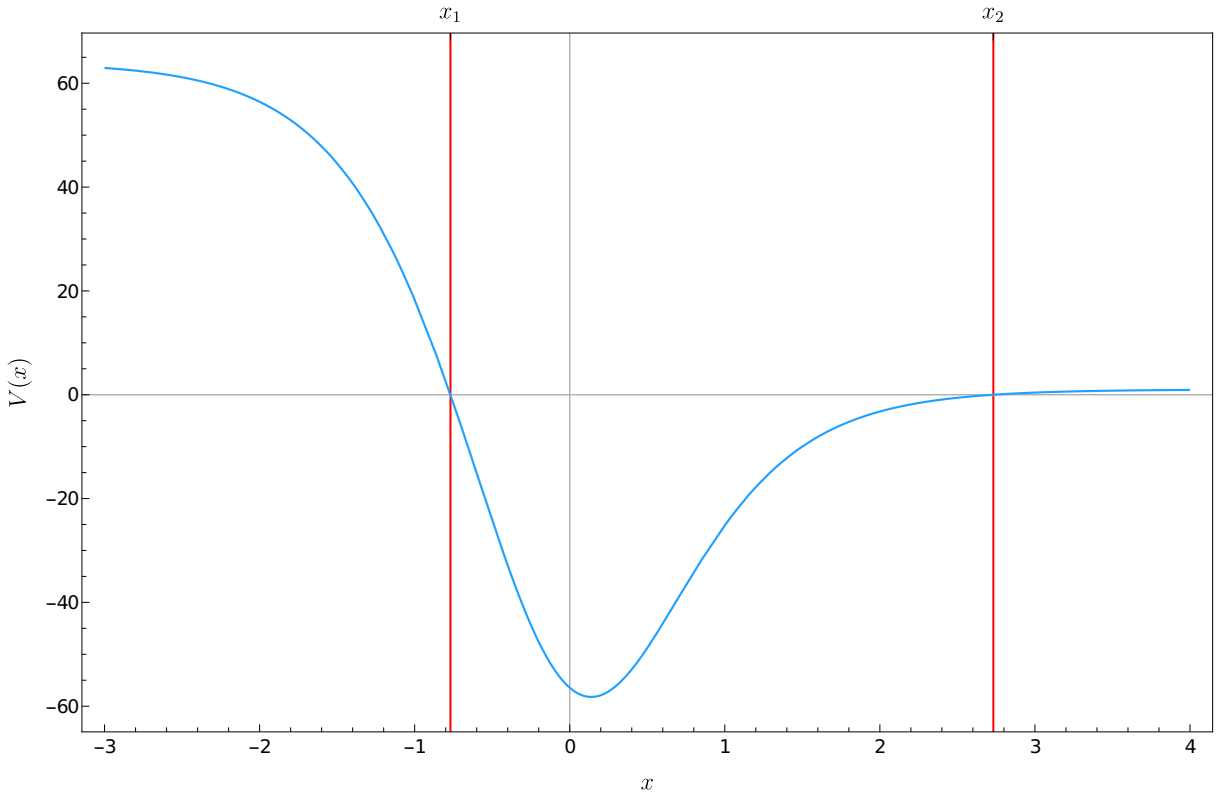

Figure 12.1: Shape of the potential for the function f, written in terms of the variable x introduced in (12.81). The specific curve plotted here corresponds to $n_1 = 2$, $n_2 = 4$, $\beta_1 = 2$, and we have chosen to fix arbitrarily $\hat{\omega}_2 = 5$.

One can see numerically that the potential satisfies the conditions (12.78), as well as (12.80) around each turning point when the frequency of the scalar, $\hat{\omega}_2$, is large. In practice, we find that $\hat{\omega}_2 \sim \mathcal{O}(10 - 100)$ is sufficient to obtain a good approximation.

The solutions away from the turning points are given by

$$f(x) = \begin{cases} V(x)^{1/4}\left(C_+^{(1)} \exp\left(\int_x^{x_1} \sqrt{V(y)}dy\right) + C_-^{(1)} \exp\left(-\int_x^{x_1} \sqrt{V(y)}dy\right)\right), & x < x_1\,, \\ |V(x)|^{1/4}\left(C_+^{(2)} \exp\left(i\int_{x_1}^{x} \sqrt{|V(y)|}dy\right) + C_-^{(2)} \exp\left(-i\int_{x_1}^{x} \sqrt{|V(y)|}dy\right)\right), & x_1 < x < x_2\,, \\ V(x)^{1/4}\left(C_+^{(3)} \exp\left(\int_{x_2}^{x} \sqrt{V(y)}dy\right) + C_-^{(3)} \exp\left(-\int_{x_2}^{x} \sqrt{V(y)}dy\right)\right), & x_2 < x\,. \end{cases} \tag{12.85}$$

These constants are of course not all independent: the solution to a second-order differential equation must only be determined by two constants. Looking at the neighborhood of each turning point, the solution is well described in terms of Airy functions (12.79), and imposing that the solution is smooth leads to relations between the integration constants on both sides of the turning point. The details of the computation can be found in [78],

one finds that the connection formulas are given by

$$\begin{aligned} C_+^{(2)} &= \frac{1}{2}e^{i\pi/4}C_+^{(1)} + e^{-i\pi/4}C_-^{(1)}\,, & C_+^{(3)} &= -\sin\Theta\, C_+^{(1)} + 2\cos\Theta\, C_-^{(1)}\,, \\ C_-^{(2)} &= \frac{1}{2}e^{-i\pi/4}C_+^{(1)} + e^{i\pi/4}C_-^{(1)}\,, & C_-^{(3)} &= \frac{1}{2}\cos\Theta\, C_+^{(1)} + \sin\Theta\, C_-^{(1)}\,, \end{aligned} \tag{12.86}$$

where

$$\Theta \equiv \int_{x_1}^{x_2} \sqrt{|V(y)|}dy\,. \tag{12.87}$$

We must now impose the boundary conditions. First, the excitation must be localized in the throat, and have a finite energy. As a consequence, the growing mode at infinity must be cancelled $C_+^{(3)} = 0$. Moreover, contrary to excitations over a black hole background, we must impose a smoothness condition at the origin, as the objective is to construct smooth microstate geometries. This translates to $C_+^{(1)} = 0$. One integration constant, $C_-^{(1)}$, is not fixed. This constant is the strength of the perturbation, and must be infinitesimally small compared to β_1.

Combining these boundary conditions with the connection formulas leads to a quantization condition:

$$\cos\Theta = 0 \quad \Longleftrightarrow \quad \frac{1}{\pi}\int_{x_1}^{x_2} \sqrt{|V(y)|}dy \;=\; N + 1/2\,, \quad N \in \mathbb{N}\,. \tag{12.88}$$

This equation has to be understood as an implicit quantization condition for the constant c_{ϕ_2}, or equivalently $\hat{\omega}_2$, which in turn determines the first-order correction to the energy of the microstratum. Recall that it is an approximation that is valid in the limit $c_{\phi_2} \gg 1$.

12.4.4 Normal modes of λ_2

We first look at an example of application of the quantization condition. Set the background to be empty AdS by putting the amplitude of the superstratum to 0, $\beta_1 = 0$. The perturbation theory around this background has been studied in Section 12.3, we know that the mode number ω_2, defined in (12.59), must be an integer[7]. If we furthermore impose $n_2 = 0$, the integral in (12.88) can be computed explicitly, and one finds:

$$\frac{1}{\pi}\int_{x_1}^{x_2} \sqrt{|V(y)|}dy \;=\; \sqrt{(\omega_2)^2 - \frac{1}{4}} - \frac{1}{2} \;\sim\; \omega_2 - \frac{1}{2} - \frac{1}{8\,\omega_2} + \dots\,. \tag{12.89}$$

From that relation and the quantization condition (12.88), we find that $N = \omega_2 - 1$, and that the error of the WKB approximation is of order $1/(8N)$.

Coming back to the general setting, $\beta_1 \neq 0$, the quantization condition can be solved numerically. In what follows, we fix as an example $n_1 = 2$, $n_2 = 4$. The figure 12.2 shows the evolution of $\delta\omega_2 \equiv \hat{\omega}_2 - \omega_2$ as a function of β_1, for different values of ω_2.

[7] As was pointed out in Section 12.3.1, this integer must be odd for the alpha-perturbation to be regular. However, for the beta-perturbation that is considered here, this is not a requirement.

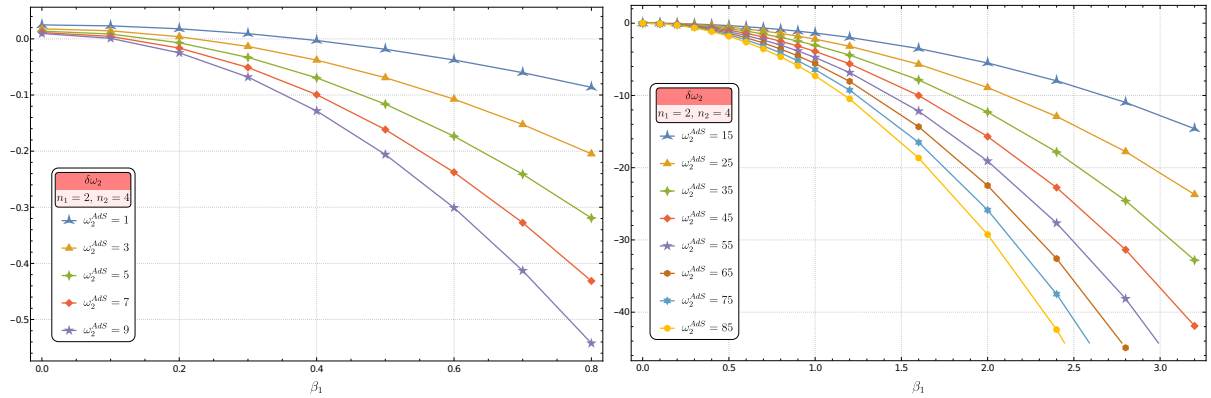

Figure 12.2: Results from the WKB analysis. Plots of $\delta\omega_2$ as a function of β_1, for $n_1 = 2$, $n_2 = 4$, and for normal modes labeled by ω_2.

The interpretation of this quantity $\delta\omega_2$ in the context of holography will be detailed in Chapter 14.

We first see that $\delta\omega_2 \leq 0$, which is in accordance with the fact that this energy comes from the attractive interaction between mutually non-BPS particles. Notice also that this energy goes to $-\infty$ in the "infinite-throat-limit", when the geometry becomes asymptotically AdS_2 (see Section 11.4.2), at

$$\beta_1^{(0)} \;=\; \frac{4n_1+2}{\sqrt{4n_1+1}} \;=\; \frac{10}{3}\,. \tag{12.90}$$

This is a sign of a break down of this analysis at some point before the limit.

We can make a further check on these numerical results, by comparing them to the perturbative solution around the vacuum. Indeed, the terms proportional to β_1^2 and β_2^2 in the shift $\delta\omega_2$ can be accessed by the perturbation theory around the vacuum. We can adapt the computations of Section 12.3, that were done at $\omega_2 = 1$, for different values of ω_2. The general analysis is complicated, but we can restrict ourselves to a specific example, for instance $n_1 = 2$, $n_2 = 4$.

This can be compared to the WKB results by fitting a polynomial in β_1^2 on the results of the WKB approximation. This polynomial fit is presented in Table 12.1. The constant term of this polynomial is a good indication of the error that is made by the WKB approximation, and we see that it diminishes as the frequency increases. The term of order β_1^2 can be compared with the perturbative analysis. The approximation grows better as one increases ω_2, as we can see in Table 12.2.

The main interest of the WKB approximation is that its results are valid for finite values of β_1, while the perturbation theory is only giving access to expansions around the vacuum. Nevertheless, we can also use the WKB analysis to learn more about the perturbation theory. Because it is much easier to get data points at large ω_2 using the WKB approximation than with the perturbation theory, one can make further analyses on these results. By fitting the coefficient of order β_1^2 with a line, we can find:

$$\delta\omega_2 \;\approx\; -\left(0.112335 + 0.0842948\,\omega_2\right)\beta_1^2 \;+\; \mathcal{O}\left(\beta_1^4,\,\beta_2^2,\,(\omega_2)^{-1}\right). \tag{12.91}$$

ω_2	Fit of $\delta\omega_2$
1	$-0.0000378819\beta_1^6 - 0.000318806\beta_1^4 - 0.173513\beta_1^2 + 0.0249378$
3	$-0.0000909752\beta_1^6 - 0.000123277\beta_1^4 - 0.347659\beta_1^2 + 0.0178344$
5	$-0.00015133\beta_1^6 + 0.0000441431\beta_1^4 - 0.520276\beta_1^2 + 0.0138782$
7	$-0.000216834\beta_1^6 + 0.000192361\beta_1^4 - 0.69175\beta_1^2 + 0.0113578$
9	$-0.000285129\beta_1^6 + 0.000326079\beta_1^4 - 0.862479\beta_1^2 + 0.00961188$
$\vdots$	$\vdots$
105	$-0.0038392\beta_1^6 + 0.00555269\beta_1^4 - 8.9661\beta_1^2 + 0.00114766$
205	$-0.00757974\beta_1^6 + 0.0109112\beta_1^4 - 17.3949\beta_1^2 + 0.000600001$

Table 12.1: Fit of a polynomial of order 3 in β_1^2 on the numerical data from the WKB analysis. The constant term, which is expected to be 0, gives an indication of the precision of the method. The term of order β_1^2 can be matched with the perturbative computation around the vacuum.

It is interesting to note that the coefficient at first-order in β_1^2 is linear in the integer zeroth-order mode number ω_2. The analysis shows that this is not true at higher orders in β_1^2. This is a prediction for the perturbation theory: if one could develop the perturbation theory for a generic frequency ω_2, up to third order in β_1, one could check the validity of this prediction, and give exact expressions for the coefficients in (12.91).

ω_2	$\delta\omega_2$ from WKB	$\delta\omega_2$ from vacuum perturbation theory
1	-0.1735	$-\dfrac{6}{35} \approx -0.1714$
5	-0.5203	$-\dfrac{14844427}{28601650} \approx -0.5190$
9	-0.8625	$-\dfrac{102879754}{119409675} \approx -0.8616$
13	-1.2026	$-\dfrac{154958717}{128927388} \approx -1.2019$
17	-1.5417	$-\dfrac{2066874954282}{1341119288509} \approx -1.5412$

Table 12.2: Comparison between the computations of the frequency shift from the WKB analysis, and from the perturbation theory around the vacuum, for a few values of ω_2. The constants that are displayed correspond to the term proportional to β_1^2 in the expansion of $\delta\omega_2$.

Chapter 13

The CFT interpretation

This Chapter aims to explain the CFT analogue of the computations that have been done in supergravity. We exclusively concentrate on the CFT, the matching with the bulk theory using holography is the purpose of the next Chapter. We review the work of [39, 42].

The three-dimensional supergravity described in Chapter 7 can be embedded in Type IIB string theory compactified on a 4-dimensional Calabi-Yau $\mathcal{M}$. The 4-dimensional compact space will play no role in our analysis and can be taken to be either $\mathbb{T}^4$ or K3[1]. The remaining six-dimensional space-time has $AdS_3 \times S^3$ asymptotics and thus our solutions are holographically dual to states of the D1-D5 CFT, that we introduced in Chapter 4. In this section we review some of the operator content of this CFT and describe the heavy states that are dual to the geometries discussed in this work. As we will see it is sometimes convenient to refer to the CFT free locus, where the theory reduces to the orbifold $\mathcal{M}^N/S_N$ ($N = n_1 n_5$ is the product of the numbers of D1 and D5 branes and S_N is the permutation group). The characterization in terms of orbifold is useful because the elementary constituents of our heavy states, even the non-BPS ones, are by themselves BPS and thus are expected to be stable across the moduli space of the CFT.

13.1 Supergravity operators of the D1-D5 CFT

The six-dimensional supergravity obtained by compactifying type IIB on $\mathcal{M}$ contains a gravity multiplet σ and N_f tensor multiplets $s^{(f)}$ (with $N_f = 5$ or 21 if $\mathcal{M} = \mathbb{T}^4$ or K3). The scalar chiral primary operators (CPO) of the D1-D5 CFT are dual to the S^3-harmonics of these fields, and are denoted respectively as σ_n and $s_n^{(f)}$: they have conformal dimension $(h, \bar{h}) = (\frac{n}{2}, \frac{n}{2})$ with n a positive integer starting from 1 for the tensor fields $s_n^{(f)}$ and from 2 for the gravity fields σ_n.

The 3D truncation we use does not allow all these operators to have freely tunable vacuum expectation values (VEV): only the operators dual to the fields that admit homogeneous and normalizable solutions of the three-dimensional supergravity equations

[1] In the theory described in Chapter 7, we have $\mathcal{M} = \mathbb{T}^4$

can take arbitrary VEVs. This does not imply that the other operators necessarily have vanishing VEVs, but these VEVs will be determined in terms of the freely tunable ones by the non-linearity of the 3D supergravity equations. Thus only a subset of the D1-D5 states can fit in our truncation but we will see that the subset is large enough to encompass non-trivial non-BPS states, including non-supersymmetric deformations of BPS states with long AdS_2 throats.

13.1.1 Light states of the single-mode truncation

For the restricted single-mode truncation considered in Section 9.2, the possible homogeneous deformations and the dual operators were identified in [39]. As we saw in Section 12.2, in that restricted truncation, only two fields, ν_1 and λ_1, have normalizable homogeneous modes. We recall them here:

$$\begin{aligned}\nu_1 =&\alpha_1\, \xi^{n_1}\, {}_2F_1\big((1-\omega_1)/2,\, n_1+(1+\omega_1)/2,\, 1+n_1,\, \xi^2\big),\\ \lambda_1 =&\beta_1\, \xi^{2\,n_1}\, {}_2F_1\big(-\omega_1,\, 2\,n_1+\omega_1,\, 1+2\,n_1,\, \xi^2\big)\,,\end{aligned} \tag{13.1}$$

where, for the perturbation to be regular, ω_1 must be an integer, and, for the ν_1 perturbation, must be odd. At linear order in α_1 the only non-trivial fields of the six-dimensional theory are a 3-form $H_{(3)} = dB_{(2)}$ and the axion $C_{(0)}$ which are given by

$$\begin{aligned}C_{(0)} &= \alpha_1 \sqrt{\frac{Q_5}{2Q_1}}\, \mathrm{Re}(B_1 Y_1)\,,\\ H_{(3)} &= \alpha_1 \sqrt{\frac{Q_1 Q_5}{2}}\, \mathrm{Re}\left[d(\star_{AdS_3} dB_1 Y_1 - B_1 \star_{S^3} dY_1)\right]\,,\end{aligned} \tag{13.2}$$

with

$$B_1 = \sqrt{1-\xi^2}\xi^n\, {}_2F_1(-m, m+n_1+1, n_1+1, \xi^2)\, e^{-i(2m+1)\tau - i n_1 \psi}\ ,\ Y_1 = \sin\theta\, e^{i\varphi_1}, \tag{13.3}$$

where $m = \frac{1}{2}(\omega_1 - 1) \in \mathbb{N}$, and $\star_{AdS_3}$, $\star_{S^3}$ the Hodge duals with respect to the undeformed AdS_3 and S^3 metrics. B_1 and Y_1 are scalar harmonics of AdS_3 and S_3, respectively: B_1 is an eigenfunction of L_0 and $\tilde{L}_0$ with eigenvalues

$$h = m + n_1 + \frac{1}{2}\,, \quad \bar{h} = m + \frac{1}{2}\,, \tag{13.4}$$

and Y_1 is an eigenfunction of J_0^3 and $\tilde{J}_0^3$ with eigenvalues

$$j = \bar{j} = \frac{1}{2}\,. \tag{13.5}$$

For $m = n_1 = 0$ the perturbation (13.2) is thus dual to the component of spin $(\frac{1}{2}, \frac{1}{2})$ of one of the tensor multiplet CPOs[2], $O_1^{(1/2,1/2)} \equiv s_1^{(7)}$. At the orbifold locus, $s_1^{(7)}$ is described

[2]For the supergravity fields, we follow the notation of [36] and references therein, which is motivated by the analysis of the 6D supergravity sketched in Appendix C.

by a bilinear of free fermions of the form $\epsilon_{AB}\,\psi^{+A}\tilde{\psi}^{+B}\quad (A,B=1,2)$ (see Chapter 4) that we schematically indicates as

$$O_1^{(1/2,1/2)} \equiv s_1^{(7)(\frac{1}{2},\frac{1}{2})} \sim \sum_{r=1}^{N} \left|\frac{1}{2},\frac{1}{2}\right\rangle^{(r)} + \dots\ , \tag{13.6}$$

where the sum is over the N copies of the sigma-model on $\mathcal{M}$ and the dots stand for possible corrections where the elementary fields are on different copies[3].

From the supergravity perspective, this state is the lowest KK mode in the S^3 reduction of one of the tensor multiplets of the 6D theory. For non-vanishing values of m, n the field (13.2) is a Virasoro descendant of the CPO given by[4]

$$L_{-1}^{n_1+m}\tilde{L}_{-1}^{m}\,|O_1^{(1/2,1/2)}\rangle\,. \tag{13.7}$$

A similar, but slightly more complicated, description applies to λ_1. Regular and normalisable solutions for λ_1 exist when $m=\frac{1}{2}(\omega_1-1)$ is either a non-negative integer or half-integer. At first order in β_1 the non-trivial fields of the truncation are the metric, the dilaton, and the three-form field strength $F_{(3)}=dC_{(2)}-C_{(0)}\,dB_{(2)}$:

$$\begin{aligned}
\frac{ds_6^2}{R_{AdS}^2} &= ds^2_{AdS_3}+ds^2_{S^3}\\
&\quad + 2\beta_1\,\mathrm{Re}\left[B_2Y_2\left(ds^2_{AdS_3}+ds^2_{S^3}-2\frac{d\theta^2}{\sin^2\theta}+2\cos^2\theta(d\varphi_1^2-d\varphi_2^2)-4i\frac{\cos\theta}{\sin\theta}d\theta d\varphi_1\right)\right]\\
&= ds^2_{AdS_3}+ds^2_{S^3}+2\beta_1\,\mathrm{Re}\left[B_2Y_2\left(ds^2_{AdS_3}-3ds^2_{S^3}\right)-B_2\overline{\nabla}_\alpha\partial_\beta Y_2\,dx^\alpha dx^\beta)\right]\,,\\
e^{2\Phi} &= \frac{Q_1}{Q_5}\left[1+4\beta_1\,\mathrm{Re}\,(B_2Y_2)\right]\,,\\
F_{(3)} &= 2Q_5\,(-\mathrm{vol}_{AdS_3}+\mathrm{vol}_{S^3})+2\beta_1\,Q_5\,\mathrm{Re}\big[\,d(B_2\star_{S^3}dY_2)\,\big]\,,
\end{aligned} \tag{13.8}$$

where $ds^2_{AdS_3}$, $ds^2_{S^3}$ are the unperturbed metrics of global AdS_3 and of the three-sphere, α,β (μ,ν) are S^3 (AdS_3) indices, the covariant derivative $\overline{\nabla}$ is computed with the unperturbed metric. The functions

$$B_2=\xi^{2n}(1-\xi^2)\,{}_2F_1(-2m,2m+2n_1+2,2n_1+1,\xi^2)\,e^{-2i(2m+1)\tau-2in_1\psi}\ ,\ Y_2=\sin^2\theta\,e^{2i\varphi_1} \tag{13.9}$$

are AdS_3 and S^3 harmonics with eigenvalues

$$h=2m+2n_1+1\,,\quad \bar{h}=2m+1\,,\quad j=\bar{j}=1\,. \tag{13.10}$$

In the CPO limit $m=n_1=0$, one finds an operator of dimension $(1,1)$ that we denote by $O_2^{(1,1)}$, and for non-vanishing m, n we have again its Virasoro descendants

$$L_{-1}^{2(n_1+m)}\tilde{L}_{-1}^{2m}\,|O_2^{(1,1)}\rangle\,. \tag{13.11}$$

[3] In the K3 case such corrections are absent for the low dimension field in (13.6), while for the dimension 2 states in (13.12) they are spelled out explicitly in [36].

[4] As usual, $|O\rangle$ indicates the state related to the operator O under the standard CFT operator-state correspondence.

The precise identification of the CPO $O_2^{(1,1)}$ is more involved: in the orbifold CFT there are two operators with the required quantum numbers, which are the operator built out of the four fermions, $\psi^{+1}\psi^{+2}\tilde{\psi}^{+1}\tilde{\psi}^{+2}$, and the supersymmetric twist field of order 3, Σ_3^{++}. Linear combinations of these two CPOs [33,36,79] form the KK modes of dimension two of a 6D tensor multiplet (different from the one associated with $O_1^{(1/2,1/2)}$) and of the 6D gravity multiplet; following the notation of [36], we denote these CPOs as $s_2^{(6)}$ and σ_2 respectively. The operator $s_2^{(6)}$ is dual to a perturbation of $\mathrm{AdS}_3 \times S^3$ [80] where only the dilaton and the anti-delf-dual part of the RR 3-form are excited, while σ_2 only perturbs the 6D metric. The linearised solution (13.8) contains both types of perturbations and thus we conclude that the CPO $O_2^{(1,1)}$ associated with μ_0 is a linear combination of the $(1,1)$ components of the operators $s_2^{(6)}$ and σ_2:

$$O_2^{(1,1)} \equiv \sqrt{3}\, s_2^{(6)(1,1)} - \sigma_2^{(1,1)} \sim \sum_{r=1}^{N} |1,1\rangle^{(r)} + \dots \,. \tag{13.12}$$

As explained, in the orbifold CFT picture, $s_2^{(6)(1,1)}$ and $\sigma_2^{(1,1)}$ are two orthogonal linear combinations of the supersymmetric twist field of order 3 and of an operator that is quadrilinear in the elementary fermions. The state in (13.12) is precisely such that the single-trace terms with four fermions cancels.

The relative coefficient between $s_2^{(6)}$ and σ_2 is determined by comparison with a simple BPS solution. The orthogonal linear combination does not have a normalisable deformation within the truncation used here, but is partially encoded in the scalars $\mu_{1,2}$. As we will see in explicit solutions, their presence is necessary for regularity since these fields can be produced at quadratic order when the deformations (12.22) are present.

13.1.2 Light states of the double-mode truncation

The more general, double-mode truncation contains, as we saw in Section 12.3, includes a larger set of homogeneous modes, including also the fields ν_2, λ_2 and $m_5 \pm m_6$, in addition to ν_1 and λ_1. The states dual to these new modes are different spin components of the states introduced above. Indeed $SO(4)$ rotations, dual to the $SU(2)_L \times SU(2)_R$ R-symmetry of the CFT, permute the fields ν_1 and ν_2 and the fields λ_1, $m_5 \pm m_6$ and λ_2. The full holographic map[5] is summarized below:

$$\begin{gathered} \nu_1 \to O_1^{(\frac{1}{2},\frac{1}{2})}\,, \quad \nu_2 \to O_1^{(\frac{1}{2},-\frac{1}{2})}\,, \\ \lambda_1 \to O_2^{(1,1)}\,, \quad m_5 + m_6 \to O_2^{(0,1)}\,, \quad m_5 - m_6 \to O_2^{(1,0)}\,, \quad \lambda_2 \to O_2^{(1,-1)}\,, \end{gathered} \tag{13.13}$$

where as before the superscript $(j,\bar{j})$ denotes the spin of each operator with respect to the R-symmetry group $SU(2)_L \times SU(2)_R$.

[5]The map depends on the choice of phase for the fields: for example the state $|\frac{1}{2},-\frac{1}{2}\rangle$ turns into $|-\frac{1}{2},\frac{1}{2}\rangle$ if one conjugates the field ν_2. The map given here corresponds to the choice of phase used in the solutions of this article.

13.2 Heavy states

The states reviewed above are "light", having a conformal dimension that does not scale with the CFT central charge $c = 6N$. We will also refer to this light operators as single-particle (or single-trace) operators, as they are dual to elementary supergravity fields. Supergravity solutions like the ones described in Chapter 12, that are large deformations of $AdS_3 \times S^3$, are dual to "heavy" states whose conformal dimension grows like c in the large central charge limit.

Heavy states can be realized as multi-particle (or multi-trace) operators made by a large (of order c) number of single-trace constituents. For supersymmetric states, a precise characterization of the multi-particle operators dual to the supergravity solutions can be given in the language of the $\mathcal{M}^N/S_N$ orbifold sigma model [31, 53, 54, 81]. We first introduce the basic formalism for a simple geometry, the single 2-charge supertube corresponding to the solution (9.25) with $n = 0$, and then generalize to 3-charge and non-BPS solutions.

The single superstratum geometry depends on one continuous parameter $\alpha_1 \equiv \alpha$ and at linear order in α_1 the only field excited is ν_1 which, as we have seen, is dual to the state in (13.6). This indicates that the heavy state dual to the geometry for finite values of α_1 is a multi-particle state made by many copies of this basic constituent of spin $(\frac{1}{2}, \frac{1}{2})$. A more precise definition is given by the following coherent-like state [53, 54, 81]

$$|\alpha_1\rangle \equiv \sum_{p=0}^{N} A_1^p \, A_0^{N-p} \left(\left|\frac{1}{2}, \frac{1}{2}\right\rangle\right)_*^p (|0\rangle)^{N-p} \quad \text{with} \quad A_1 = \sqrt{N}\,\frac{\alpha_1}{2}\,, \; A_0 = \sqrt{N}\left(1 - \frac{\alpha_1^2}{4}\right)^{1/2}\,, \tag{13.14}$$

where $|0\rangle$ is the NS-sector[6] vacuum and $(|\frac{1}{2}, \frac{1}{2}\rangle)_*^p$ denotes a multi-particle state made by p copies of the state $|\frac{1}{2}, \frac{1}{2}\rangle$, which will be more explicitly defined below. In the large N limit, the sum over p in (13.14) is peaked over the average value

$$\bar{p} = A_1^2 = N\,\frac{\alpha_1^2}{4} \equiv N_1\,, \tag{13.15}$$

as it can be checked by calculating the norm of the state (13.14), see for instance [31]. For many purposes it suffices to approximate the sum with its average:

$$|\alpha_1\rangle \sim \left(\left|\frac{1}{2}, \frac{1}{2}\right\rangle\right)_*^{N_1} \quad \text{with} \quad \frac{N_1}{N} = \frac{\alpha_1^2}{4}\,; \tag{13.16}$$

the precise form of the state (13.14) is however needed to compute expectation values of operators that mix the constituents $|\frac{1}{2}, \frac{1}{2}\rangle$ and $|0\rangle$ in the heavy state.

A crucial point for us is the definition of the product $(|\frac{1}{2}, \frac{1}{2}\rangle)_*^p$ and for this purpose we must recall a basic fact about the orbifold $\mathcal{M}^N/S_N$: All operators must be invariant

[6] We represent the states in the NS sector in this article. Of course an alternative representation can be given by spectrally flowing to the R sector. As far as one works with asymptotically AdS solutions the two representations are equivalent, but one should keep in mind that only the R-sector states can be extended to asymptotically-flat solutions.

under the exchange of the copies of the sigma-model on each $\mathcal{M}$. A simple way to achieve this for the heavy state is to define each term in (13.14) as

$$\left(\left|\frac{1}{2},\frac{1}{2}\right\rangle\right)^p_* \equiv \sum_{\substack{r_1,r_2,\dots,r_p \\ r_1\neq r_2\neq\dots\neq r_p}} \left|\frac{1}{2},\frac{1}{2}\right\rangle^{(r_1)}\left|\frac{1}{2},\frac{1}{2}\right\rangle^{(r_2)}\dots\left|\frac{1}{2},\frac{1}{2}\right\rangle^{(r_p)}, \tag{13.17}$$

so that any of the N copies is either occupied by *one* CPO $|\frac{1}{2},\frac{1}{2}\rangle^{(r)}$ or by the vacuum. Another approach, more natural at a generic point in the CFT moduli space, is to consider the (non-singular) OPE product of p single-particle operators

$$\left(\left|\frac{1}{2},\frac{1}{2}\right\rangle\right)^p \equiv \lim_{z_i\to 0} O_1^{(\frac{1}{2},\frac{1}{2})}(z_1)\dots O_1^{(\frac{1}{2},\frac{1}{2})}(z_p)\,|0\rangle\,. \tag{13.18}$$

This is *not* the definition of the multi-particle operator in (13.14): in that heavy state one removes the copies where more than one operator $|\frac{1}{2},\frac{1}{2}\rangle^{(r)}$ acts simultaneously, and also the multi-trace corrections mentioned in (13.6).

The fact that the superstratum geometry is dual to the state (13.14) with the definition (13.17) has been confirmed by several precision-holography checks [31, 33, 36, 82], where the difference between (13.17) and (13.18) plays a crucial role.

A legitimate question is what is the gravity dual of a heavy state defined in terms of the multi-particle (13.18) that is more natural from the OPE point of view. As discussed in Section 11.2, in the 3D theory there is an extended family of supersymmetric solutions parametrized by the two real numbers α_1, β_1. Choosing $\beta_1 = 0$ results in the superstrata geometry (9.25), whose dual is the state $|\alpha_1\rangle$ in (13.14). On the other hand, the solution with $\beta_1 = -\frac{\alpha_1^2}{4}$ is the so-called "special-locus" solution, described in Section 12.2.3, that exhibits a remarkable simplicity and, in particular, its scalar matrix m has a single non-trivial eigenvalue and thus it enjoys an $SO(3)$ symmetry. As we will see in the next Section, this structure of the matrix m is naturally explained by assuming that the state dual to the "special-locus" geometry has the leading order form[7]

$$|\alpha_1\rangle_{s.l.} \sim \left(\left|\frac{1}{2},\frac{1}{2}\right\rangle\right)^{N_1} \quad \text{with} \quad \frac{N_1}{N} = \frac{2\alpha_1^2}{8+\alpha_1^2}\,, \tag{13.19}$$

where the multi-particle $(|\frac{1}{2},\frac{1}{2}\rangle)^{N_1}$ is defined as in (13.18). The precise form of the state $|\alpha_1\rangle_{s.l.}$, analogous to (13.14), has not yet been determined, but it is important to keep in mind that (13.19) represents only the leading order term of the state and, like in (13.14), the actual state also contains terms with $(|\frac{1}{2},\frac{1}{2}\rangle)^p$, where p is spread around the average value N_1. These terms are relevant when computing generic 1-point functions of CPOs in the state $|\alpha_1\rangle_{s.l.}$.

It is straightforward to generalise the CFT description of the states to the 3-charge BPS geometries and then to the non-BPS solutions constructed in the previous section. For simplicity, we will only give the leading order form of the state, in the spirit of (13.16)

[7]The relation between the supergravity parameter α_1 and N_1 can be found for example by comparing the angular momenta of the gravity solution with those of the CFT state $|\alpha_1\rangle_{s.l.}$.

and (13.19). Adding the momentum charge n_1 amounts to replace the CPO $|\frac{1}{2},\frac{1}{2}\rangle$ by its descendant $L_{-1}^{n_1}|\frac{1}{2},\frac{1}{2}\rangle$. Thus the 3-charge superstratum and the special locus solutions are dual to

$$|\alpha_1, n_1\rangle \sim \left(L_{-1}^{n_1}\Big|\frac{1}{2},\frac{1}{2}\Big\rangle\right)_*^{N_1} \quad \text{with} \quad \frac{N_1}{N} = \frac{\alpha_1^2}{4}\,, \tag{13.20a}$$

$$|\alpha_1, n_1\rangle_{s.l.} \sim \left(L_{-1}^{n_1}\Big|\frac{1}{2},\frac{1}{2}\Big\rangle\right)^{N_1} \quad \text{with} \quad \frac{N_1}{N} = \frac{2(2n_1+1)\alpha_1^2}{8(2n_1+1)+\alpha_1^2}\,, \tag{13.20b}$$

where the starred and un-starred multi-particle operators are defined as in (13.17) and (13.18) respectively. One also has the "pure NS" superstratum of Section 11.4.1, which depends on the single parameter β_1 associated with the CPO defined in (13.12). We thus expect the heavy state dual to the pure NS superstratum to be of the form

$$|\beta_1, n_1\rangle \sim (L_{-1}^{2n_1}|1,1\rangle)^{N_1} \quad \text{with} \quad \frac{N_1}{N} = \frac{(2n_1+1)\beta_1^2}{4\,(2n_1+1)^2+\beta_1^2}\,. \tag{13.21}$$

Based on the existence of non-BPS deformations of the state $|\beta_1, n_1\rangle$ within the Q-ball ansatz (see the perturbation theory of Section 12.4), we conjecture that the multi-particle constituents appearing in this state are constructed following the same approach as (13.18). For instance, in the $n_1 = 0$ case the coherent-like sum (13.14) should run over the states

$$\Big(|1,1\rangle\Big)^p \equiv \lim_{z_i\to 0} O_2^{(1,1)}(z_1)\dots O_2^{(1,1)}(z_p)\,|0\rangle\,. \tag{13.22}$$

This is to be contrasted with the geometries defined through the Lunin-Mathur profile [53] which involve linear combinations between single and multi-trace operator that are different from the one needed to define $O_2^{(1,1)}$, see [33, 36]. We do not present, however, any direct check of this conjecture, since this would require computing the VEVs of dimension-four CPOs a task that is unfeasible with our current holographic tools.

13.2.1 Non-BPS heavy states in the single-mode truncation

The heavy states dual to the non-BPS single-mode solutions presented in Section 12.2 are constructed following the same procedure as for the 3-charge superstrata: by building multi-particle heavy states out of many light constituents. As in the perturbative analysis, we limit the study to $\omega_1 = 3$, or equivalently $m = 1$. The schematic, leading order representation of the dual states is expected to be

$$|\alpha_1, n_1, m=1\rangle \;\sim\; \left(L_{-1}^{n+1}\tilde{L}_{-1}\,|O_{\frac{1}{2},\frac{1}{2}}\rangle\right)^{N_1}\,, \tag{13.23}$$

where, based on the superstrata relation (13.20a), the link between the number of strands N_1 and the quantities α_1, n_1 should have the form

$$\frac{N_1}{N} \;=\; \frac{\alpha_1^2}{4} + O(\alpha_1^4)\,. \tag{13.24}$$

The first order correction to this equality will be computed in the next Chapter. Note that the state $|\alpha_1, n_1, m=1\rangle$ is indeed non-BPS, as each of its single-particle constituents is non-BPS on its own.

It is important to clarify why in (13.23) we have used the multi-particle definition (13.18) rather than the one in (13.17). Both options lead to perfectly acceptable heavy states which should have a dual representation in supergravity. It was however a non-trivial outcome of the supergravity analysis of Section 12.2 that the only non-BPS geometries that fit in the Q-ball ansatz are at the special locus ; they are dual to the state in (13.23). A rough explanation of this finding rests on two facts: first, the Q-ball ansätze of Chapter 9 require the phases present in the matrix m (associated with $\lambda_{1,2}$ modes) to be exactly twice the ones present in the scalar χ (the $\nu_{1,2}$ modes) and, second, the scalar matrix of the special locus geometry enjoys an $SO(3)$ symmetry. It is conjectured that this symmetry protects the ratio of the phases of the scalar modes against the non-BPS corrections and locks it to the value required by the Q-ball Ansatz.

Analogously one can consider the non-BPS multi-particle state based on the constituents of the β_1 perturbation:

$$|\beta_1, n_1, m = 1\rangle \sim (L_{-1}^{2\,(n_1+1)} \tilde{L}_{-1}^2 |1,1\rangle)^{N_1}\,, \tag{13.25}$$

where

$$\frac{N_1}{N} = \frac{\beta_1^2}{4\,(2n_1+1)} + O(\beta_1^4)\,. \tag{13.26}$$

13.2.2 Non-BPS heavy states in the double-mode truncation

The situation is somewhat different for the non-BPS microstates of the double-mode truncation that were constructed in Section 12.3. They can be obtained by starting from one of the BPS solutions reviewed above and by adding single-particle constituents that do not preserve the same supercharges of the original constituents. Hence, though each single-particle component is by itself BPS, and as such it is dual to a certain supergravity mode, the supersymmetry of the full state is broken by the non-trivial interaction between the mutually non-BPS constituents. For example the states $|\frac{1}{2},\frac{1}{2}\rangle$ and $|\frac{1}{2},-\frac{1}{2}\rangle$ preserve different supercharges on the right sector but the same on the left sector, and thus a multi-particle state containing both states is still BPS; to break the remaining supersymmetries one excites the left sector by acting, for instance, with some power of the Virasoro generator L_{-1}. One is thus led to consider the state

$$|\alpha_1, \alpha_2, n_1, n_2\rangle \sim \left(L_{-1}^{n_1}\Big|\frac{1}{2},\frac{1}{2}\Big\rangle\right)^{N_1}\left(L_{-1}^{n_2}\Big|\frac{1}{2},-\frac{1}{2}\Big\rangle\right)^{N_2}\,, \tag{13.27}$$

where the relation between the microscopic quantities, N_1, N_2, and the macroscopic ones, α_1, α_2, should have the general form

$$\frac{N_1}{N} = \frac{2(2n_1+1)\alpha_1^2}{8(2n_1+1)+\alpha_1^2} + O(\alpha_1^2\alpha_2^2)\,, \quad \frac{N_2}{N} = \frac{2(2n_2+1)\alpha_2^2}{8(2n_2+1)+\alpha_2^2} + O(\alpha_1^2\alpha_2^2)\,. \tag{13.28}$$

We will provide a derivation of the first non-trivial correction terms of order $O(\alpha_1^2, \alpha_2^2)$ in the next Chapter. While the state $|\alpha_1, \alpha_2, n_1, n_2\rangle$ is non-BPS for generic values of n_1 and

n_2, it is BPS for $n_1 = n_2$, since it can be obtained by acting with a finite $SU(2)_R$ rotation generated by $\tilde{J}_0^-$ on the supersymmetric state $|\alpha_1, n_1\rangle_{s.l.}$ (this follows from $\tilde{J}_0^-|\frac{1}{2},\frac{1}{2}\rangle = |\frac{1}{2},-\frac{1}{2}\rangle$ and $(\tilde{J}_0^-)^k|\frac{1}{2},\frac{1}{2}\rangle = 0$ for $k > 1$).

Note that in (13.27), we have once again used the multi-particle definition (13.18) rather than the one in (13.17). this is for exactly the same reason as in the previous Section: the only non-PS solutions that fit the Q-ball truncation are on the special locus.

Analogously one can consider the "pure NS" non-BPS state

$$|\beta_1, \beta_2, n_1, n_2\rangle \sim (L_{-1}^{2\,n_1}|1,1\rangle)^{N_1}(L_{-1}^{2\,n_2}|1,-1\rangle)^{N_2}\,, \tag{13.29}$$

where

$$\frac{N_1}{N} = \frac{(2n_1+1)\beta_1^2}{4\,(2n_1+1)^2+\beta_1^2} + O(\beta_1^2\beta_2^2) \quad , \quad \frac{N_2}{N} = \frac{(2n_2+1)\beta_2^2}{4\,(2n_2+1)^2+\beta_2^2} + O(\beta_1^2\beta_2^2)\,. \tag{13.30}$$

This state is non-BPS for the same reason explained before (13.27) but, contrary to the state $|\alpha_1, \alpha_2, n_1, n_2\rangle$, it remains non-BPS even for $n_1 = n_2 \neq 0$. Indeed, since $\tilde{J}_0^-|1,1\rangle = |1,0\rangle$ and $(\tilde{J}_0^-)^2|1,1\rangle = |1,-1\rangle$, acting with a finite rotation generated by $\tilde{J}_0^-$ on the BPS state $|\beta_1, n_1\rangle$ produces both copies of type $|1,0\rangle$ and $|1,-1\rangle$ and does not yield the state $|\beta_1, \beta_2, n_1, n_1\rangle$.

13.2.3 The holographic charges

We start by briefly reviewing the relevant holographic formulas (following [39,54]) needed to extract the angular momenta, J^a, $\tilde{J}^a$, and the conformal dimensions, h, $\bar{h}$, from the geometry. To compute these quantities one only needs the 3D Einstein metric ds_3^2 (7.18) and the gauge fields $\tilde{A}^{ij}$ (9.5). We will use an AdS_3 radial coordinate z, related to our previous coordinate ξ, and coordinates $x^\mu \equiv \{\tau, \sigma\}$ on the boundary, where τ coincides with the coordinate used in (7.12) up to a rescaling, while the normalisation of σ cannot be changed since we need to preserve the periodicity 2π. The relation between ξ and z is chosen in such a way that the 3D metric (7.18) has the asymptotic form as $z \to 0$ [83]

$$-ds_3^2 = \frac{dz^2}{z^2} + \frac{-d\tau^2 + d\sigma^2}{z^2} + g_{\mu\nu}^{(2)} dx^\mu dx^\nu + O(z^2)\,. \tag{13.31}$$

The z (or ξ) component of the gauge fields should vanish at $z = 0$ ($\xi = 1$) and the asymptotic values of the τ and ψ components are denoted by $\Phi_i^{(\infty)}$, $\Psi_i^{(\infty)}$ $(i = 1,2,3,4)$. In terms of these asymptotic values, the $SU(2)_L \times SU(2)_R$ angular momenta J^a, $\tilde{J}^a$ $(a = 3, \pm)$ are

$$J^3 = -\frac{N}{2}\left(\Phi_1^{(\infty)} + \Phi_2^{(\infty)} + 2(\Psi_1^{(\infty)} + \Psi_2^{(\infty)})\right) \;,\; J^\pm = \frac{N}{2}\left(\Phi_3^{(\infty)} + \Phi_4^{(\infty)} + 2(\Psi_3^{(\infty)} + \Psi_4^{(\infty)})\right)\,, \tag{13.32a}$$

$$\tilde{J}^3 = -\frac{N}{2}\left(\Phi_1^{(\infty)} - \Phi_2^{(\infty)}\right) \;,\; \tilde{J}^\pm = \frac{N}{2}\left(\Phi_3^{(\infty)} - \Phi_4^{(\infty)}\right)\,. \tag{13.32b}$$

Note that these formulas are also valid in the single-sector truncation, where some of the gauge fields vanish $\Phi_{3,4} = \Psi_{3,4} = 0$. In this case, we find immediately $J^{\pm} = \tilde{J}^{\pm} = 0$, which matches with the momenta of the CFT states (13.23), (13.25).

The values of the left and right conformal dimensions, h and $\bar{h}$, are computed from

$$h = \frac{N}{4}\left(1 + g^{(2)}_{\tau\tau} + 2g^{(2)}_{\tau\sigma} + g^{(2)}_{\sigma\sigma}\right) + \frac{(J^3)^2 + J^+J^-}{N}\,, \tag{13.33a}$$

$$\bar{h} = \frac{N}{4}\left(1 + g^{(2)}_{\tau\tau} - 2g^{(2)}_{\tau\sigma} + g^{(2)}_{\sigma\sigma}\right) + \frac{(\tilde{J}^3)^2 + \tilde{J}^+\tilde{J}^-}{N}\,. \tag{13.33b}$$

Note that the formulas (13.32) assume the Axial gauge, but the general result follows simply by transforming the guage fields: under a generic $SO(4)$ gauge rotation, $\mathcal{U}$, the matrix of the gauge fields, $\tilde{A}$, transforms as $\tilde{A} \to \mathcal{U}\tilde{A}\mathcal{U}^{-1} + \frac{1}{2}d\mathcal{U}\mathcal{U}^{-1}$. In particular, for a block-diagonal phase rotation of the form

$$\mathcal{U} = \begin{pmatrix} \mathcal{U}_1 & 0 \\ 0 & \mathcal{U}_2 \end{pmatrix} \quad \text{with} \quad \mathcal{U}_i = \begin{pmatrix} \cos\delta_i & -\sin\delta_i \\ \sin\delta_i & \cos\delta_i \end{pmatrix} \quad \text{and} \quad \delta_i = \delta_i^{\tau}\,\tau + \delta_i^{\psi}\,\psi\,, \tag{13.34}$$

so the angular momenta transform as

$$\begin{aligned} J^3 &\to J^3 + \frac{N}{4}(\delta_1^{\tau} + \delta_2^{\tau} + 2(\delta_1^{\psi} + \delta_2^{\psi})) \quad , \quad J^{\pm} \to J^{\pm} e^{\pm i(\delta_1+\delta_2)}\,, \\ \tilde{J}^3 &\to \tilde{J}^3 + \frac{N}{4}(\delta_1^{\tau} - \delta_2^{\tau}) \quad , \quad \tilde{J}^{\pm} \to \tilde{J}^{\pm} e^{\pm i(\delta_1-\delta_2)}\,. \end{aligned} \tag{13.35}$$

13.3 Precision holography tests for supersymmetric states

In this section we provide some explicit checks supporting the identification between the supergravity solutions and the heavy states introduced in the previous section. In order to have a precise, quantitative check, we focus on protected physical observables, such as discrete quantum numbers and supersymmetric 3-point correlators [84]. In particular for the 3-point correlators we follow the approach initiated by [53, 54, 81]: we extract the expectation values of the BPS operators dual to single particle states from the asymptotic expansion of the supergravity solutions at the AdS boundary and then match these results against those obtained in the CFT description. The main goal of this section is to show how the different definitions of the multiparticle heavy states are reflected in the corresponding supergravity solutions, thus providing support for our proposed identification.

We will focus on the 1/4-BPS case which is technically simpler, but still contains all the interesting features needed for our analysis. In particular we show that the special locus constraint $\beta_1 = -\frac{\alpha_1^2}{4}$ is directly related to the standard definition of multiparticle states (13.18). In contrast the more familiar 2-charge solution with $\beta_1 = 0$ is dual to the state (13.14) as discussed in [53]. The most interesting information is derived from the expectation values of the operators of dimension 2 [33, 36]. This requires a careful analysis of the supergravity solutions since the corresponding expectation values are related

to subleading terms at the AdS boudary with respect to the contributions relevant for dimension 1 operators. In the 1/4-BPS case, we can bypass the problem by working in the gauged-fixed approach summarised in Appendix D of [36] which is the approach we follow in Section 13.3. The main result is that all operators of dimension 2 have a vanishing expectation value in the special locus geometry (11.14) with $p = 0$. This is consistent with the dual state (13.19) since these vanishing expectation values are proportional to extremal 3-point correlators or equivalently 2-point correlators between a single and a double-particle state. These quantities are known to be sensitive to the mixing between multi-particle operators [85] and they vanish when using the natural holographic dictionary [86, 87] derived from the standard OPE product (13.18). This is to be contrasted with what happens for the state (13.14), where one can use the free orbifold description to check that there are non-zero expectation values for opreators of dimensions 2. Thanks to the non-renormalisation properties of these observables [84], we can match the CFT results with those obtained from the solution with $\beta_1 = 0$ and check that there is a non-trivial agreement as done in [33, 36].

This analysis can be extended to the case of 1/8-BPS geometries thanks to the fact that a chiral part of the supersymmetry is preserved, but this will not be discussed here.

The 1/4-BPS case

In this section we use Eq. [D.2] and [D.4] of [36] to read the holographic expectation values. We start the 6D uplift of Appendix C and use for instance, Eq. [C.1] of [36] to read the functions $Z_{1,2,4}$, thus we need to work in the Ramond sector. From the scalars parametrised as in (C.1) and (C.13) we have

$$\frac{Z_4}{Z_2} = C_4 = \sqrt{\frac{Q_1}{2Q_5}} X \ , \quad \frac{Z_1}{Z_2} = V_4^2 = \frac{Q_1}{2Q_5}\left(X^2 + 2\Delta\right) \ , \quad \mathcal{P} \equiv Z_1 Z_2 - Z_4^2 = \frac{Q_1}{Q_5}\Delta\, Z_2^2 \ . \tag{13.36}$$

Looking now at 6D Einstein metric ds_6^2 (C.9), we should rewrite it in the form of Eq. [C.1] of [36]. In order to apply the gauged-fixed approach of that reference, we first need to fix the constants in Ω_1 and perform an appropriate transformation (13.34) on the 3D gauge fields so as to reproduce the values expected for the CFT in the Ramond sector. Then we should choose coordinates such that the 4D metric in [C.1] takes the form $d\rho^2 + \rho^2\left(d\theta^2 + \sin^2\theta d\varphi_1^2 + \cos^2\theta d\varphi_2^2\right)$, where the relation between ξ and ρ is given in (7.12). In general this requires a change of coordinates that we can derive perturbatively around the AdS boundary

$$\rho \to c_\rho \hat{\rho} + \frac{f_\rho(\hat{\theta}, \hat{\varphi}_i)}{\hat{\rho}} + \dots \ , \quad \theta \to \hat{\theta} + \frac{f_\theta(\hat{\theta}, \hat{\varphi}_i)}{\hat{\rho}^2} + \dots \ , \quad \varphi_j \to \hat{\varphi}_j + \frac{f_{\varphi_j}(\hat{\theta}, \hat{\varphi}_i)}{\hat{\rho}^2} + \dots \ , \tag{13.37}$$

where the dots stand for subleading terms in the large ρ expansion.

Let us first start from the configuration described in Eq. (9.25) with $n = n_1$. In order to satisfy (13.31) we need to perform a rescaling of τ which amounts to choose

$$\Omega_1 = 1 - \frac{\alpha_1^2}{4} \ , \tag{13.38}$$

while to reproduce the angular momenta from (13.32) we need to perform the $SO(4)$ rotation (13.34) with parameters[8]

$$\delta_i^\tau = 0 \,, \quad \delta_1^\psi = n_1 \,, \quad \delta_2^\psi = -1 \,. \tag{13.39}$$

Finally the change of variables (13.37) needed reads

$$c_\rho = \sqrt{1-\frac{\alpha_1^2}{4}} \,, \quad f_\rho(\hat\theta,\hat\varphi_i) = \frac{1}{8}\sqrt{1-\frac{\alpha_1^2}{4}}\,(1{+}2\cos(2\theta)) \,, \quad f_\theta(\hat\theta,\hat\varphi_i) = -\frac{1}{4}\left(1-\frac{\alpha_1^2}{4}\right)\sin(2\theta) \,, \tag{13.40}$$

while $f_{\varphi_j} = 0$. In the 1/4-BPS case, which has $n_i = 0$, was first obtained in [53] where also the dual interpretation in terms of the state (13.14) was introduced. For this geometry, we see that Z_2 does not depend on the S^3 coordinates. By using (C.8) and the explicit expressions in (9.25) in the equations above, one can expand $\frac{Z_4}{Z_2}$ in spherical harmonics[9] and read from (D.4) of [36] the leading order result for the expectation value of the operator (13.6)

$$\langle s_1^{(7)(\pm\frac{1}{2},\pm\frac{1}{2})}\rangle = \frac{\alpha_1}{\sqrt{2}}\lim_{\xi\to 1}\left(\hat\rho\,\sqrt{1-\xi^2}\right) = \frac{\alpha_1}{\sqrt{2}}\sqrt{1-\frac{\alpha_1^2}{4}} \,. \tag{13.41}$$

Moving to the harmonics of order 2, one can check that the operator O_2 has vanishing expectation value in the solution defined by (9.25). The only components that can be potentially non-trivial are $(\pm1,\pm1)$ and in that case there is a cancellation between the two terms in (13.12) which separately are non-zero

$$s_2^{(6)(\pm1,\pm1)} = \frac{1}{\sqrt{3}}\sigma_2^{(\pm1,\pm1)} = \frac{1}{2\sqrt{2}}\frac{\alpha_1^2}{4}\left(1-\frac{\alpha_1^2}{4}\right) \quad \Rightarrow \quad \langle O_2^{(\pm1,\pm1)}\rangle = 0 \,. \tag{13.42}$$

Then the orthogonal combination

$$C_2^{(\pm1,\pm1)} \equiv \sqrt{3}\,\sigma_2^{(\pm1,\pm1)} + s_2^{(6)(\pm1,\pm1)} \tag{13.43}$$

has a non-trivial expectation value in the heavy state dual to (9.25)

$$\langle C_2^{(\pm1,\pm1)}\rangle = \frac{\alpha_1^2}{2\sqrt{2}}\left(1-\frac{\alpha_1^2}{4}\right) \,. \tag{13.44}$$

Let us now consider the 1/4-BPS version of the "special locus" solution discussed in Section 11.1, which is obtained by setting $n_1 = 0$ in (11.14). In this case we have

$$c_\rho = \sqrt{\frac{8-\alpha_1^2}{8+\alpha_1^2}} \tag{13.45}$$

and, thus, he expectation value for the operator (13.6) now reads

$$\langle s_1^{(7)(\pm\frac{1}{2},\pm\frac{1}{2})}\rangle = \frac{4\sqrt{2}}{8+\alpha_1^2} \,. \tag{13.46}$$

[8] In the Neveu-Schwarz sector we have $\delta_2^\psi = 0$ and the potentials $\Psi_{1,2}$ vanish at $\xi = 0$.

[9] We follow [36] also for the conventions of the spherical harmonics, see their Appendix A.

Moving to the harmonics of order 2, one can start again from [D.4] of [36] and evaluate the second equation in (13.36). The surprise is that it does not depend on the S^3 coordinates and so the expectation value of $s_2^{(6)}$ vanishes for the 1/4-BPS "special-locus" solution. The analysis of the expectation values for σ_2 is more involved. For the $(\pm 1, \pm 1)$ components, the terms proportional to the second harmonics of $Z_{1,2}$ and those proportional to the square of the first harmonics of Z_4 are separately non-trivial, but cancel in the combination in [D.4] of [36]. For the $(0, 0)$ component, also the term proportional to the square of the first harmonic of the vectors contributes, but again there is a non-trivial cancellation when all contributions to [D.4] are combined. In summary also all components of σ_2 vanish, which implies $\langle C_2 \rangle = \langle O_2 \rangle = 0$, and so there are no dimension-2 expectation values for this "special locus" solution.

Chapter 14

Holographic analysis of non-BPS microstates

In this Chapter, we explain how to establish the link between the CFT picture described in Chapter 13, and the bulk perturbation theory of Chapter 12. It is based on the work presented in [39, 42].

The non-BPS solutions constructed in Chapter 12 are holographically related to the heavy CFT states reviewed in Section 13.2. Establishing the precise relation and verifying its consistency requires, however, some further analysis. We will first outline our general approach and then discuss in more detail the alpha and beta classes of solutions, in both the single-mode and double-mode truncation.

14.1 The approach

When dealing with non-BPS configurations the set of precise-holography tools that has been used to conjecture and verify with great accuracy the map between asymptotically AdS_3 geometries and D1-D5 supersymmetric states [31, 33, 36, 53, 54] shrinks considerably. This is because three-point functions where some of the operators break all supersymmetries generically depend on the CFT moduli and their values at the gravity point are unknown. The only available link between gravity and CFT is provided by few quantized charges, the momentum charge, $n_p = h - \bar{h}$, and the $SU(2)_L \times SU(2)_R$ angular momenta, J^a and $\tilde{J}^a$ $(a = 3, \pm)$. The holographic formulas for these quantities is given for example in [54, 88].

The formulae for the angular momenta depend on the asymptotic values of the gauge fields, and thus are sensitive to the gauge in which the bulk solution sits. As it was explained in [88], in the quantum theory large gauge transformations are anomalous, and the choice of gauge has the physical effect of changing the state. An example of this phenomenon is the spectral flow transformation that relates the R and NS sectors of the CFT.

In our theory, the $U(1)^2$ gauge rotating the (12) and (34) components will play an important role, as it shifts the gauge fields Φ_1 and Φ_2, and changes the τ- and ψ-dependence

of the scalars. The gravity computations of Chapter 12 have been performed in a particularly convenient gauge where, in particular, all the dependence on the worldsheet coordinates τ and ψ has been gauged away. Using this gauge, the computed quantized charges do not reproduce the values expected from the CFT. A first step for a holographic interpretation of our gravity solutions is to perform the appropriate rotation that yields the values of the angular momenta predicted by the CFT.

A further step is finding the relation between the microscopic quantities, N_1, N_2, and the gravity parameters, α_1, α_2, β_1, β_2, expressed by the perturbative relations (13.24) and (13.26) in the single-sector truncation, and by (13.28) and (13.30) in the double-sector truncation. In the single-sector truncation, this relation can be computed by simply matching the momentum charge $h - \bar{h}$. However, as we will see, this is not enough in the double-sector truncation, and we will need to also match the energy $h + \bar{h}$.

This second point requires some clarification: Unlike the quantized momentum, the energy is a non-protected (moduli-dependent) quantity, which receives corrections from the interactions between the mutually non-BPS single-particles constituents of the heavy states (13.27), (13.29). From the CFT perspective, these corrections correspond to the anomalous dimensions of the non-BPS multi-particle operators formed by the interacting single-particles and are interesting dynamical data that are, generically, unknown. These energy corrections can be read off from the geometry in two different ways: from the τ-dependence of fields and from the asymptotic behavior of (τ, ψ) component of the metric (the precise formulas will be reviewed below). Thus, though we cannot predict the energy corrections from the CFT, requiring the consistency[1] between these two ways of extracting them imposes a non-trivial constraint, which allows us to completely determine the holographic dictionary and the energy corrections order by order in perturbation theory.

A schematic summary of our procedure is as follows:

(i) Start from the solutions of Chapter 12 and perform an $SO(4)$ rotation such that: the angular momenta of the rotated solution have the values expected from the CFT, the ξ-components of the gauge fields vanish at infinity, $\xi = 1$ (this is the gauge where one usually computes the angular momenta), and the ψ-components of the gauge fields vanish at the origin, $\xi = 0$ (this is needed for regularity, since the ψ coordinate degenerates at the origin);

(ii) Extract the conformal dimensions h, $\bar{h}$ from the metric (with the holographic formulas reviewed below) and determine the relation between N_1, N_2 and the supergravity parameters α_1, α_2, β_1, β_2 by matching the momentum $h - \bar{h}$ with the CFT value, and, in the double-mode truncation, the energy $h + \bar{h}$ with the value inferred from the frequency of the supergravity fields.

Since the procedure requires extracting the angular momenta, J^a, $\tilde{J}^a$, and the conformal dimensions, h, $\bar{h}$, from the geometry, we first briefly review the relevant holographic

[1] We will make an independent check of this consistency requirement in the single-mode truncation. In the double-mode truncation, we turn things around and impose by hand the consistency, as a way to infer the relations (13.28) and (13.30).

formulas (following [39, 54]) and then give some details of the computations for the alpha and beta class of solutions at the lowest perturbative orders.

14.2 Matching in the single-mode truncation

We start to derive the matching in the simpler case of the single-mode truncation, and we focus on the alpha class of solutions. In the bulk, the solution has been computed perturbatively in Section 12.2.2. The proposed identification for the CFT state was given in (13.23).

As we explained, the first step is to rewrite the metric in the Feffermann-Graham form. We then need to find the correct gauge to match the CFT quantized charges.

The radial coordinate z is defined such that the metric is asymptotic to

$$ds_3^2 = \frac{dz^2}{z^2} + \frac{-d\tau^2 + d\sigma^2}{z^2} + g^{(2)}_{\mu\nu} dx^\mu dx^\nu + O(z^2)\,. \tag{14.1}$$

Using the perturbative expansion, we find that the coordinates z and ξ are related as

$$\frac{\xi}{\sqrt{1-\xi^2}} = \left(1 + \frac{3}{8(n_1+1)^2}\alpha_1^2 + c_\rho^{(0)}\alpha_1^4 + O(\alpha_1^6)\right) z^{-1} \left[1 - \frac{z^2}{4}\left(1 + c_\rho^{(1)}\alpha_1^4 + O(\alpha_1^6)\right) + O(z^4)\right], \tag{14.2}$$

where $c_\rho^{(0)}$, $c_\rho^{(1)}$ are n_1-dependent rational numbers :

$$c_\rho^{(0)} = \frac{72\big(3n_1(n_1+3)+4\big)\Big(-3H_{n_1+1} + H_{n_1+\frac{5}{2}} + \log 4\Big) + 3(1+2n_1)\big(89 + 4n_1(35+9n_1)\big)}{128(2n_1+1)(2n_1+3)(2n_1+5)(n_1+1)^4}, \tag{14.3}$$

$$c_\rho^{(1)} = \frac{36\big(3n_1(n_1+3)+4\big)\Big(H_{n_1+1} - H_{n_1+\frac{5}{2}} - \log 4\Big) - 24n_1(6n_1^2+13n_1-12) + 231}{32(2n_1+1)(2n_1+3)(2n_1+5)(n_1+1)^4}, \tag{14.4}$$

and we have defined

$$H_k = \int_0^1 \frac{1-x^k}{1-x} dx, \tag{14.5}$$

which is equal to the k-th harmonic number when k is an integer. Note that to obtain the holographic matching it is indeed necessary the expansion of the metric up to $O(\alpha_1^4)$.

The CFT quantized charges can be read-off from the state (13.23):

$$J^3 = \tilde{J}^3 = \frac{N_1}{2}\,, \quad J^\pm = \tilde{J}^\pm = 0\,, \quad h = \left(n_1 + \frac{3}{2}\right)N_1\,, \quad \bar{h} = \frac{3}{2}N_1\,. \tag{14.6}$$

To compare these predictions with the supergravity values, we first need to establish the dictionary between the scale of the perturbation, α_1, and the number of non-BPS strands, N_1. While h and $\bar{h}$ depend on the moduli and thus cannot be matched directly,

the momentum charge $h - \bar{h}$ can. Using the formulas (13.33), it can computed in the supergravity in a perturbative expansion in α_1, and then matched with (14.6). We obtain

$$g^{(2)}_{\tau\sigma} \;=\; n_1 \frac{N_1}{N}\,; \tag{14.7}$$

and we can invert the series in α_1 on the left-hand side, to obtain:

$$\frac{\alpha_1^2}{4} \;=\; \frac{N_1}{N}\left[1 + c_{N_1}\frac{N_1}{N} + O\left(\frac{N_1}{N}\right)^2\right]. \tag{14.8}$$

where c_{N1} are n_1-dependent rational numbers:

$$c_{N1} \;=\; \frac{12\big(3n_1(n_1+3)+4\big)\Big(3H_{n_1+1} - H_{n_1+\frac{5}{2}} - \log 4\Big) + 4n_1(4n_1+21) + 39}{2(2n_1+1)(2n_1+3)(2n_1+5)}\,. \tag{14.9}$$

Having this dictionary, we can now match the angular momenta. As noted in the previous Section, it is necessary to first perform a large gauge transformation on the gravity side. In the single-mode truncation, a simple block-diagonal rotation of the form (13.34) is enough, and we find that we can match the angular momenta with

$$\Delta\omega_1 \;\equiv\; \delta\omega_1 \;=\; -\,c_\omega \frac{N_1}{N} + O\left(\frac{N_1}{N}\right)^2, \qquad \Delta\omega_2 \;=\; 0\,, \tag{14.10}$$

with c_ω an n_1-dependent positive rational number:

$$c_\omega \;=\; \frac{1}{8}\left(64 - \frac{3}{2n_1+1} - \frac{66}{2n_1+3} - \frac{3}{2n_1+5}\right). \tag{14.11}$$

It is natural to interpret the frequency shift $\delta\omega_1$ as the correction to the energy of a single particle constituents $L_{-1}^{n_1+1}\tilde{L}_{-1}\,|O_{\frac{1}{2},\frac{1}{2}}\rangle$ due to the (attractive) interaction with the other elements of the bound state: this correction should be proportional to the number of elements N_1 (for $N_1 \gg 1$) and to the Newton's constant $G_N \sim N^{-1}$, in agreement with (14.10). To check the numerical coefficient c_ω would require to compute an anomalous dimension of the operator $L_{-1}^{n+1}\tilde{L}_{-1}\,O_{\frac{1}{2},\frac{1}{2}}$ in the strongly coupled CFT, a task that is at the moment out of reach.

Even without an independent verification of (14.10), we can still make a non-trivial check of our interpretation of $\delta\omega_1$ and of the consistency of our supergravity construction by comparing with the energy $h+\bar{h}$ extracted from the metric via the holographic relations (13.33). Indeed, using these relations we compute the energy at order $\mathcal{O}(\alpha_1^4)$ and find

$$h + \bar{h} = N_1\left[(3+n_1) + \frac{\delta\omega_1}{2} + O\left(\frac{N_1}{N}\right)^2\right]. \tag{14.12}$$

On the other hand, this quantity represents the energy of the full state (13.23) and thus should be, in first approximation, $(3+n_1)N_1$ which is the sum of the free energies of the elementary constituents of the bound state. Then we should include the dynamical

correction: in the regime $1 \ll N_1 \ll N$ this is given by the interaction energy between any single pair of constituents, times the number of pairs. But according to our interpretation of $\delta\omega_1$ the interaction energy between one pair should be identified with $\frac{\delta\omega_1}{N_1}$, and the number of pairs is $\approx \frac{N_1^2}{2}$ for $N_1 \gg 1$. This way of calculating $h + \bar{h}$ reproduces the holographic result (14.12), including the N_1/N correction in the square parenthesis.

14.3 Matching in the double-mode truncation

We now turn to the more difficult case of the double-mode truncation. We follow the same method as previously, however the computations are more challenging. In particular, the large gauge transformation needed to match the angular momenta is no longer a simple block-diagonal rotation.

14.3.1 Alpha class

We focus here on the gravity solution constructed in Section 12.3.2 and show that, after an appropriate $SO(4)$ rotation, it is dual to the heavy state described schematically in (13.27).

Our guides in finding the correct gauge are, once again, the CFT quantized charges, that can be easily extracted from (13.27):

$$J^3 = \frac{1}{2}(N_1+N_2)\,,\ J^\pm = 0\,,\ \tilde{J}^3 = \frac{1}{2}(N_1-N_2)\,,\ \tilde{J}^\pm = -\delta_{n_1,n_2}\sqrt{N_1 N_2}\,,\ n_p = h-\bar{h} = n_1 N_1 + n_2 N_2\,. \tag{14.13}$$

The only point that might deserve a clarification is the value of $\tilde{J}^\pm$: it can be understood by remembering that the heavy states are actually defined by coherent state superpositions, like in (13.14), and by noting that the state $\tilde{J}_0^+\left(L_{-1}^{n_2}\left|\frac{1}{2},-\frac{1}{2}\right\rangle\right) = L_{-1}^{n_2}\left|\frac{1}{2},\frac{1}{2}\right\rangle$ is orthogonal to $L_{-1}^{n_1}\left|\frac{1}{2},\frac{1}{2}\right\rangle$ unless $n_1 = n_2$; hence, when $n_1 = n_2$ acting with $\tilde{J}^\pm$ on the heavy state gives a state that has non-vanishing overlap with itself, but this does not happen for the non-BPS state with $n_1 \neq n_2$. This shows that we have to treat the BPS and non-BPS cases separately in the alpha class of solutions and we cannot simply set $n_1 = n_2$ in the expressions (for the beta class, $n_1 = n_2$ is still non-BPS, as explained after (13.30), and there is no such issue there). In the following we will mostly focus on the non-BPS solutions with $n_1 \neq n_2$.

Comparison of the CFT predictions (14.13) with the supergravity values computed from the holographic formulas (13.32), (13.33), requires the dictionary between the CFT variables, N_1, N_2, and the gravity ones, α_1, α_2, which is only known in the BPS limits, $\alpha_1 = 0$ or $\alpha_2 = 0$ (see (13.28)), while the corrections have to be inferred order by order in the double perturbative expansion in α_1, α_2. Already at zeroth order in both α_1 and α_2 one sees that the gauge used in the supergravity construction is not the one that describes

a proper CFT state. At this order, the non-vanishing gauge fields are constants:

$$\Phi_1 = \Phi_2 = \frac{1}{2} \quad , \quad \Psi_1 = \frac{n_1}{2} \quad , \quad \Psi_2 = \frac{n_2}{2} \, . \tag{14.14}$$

A regular solution must have $\Psi_i = 0$ at the origin and moreover the CFT requires, at this order, $J_3 = \tilde{J}_3 = 0$ and thus, via (13.32), $\Phi_1^{(\infty)} = \Phi_2^{(\infty)} = 0$. Hence, one has to apply a gauge rotation of the form (13.34) with

$$\delta_1 = \tau + n_1 \, \psi \quad , \quad \delta_2 = \tau + n_2 \, \psi \, , \tag{14.15}$$

to cancel the constant parts of the gauge fields. Note than when this transformation acts on the $SO(4)$ vector χ_I, as $\chi \to \mathcal{U}\chi$, it induces the phases $\chi_1 + i\chi_2 \sim e^{i\delta_1}$ and $\chi_3 + i\chi_4 \sim e^{i\delta_2}$ which are the phases expected for the states $L_{-1}^{n_1}\Big|\frac{1}{2},\frac{1}{2}\Big\rangle$ and $L_{-1}^{n_2}\Big|\frac{1}{2},-\frac{1}{2}\Big\rangle$, respectively, based on the values of the energy and momentum. Turning things around, this is the reason why in the supergravity construction one has chosen the constants (14.14) for the gauge fields.

The "non-abelian" gauge fields, Φ_i, Ψ_i with $i = 3, 4$, first appear at order $\alpha_1\alpha_2$ and are given in (12.65). Using the holographic formulas (13.32) to extract the values of the angular momenta from the asymptotic values of these gauge fields we obtain $J^\pm \neq 0$ and $\tilde{J}^\pm = 0$, while for the non-BPS states with $n_1 \neq n_2$ one expects both $J^\pm$ and $\tilde{J}^\pm$ to vanish (see (14.13)). This signals the necessity to perform a further gauge transformation to rotate $J^\pm$ away. The regularity condition that $\Psi_i(\xi = 0) = 0$ and the requirement that the ξ-components of the gauge fields vanish at $\xi = 1$ partially constrain the transformation, and a possible choice is

$$\mathcal{U} = \mathbf{1} + \alpha_1\alpha_2 \frac{\xi^{n_1+n_2}\big((n_1+n_2)\xi^2 - (n_1+n_2+2)\big)}{2(n_1-n_2)(n_1+n_2)^2(n_1+n_2+2)} \begin{pmatrix} 0 & 0 & u_1 & 0 \\ 0 & 0 & 0 & u_2 \\ -u_1 & 0 & 0 & 0 \\ 0 & -u_2 & 0 & 0 \end{pmatrix} , \tag{14.16}$$

where $u_1 = n_1 + n_2 + 2\, n_1\, n_2$ and $u_2 = n_1\,(n_1+1) + n_2\,(n_2+1)$. This transforms the gauge fields to

$$\begin{aligned}
\Phi_3 = \Phi_4 &= \alpha_1\,\alpha_2 \frac{n_1^2 - n_2^2 + (n_1-n_2)\,\xi^{n_1+n_2}\big((n_1+n_2)\xi^2 - (n_1+n_2+2)\big)}{4\,(n_1+n_2)^2(n_1+n_2+2)} \, , \\
\Psi_3 &= -\alpha_1\,\alpha_2 \frac{(n_2+1)\Big(n_1+n_2+\xi^{n_1+n_2}\big(2+(1-\xi^2)(n_1+n_2)\big)\Big)}{4(n_1+n_2)(n_1+n_2+2)} \, , \\
\Psi_4 &= \alpha_1\,\alpha_2 \frac{(n_1+1)\Big(n_1+n_2+\xi^{n_1+n_2}\big(2+(1-\xi^2)(n_1+n_2)\big)\Big)}{4(n_1+n_2)(n_1+n_2+2)} \, , \\
\Psi_5 &= \alpha_1\,\alpha_2 \frac{(n_1+n_2+2\,n_1\,n_2)}{4(n_1^2-n_2^2)}(1-\xi^2)\,\xi^{n_1+n_2-1} \, , \\
\Psi_6 &= \alpha_1\,\alpha_2 \frac{n_1\,(n_1+1)+n_2\,(n_2+1)}{4(n_1^2-n_2^2)}(1-\xi^2)\,\xi^{n_1+n_2-1} \, .
\end{aligned} \tag{14.17}$$

It appears that $\Psi_{5,6}$ are singular at the origin for $n_1 = n_2$, but, in fact, the state is then BPS, whereas the transformation above applies only in the non-BPS case. The former is discussed further down.

Having obtained the expected values of $J^\pm$ and $\tilde{J}^\pm$, one should also consider J^3 and $\tilde{J}^3$: discarding terms of order $\alpha_2^2 \sim N_2$ and higher, one should have $J^3 = \tilde{J}^3 = \frac{N_1}{2} \sim N\frac{\alpha_1^2}{4}$, where we stop at order $O(\alpha_1^2)$ for now. At this order, the existence of a normalisable solution for ν_2 requires adjusting the constant term in Φ_2 and the asymptotic values of the gauge fields are corrected with respect to the zero-th order values (14.14) to (see (12.65))

$$\begin{aligned}
&\Phi_1^{(\infty)} = \frac{1}{2} - \frac{\alpha_1^2}{8}\,, \quad \Phi_2^{(\infty)} = \frac{1}{2} + \frac{1}{8}\left[-1 + \frac{2\,(n_1-n_2)^2}{(n_1+n_2)(n_1+n_2+1)(n_1+n_2+2)}\right]\alpha_1^2\,,\\
&\Psi_1^{(\infty)} = \frac{n_1}{2}\,, \quad \Psi_2^{(\infty)} = \frac{n_2}{2} - \frac{\alpha_1^2}{8}\,.
\end{aligned} \tag{14.18}$$

To obtain the expected values of J^3 and $\tilde{J}^3$ it is necessary to correct the phase δ_2 in the gauge transformation (13.34) to

$$\delta_2 \to (1+\delta\omega_2)\,\tau + n_2\,\psi \tag{14.19}$$

with

$$\delta\omega_2 = -2\frac{N_1}{N}\left[1 - \frac{(n_1-n_2)^2}{(n_1+n_2)(n_1+n_2+1)(n_1+n_2+2)}\right] + O\left(\frac{N_1}{N}\frac{N_2}{N}, \left(\frac{N_1}{N}\right)^2\right) \quad \text{for} \quad n_1 \neq n_2\,. \tag{14.20}$$

This quantity has an important microscopic meaning: it represents the interaction energy of a particle of type $L_{-1}^{n_2}\left|\frac{1}{2},-\frac{1}{2}\right\rangle$ with the N_1 particles of type $L_{-1}^{n_1}\left|\frac{1}{2},\frac{1}{2}\right\rangle$ or, in CFT language, the anomalous dimension of the non-BPS double-trace operator $:\partial^{n_1} s_1^{(1)(\frac{1}{2},\frac{1}{2})}\partial^{n_2} s_1^{(1)(\frac{1}{2},-\frac{1}{2})}:$. Since this energy shift originates from the attractive interaction between oppositely charged particles, one expects $\delta\omega_2 < 0$, in agreement with the expression in (14.20), for any $n_1, n_2 \geq 0$. One could wonder why $\delta\omega_2$ does not vanish for the BPS state with $n_1 = n_2$. The point is that, as we emphasised after (14.13), the limit $n_1 \to n_2$ is not smooth and the analysis above only applies when $n_1 \neq n_2$. When $n_1 = n_2$ one has $\tilde{J}^\pm \neq 0$ (see (14.13)), and this requires modifying the gauge-transformation (14.16) to

$$\mathcal{U} = \mathbf{1} + \frac{\alpha_1\tau}{4}\begin{pmatrix} 0 & 0 & 0 & \alpha_2 \\ 0 & 0 & -\alpha_2 & 0 \\ 0 & \alpha_2 & 0 & 2\alpha_1 \\ -\alpha_2 & 0 & -2\alpha_1 & 0 \end{pmatrix}\,, \tag{14.21}$$

which is ξ-independent but τ-dependent and it changes the energy shift $\delta\omega_2$ at order α_1^2 to

$$\delta\omega_2 = 0 \quad \text{for} \quad n_1 = n_2\,, \tag{14.22}$$

as expected for a supersymmetric state.

Both the supergravity and the CFT pictures have a symmetry under the exchange of the states $L_{-1}^{n_1}\left|\frac{1}{2},\frac{1}{2}\right\rangle$ and $L_{-1}^{n_2}\left|\frac{1}{2},-\frac{1}{2}\right\rangle$, which interchanges the labels 1 and 2. This implies that the energy of the particles of type $L_{-1}^{n_1}\left|\frac{1}{2},\frac{1}{2}\right\rangle$ is shifted by

$$\delta\omega_1 = -2\frac{N_2}{N}\left[1-\frac{(n_1-n_2)^2}{(n_1+n_2)(n_1+n_2+1)(n_1+n_2+2)}\right]+O\left(\frac{N_1}{N}\frac{N_2}{N},\left(\frac{N_2}{N}\right)^2\right) \quad \text{for} \quad n_1\neq n_2\,, \tag{14.23}$$

when interacting with the N_2 particles of type $L_{-1}^{n_2}\left|\frac{1}{2},-\frac{1}{2}\right\rangle$. Moreover the total energy of the non-supersymmetric bound state should be given by the (1-2) symmetric expression

$$h+\bar{h} = (n_1+1)\,N_1+(n_2+1)\,N_2-2\frac{N_1N_2}{N}\left[1-\frac{(n_1-n_2)^2}{(n_1+n_2)(n_1+n_2+1)(n_1+n_2+2)}\right], \tag{14.24}$$

up to higher order corrections in N_1/N, N_2/N; the first term, N_1+N_2, is just the energy of the particles in the free theory and second term is the attractive interaction energy, proportional to the numbers of particle N_1 and N_2 and to the 3D Newtons's constant $G_3\sim 1/N$, as expected from the bulk perspective.

One could try to verify the relation (14.24) by extracting the energy $h+\bar{h}$ from the 3D metric ds_3^2, computed up to oder $\alpha_1^2\alpha_2^2$, using the holographic formulas (13.33). However one faces a difficulty: the prediction (14.24) is expressed in terms of the microscopic numbers N_1, N_2, while the holographic computation yields $h+\bar{h}$ as a function of the gravity parameters α_1, α_2. The comparison thus requires the relation between (N_1,N_2) and (α_1,α_2) up to order $\alpha_1^2\alpha_2^2$; keeping into account the (1-2)-exchange symmetry, this relation could have the general form

$$\frac{N_1}{N}=\frac{\alpha_1^2}{4}+c(n_1,n_2)\,\alpha_1^2\,\alpha_2^2+O\big(\alpha_1^4,\,\alpha_1^2\,\alpha_2^4\big) \quad , \quad \frac{N_2}{N}=\frac{\alpha_2^2}{4}+c(n_2,n_1)\,\alpha_1^2\,\alpha_2^2+O\big(\alpha_2^4,\,\alpha_1^4\,\alpha_2^2\big)\,, \tag{14.25}$$

for some function $c(n_1,n_2)$ that should be neither symmetric nor anti-symmetric under the exchange of n_1 and n_2. The only constraint one has on $c(n_1,n_2)$ is the one coming from the momentum $h-\bar{h}$:

$$h-\bar{h}=n_1\,N_1+n_2\,N_2=\frac{n_1\,\alpha_1^2+n_2\,\alpha_2^2}{4}+(n_1\,c(n_1,n_2)+n_2\,c(n_2,n_1))\,\alpha_1^2\alpha_2^2+O\big(\alpha_1^4,\,\alpha_2^4\big)\,, \tag{14.26}$$

which can again be computed from the gravity solution using (13.33). This lone constraint is not sufficient to determine $c(n_1,n_2)$; one can, however, turn things around[2] and assume both (14.26) *and* (14.24), and thus determine $c(n_1,n_2)$. Computationally, this requires obtaining the perturbative solution for general n_1 and n_2 to at least 4th order. We managed to do this only for the alpha class of solutions, due to the simplifications of the

[2] In [39] an independent check of a relation analogous to (14.24) was performed: the non-supersymmetric states studied in that article depended on a single parameter α and thus the constraint coming from the momentum charge was sufficient to completely determine the gravity-CFT map. The non-triviality of that check, gives us further motivation for assuming (14.24) in our context.

special locus. We have:

$$
\begin{aligned}
c(n_1,n_2) = \frac{1}{16}\Bigg[& \frac{4\,n_1^2}{(n_1+n_2)^2} - \frac{5\,n_1(n_1+2)}{n_1+n_2} + \frac{1}{n_1-n_2} - \frac{2\,(2\,n_1+1)^2}{(n_1+n_2+1)^2} + \frac{4(n_1+1)^2}{(n_1+n_2+2)^2} \\
& + \frac{2+2\,n_1\big(5\,n_1(n_1+3)+8\big)}{n_1\,(n_1+n_2+1)} - \frac{(n_1+1)\big(5\,n_1\,(n_1+3)+4\big)}{n_1\,(n_1+n_2+2)}\Bigg] \\
& + \frac{(n_1-n_2)^2\big(\psi^{(0)}(n_1+n_2)-\psi^{(0)}(n_1)\big)}{8\,(n_1+n_2)(n_1+n_2+1)(n_1+n_2+2)},
\end{aligned}
\tag{14.27}
$$

where $\psi^{(m)}(z)$ is the polygamma function of order m. $\psi^{(0)}(z)$ is also known as the digamma function.

The coefficients $c(n_1,n_2)$ do not have an intrinsic physical meaning, they just encode the dictionary between gravity and CFT, but their knowledge is useful because it allows us to push the computation of the energy shifts, $\delta\omega_1$, $\delta\omega_2$, one step further and include the corrections proportional to N_1N_2:

$$
\begin{aligned}
\delta\omega_1 &= -2\frac{N_2}{N}\left[1-\frac{(n_1-n_2)^2}{(n_1+n_2)(n_1+n_2+1)(n_1+n_2+2)}\right] + \frac{N_1N_2}{N^2}\,d(n_1,n_2) \\
\delta\omega_2 &= -2\frac{N_1}{N}\left[1-\frac{(n_1-n_2)^2}{(n_1+n_2)(n_1+n_2+1)(n_1+n_2+2)}\right] + \frac{N_1N_2}{N^2}\,d(n_2,n_1)\,,
\end{aligned}
\tag{14.28}
$$

where we have again implemented the (1-2) symmetry and introduced the unknown coefficients $d(n_1,n_2)$. The procedure to determine these unknowns is conceptually the same we used to arrive at (14.20): one computes the corrections of order $\alpha_1^2\alpha_2^2$ to the gauge fields, and in particular to the constant part of Φ_1, Φ_2 (see eq. (14.18)), which is needed to have normalisable solutions for ν_1 (resp. ν_2) at order $\alpha_1^3\alpha_2^2$ (resp. $\alpha_1^2\alpha_2^3$); one then determines the corrections to the phases, δ_1, δ_2, of the gauge transformation (13.34) in such a way to obtain the CFT-expected values of the angular momenta J^3 and $\tilde{J}^3$ in (14.13) – it is at this step that one needs the map (14.25). The energy shifts, $\delta\omega_1$, $\delta\omega_2$ in (14.28), follow from the rotation parameters δ_1, δ_2. As for $c(n_1,n_2)$, we only have an expression

for $d(n_1,n_2)$ for generic n_1, n_2 for the alpha class of solutions, namely:

$$
\begin{aligned}
d(n_1,n_2) &= -\frac{16\,n_1^4}{(n_1+n_2)^3} + \frac{8\,n_1^3\,(5\,n_1+2)}{(n_1+n_2)^2} + \frac{4\,n_1^2}{n_2\,(n_1^2+3\,n_1+2)^2} - \frac{4\,n_1\,(n_1^2(n_1\,(14\,n_1+31)+26)-3)}{(2\,n_1+1)(n_1+n_2)} \\
&- \frac{4(3\,n_1+1)^2}{(n_1+1)^2(2\,n_1+n_2+1)} + \frac{4\,(3\,n_1+2)^2(n_1(n_1+6)+4)}{(n_1+1)^2(n_1+2)^2(2\,n_1+n_2+2)} - \frac{4\,(2\,n_1+1)^4}{(n_1+n_2+1)^3} - \frac{16\,(n_1+1)^4}{(n_1+n_2+2)^3} \\
&+ \frac{4\,(2\,n_1+1)^2(n_1(n_1+1)(2\,n_1\,(3\,n_1+5)+7)+1)}{n_1\,(n_1+1)(n_1+n_2+1)^2} + \frac{16(n_1+1)^3(n_1\,(n_1\,(n_1+4)+6)+2)}{n_1\,(n_1+2)(n_1+n_2+2)^2} \\
&+ \frac{4\,(n_1+1)(n_1\,(n_1\,(n_1\,(n_1\,(2\,n_1\,(3\,n_1\,(10\,n_1+67)+527)+1373)+914)+244)-68)-72)-16)}{n_1^2(n_1+2)^2(2\,n_1+1)(n_1+n_2+2)} \\
&+ \frac{2\,n_1\,(n_1\,(n_1\,(n_1\,(2\,n_1\,(16\,n_1\,(n_1^2-9)-329)-727)-460)-165)-30)-4}{n_1^2(n_1+1)^2(n_1+n_2+1)} \\
&+ \frac{4\,\gamma\,(n_1-n_2)^2(n_1^3+(3\,n_2+4)\,n_1^2+(n_2\,(3\,n_2+4)+2)\,n_1+n_2(n_2(n_2+4)+2))}{(n_1+n_2)^2(n_1+n_2+1)^2(n_1+n_2+2)^2} \\
&+ \left[\frac{4\,n_1^4}{n_1+n_2} + \frac{(2\,n_1+1)^4}{n_1+n_2+1} + \frac{4\,(n_1+1)^4}{n_1+n_2+2}\right]\left(4\,\psi^{(1)}(n_1) - \frac{2\pi^2}{3}\right) \\
&+ \frac{4\,(n_1-n_2)^2\,\psi^{(0)}(n_1+n_2)}{(n_1+n_2)(n_1+n_2+1)(n_1+n_2+2)}\left(1 - \frac{(n_1-n_2)^2}{(n_1+n_2)(n_1+n_2+1)(n_1+n_2+2)}\right) \\
&+ \frac{4(n_1-n_2)^2(n_1^3+(3\,n_2+4)\,n_1^2+(n_2\,(3\,n_2+4)+2)\,n_1+n_2\,(n_2\,(n_2+4)+2))}{(n_1+n_2)^2(n_1+n_2+1)^2(n_1+n_2+2)^2}\,\psi^{(0)}(n_1) \\
&- \frac{4(n_1-n_2)^2(n_1^3+(3\,n_2+2)\,n_1^2+(n_2\,(3\,n_2+8)+2)\,n_1+n_2\,(n_2\,(n_2+2)+2))}{(n_1+n_2)^2(n_1+n_2+1)^2(n_1+n_2+2)^2}\,\psi^{(0)}(n_2) \\
&+ \sum_{p=1}^{n_1}\left(\frac{(p+n_1-1)^2}{8\,(p-n_1-3)(p-n_1-2)(p-n_1-1)(p+n_2-1)} + \frac{(2\,n_1+p+2)^4}{8\,p^2(p+1)^2(p+2)^2(n_1+n_2+p+2)}\right),
\end{aligned}
\tag{14.29}
$$

where γ is the Euler–Mascheroni constant. Somewhat surprisingly, the result is non-vanishing, implying that the strands of type 2 feel a force proportional to the number of strands of the same type, in the presence of strands of type 1 (and the same with 1 and 2 interchanged, of course); in other words, the strands of type 1 deform the strands of type 2 in such a way that they are no longer mutually BPS with each other. From a CFT point of view, as the term proportional to N_1 in $\delta\omega_2$ is identified with the anomalous dimension of the double-trace operator mentioned after (14.20), the term of oder N_1N_2 computes the anomalous dimension of a triple-trace operator of the form $:\partial^{n_1}\sigma_1^{(\frac{1}{2},\frac{1}{2})}\partial^{n_2}\sigma_1^{(\frac{1}{2},-\frac{1}{2})}\partial^{n_2}\sigma_1^{(\frac{1}{2},-\frac{1}{2})}:$.

14.3.2 Beta class

An analogous analysis can be performed for the non-BPS state (13.29), whose charges readily follow from its CFT representation:

$$
J^3 = N_1+N_2 \quad , \quad J^\pm = 0 \quad , \quad \tilde{J}^3 = N_1-N_2 \quad , \quad \tilde{J}^\pm = 0 \quad , \quad n_p = h-\bar{h} = n_1N_1+n_2N_2\,.
\tag{14.30}
$$

The non-BPS perturbation at first order in the perturbation parameter β_2 is controlled by a single field λ_2 and this greatly simplifies the linear-order analysis: in particular one can study the perturbation at first order in β_2 and all orders in β_1 using a WKB approach that is discussed in Section 12.4. Here we briefly comment on the double-perturbative approach in β_1 and β_2, along the lines of the previous subsection.

At first order in β_2, the fact that all the "non-abelian" gauge fields Φ_i, Ψ_i with $i = 3, 4$ vanish, trivialises the agreement with the constraints $J^{\pm} = \tilde{J}^{\pm} = 0$. A non-trivial input comes from the CFT-gravity matching of J^3, $\tilde{J}^3$. At lowest non-trivial order in β_1, the asymptotic values of the gauge fields are

$$\begin{aligned} \Phi_1^{(\infty)} &= \frac{1}{2} - \frac{\beta_1^2}{4\,(2\,n_1+1)} \quad , \quad \Psi_1^{(\infty)} = \frac{n_1}{2} \quad , \\ \Phi_2^{(\infty)} &= \frac{1}{2} + \frac{(n_1+n_2-1)\,\beta_1^2}{4\,(2\,n_1+1)(n_1+n_2+1)} \quad , \quad \Psi_2^{(\infty)} = \frac{n_2}{2} - \frac{\beta_1^2}{4\,(2\,n_1+1)}\,, \end{aligned} \tag{14.31}$$

where, in particular, the constant part of Φ_2 is determined by the existence of a normalisable solution for λ_2. The angular momenta implied by these gauge fields are consistent with the ones predicted by the CFT only after a gauge rotation (13.34) with

$$\delta\omega_2 = -\frac{n_1+n_2}{(2n_1+1)(n_1+n_2+1)}\beta_1^2 \approx -4\frac{N_1}{N}\frac{n_1+n_2}{n_1+n_2+1}\,; \tag{14.32}$$

note that, due to the form of the 6D ansatz, the phase of the field λ_2 is $2\delta\omega_2$, and thus (14.32) represents half of the interaction energy between a particle of type $L_{-1}^{n_2}|1,-1\rangle$ and N_1 particles of type $L_{-1}^{n_1}|1,1\rangle$. It is a non-trivial consistency check that this interaction energy, when expressed in terms of the microscopic number N_1, is symmetric under exchange of n_1 and n_2, and also that it is always negative, as expected on physical grounds. In CFT terms this energy shift encodes the anomalous dimension of the double-trace operator $:\partial^{n_1}(\sqrt{3}\,s_2^{(2)(1,1)} - \sigma_2^{(1,1)})\partial^{n_2}(\sqrt{3}\,s_2^{(2)(1,-1)} - \sigma_2^{(1,-1)}):$. Following the same steps explained in the previous subsection for the "alpha class" of solutions, one can include the corrections of order $\beta_1^2\beta_2^2$ to the energy shift:

$$\delta\omega_2 = -4\frac{N_1}{N}\frac{n_1+n_2}{n_1+n_2+1} + \frac{N_1N_2}{N^2}\,\tilde{d}(n_1,n_2)\,, \tag{14.33}$$

where the coefficients $\tilde{d}(n_1,n_2)$ capture the triple-trace anomalous dimension. For some values of n_1, n_2, one finds ...

Chapter 15

The numerical approach

All results presented up to now have been derived in a perturbative regime. However, we can also solve the full system of non-linear equations numerically and in this chapter we will outline our schemes for doing so and discuss our findings, comparing them with what we already know from perturbation theory. This Chapter is based on [38, 42].

We construct numerical solutions based on two different methods. The first one was used in [38], to study the solutions of the single-mode truncation. The second method, from [42], produced more reliable results in a special instance of the double-mode truncation.

15.1 First method in the single-mode truncation

In this section we present the method used in [38] to construct non-BPS solutions in the single-mode truncation. These computations provided an important insight into the form of solutions of the systems, and lead to the discovery of the special locus. However, the results of [38] were obtained before we really understood the signification of the special locus, the CFT interpretation, and the resolution of log-divergences in perturbation theory, in [39]. As such, most of the results in [38] were either wrong or no longer relevant. For this reason, we will only present the method behind the computation and abstain from presenting these results in this section. In the next section, we present updated results obtained from a different method.

15.1.1 Solving the boundary value problem

We have to solve for the eleven functions given in the list, $\mathcal{F}_{\text{s.m}}$, given in (9.6). The equations of motion (9.7) give us eleven second-order differential equations with three integrals of motion given in Section 9.1.1. To solve this system we need essentially 22 pieces of data. Much of this data is encompassed by requiring that the solution is smooth at $\xi = 0$ and $\xi = 1$, however, as we saw in Section 12.1 this is not sufficient and so we will also impose the same boundary conditions that we imposed on the linear system: The

gauge fixing of the Maxwell potentials, (12.7)[1], the asymptotics of the metric functions, (12.4) and (12.8), and the requirement that the scalars approach the supersymmetric critical point at infinity, (12.6).

Having done this, the linear system still had four degrees of freedom, ω_1, n_1, and trwo continuous parameters, that were named α_1 and β_1 in the perturbation theory. We will fix $\omega_1 = 3$ and $n_1 = 2$. A canonical choice for the continuous variables would be to fix:

$$\hat{\alpha}_1 \equiv \partial_\xi^2 \nu(0) \quad \text{and} \quad \hat{\beta}_1 \equiv \partial_\xi^4 \lambda_1(0)\,. \tag{15.1}$$

This choice has the advantage of matching exactly with the perturbation theory. However, using conditions on derivatives can lead to loss of numerical precision, and so our numerical analysis is configured somewhat differently: we use α to parametrize the constant value of ν_1 at infinity, $\alpha \equiv \nu_1(1)$. As for β, we use $\beta \equiv -1/2\partial_\xi \lambda_1(1)$.[2]

This characterizes the families of solutions we seek. However, one cannot simply plug these constraints into a numerical algorithm. The primary challenge is that $\xi = 0$ and $\xi = 1$ are regular singular points of all the differential equations, and almost all these equations have singular branches. This means that if one "shoots" from one end of the ξ-interval, $(0, 1)$, then the numerical solution will, through the accumulation of numerical errors, pick up one of the singular branches and diverge hopelessly at the other end of the interval.

Our first method to dealing with this problem is to use a "double-shooting" method. That is, we completely specify initial data near $\xi = 0$ and use standard algorithms (such as Runge-Kutta) to evolve it towards $\xi = 1$. Similarly, we completely specify initial data near $\xi = 1$ and numerically evolve the solution towards $\xi = 0$. We then examine both solutions at some intermediate point, which we take to be $\xi_{mid} \equiv \frac{3}{5}$, and try to match the two solutions by adjusting the initial data at both ends while respecting the boundary conditions we wish to impose.

There is a further issue: the fact that $\xi = 0$ and $\xi = 1$ are singular points of the differential equations means that we cannot simply specify the initial conditions at these points. We have to determine the solution at an infinitesimal displacement away from the end points and then shoot from these displaced initial points. Specifically, we take the initial points for the numerics to be $\xi_0 = 1/100$ and $\xi_1 = 995/1000$. We expand every one of the eleven functions in series about $\xi = 0$ and in series about $\xi = 1$, and impose the boundary data on these series and choose values of α and β. We then use the equations of motion to determine the series as much as as possible. In this way we obtain approximate solutions at ξ_0 and at ξ_1. These approximate solutions still have undetermined coefficients and these become the data that must be varied in order to find a matched solution at the "mid-point," $\xi_{mid} = \frac{3}{5}$. Obviously the match will not be perfect, and we express the mismatch in terms of a *cost function*. The complete numerical algorithm then involves the minimization of this cost function.

[1] Since we are in the single-mode truncation, we can choose $n_2 = 0$, and furthermore $\Phi_2(1) = 0$, this was discussed in the end of Section 12.1

[2] This uses only one derivative, and is thus a direct input for the numerics.

15.1.2 Series expansions at the boundaries

Our purpose here is to use series expansions to generate approximate solutions at $\xi_0 = 1/100$ and $\xi_1 = 995/1000$. Motivated by the expectation that the normalizable modes lead to simple power series solutions, we are going to ignore all logs, both leading, and sub-leading. This is consistent with what we saw from the perturbation theory.

At $\xi = 0$ we take:

$$\begin{aligned}
\nu_1 &= \sum_{n\geq 2} \nu_n^{(0)}\, \xi^n \ , & \lambda_1 &= \beta\, \xi^4 + \sum_{n\geq 5} \lambda_{1,n}^{(0)}\, \xi^n \ , \\
\mu_1 &= \sum_{n\geq 0} \mu_{1,n}^{(0)}\, \xi^n \ , & \mu_2 &= \sum_{n\geq 0} \mu_{2,n}^{(0)}\, \xi^n \ , \\
\Phi_1 &= \sum_{n\geq 0} \phi_{1,n}^{(0)}\, \xi^n \ , & \phi_2 &= \sum_{n\geq 1} \phi_{2,n}^{(0)}\, \xi^n \ , \\
\Psi_1 &= \sum_{n\geq 1} \psi_{1,n}^{(0)}\, \xi^n \ , & \Psi_2 &= \sum_{n\geq 1} \psi_{2,n}^{(0)}\, \xi^n \ , \\
\Omega_0 &= \sum_{n\geq 0} \omega_{0,n}^{(0)}\, \xi^n \ , & \Omega_1 &= \sum_{n\geq 0} \omega_{1,n}^{(0)}\, \xi^n \ , \\
k &= \sum_{n\geq 2} k_n^{(0)}\, \xi^n \ .
\end{aligned} \tag{15.2}$$

and at $\xi = 1$ we take:

$$\begin{aligned}
\nu_1 &= \alpha + \sum_{n\geq 1} \nu_n^{(\infty)}\, (1-\xi^2)^n \ , & \lambda_1 &= \sum_{n\geq 1} \lambda_{1,n}^{(\infty)}\, (1-\xi^2)^n \ , \\
\mu_1 &= \sum_{n\geq 1} \mu_{1,n}^{(\infty)}\, (1-\xi^2)^n \ , & \mu_2 &= \sum_{n\geq 1} \mu_{2,n}^{(\infty)}\, (1-\xi^2)^n \ , \\
\Phi_1 &= \sum_{n\geq 0} \phi_{1,n}^{(\infty)}\, (1-\xi^2)^n \ , & \Phi_2 &= \sum_{n\geq 0} \phi_{2,n}^{(\infty)}\, (1-\xi^2)^n \ , \\
\Psi_1 &= \sum_{n\geq 0} \psi_{1,n}^{(\infty)}\, (1-\xi^2)^n \ , & \Psi_2 &= \sum_{n\geq 0} \psi_{2,n}^{(\infty)}\, (1-\xi^2)^n \ , \\
\Omega_0 &= 1 + \sum_{n\geq 1} \omega_{0,n}^{(\infty)}\, (1-\xi^2)^n \ , & \Omega_1 &= \sum_{n\geq 0} \omega_{1,n}^{(\infty)}\, (1-\xi^2)^n \ , \\
k &= \frac{1}{\omega_{1,0}^{(\infty)}} + \sum_{n\geq 1} k_n^{(\infty)}\, (1-\xi^2)^n \ .
\end{aligned} \tag{15.3}$$

We then substitute these expansions in the equations of motions and solve for the coefficients order by order.

The result is that all but 19 of the coefficients are fixed by the equations of motion. We can furthermore fix two of them using the conserved quantities defined in Section 9.1.1. Indeed, since these quantities are independent of ξ, they can be used to relate some of

the coefficients at infinity with the coefficients at the origin:

$$\phi_{1,0}^{(\infty)} \;=\; \phi_{1,0}^{(0)} \;-\; e^{4\mu_{1,0}^{(0)}}\,\frac{\psi_{2,2}^{(0)}}{\omega_{0,0}^{(0)}} \quad \text{and} \quad \psi_{1,0}^{(\infty)} \;=\; 0\;. \tag{15.4}$$

The constant terms in Φ_2 and Ψ_2 are special in that they do not enter the dynamics, and so, *a priori*, $\phi_{2,0}^{(0)}$, $\psi_{2,0}^{(0)}$, $\phi_{2,0}^{(\infty)}$ and $\psi_{2,0}^{(\infty)}$ can be set to arbitrary values in the shooting process. Indeed we start by setting them to zero. However, the *potential differences* $\phi_{2,0}^{(\infty)}-\phi_{2,0}^{(0)}$ and $\psi_{2,0}^{(\infty)}-\psi_{2,0}^{(0)}$ do have physical meaning, and are determined by the dynamics. What this means is that when we evolve the solutions from their zero initial values at $\xi=0$ and $\xi=1$, the solutions from each end will have a constant offset relative to one another at the mid-point, $\xi_{mid}=\frac{3}{5}$. A smooth solution is then obtained by uniformly shifting either the solution from $\xi=0$, or the solution from $\xi=1$, by the constant offset. We therefore determine the potential differences between $\xi=0$ and $\xi=1$ from these offsets at ξ_{mid}. The important point here is that the data $\phi_{2,0}^{(0)}$, $\psi_{2,0}^{(0)}$, $\phi_{2,0}^{(\infty)}$ and $\psi_{2,0}^{(\infty)}$ is irrelevant to solving the shooting problems, but the potential differences are easily read off from the solutions.

We are thus left with 15 parameters that must be varied in order to find the solution:

$$\begin{aligned}\mathcal{P} \;=\; \Big\{&\nu_2^{(0)}\;,\;\lambda_{1,0}^{(0)}\;,\;\mu_{2,0}^{(0)}\;,\;\psi_{1,2}^{(0)}\;,\;\psi_{2,2}^{(0)}\;,\;k_2^{(0)}\;,\;\omega_{0,0}^{(0)}\;,\;\omega_{1,0}^{(\infty)}\;,\\ &\mu_{0,1}^{(\infty)}\;,\;\mu_{1,1}^{(\infty)}\;,\;\mu_{1,2}^{(\infty)}\;,\;\phi_{2,1}^{(\infty)}\;,\;\psi_{1,1}^{(\infty)}\;,\;k_1^{(\infty)}\;,\;k_2^{(\infty)}\Big\}\;.\end{aligned} \tag{15.5}$$

15.1.3 The minimization procedure

The first step is to choose fixed values of α, β and $\omega_1 = 1, 3$ or 5. We then choose a set of values of the parameters, $\mathcal{P}$, (15.5), and use them to fix the values of all the fields and their derivatives close to both ends of the segment, at $\xi_0 = 1/100$ and $\xi_1 = 995/1000$. This provides initial conditions for the shooting process from each end. Finally, we select a value of ω close to ω_1. We apply the shooting algorithm from both ends, to get two solutions in the bulk. We denote these solutions respectively $\mathcal{S}_0$ and $\mathcal{S}_1$.

We then compare these solutions at a "mid-point" in the bulk, which we take to be $\xi_{mid}=\frac{3}{5}$. The comparison is made by defining a cost function:

$$C(\mathcal{P}) \;=\; \sum_{v\in\mathcal{F}_{\rm s.m}\setminus\{\Phi_2,\Psi_2\}} \big(v_{\mathcal{S}_0}(\xi_{mid})-v_{\mathcal{S}_1}(\xi_{mid})\big)^2 \;+\; \sum_{v\in\mathcal{F}_{\rm s.m}} \big(v'_{\mathcal{S}_0}(\xi_{mid})-v'_{\mathcal{S}_1}(\xi_{mid})\big)^2 \tag{15.6}$$

where $\mathcal{F}_{\rm s.m}=\{\nu_1,\lambda_1,\mu_1,\mu_2,\Phi_1,\Phi_2,\Psi_1,\Psi_2,\Omega_0,\Omega_1,k\}$ is the set of all the fields. Note that, for the reasons explained above, we do not match on the values of Φ_2 and Ψ_2.

The goal is now to compute numerically the values of $\mathcal{P}$ that minimize $C(\mathcal{P})$.

We do this by using numerical algorithms built into *Mathematica,* and, in particular, we use *ParametricNDSolve* for the shooting and *FindMinimum* to compute the minimum of the cost function. Rather than simply treat the latter as a black box, we summarize what is going on inside the algorithm and how we adapted some of the options to make the solution technique more effective.

We use the Levenberg-Marquardt algorithm (a refinement of the Gauss-Newton algorithm), implemented in *FindMinimum*. This algorithm makes successively more accurate approximations of the minimum by using *quadratic* approximations to the cost function. This method is particularly well-adapted for minimization problems for which the cost function is written as a sum of squares, $C = \sum r_i^2$. The schematic process is then:

Step 1 Choose a first estimate of the solution $\mathcal{P}$. These values are used as a seed for the algorithm. Such seeds can be based on other known solutions, or starting from the exactly known superstratum result. The seed must be close enough to the solution, or at least not so far as to make the results from the shooting diverge before reaching ξ_{mid}.

Step 2 Use this data and *ParametricNDSolve* to compute a solution and calculate the value of the cost function, $C(\mathcal{P})$. Next compute numerically the Jacobian J of the functions, r_i, at this point by computing the difference between the original value of the r_i, and the new values obtained using small perturbations of the parameters.

Step 3 Ideally a quadratic approximation would involve computing the Hessian of the cost function, but this is numerically very demanding and compounds numerical errors. Instead, the Gauss-Newton algorithm uses the Jacobian to construct an approximation to the Hessian and makes a quadratic approximation based on this. The displacements of the parameters, $\Delta\mathcal{P}$, that move the solution towards the minimum are thus estimated by computing the minimum of the quadratic approximation:

$$\sum_{ij} \left[r_i(\mathcal{P})\, J_{ji}\, \Delta\mathcal{P}_j + \frac{1}{2} \Delta\mathcal{P}_i (JJ^\top)_{ij} \Delta\mathcal{P}_j \right] . \tag{15.7}$$

Step 4 The danger, as ever, with such an algorithm is that it might overshoot, or oscillate around, the minimum. So *FindMinimum* actually treats $\Delta\mathcal{P}$ as a displacement in the parameters space and then finds a better estimate of the minimum of the cost function in the one-dimensional space along this direction. This is the primary function of the "step control" within *FindMinimum*. The result is a new estimate of the parameters of the solution given by $\mathcal{P}+\lambda\Delta\mathcal{P}$, where λ is a step in the minimizing direction deemed good enough by *FindMinimum*.

Step 5 Then *FindMinimum* repeats steps 2 to 4 with the new estimates, and does so until it achieves a good level of convergence[3]

15.2 Second method

We now present a different method for solving the equations of motion numerically, that we use in the double-mode truncation.

[3]It can also generate errors where it has failed to converge adequately and then one must adjust the values of $\mathcal{P}$ and restart the search.

That will only be done for the $\mathbb{Z}_2$ symmetric beta class of solutions, that is - we work with $n_1 = n_2 = n$ and $\beta_1 = \beta_2 = \beta$. The states in this restricted case are still non-BPS, they were computed perturbatively in Section 12.3.4. The reason we make this choice is not because we cannot perform the numerics in the other cases, but due to the fact that this is the only scenario in which we can exactly map all CFT parameters to bulk quantities using the holographic dictionary. To elaborate, in the general case, when $n_1 \neq n_2$, for either the alpha or beta class of solutions, we have different numbers of constituents of the given species in the two sectors, $N_1 \neq N_2$. Perturbatively, these are related to the gravity amplitudes that drive the bulk solution via (13.28) and (13.30). Unfortunately, we cannot obtain exact expressions for them as that requires the precise form of $h + \bar{h}$ in terms of the full energy shifts $\delta\,\omega_{1,2}$, thus making it impossible to read off $N_{1,2}$ from the bulk, numerical solution.

In the $\mathbb{Z}_2$ symmetric case, $N_1 = N_2$, so we only need a single relation, which we get from $h - \bar{h} = n_p$. The equations that we will solve are given in Appendix D, namely (D.1). These are seven second-order, ordinary differential equations. The reduced number comes about because $n_1 = n_2 = n$ and $\beta_1 = \beta_2 = \beta$ imply that $\mu_1 = \mu_2$, $\lambda_1 = \lambda_2$, $\Phi_1 = \Phi_2$ and $\Psi_1 = \Psi_2$, as easily seen in perturbation theory. We should note that a linear combination of the Φ_1, Ψ_1 and κ EoMs leads to a first-order, differential equation, given in (D.2). This is a genuine EoM for one of the fields, but we did not use it in the numerical procedure, as it seemed to have slightly worse convergence properties.

Our system of equations also contains three first-order constraints. The ones coming from the Maxwell sector are automatically satisfied. Only the constraint from Einstein equations, $E_{R_{\tau\psi}}$, remains and it is a constant of motion by the EoMs, given in Appendix D for this case. It is used to monitor the convergence of our solutions, as seen in Figure 15.1, where the maximum value of the constraint over the whole space is plotted as a function of the number of grid points, N_ξ, for a highly non-BPS solution. All results presented in this work have $\max|E_{R_{\tau\psi}}(\xi)| \leq 10^{-50}$.

We solve for $\{\lambda_1,\, \mu_1,\, \Phi_1,\, \Psi_1,\, \Omega_0,\, \Omega_1,\, \kappa\}$ as functions of the radial variable $\xi \in [0, 1]$, where $\xi = 0$ is the origin of space, $\xi = 1$ is the AdS boundary, and κ is defined via $k = \xi\,\kappa$. The numerical integration is carried out by using spectral collocation methods on a Chebyshev-Gauss-Lobatto grid and implementing a standard Newton-Raphson iteration (see [89] for a review of such methods applied to gravity) with increased precision (50 digits). We need to impose appropriate boundary conditions to ensure a well-posed problem. These were discussed in detail in Section 12.1, but we will briefly outline them for completeness.

At the origin, $\xi = 0$, regularity enforces Neumann boundary conditions on almost all fields, except[4] for Ψ_1 and κ:

$$\begin{aligned} \partial_\xi\, X(\xi)|_{\xi=0} = 0, \quad \text{for}\, X \in \{\lambda_1,\, \mu_1,\, \Phi_1,\, \Omega_0,\, \Omega_1\}, \\ \kappa(\xi = 0) = 0, \quad \Psi_1(\xi = 0) = \frac{n}{2}. \end{aligned} \tag{15.8}$$

[4]Remember that $k(\xi = 0) \sim \xi^2$ and we have defined $k(\xi) = \xi\,\kappa(\xi)$.

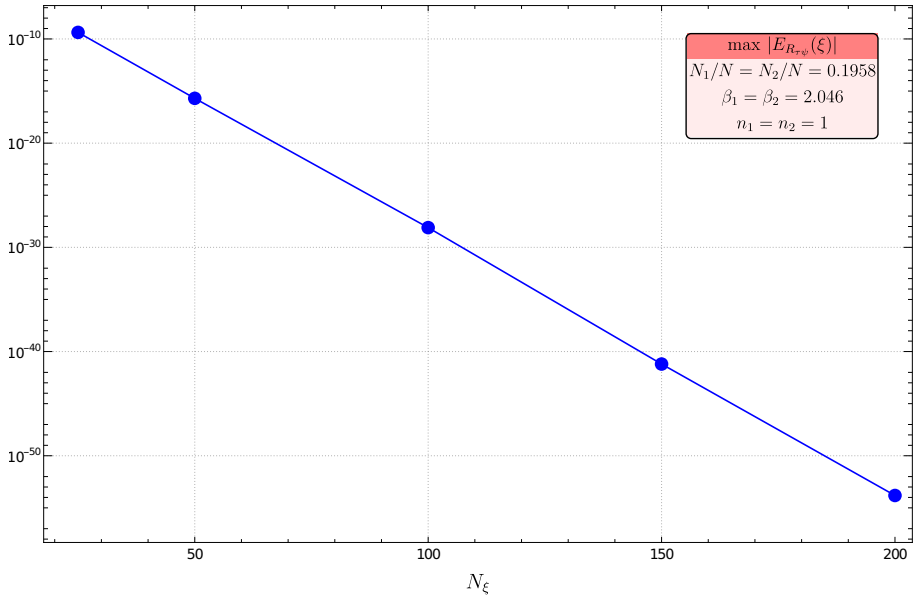

Figure 15.1: Maximum of the absolute value of the Einstein constraint, $E_{R_{\tau\psi}}$, over the whole integration domain for a highly non-BPS state as a function of the number of points used in the numerics, N_ξ. $\omega_1 = \omega_2 = 1$.

In fact, it can be shown that the first $2\,n - 1$ derivatives of λ_1 vanish at the origin, in agreement with expectations from perturbation theory.

At the AdS boundary, $\xi = 1$, we impose a conformally Minkowski metric, which requires

$$\Omega_0(\xi = 1) = 1, \quad \Omega_1(\xi = 1) = \frac{1}{\kappa(\xi = 1)}, \quad \partial_\xi \kappa|_{\xi=1} = 1. \tag{15.9}$$

The scalars are fixed by demanding that, in addition, we approach the supersymmetric vacuum at the boundary, so that:

$$\lambda_1(\xi = 1) = 0, \quad \mu_1(\xi = 1) = 0. \tag{15.10}$$

Our solutions is specified by 2 parameters, n and β. The former is set at the origin, (15.8). In the perturbation theory, we identify $\beta_{1,2}$ with the $2\,n_{1,2}$-th derivatives of $\lambda_{1,2}$. However, enforcing a boundary condition at the origin with so many derivatives is very hard to implement numerically, especially if we want to access values of $n_1 = n_2 = n > 1$. Therefore, for $\beta_1 = \beta_2 = \beta$, we have found that numerically it is easiest to dial it using the value of Φ_1 at infinity. Thus, we set

$$\Phi_1(\xi = 1) = \tilde{\phi}_1, \tag{15.11}$$

and use $\tilde{\phi}_1$ to explore the moduli space of solutions for fixed n. Nevertheless, we need the value of β to compare our numerical results with the perturbative predictions. To extract it precisely we resorted to obtaining our solutions with extended precision of 50 digits, so that we can trust the derivatives.

We do not need to provide a boundary condition for Ψ_1 at infinity since the existence of (D.2) implies that we have in fact 6 second-order differential equations and 1 first-order equation, and, even though, we do not integrate (D.2) explicitly, it can be used to argue that a single boundary condition on Ψ_1 at the origin is sufficient, as numerically we are solving for smooth functions.

15.2.1 Holographic extraction

Here we discuss the procedure for extracting the holographic quantities from the numerical solutions. First we need to expand the EoMs, (D.1), in series about the conformal boundary, $\xi = 1$, using

$$X = \sum_{k=0}^{\infty} (1-\xi^2)^k \, q_X^{(k)}, \quad \text{for } X \in \{\lambda_1,\, \mu_1,\, \Phi_1,\, \Psi_1,\, \Omega_0,\, \Omega_1,\, \kappa\}. \tag{15.12}$$

Similarly to what happened in Section 15.1.2, some of the coefficients in the expansion above get fixed by the EoMs, (D.1), together with the boundary conditions. The ones that remain unspecified are:

$$q_{\lambda_1}^{(1)},\, q_{\mu_1}^{(2)},\, q_{\Phi_1}^{(1)},\, q_{\Psi_1}^{(0)},\, q_{\Omega_0}^{(2)},\, q_{\kappa}^{(0)}. \tag{15.13}$$

Then, we write the metric in Fefferman-Graham form for an asymptotically, locally AdS space, as in (13.31):

$$\begin{aligned} ds^2 &= \frac{R_{AdS}^2}{z^2}\Big[dz^2 + g_{ij}(x,z)\, dx^i\, dx^j\Big], \\ g(x,z) &= g_{(0)} + z^2\, g_{(2)} + \cdots + z^d\, g_{(d)} + h_{(d)}\, z^d\, \log z^2 + \mathcal{O}\big(z^{d+1}\big), \end{aligned} \tag{15.14}$$

where d is the number of boundary dimensions ($d = 2$ here) and the radial coordinate z is such that the conformal boundary is located at $z = 0$. Only even powers of z appear in the expansion up to order z^{d-1} and the logarithmic term is only present in odd bulk dimensions – it is linked to the conformal anomaly of the boundary CFT. Moreover, $g_{(0)}$ specifies the conformal class of the boundary metric, which we pick as flat Minkowski, implying that the conformal anomaly vanishes and $h_{(d)} = 0$ here as well [83].

To obtain (15.14) we change coordinates asymptotically using

$$\xi = \sum_{k=0}^{\infty} a_k\, z^k, \tag{15.15}$$

where the coefficients a_k are determined order by order in z by taking our metric ansatz, (7.18), plugging in the function expansions (15.12), applying the above coordinate transformation and matching with (15.14). For our purposes we only need:

$$a_0 = 1, \quad a_1 = 0, \quad a_2 = -\frac{1}{2\, q_\kappa^{(0)}}, \quad a_3 = 0, \quad a_4 = \frac{1}{8\,\big(q_\kappa^{(0)}\big)^2}. \tag{15.16}$$

Finally, we use (14.30), which for the $\mathbb{Z}_2$ symmetric case reduce to[5] $J^3 = 2\,N_1$, $\tilde{J}^3 = 0$ (which is automatically satisfied since $\Phi_1 = \Phi_2$) and $n_p = h - \bar{h} = 4\,n\,N_1$ to determine $N_1/N = N_2/N$ and $\delta\omega_1 = \delta\omega_2$ as functions of the gravity parameters. As desired we have equal number of equations and unknowns. The result is:

$$\begin{aligned} \delta\omega_1 = \delta\omega_2 =& -1 + 2\big(\tilde{\phi}_1 + 2\,q_{\Psi_1^{(0)}}\big) + K, \\ N_1/N = N_2/N =& \frac{n}{2} + \frac{K}{4}, \end{aligned} \tag{15.17}$$

where

$$\begin{aligned} K = -\frac{1}{\sqrt{3}\left(q_\kappa^{(0)}\right)^2}\Bigg[& -\left(q_\kappa^{(0)}\right)^2\left(3 + 8\left(q_\kappa^{(0)}\right)^4\Big(\left(q_{\lambda_1}^{(1)}\right)^2\tilde{\phi}_1^{\,2} + \left(q_{\Phi_1}^{(1)}\right)^2\Big)\right) \\ & - \left(q_\kappa^{(0)}\right)^4\Big(3 + 12\,n^2 - 4\left(q_{\lambda_1}^{(1)}\right)^2 - 18\,q_{\Omega_0}^{(2)}\Big)\Bigg]^{\frac{1}{2}}. \end{aligned} \tag{15.18}$$

The expression for the total energy in terms of bulk quantities can be determined from (13.33) as

$$\frac{h + \bar{h}}{N} = \frac{1}{2}\left(1 - \frac{1}{\left(q_\kappa^{(0)}\right)^2}\right) + n\left(2\,n + K\right). \tag{15.19}$$

15.2.2 Results

For the beta class of solutions, (12.61) implies that half-integer values of $n_{1,2}$ are also allowed. We have obtained numerical results for six different values: $n_1 = n_2 = n \in \{\frac{1}{2}, 1, \frac{3}{2}, 2, \frac{5}{2}, 3\}$ with $\omega_1 = \omega_2 = 1$. All of them have qualitatively the same behaviour, except for $n = \frac{1}{2}$, which will be discussed further below.

The space of geometries is explored by using the perturbative solutions as seeds to the Newton-Raphson method. We start from $\tilde{\phi}_1 \sim \omega_1/2$, equivalent[6] to $\beta \ll 1$, and decrease its value, equivalent to increasing β. In practice, we will present our results as a function of the fraction of single-particle constituents, $N_1/N = N_2/N$, hence we start with its plot as a function of $\beta_1 = \beta_2 = \beta$. The latter is read off from the gravity solutions as

$$\beta = \frac{1}{n!}\,\partial_\xi^{2\,n}\lambda_1\big|_{\xi=0}\,, \tag{15.20}$$

whereas the former is given by (15.17). When extracting β, we make sure that the value we get is stable to 10^{-50} when varying the grid size. The results are shown in Figure 15.2. The right graph exhibits the agreement of our numerics (solid markers) with the perturbative expression (dashed curves and hollow markers, which are added to make the comparison easier), given as P_n in the plot, and which can be obtained from (13.30) by expanding for

[5] $J^\pm$ and $\tilde{J}^\pm$ don't change.

[6] From perturbation theory we know that for the $\mathbb{Z}_2$ symmetric beta class we have: $\Phi_1(\xi = 1) = \omega_1/2 - (n\,\beta^2)/(1 + 2\,n)^2 + \mathcal{O}(\beta^4)$.

$\beta_1 = \beta_2 = \beta \ll 1$ and setting $n_1 = n_2 = n$. As β increases the exact and perturbative results deviate significantly and we have omitted the latter for clarity from the left figure, which shows all our numerical data. For $n \geq 1$ the points reach very close to the CTC bound and the behaviour far away from the perturbative regime appears linear in β. The only exception is $n = \frac{1}{2}$, where the curve turns around and $N_1/N = N_2/N$ stops being a single-valued function of β.

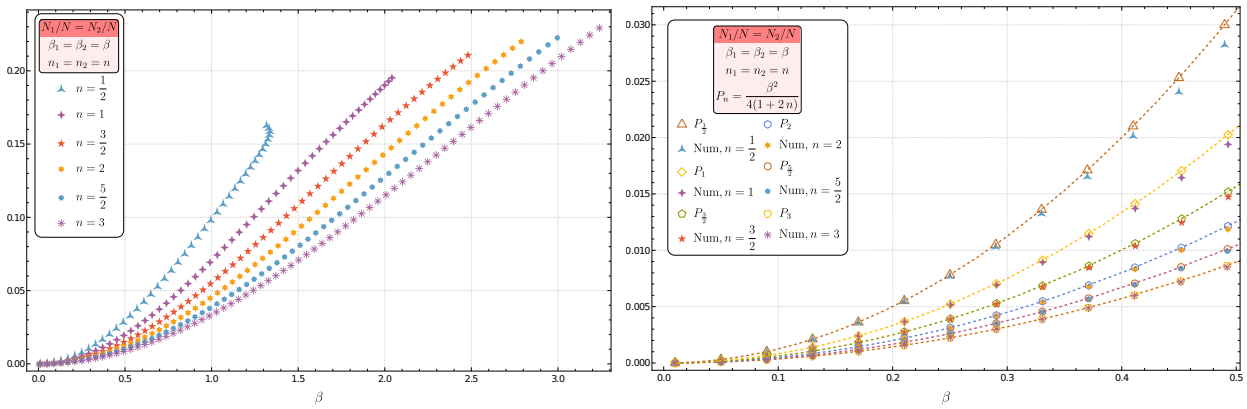

Figure 15.2: N_1/N as a function of β for six different values of n. $\omega_1 = \omega_2 = 1$. On the right we zoom in for small β and show a comparison with the perturbative result, P_n, given by dashed curves and additional hollow markers to facilitate the comparison. Both graphs use solid markers for the numerical results.

The theoretical limit to decreasing $\tilde{\phi}_1$ is the point at which CTCs become present in the spacetime. We monitor the value of Ω_1 at $\xi = 1$, which approaches zero, where the bound is attained and changes sign once CTC are present. One can then see the development of a finite-length, BTZ-like throat, as depicted in Figure 15.3. As n increases, larger values of β, and thus N_1/N, become attainable before hitting the bound. Our observations suggest that it comes at a lower value of β or N_1/N in the non-BPS case than in the BPS one.

The energy shift of our solutions is probably the most interesting when it comes to analysing them. A non-zero value indicates that the state is indeed non-BPS. Figure 15.4 demonstrates that all our solutions break supersymmetry. $\delta\omega_1 = \delta\omega_2 = 0$ is possible for $\beta = 0$, when the solutions is just the AdS_3 vacuum, or for $n = 0$ (and non-zero β or N_1/N), which results in a non-trivial geometry that we have constructed, but is not presented here, and it does have vanishing interaction energy. The x-axis is given in terms of the momentum charge. For $n \geq 1$ the curves approach $\delta\omega_1 = \delta\omega_2 = -1$ as n_p grows and our numerics approach the CTC bound. It is interesting that this can happen, as $\delta\omega_i$ is the correction to the phase of the $SO(4)$ transformation that puts us in the correct gauge to identify the CFT states. The coefficient of τ that gets corrected by the energy shifts is the twist of the L_{-1}^{2n} operator that acts on the state $|1, \pm 1\rangle$. $\delta\omega_i \to -1$ would then correspond to the vanishing of that twist.

As before, $n = 1/2$ displays a qualitatively different behaviour in that it does not approach the limit of -1. The numerics for this case are the hardest, as the gradients in

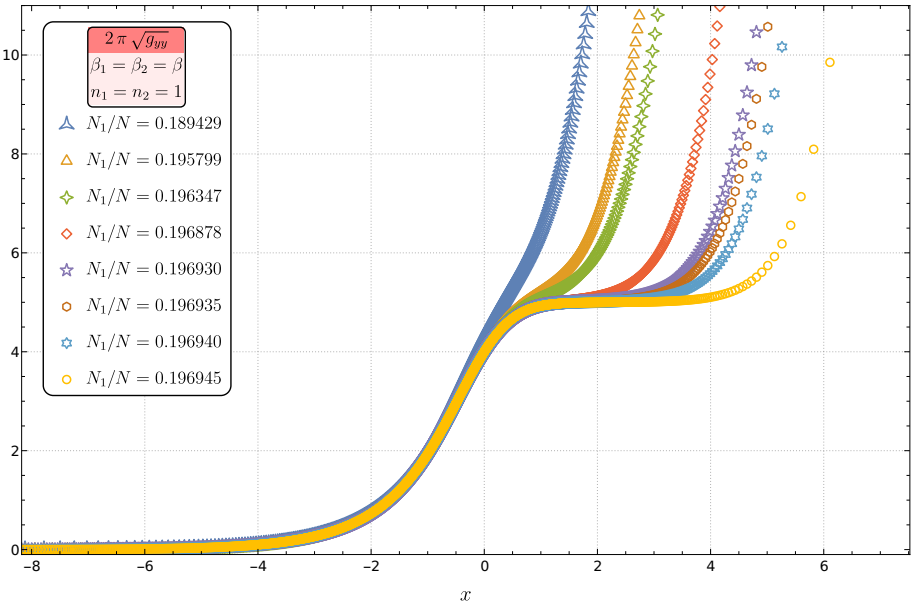

Figure 15.3: The radius of the $y-$circle $2\,\pi\,\sqrt{g_{yy}}$ for $n = 1$ and different values of N_1/N, approaching the CTC bound. The x-axis uses a rescaled radial coordinate, $\xi = e^x/\sqrt{e^{2\,x}+1}$. $\omega_1 = \omega_2 = 1$.

the functions are the steepest, but we do not believe it is possible to reach -1.

Figure 15.5 shows the agreement of the numerical data with the predictions from perturbation theory, (14.32) with $n_1 = n_2 = n$, for small values of N_1/N - i.e. small β. We have omitted the perturbative results from the main plot, Figure 15.4, for clarity.

Finally, we also show a plot of the total energy, (15.19), of our states, Figure 15.6. The right plot again depicts the excellent agreement with our perturbative results for small values of N_1/N (β), whereas on the left we have all the numerical data.

15.2.3 Perturbation theory comparison with numerical results

In this work, we have relied heavily on perturbation theory to explore the space of solutions in our system and analyse their properties. To this end, it is instructive to also compare the perturbative results with solutions to the full non-linear system of equations.

It turns out that for small values of β the perturbative expansion to third order gives remarkably good approximation to the full solution. This can be seen in Fig. 15.7, where we show a comparison for all the relevant fields in our case, with $\beta \sim \frac{1}{4}$, $n_1 = n_2 = 1$ and $\omega_1 = \omega_2 = 1$. Note that the plots show κ instead of k, defined via $k = \xi\,\kappa$.

For $n = 1$, the maximum value of β is ~ 2.05 (before the appearance of closed timelike curves (CTCs) in the spacetime). Given that we are using only third order perturbation theory, the accuracy at $\beta \sim 1/4$ is surprisingly good, except for μ_1. The latter receives its first non-trivial correction at fourth order[7] in β, hence the visible disagreement on our

[7]We have checked this for explicit values of n_1 and n_2 in the non-$\mathbb{Z}_2$ symmetric case and have no reasons to believe that the behaviour here will be different, as the beta class is continuous in taking the

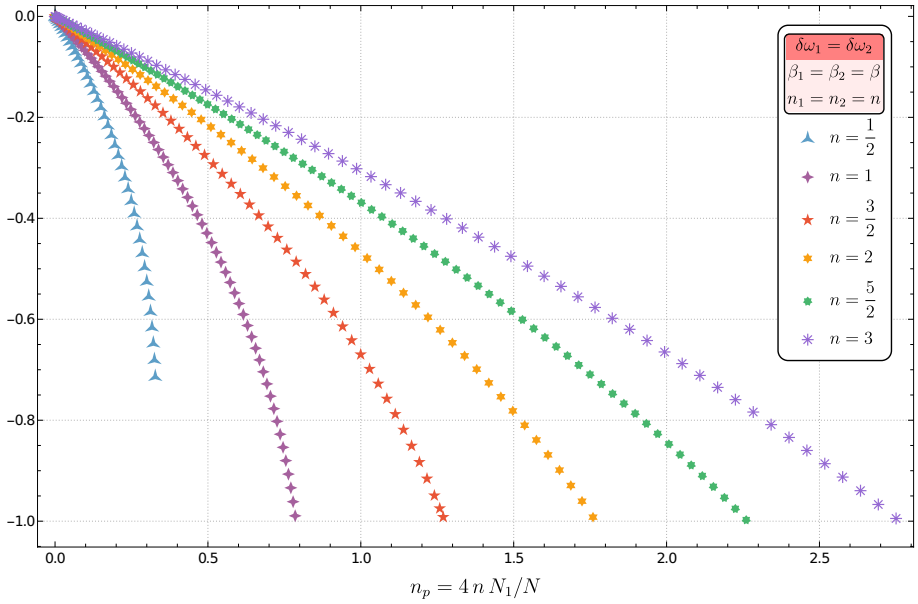

Figure 15.4: The energy shift $\delta\omega_1 = \delta\omega_2$ as a function of the momentum charge n_p for six different values of n. $\omega_1 = \omega_2 = 1$. For $n \geq 1$ the curves approach the limiting value -1, as we get close to the CTC bound. $n = 1/2$ is an exception and our numerics suggest -1 will not be reached.

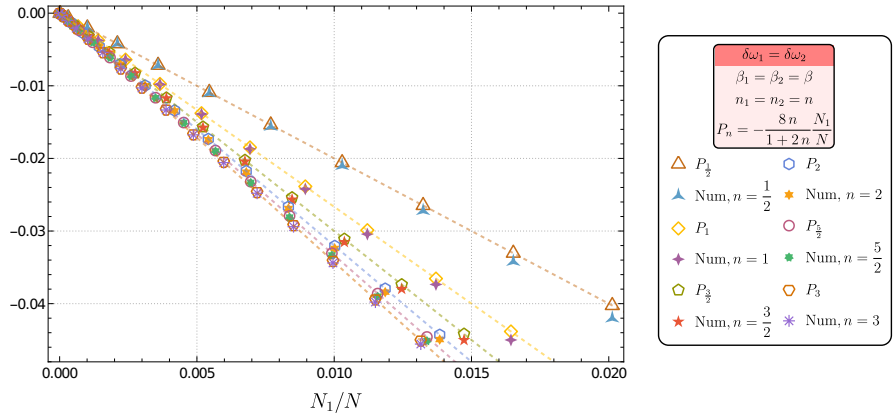

Figure 15.5: The energy shift $\delta\omega_1 = \delta\omega_2$ in comparison with our perturbative results, P_n, given by dashed curves and additional hollow markers to facilitate the comparison, for six different values of n. $\omega_1 = \omega_2 = 1$. Both graphs use solid markers for the numerical results. P_n is given in (14.32) with $n_1 = n_2 = n$.

plots. Moreover, at third order Ω_1 is just a constant, nevertheless, the horizontal scale shows that the fully backreacted solution is very close to that value.

Figures 15.8 and 15.9 are analogues to Fig. 15.7, but for larger values of β, namely at $\beta \sim 1$ and close to the maximum $\beta \sim 2.05$, respectively. They are meant to illustrate how the increasing amount of non-BPSness deforms the solution, all the way to the CTC bound. The fields that change the most are Φ_1, Ω_1 and κ. In particular, κ increases

$n_1 = n_2$ limit.

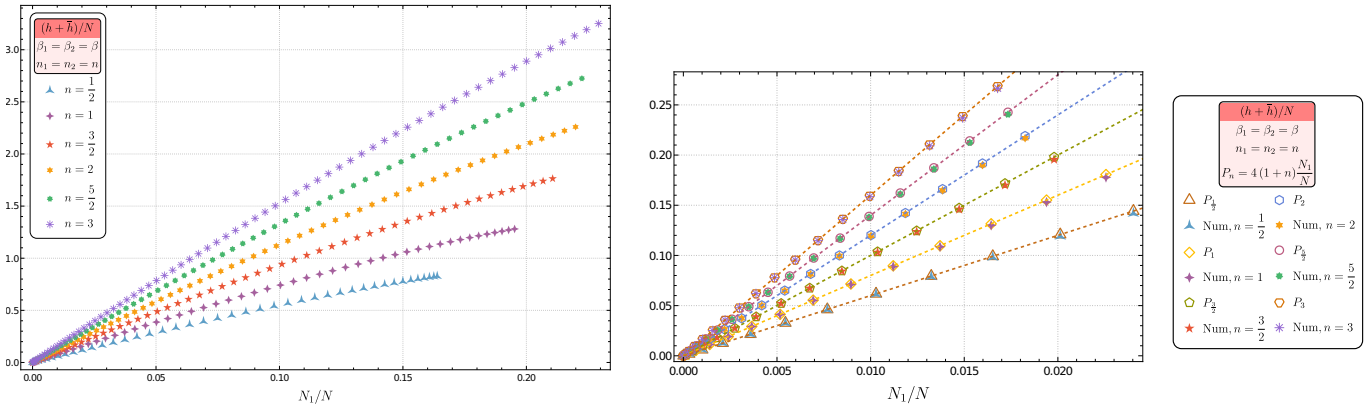

Figure 15.6: The total energy $(h + \bar{h})/N$ as a function of N_1/N for six different values of n. $\omega_1 = \omega_2 = 1$. On the right we zoom in for small N_1/N and show a comparison with the perturbative result, P_n, given by dashed curves and additional hollow markers to facilitate the comparison. Both graphs use solid markers for the numerical results.

massively in value at infinity, as one gets closer to the maximum value of β, which together with (12.1) and (12.5) implies that Ω_1 decreases quickly towards 0 as $\xi \to 1$.

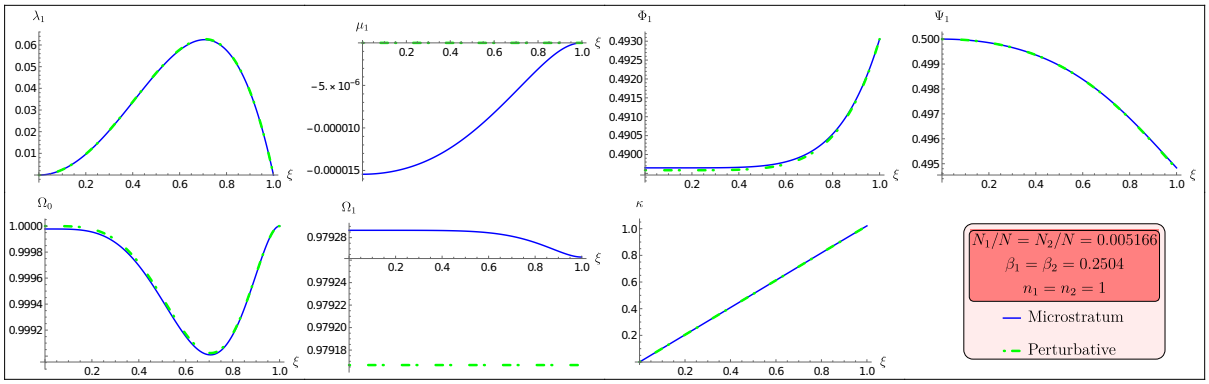

Figure 15.7: The non-zero fields in the $\mathbb{Z}_2$ symmetric beta class of solutions, where $\beta_1 = \beta_2$, $n_1 = n_2$ and $\lambda_1 = \lambda_2$, $\mu_1 = \mu_2$, $\Phi_1 = \Phi_2$, $\Psi_1 = \Psi_2$. We compare the full numerical results to the perturbative solution. $\omega_1 = \omega_2 = 1$.

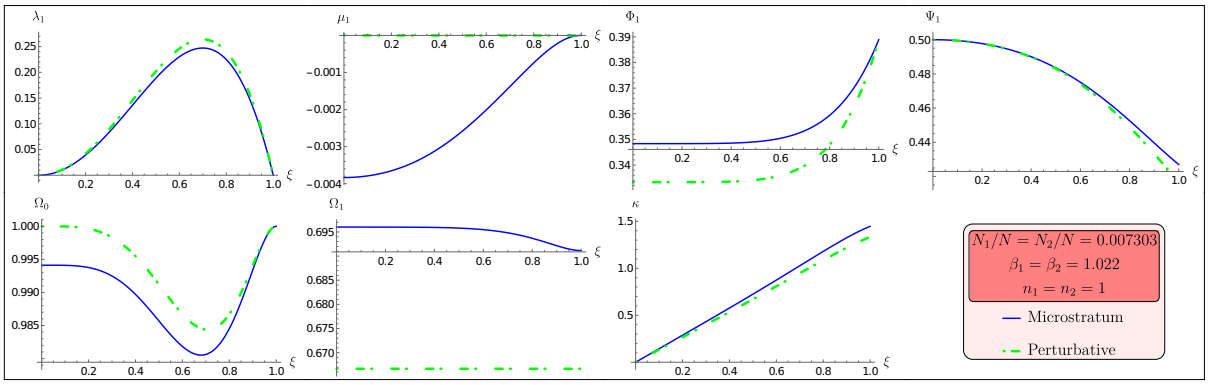

Figure 15.8: The non-zero fields in the $\mathbb{Z}_2$ symmetric beta class of solutions, where $\beta_1 = \beta_2$, $n_1 = n_2$ and $\lambda_1 = \lambda_2$, $\mu_1 = \mu_2$, $\Phi_1 = \Phi_2$, $\Psi_1 = \Psi_2$. We compare the full numerical results to the perturbative solution. $\omega_1 = \omega_2 = 1$.

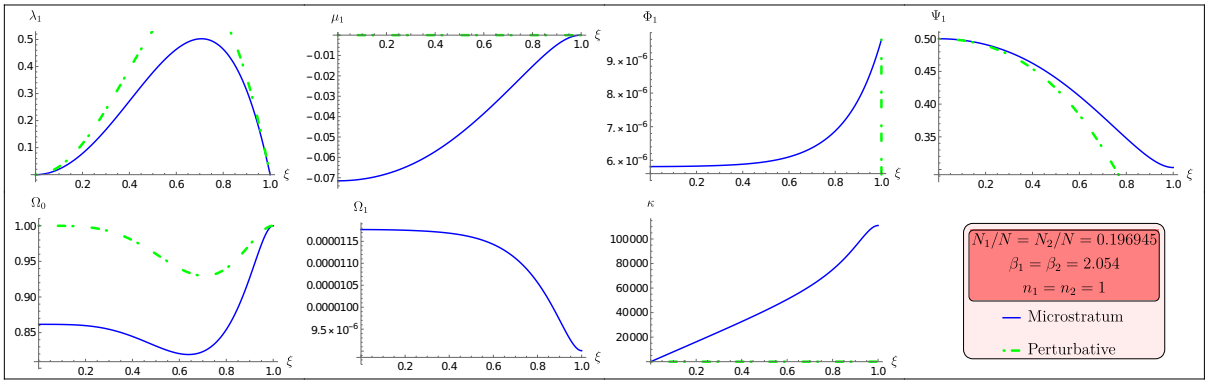

Figure 15.9: The non-zero fields in the $\mathbb{Z}_2$ symmetric beta class of solutions, where $\beta_1 = \beta_2$, $n_1 = n_2$ and $\lambda_1 = \lambda_2$, $\mu_1 = \mu_2$, $\Phi_1 = \Phi_2$, $\Psi_1 = \Psi_2$. We compare the full numerical results to the perturbative solution. $\omega_1 = \omega_2 = 1$.

Chapter 16

Final Comments

We have constructed, both in perturbation theory and numerically, families of non-extremal microstrata, along with their CFT dictionaries. These states are non-BPS analogues of the superstrata and share with them many qualitative features but they also display new dynamical properties. There is excellent accord between the numerical and perturbative results and this gives us a high level of confidence in the accuracy of our solutions.

The solutions separates into two families, that we named alpha-class and beta-class. In the alpha-class, we have pointed out that if one turns on the $\nu_{1,2}$-perturbation at linear order, one has to fine-tune the coefficient of the other independent ($\lambda_{1,2}$) perturbations at the higher orders to ensure regularity and not to spoil the asymptotic behaviour. We called this condition the "special locus", and we provided an interpretation in the CFT of this condition. The solutions in the beta-class are simpler, as many fields vanish, and this allowed us to analyze them further. Using WKB techniques, we add a non-BPS excitation to a very deep BPS microstate, we have compared them to the perturbative results around the vacuum, and computed the normal modes of these solutions in the regime of large redshift.

Using holography and the tools of the CFT, we determined the dependence of microstratum frequencies, and energies, on their amplitudes. In retrospect, this dependence should not be very surprising. The normal modes of oscillation will naturally depend on the shape of the geometry and particularly upon the depth, or red-shift, between the cap and the top of the AdS throat. Since we know that these geometric features depend on the amplitudes of the microstratum, it must follow that these amplitudes lead to non-linear shifts in the frequencies of the normal modes. It is, however, gratifying to see this explicitly and it also suggests how microstate-geometry fluctuations will lead to the development of a chaotic spectrum. The non-linear dynamics will re-shuffle the spectrum, and may well result in the eigenvalue repulsion that is characteristic of non-integrable field theories.

We also have examined the BPS equations for the three-dimensional supergravity theory. We have used this BPS system to significantly extend the known families of superstrata to obtain "generalized superstrata," that include a family of elliptical deformations of the supertube that underlies the superstratum. The resulting geometries have reduced

symmetry (compared to standard superstrata) and it would have been very challenging to construct them directly in six dimensions. We have determined the CFT dual of these new BPS geometries and made some precision holographic test that confirmed the identification. Of note is the existence of a special locus of solutions, whose duals in the CFT take a very simple and natural form, as an OPE product of light states. These states in the CFT are simpler than the standard superstrata, which rely on the particularities of the orbifold point for their definition. They enjoy the same properties as the non-BPS special locus, in particular the $SO(3)$ invariance. We have also a family of "pure-NS" superstrata ; these solutions can be dualized in the NS5-F1 frame to a solution with no Ramond excitations, possibly enabling a worldsheet description.

There are a multitude of possible future directions arising from our results. First, we constructed our microstrata by making reductions, consistent truncations, implementing a Q-ball Ansatz, and focussing on single-mode or double-mode solutions. There are obvious directions for generelizations of our results, the foremost is certainly trying to generate solutions with more modes, to observe the cascade of frequencies and a possibly chaotic spectrum. Moving in a more ambitious direction, one can try to find solutions that depend on more that one variable.

It may be possible to distill the core elements of the "Q-ball" trick we found in three dimensions and implement it directly in six dimensions. Doing this might enable one to get beyond the limitations imposed by the consistent truncation. One of the issues with this ansatz is that it restricts generic (k, m, n) superstrata to $k = 1$, and these have rather weak fall-off at infinity. Making the Q-ball trick work for higher values of k would be most interesting.

Another important aspect is the question of whether one can couple microstrata to asymptotically-flat space. All the solutions have been built in asymptotically AdS space, which allowed us to construct time-independent solutions, for which the geometry is in equilibrium with its radiation. But a genuinely non-BPS solution in flat space would radiate, and depend explicitly on time. Constructing such a solution would provide an analogue of Hawking radiation for microstrata, and one would be able to check explicitly that (at least some) microstates can decay without violating unitarity.

Part III

Brane fractionation and microstate counting

Chapter 17

The (amazing) Super-Maze

This Chapter reviews the work of [43].

String Theory is famous for its ability to count the degrees of freedom that give rise to the entropy of supersymmetric black holes, but this counting is always done in a regime of parameters where the interactions are weak and the classical black-hole solution does not exist [10, 90, 91]. This leaves open the question of how these microscopic degrees of freedom look like in the regime of parameters where the classical black hole solution exists. This question is hard to answer, because it is difficult to track these degrees as one moves to this regime of parameters, and also because the black-hole microscopic degrees of freedom look different in different duality frames.[1]

Historically, the quest for understanding the black hole degrees of freedom has been pursued from the opposite direction: people have first constructed solutions with black-hole charges that do not have a horizon and that exist in the same regime of parameters as the classical black hole solution [18,20–30,37,38,40,50,68,92–106]. By construction, these solutions (known as microstate geometries) describe *some* of the black-hole microstates. The second step was to use holographic tools to relate some of them to the corresponding states in the CFT that counts the black-hole entropy [31–36,39,53,54,79]. This endeavor has been very successful, and has produced some of the finest checks of the power of holography to date. However, despite the tremendous amount of geometries constructed[2], it has not been possible to construct geometries dual to the states that account for the total black-hole entropy.

Here we take the opposite approach: We start from a weakly-coupled system whose degrees of freedom count the entropy of the black hole, and attempt to track these degrees of freedom to the regime of parameters where the classical black-hole solution exists. Our starting point is the F1-NS5-P black hole in Type IIA string theory, whose entropy comes from the fractionation of each of the N_1 fundamental strings into N_5 *little strings* living in the worldvolume of the NS5-branes [109,110]. The resulting $N_1 \times N_5$ little strings wrap

[1] For example, the entropy of the D1-D5-P black hole for example comes from 1-5 strings carrying fractional momentum quanta, while the entropy of the U-dual IIA F1-NS5-P black hole comes from fractionated little strings carrying integer momenta.

[2] Of order $e^{\sqrt{N_1 N_5 N_p^{1/2}}}$ for the D1-D5 system [107,108].

the common F1-NS5 direction and can carry momentum along this direction by transverse oscillations in the other four internal directions of the NS5 branes [91][3]. It is not hard to see that in the Cardy limit the entropy of these oscillations and of their fermionic superpartners is $S_{\text{little strings}} = 2\pi\sqrt{(4+2)\frac{N_1 N_5 N_p}{6}}$, reproducing precisely the entropy of the F1-NS5-P black hole.

The M-theory uplift of this system makes the little strings less mysterious: One obtains N_5 M5 branes wrapping the common 1-5 direction (that we will henceforth call y) and that are located at different points of the M-theory circle. One fundamental string uplifts to an M2 brane wrapping y and the M-theory circle, x^{11}, and this M2 brane can break into N_5 "strips" stretching between two adjacent M5 branes. As one can see from Figure 17.1, these M2 strips can move independently along the other internal directions of the M5 branes. Hence, the fractionation of an F1 string into N_5 little strings has a clear geometric picture in M-theory, as the breaking of an M2 brane into N_5 strips.

The purpose of this chapter is to begin tracking the fractionated little strings, from the "zero backreaction" regime, where their counting reproduces the the F1-NS5-P black-hole entropy, to the regime of parameters where their backreaction becomes important. We will show that the momentum-carrying fractionated strings coalesce into 4-supercharge brane bound-states that have locally 16 supersymmetries.

The first step in our endeavor is to understand the backreaction of the M2 strips ending on a single M5 brane. We show that their behavior is similar to that of the *Callan-Maldacena spikes* describing backreacted F1 strings ending on D3 branes [111]. Since the M5 branes and the M2 branes extend along a common direction, the M2 branes will now form "furrows" on the M5 brane worldvolume, whose transverse section will look like a Callan-Maldacena spike. A key feature of these bound-states is that they preserve 8 supersymmetries, but if one zooms on a piece of the spike or of the furrow, one finds that locally there are 16 preserved supersymmetries, as a result of the presence of extra "dipolar" charges.

Besides the infinite M5-M2 brane furrow, one can consider more complicated bound state of multiple M5 branes and multiple M2 strips stretching between them (like the system in Figure 17.1). This will result in a complicated maze of furrows, that connect these M5 branes. This super-maze preserves the same supersymmetries and the M5 branes and M2 branes whose charges it carries, but if one zooms in on a piece of maze, one expects that the supersymmetry will be locally enhanced from 8 to 16 supercharges.

Note that each of the $N_1 N_5$ M2 brane strips whose pull on the M5 branes gives the super-maze can be located at an arbitrary position inside the T^4 or $K3$ wrapped by the

[3]In the rest of this chapter, we refer to these microstates as "Dijkgraaf-Verlinde-Verlinde (DVV) microstates" or "little-string microstates." It is important to note that the DVV microscopic counting is different in spirit from the Strominger-Vafa/D1-D5 counting: here the momentum is carried by $N_1 N_5$ fractionated strings carrying integer momenta, while in the D1-D5 CFT we have a single long effective string with modes with momentum quantized in units of $1/N_1 N_5$. Hence, the entropy of the DVV microstates comes from fractionating the F1 strings, while the Strominger-Vafa entropy comes from fractionating the momentum carriers.

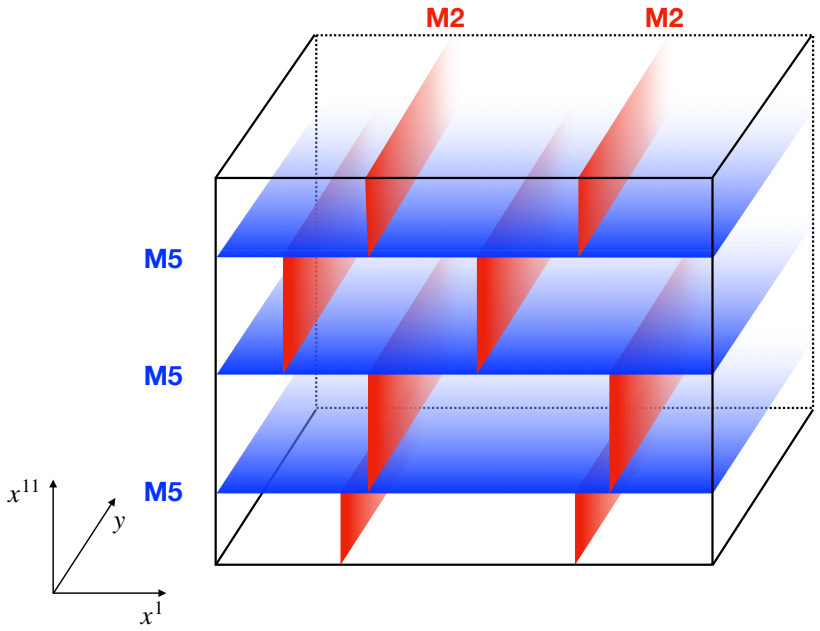

Figure 17.1: Cross-section of $N_1 = 2$ M2 branes splitting into strips between $N_5 = 3$ M5 branes. The vertical axis is the M-theory direction, and the horizontal axis represents one of the internal directions of the M5 branes, x^1. The strips can carry momentum along the y-circle, which is common to the M2 and M5 branes.

M5 branes. Therefore, the dimension of the moduli space of super-mazes is $4N_1N_5$. This matches, as expected, the dimension of the moduli space of the D1-D5 (F1-NS5) system deformations that preserve rotational invariance in the transverse space [14, 17, 112]

The second step in our endeavour is to add momentum to the super-maze, in order to construct a brane bound-state configuration that has 16 supercharges locally and that carries the charges of a black hole with a macroscopically-large event horizon. To do this, we will first construct the two-charge bound states formed by M2 branes and momentum, and by M5 branes and momentum. The former is the M-theory uplift of the F1-P system, whose solutions have been described in supergravity in [113]. The momentum is carried by the transverse oscillations of the M2 branes and, if one zooms in near a piece of the momentum-carrying M2 brane one finds that the supersymmetry is enhanced to 16 supercharges.

Similarly, the M5 branes can carry momentum by transverse fluctuations, that we can restrict to be oriented only along the M-theory direction, so that the resulting solution is spherically symmetric in the non-compact spacetime directions. This system is the uplift

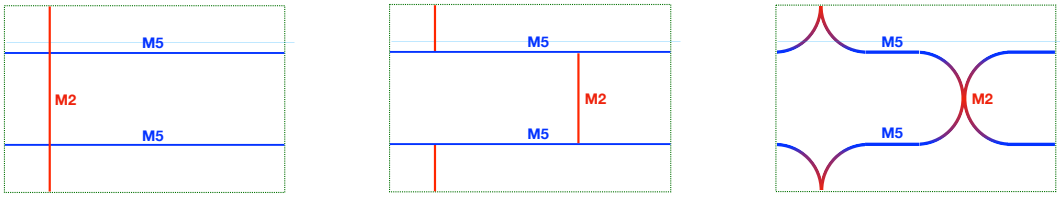

Figure 17.2: The fractionation of M2 branes into strips and the super-maze: Before the fractionation (left panel) the M2 brane does not interact with the M5 branes, and can be freely taken away. After the fractionation, each strip of the M2 branes can move independently, giving the naïve configuration in the middle panel. However, the M2 strips pull on the M5 brane, creating the super-maze depicted in the right panel.

of the NS5-P-D0-D4 solution found in [69]. This solution also preserves 8 supersymmetries, but locally the supersymmetry is enhanced to 16. For both the M2-P and the M5-P system, this is ensured by the presence of dipolar charges, which can be thought of as the "glue" needed to construct the bound states of two-charge system. Of course, for the M5-P system one can consider other types of glue, coming for example from 2 species of M2 branes inside the M5-brane worldvolume. The resulting configuration is called a magnetube, and its supergravity solution was constructed in [114, 115].

The main result of this chapter is to identify the ingredients needed to construct the bound states of the NS5-F1-P Type IIA system and of its M-theory M2-M5-P uplift. These bound states describe the DVV little strings carrying momentum in the regime of parameters where the brane interactions are taken into account. We show that there exists a supersymmetry projector corresponding to a brane configuration that has 16-supersymmetries locally and 4 globally, and which describes the zooming in on a piece of the momentum-carrying M2-M5 maze. Besides the M2, M5 and P charges of the black hole, this system has 6 other dipolar charges, which are necessary to form the glue that transforms these branes into a bound state.

The entropy of the DVV little strings carrying momentum reproduces (upon taking into account all bosonic and fermionic polarizations) the entropy of the F1-NS5-P black hole [91], and our result shows that the microstates carrying this entropy correspond (upon taking brane interactions into account) to a momentum-carrying super-maze whose supersymmetry is enhanced everywhere to 16 supercharges locally.

It is important to emphasize that the local enhancement of supersymmetry to 16 supercharges is the hallmark of the existence in certain duality frames of smooth supergravity solutions that result from the backreaction of these configurations and, more generally, of the absence of event horizons. We will explain the connection between local enhancement of supersymmetry and smooth horizonless solutions in more detail in Section 17.4. Confirming that the entropy of this black hole comes from horizonless super-mazes would constitute a proof of the fuzzball proposal for three-charge supersymmetric black holes in

String Theory, and we are looking forward to the construction of the fully-backreacted solution corresponding to the brane microstates we have discovered.

Our result points towards a change of strategy in the fuzzball/microstate geometry programme of constructing horizonless solutions dual to microstates of string-theory black holes. Until now, the strategy of this programme has been to "blow up" the delta-function source of the harmonic functions of the branes making up the black hole, and replace it by an extended source in the *non-compact* spatial dimensions. This has resulted in a huge plæthora of solutions [18, 20–30, 37, 38, 40, 50, 68, 92–106], all of which break the spherical symmetry of the black-hole horizon. However, the connection between these solutions and the microstates that give rise to the black-hole entropy at weak coupling is difficult to establish, and has only been worked out for superstrata, whose entropy is parametrically smaller than that of the black hole [107, 108]. Furthermore, all the known superstrata have at least one unit of angular momentum in one of the non-compact angular directions in which supersymmetric black holes cannot rotate[4].

Our work points out a new route for constructing microstate geometries that solves these two challenges at the same time: the momentum-carrying super-maze preserves the same spacetime spherical symmetry as the black-hole solution, and it is directly connected to DVV fractionated strings that give rise to the entropy of the F1-NS5-P black-hole in Type IIA String Theory. Furthermore, as we will explain in Section 17.4 the fact that locally the supersymmetry is enhanced to 16 supersymmetries indicates that the fully-backreacted super-mazes will give rise to smooth horizonless black hole microstate geometries, and will not have an event horizon.

In Section 17.1 we review the construction of two-charge bound states and the role of branes that act as "glue" and transform singular configurations of branes into bound states preserving locally 16 supercharges. In Section 3 we describe the construction of the new three-charge bound state, which preserves 16 supercharges locally and is a piece of the super-maze coming from the backreaction of DVV black-hole microstates. In Section 17.3 we explain the link between the projector and the local orientation of the branes that make up the super-maze, and confirm our construction by showing that the energy of the super-maze saturates the BPS bound. In Section 17.4 we discuss the relation between smooth horizonless supergravity solutions and brane configurations preserving locally 16 supercharges, and argue that the backreaction of the super-maze will give rise to bubbling horizonless solutions. In Appendix 1 we collect the projectors corresponding to branes, strings, KK Monopoles and momentum in String and M Theory.

Note on nomenclature: Throughout this chapter we will refer to two- and three-charge systems as systems of two or three sets of branes that preserve 8 respectively 4 common supersymmetries and that exert no force on each other. Thus, a system of D5 branes and parallel D1 branes can be properly called a two-charge system, but a system of D3 branes and parallel D1 branes is not: the D1 branes are attracted to the D3 branes and form a bound state that has 16 supercharges everywhere and is T-dual to a single

[4]The five-dimensional supersymmetric three-charge black holes can have finite J_L, but their J_R must be zero. In contrast superstrata always have $J_R \neq 0$.

oblique stack of parallel D2 branes. Similarly a D7 brane and a parallel D1 brane do not constitute a two-charge system, because the D1 branes run away from the D7 branes.

17.1 Making two-charge bound states out of strings and branes

The vacuum of Type II String Theory preserves 32 supersymmetries. Adding excitations such as strings or branes decreases the number of preserved supersymmetries. Indeed, one can derive using the BPS equations that the presence of branes imposes a constraint on the Killing spinor ϵ:

$$P\,\epsilon \;=\; -\,\epsilon\,, \quad \text{or equivalently} \quad \Pi\,\epsilon \;\equiv\; \frac{1}{2}(1+P)\,\epsilon \;=\; 0\,, \tag{17.1}$$

where P is a traceless *involution* ($P^2 = 1$), typically a product of gamma matrices, that depend on the exact type and orientation of the object considered. Thus Π is a projector, verifying $\Pi^2 = \Pi$. A list of the involutions corresponding to branes, strings, solitons and momentum waves is given in Appendix E. The constraint (17.1) divides the number of preserved global supersymmetries by two.

If one considers configurations with several types of branes whose supersymmetries are compatible, the constraints add up. For example, for a two-charge system, the Killing spinor must respect

$$\Pi_1\,\epsilon \;=\; 0\,, \quad \text{and} \quad \Pi_2\,\epsilon \;=\; 0\,. \tag{17.2}$$

In other words, the Killing spinor must lie in the intersection of the kernels of Π_1 and Π_2. The dimension of this intersection is the number of preserved global supersymmetries (8).

The number of states of a two-charge system is however much larger than one can surmise by considering the individual motion of its component branes. Indeed, the branes can form bound states[5], which contain more fields than those of the naïve multi-brane solution. These fields can be thought of as coming from the dipolar branes that act as the "glue" needed to form the bound state, and which also give rise to a local enhancement of the number of preserved supersymmetries to 16.

For a general bound state, the Killing spinor satisfies

$$\hat{\Pi}\,\epsilon \;\equiv\; \frac{1}{2}(1+\alpha_1 P_1+\cdots+\alpha_n P_n)\,\epsilon \;=\; 0\,, \tag{17.3}$$

where P_i are the traceless involutions associated to the branes whose charges the bound state has and where, for each species of brane, i, the coefficient α_i is the ratio between the charge density corresponding to this brane, Q_i,[6] and the mass density of the full bound

[5] In the D0-D4 system for example, the individual motion of the branes corresponds to the Coulomb branch, where the branes do not form a bound state. However, the large degeneracy of the system comes from the Higgs branch, which describes bound states of D0 branes inside the D4 branes.

[6] Note that the dependence in the string coupling, g_s, enters in the Q_i's.

state, M:

$$\alpha_i \equiv \frac{Q_i}{M}\,. \tag{17.4}$$

Hence, the projector can be written as

$$\hat{\Pi} \;\equiv\; \frac{1}{2M}(M + Q_1 P_1 + \cdots + Q_n P_n)\,. \tag{17.5}$$

The number of preserved supersymmetries is now the dimension of the kernel of $\hat{\Pi}$. This operator is in general not a projector, but when it is, the configuration preserves 16 global supersymmetries.

It is thus possible to reveal the extra dipole charges needed to construct the bound states of a two- or three-charge system by finding involutions corresponding to suitable branes and tuning their charges to make $\hat{\Pi}$ a projector. For a given bound state, the solution for α_i is often not unique: There often exists a whole moduli space of values of the charges that make $\hat{\Pi}$ a projector. One can then imagine varying these charge densities along the internal dimensions of the bound state, so that the constraint becomes:

$$\hat{\Pi}(\vec{x})\,\epsilon(\vec{x}) \;\equiv\; \frac{1}{2}\Big[1 + \alpha_1(\vec{x})P_1 + \cdots + \alpha_n(\vec{x})P_n\Big]\epsilon(\vec{x}) \;=\; 0\,, \tag{17.6}$$

where $\vec{x}$ denotes the internal dimensions of the bound state. Doing so, the number of *local* preserved supersymmetries is still 16. However, the number of *global* supersymmetries can be much less: it is the dimension of the common kernel to the projectors at all possible values of $\vec{x}$. The global Killing spinor does not depend on the position $\vec{x}$, and it must satisfy

$$\forall\,\vec{x}\,, \quad \hat{\Pi}(\vec{x})\,\epsilon \;=\; 0\,, \tag{17.7}$$

where ϵ must be constant.

A common way to ensure that at least some amount of supersymmetry is preserved globally is to rewrite the projectors as

$$\hat{\Pi}(\vec{x}) \;=\; f_1(\vec{x})\Pi_1 + \cdots + f_k(\vec{x})\Pi_k \tag{17.8}$$

where $\Pi_1, \ldots, \Pi_k$ are commuting projectors, and $f_1, \ldots, f_k$ can be any matrix-valued functions. Then, satisfying (17.7) is equivalent to

$$\Pi_1\,\epsilon \;=\; \ldots \;=\; \Pi_k\,\epsilon \;=\; 0\,, \tag{17.9}$$

so the number of preserved global supersymmetries is the dimension of the intersection of the kernels of $\Pi_1, \ldots, \Pi_k$.

When constructing bound states, one typically starts with the set of global charges and their projectors, $\Pi_1, \ldots, \Pi_k$. Combining (17.6) with (17.8) then leads to constraints on the charges of each constituent, Q_i, and hence on α_i.

The distinction between local and global supersymmetries is important, and is at the core of the results of this chapter. As we explained in the Introduction, by constructing

two- and three-charge bound states preserving 16 local supersymmetries, we ensure that we construct microstates of these two- or three-charge systems and that furthermore their backreaction will not give rise to an event horizon.

This bound-state making philosophy was first used to conjecture the existence of superstrata [116], but the method presented here is a generalization of that of [116], where an orthogonal momentum, P(ψ), was imposed to be one of the dipoles. In the following Subsection, we will first illustrate the bound-state making philosophy with several examples of two-charge bound states.

17.1.1 The F1-P bound state

Consider an F1-P system where the strings wrap a compact direction, y, and momentum is also along y direction. The involutions and projectors associated to them are (see Appendix E):

$$\begin{aligned} P_{\mathrm{F1}(y)} &= \Gamma^{0y}\sigma_3\,, \qquad \Pi_{\mathrm{F1}(y)} = \frac{1}{2}(1+P_{\mathrm{F1}(y)})\,, \\ P_{\mathrm{P}(y)} &= \Gamma^{0y}\,, \qquad \Pi_{\mathrm{P}(y)} = \frac{1}{2}(1+P_{\mathrm{P}(y)})\,. \end{aligned} \tag{17.10}$$

When the F1 and P do not form a bound state, the constraints on the Killing spinor add up

$$\Pi_{\mathrm{F1}(y)}\epsilon = \Pi_{\mathrm{P}(y)}\epsilon = 0\,. \tag{17.11}$$

and the system preserves 8 supersymmetries everywhere.

It is possible to form a bound state possessing the same global charges as this system, but preserving locally 16 supersymmetries. In order to do so, one needs to add dipolar transverse strings and momentum which we choose to be along a single transverse direction inside the T^4, that we call x_1 (more complicated choices are also possible but not illustrative for our purpose here):

$$\begin{aligned} P_{\mathrm{F1}(1)} &= \Gamma^{01}\sigma_3\,, \qquad \Pi_{\mathrm{F1}(1)} = \frac{1}{2}(1+P_{\mathrm{F1}(1)})\,, \\ P_{\mathrm{P}(1)} &= \Gamma^{01}\,, \qquad \Pi_{\mathrm{P}(1)} = \frac{1}{2}(1+P_{\mathrm{P}(1)})\,. \end{aligned} \tag{17.12}$$

The objective is to construct a local projector, $\Pi_{\text{F1-P bound}}$, that can be written in two ways:

$$\Pi_{\text{F1-P bound}} = \frac{1}{2}\big(1+\alpha_1 P_{\mathrm{F1}(y)}+\alpha_2 P_{\mathrm{P}(y)}+\alpha_3 P_{\mathrm{F1}(1)}+\alpha_4 P_{\mathrm{P}(1)}\big) \tag{17.13}$$

$$= f_1\Pi_{\mathrm{F1}(y)}+f_2\Pi_{\mathrm{P}(y)} \tag{17.14}$$

where $\alpha_1,\ldots,\alpha_4$ are real numbers, and f_1, f_2 are matrices.

The equation $\Pi^2_{\text{F1-P bound}} = \Pi_{\text{F1-P bound}}$ first leads to

$$\alpha_1^2+\alpha_2^2+\alpha_3^2+\alpha_4^2 = 1\,, \qquad \alpha_1\alpha_4+\alpha_2\alpha_3 = 0\,, \tag{17.15}$$

while equalizing (17.13) and (17.14) leads to

$$\begin{aligned} \alpha_3 + \alpha_4 &= 0\,, \qquad \alpha_1 + \alpha_2 &= 1\,, \\ f_1 &= \alpha_1 - \alpha_4 \Gamma^{y1}\sigma_3\,, \qquad f_2 &= \alpha_2 - \alpha_3 \Gamma^{y1}\sigma_3\,. \end{aligned} \tag{17.16}$$

The solution given here for f_1 and f_2 is not unique.

Solving these equations is straightforward, the solution depends on the choice of an arbitrary angle, θ:

$$\begin{aligned} \Pi_{\text{F1-P bound}} &= \frac{1}{2}\big[1 + c^2 P_{\text{F1}(y)} + s^2 P_{\text{P}(y)} + cs P_{\text{F1}(1)} - cs P_{\text{P}(1)}\big] \\ &= c\big(c + s\,\Gamma^{y1}\sigma_3\big)\Pi_{\text{F1}(y)} \;+\; s\big(s - c\,\Gamma^{y1}\sigma_3\big)\Pi_{\text{P}(y)}\,, \end{aligned} \tag{17.17}$$

where $c \equiv \cos\theta$ and $s \equiv \sin\theta$.

Geometrically, the angle θ corresponds to the inclination of the string in the (y, x_1) plane. If θ is constant, the configuration is a straight string tilted in the (y, x_1)-plane, with transverse momentum. This transversely boosted F1 string preserves 16 supersymmetries.[7] In the limit $\theta = 0$, this is a pure F1 string along y, and when $\theta = \pi/2$ this is a pure momentum wave along y.

One can bend the string by allowing θ to vary along it. The resulting configuration still preserves 16 supersymmetries locally, but only 8 globally.

17.1.2 The NS5-P bound state

The same exercise can be done for the NS5-P system in type IIA. We start with NS5 branes extending along the directions $y, x_1, \ldots, x_4$, and momentum along y. The involutions associated to them are:

$$P_{\text{NS5}(y1234)} = \Gamma^{0y1234}\,, \qquad P_{\text{P}(y)} = \Gamma^{0y}\,. \tag{17.18}$$

Once again, if these constituents do not form a bound state the configuration preserves 8 supersymmetries. They can also form bound states that preserve locally 16 supersymmetries. Contrary to the fundamental string, the NS5-brane does not need to bend in the transverse directions to carry momentum. To make the bound state, one possibility is to use internal dipolar D4-branes (extending along the directions $x_1, \ldots, x_4$) and D0-branes [69]:

$$P_{\text{D4}(1234)} = \Gamma^{01234} i\sigma_2\,, \qquad P_{\text{D0}} = \Gamma^{0} i\sigma_2\,. \tag{17.19}$$

Note that this is not the only possible choice of dipoles. We can also form an F1-NS5 bound state by adding as "glue" two orthogonal sets of D2 branes. This system can be obtained from the one we have by two T-dualities along the NS5 internal directions that are not wrapped by the F1 strings. Its M-theory uplift is know as the magnetube [114, 115].

[7] For an illustration, see Figure 2 and Figure 3 in [69].

Another possibility to construct bound states with P and NS5 charges is to put a momentum-carrying transverse wave on the NS5 brane. This configuration can easily be obtained by dualizing the F1 strings with a transverse momentum wave described above and its "glue" consists of a dipolar NS5 charge and angular momentum. This solution breaks the spherical symmetry of the black-hole solution. Since in this chapter we are interested in constructing bound states that respect this spherical symmetry and can describe locally the backreaction of the DVV microstates, we will describe in detail the brane bound states created using D0-D4 glue.

One needs to construct a projector satisfying

$$\begin{aligned} \Pi_{\text{NS5-P bound}} &= \frac{1}{2}\big(1+\alpha_1 P_{\text{NS5}(y1234)}+\alpha_2 P_{\text{P}(y)}+\alpha_3 P_{\text{D0}}+\alpha_4 P_{\text{D4}(1234)}\big) && (17.20)\\ &= f_1\Pi_{\text{NS5}(y1234)}+f_2\Pi_{\text{P}(y)} && (17.21)\end{aligned}$$

as well as the usual condition on projectors $\Pi^2_{\text{NS5-P bound}} = \Pi_{\text{NS5-P bound}}$, for some real numbers $\alpha_1,\ldots,\alpha_4$ and matrices f_1, f_2.[8]

The solution to this system is:

$$\begin{aligned} \Pi_{\text{NS5-P bound}} &= \frac{1}{2}\big[1+c^2 P_{\text{NS5}(y1234)}+s^2 P_{\text{P}(y)}+csP_{\text{D0}}-csP_{\text{D4}(1234)}\big]\\ &= c(c+s\,\Gamma^y i\sigma_2)\Pi_{\text{NS5}(y1234)} \;+\; s(s-c\,\Gamma^y i\sigma_2)\Pi_{\text{P}(y)}\,,\end{aligned} \tag{17.22}$$

where again $c\equiv\cos\theta$ and $s\equiv\sin\theta$.

17.1.3 The NS5-F1 bound state

One can form an NS5-F1 bound state in type IIA using a similar procedure. Consider an NS5-F1 system where the NS5 extends along the directions $y, x_1, \ldots, x_4$, and the string is along y. The involutions associated to them are

$$P_{\text{NS5}(y1234)} = \Gamma^{0y1234}\,, \qquad P_{\text{F1}(y)} = \Gamma^{0y}\sigma_3\,. \tag{17.23}$$

The bound state can be obtained from the NS5-P system by performing two T-dualities along the directions y and x_1. Again, the choice of x_1 among the four torus directions is at this point arbitrary.

The dipole charges needed to form it are D4-branes extending along the directions $y, x_2\ldots, x_4$, and D2-branes along the direction y and x_1:

$$P_{\text{D4}(y234)} = \Gamma^{0y234}i\sigma_2\,, \qquad P_{\text{D2}(y1)} = \Gamma^{0y1}\sigma_1\,. \tag{17.24}$$

The projector of this bound state is

$$\begin{aligned} \Pi_{\text{NS5-F1 bound}} &= \frac{1}{2}\big[1+c^2 P_{\text{NS5}(y1234)}+s^2 P_{\text{F1}(y)}+csP_{\text{D2}(y1)}+csP_{\text{D4}(y234)}\big]\\ &= c\big(c+s\,\Gamma^1 i\sigma_2\big)\Pi_{\text{NS5}(y1234)} \;+\; s\big(s-c\,\Gamma^1 i\sigma_2\big)\Pi_{\text{F1}(y)}\,.\end{aligned} \tag{17.25}$$

[8] It is not necessary to do this computation again. One can find the result by dualizing the F1-P system (if the directions are not compact, a T-duality can be seen as a solution-generating technique rather than a proper duality). The duality chain is $T_1 - S - T_{1234} - S - T_1$.

where again $c \equiv \cos\theta$ and $s \equiv \sin\theta$, and the angle θ is a function of the coordinates $y, x_1, \ldots, x_4$.

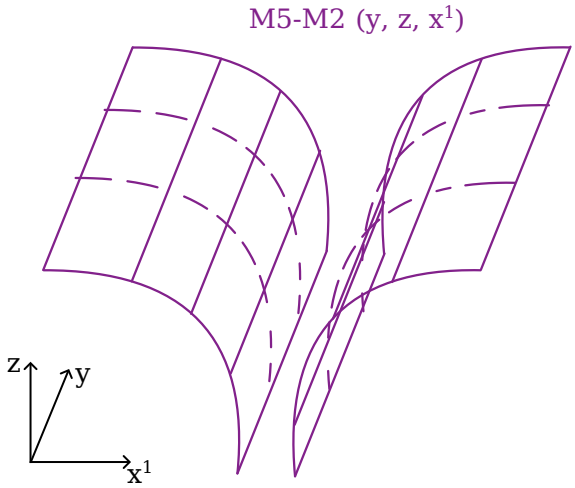

Figure 17.3: The backreaction of the M5-M2 bound state, projected onto the space (y, x_1, z). The M2-branes pull the M5-branes, forming a furrow. The mechanism is similar to the formation of a Callan-Madacena spike in the D3-F1 brane system.

The angle θ and the form of the projector have a clear geometric interpretation for the F1-P bound state (as the tilt of the string). For the NS5-F1 bound state, the interpretation is more complicated: one needs first to uplift the configuration to M-theory. The projector is then given by:

$$\Pi_{\mathrm{M5-M2}} = \frac{1}{2}\left[1 + c^2 P_{\mathrm{M5}(y1234)} + s^2 P_{\mathrm{M2}(y\,z)} - csP_{\mathrm{M5}(y234\,z)} + csP_{\mathrm{M2}(y1)}\right]. \tag{17.26}$$

The brane system then consists of M5-branes and M2-branes sharing one common direction, y. The M2-branes are also extended along the M-theory circle, denoted by z. It is easy to see that M2 branes terminating on the M5 branes will pull them along the (previously orthogonal) M-theory direction. This mechanism is similar to the formation of a Callan-Maldacena spike (see Fig. 17.3). At each location on the M5-brane, the angle θ corresponds to the tilt of the brane in the z direction. Of course, for a generic spike, the pull of the M2 brane will affect all the 4 directions of the NS5 brane, (x_1, x_2, x_3, x_4), and the spike will be described by a complicated function of all these four variables. To obtain the bound state depicted in Figure (17.3), corresponding to the projector (17.25), we can either smear the M2 branes along the directions (x_2, x_3, x_4) or one can zoom in at a location of the spike where the tangent to the spike is orthogonal to x_1.

Another (more familiar) possibility to construct bound states with F1 and NS5 charges is to add a dipolar KKM charge (extending in the space transverse to the NS5 worldvolume and with the special direction along the F1-NS5 common direction) as well as angular momentum, J. This gives rise to a F1-NS5 supertube with KKM-J dipole charge, and its

supergravity solution is the S-dual of the well-known Lunin-Mathur geometry [52, 117]. Much like its better known supertube cousins [118, 119], the KKM can wrap an arbitrary curve in the four dimensions transverse to the NS5 branes, and the solution preserves 8 supercharges. As reviewed in [116], when one zooms near the supertube profile this configuration preserves locally 16 supercharges and this enhancement of supersymmetry comes from the presence of the KKM and angular-momentum "glue", and is equivalent to the fact that the supergravity solution corresponding to the F1-NS5-KKM-J supertube is smooth [120].

Starting from this two-charge bound state one can also add momentum, and build three-charge superstrata: bound states that have the same charges as an F1-NS5-P black hole and give rise to a smooth supergravity solution [18]. However, since our purpose in this chapter is to build three-charge brane bound states that have the same charges as a black hole but that do not break the rotational symmetry of the black-hole horizon, we will not use the "KKM-angular momentum glue", and focus instead on the "D4-D2 glue".

17.1.4 The relation between the M5-M2 furrow and the Callan-Maldacena spike

There are two ways to relate the M2-M5 furrow whose Type-IIA reduction gives rise to the NS5-F1 bound state to the better known F-string and D-string spikes constructed in the D3 brane worldvolume by Callan and Maldacena [111, 121].

The first is to start with a D4-brane in the directions 1234, and an F1-string along the direction y, ending on the D4-brane. This picture is valid when $g_s \ll 1$. As one increases g_s or the number of F1 strings, these strings pull on the D4 brane and give rise to a spike. Much like the D3-F1 spike, this D4-F1 spike can be constructed as a solution to the D4-brane DBI action.

The M5-M2 bound state we consider is dual to the D4-F1 spike, after 11-dimensional uplift along z, and a flip in the coordinates (y, z):

$$\begin{pmatrix} \mathrm{D4}(x^1x^2x^3x^4) \\ \mathrm{F1}(y) \end{pmatrix}_{\mathrm{IIA}} \xrightarrow{\text{uplift on } z} \begin{pmatrix} \mathrm{M5}(z, x^1x^2x^3x^4) \\ \mathrm{M2}(z, y) \end{pmatrix}_{\mathrm{M}} \xrightarrow{(z,y)\text{-flip}} \begin{pmatrix} \mathrm{M5}(y, x^1x^2x^3x^4) \\ \mathrm{M2}(y, z) \end{pmatrix}_{\mathrm{M}}. \tag{17.27}$$

Another way to obtain an M2-M5 furrow – but this time smeared over one of the internal directions – is to construct the furrow corresponding to a D2 along the directions $0, y, z$ that ends on a D4 brane extended along $0, y, 1, 2, 3$. From the perspective of the D4 brane DBI action, this smeared furrow has exactly the same solution as a D1-D3 spike [121]. This furrow can also be constructed using the non-Abelian DBI action of the D2 brane; the D2 non-commuting worldvolume fields are the same as the D6 brane fields describing a D6 brane ending on a D8 brane [122]. Upon uplifting the D2-D4 furrow to 11 dimensions, one obtains a solution smeared along this direction, which is precisely the same as an M2-M5 furrow smeared along one of the M5-brane worldvolume directions:

$$\begin{pmatrix} \text{D3}(x^1x^2x^3) \\ \text{D1}(z) \end{pmatrix}_{\text{IIB}} \xrightarrow{\text{T}_y} \begin{pmatrix} \text{D4}(y, x^1x^2x^3) \\ \text{D2}(y, z) \end{pmatrix}_{\text{IIA}} \xrightarrow{\text{uplift on } x^4} \begin{pmatrix} \text{M5}(y, x^1x^2x^3\widetilde{x^4}) \\ \text{M2}(y, z) \end{pmatrix}_{\text{M}} . \tag{17.28}$$

17.2 The three-charge NS5-F1-P bound state

This section is devoted to the construction of the bound states of the three-charge system. As explained in the Introduction, we expect the bound state to have both the three charges of the NS5-F1-P system, but also several dipolar charges, which constitute the glue needed to construct a bound state that has locally 16 supercharges.

17.2.1 Constructing the projector

We consider the Type IIA three-charge system with NS5-branes extending along the directions $y, x_1, \ldots, x_4$, as well as F1 strings and momentum along the direction y. The involutions that enter in the construction of their corresponding projectors are:

$$P_{\text{NS5}(y1234)} = \Gamma^{0y1234}, \qquad P_{\text{F1}(y)} = \Gamma^{0y}\sigma_3, \qquad P_{\text{P}(y)} = \Gamma^{0y}. \tag{17.29}$$

In order to form a bound state, one needs to find the dipole charges that bind these branes into a configuration with 16 supersymmetries locally. In Section 17.1 we explained how to construct two-charge bound states for the F1-P, NS5-F1 and NS5-P systems: For each system, we found several pairs of dipole charges acting as a glue between the constituents to form bound states. However, upon demanding that these bound states preserve the rotational invariance of the black-hole horizon, only a limited choice of dipole-brane glue remained. The intuitive first attempt at constructing the NS5-F1-P three-charge bound state is to add all the six dipole charges that enter in the construction of the rotationally-invariant two-charge bound states (summarized in Table 17.1), and to try to construct a projector. We can easily find that this only works if the dipole charges of the F1-P bound state are oriented along the same direction, x_1, as the dipole charges of the NS5-F1 bound state.

NS5(y1234)	F1(y)	P(y)	D4(y234)	D2(y1)	D4(1234)	D0	F(1)	P(1)
$\otimes$	$\otimes$		$\times$	$\times$				
$\otimes$		$\otimes$			$\times$	$\times$		
	$\otimes$	$\otimes$					$\times$	$\times$

Table 17.1: Each line describes a two-charge bound state whose charges are two of the three charges of the NS5-F1-P brane systems (denoted by $\otimes$). Each bound state contains two more dipole charges, denoted by $\times$. We attempt to construct a three-charge bound state with NS5-F1-P and all six dipole charges.

Constructing the projector for this bound state follows the same rules as for the two-charge systems. One needs to determine the local charges, α_i, and the matrices, f_j, such that the expression:

$$\begin{aligned}\Pi_{\text{NS5-F1-P bound}} &= \frac{1}{2}\Big[1+\alpha_1 P_{\text{NS5}(y1234)}+\alpha_2 P_{\text{F1}(y)}+\alpha_3 P_{\text{P}(y)}+\alpha_4 P_{\text{D4}(y234)} \\ &\qquad +\alpha_5 P_{\text{D2}(y1)}+\alpha_6 P_{\text{P}(1)}+\alpha_7 P_{\text{F1}(1)}+\alpha_8 P_{\text{D4}(1234)}+\alpha_9 P_{\text{D0}}\Big]\,. \qquad (17.30)\\ &= f_1\Pi_{\text{NS5}(y1234)}+f_2\Pi_{\text{F1}(y)}+f_3\Pi_{\text{P}(y)}\,, \qquad (17.31)\end{aligned}$$

is a projector ($\Pi^2_{\text{NS5-F1-P bound}}=\Pi_{\text{NS5-F1-P bound}}$) and moreover, as the second line illustrates, is compatible everywhere with the supersymmetries of the NS5-F1-P system.

From (17.30) and (17.31) we find:

$$\begin{aligned}\alpha_1+\alpha_2+\alpha_3 &= 1\,,\quad \alpha_4-\alpha_5 = 0\,,\quad \alpha_6+\alpha_7 = 0\,,\quad \alpha_8+\alpha_9 = 0\,,\\ f_1 &= \alpha_1+\alpha_4\,\Gamma^1 i\sigma_2-\alpha_8\,\Gamma^y i\sigma_2\,,\\ f_2 &= \alpha_2-\alpha_5\,\Gamma^1 i\sigma_2-\alpha_6\,\Gamma^{y1}\sigma_3\,,\\ f_3 &= \alpha_3-\alpha_9\,\Gamma^y i\sigma_2-\alpha_7\,\Gamma^{y1}\sigma_3\,.\end{aligned} \qquad (17.32)$$

Here again the values of the functions f_j are not unique. The equation $\Pi^2_{\text{NS5-F1-P bound}}=\Pi_{\text{NS5-F1-P bound}}$ leads to:

$$\sum_{i=1}^{9}\alpha_i^2 = 1\,, \qquad (17.33)$$

$$\alpha_2\alpha_3+\alpha_6\alpha_7 = 0\,,\qquad \alpha_3\alpha_5+\alpha_7\alpha_9 = 0\,,\qquad \alpha_2\alpha_9-\alpha_5\alpha_6 = 0\,, \qquad (17.34)$$

$$\alpha_3\alpha_4+\alpha_6\alpha_8 = 0\,,\qquad \alpha_1\alpha_3+\alpha_8\alpha_9 = 0\,,\qquad \alpha_1\alpha_2-\alpha_4\alpha_5 = 0\,, \qquad (17.35)$$

$$\alpha_1\alpha_6-\alpha_4\alpha_9 = 0\,,\qquad \alpha_1\alpha_7-\alpha_5\alpha_8 = 0\,,\qquad \alpha_2\alpha_8-\alpha_4\alpha_7 = 0\,. \qquad (17.36)$$

The solutions to this system can be expressed in terms of three real numbers (a,b,c) satisfying $a^2+b^2+c^2=1$:

$$\alpha_1 = a^2\,,\qquad \alpha_2 = b^2\,,\qquad \alpha_3 = c^2\,, \qquad (17.37a)$$

$$\alpha_4 = ab\,,\qquad \alpha_5 = ab\,,\qquad \alpha_6 = bc\,, \qquad (17.37b)$$

$$\alpha_7 = -bc\,,\qquad \alpha_8 = -ac\,,\qquad \alpha_9 = ac\,. \qquad (17.37c)$$

Then the projector is:

$$\begin{aligned}\Pi_{\text{NS5-F1-P bound}} &= \frac{1}{2}\Big[1+a^2 P_{\text{NS5}(y1234)}+b^2 P_{\text{F1}(y)}+c^2 P_{\text{P}(y)}+ab\left(P_{\text{D4}(y234)}+P_{\text{D2}(y1)}\right)\\ &\qquad +bc\left(P_{\text{P}(1)}-P_{\text{F1}(1)}\right)-ac\left(P_{\text{D4}(1234)}-P_{\text{D0}}\right)\Big]\,.\end{aligned} \qquad (17.38)$$

This projector preserves locally 16 supersymmetries. We now allows the parameters a, b, c to be functions of the coordinates $y, x_1, \ldots, x_4, z$. The supersymmetries rotate, but the projector still preserves the 4 global supercharges of the NS5-F1-P brane system:

$$\begin{aligned}\Pi_{\text{NS5-F1-P bound}} &= a\,(a + b\,\Gamma^1 i\sigma_2 + c\,\Gamma^y i\sigma_2)\;\Pi_{\text{NS5}(y1234)} \\ &+\; b\,(b - a\,\Gamma^1 i\sigma_2 - c\,\Gamma^{y1}\sigma_3)\;\Pi_{\text{F1}(y)} \\ &+\; c\,(c - a\,\Gamma^y i\sigma_2 + b\,\Gamma^{y1}\sigma_3)\;\Pi_{\text{P}(y)}\,.\end{aligned} \tag{17.39}$$

We represent the relative densities of the branes whose charges enter in this projector in Figure 17.4.

Of course, in order for the projector (17.38) to correspond to a physical brane configuration the densities of branes wrapping a certain direction should not be functions of this direction. Since these densities are related to the coefficients in the projector via equation (17.4) this puts certain constraints on the parameters a, b and c. These constraints will be further explained in Section 17.3.

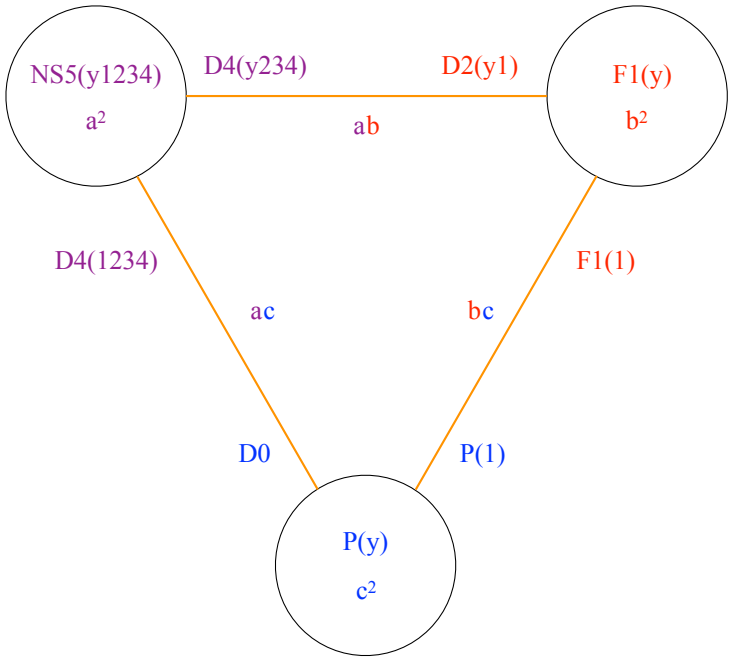

Figure 17.4: Schematic representation of the three-charge NS5-F1-P bound state. The nodes represent the three charges of the bound state. Every combination of two nodes and the orange line joining them corresponds to a two-charge bound state, and the dipole charges and their coefficients in the projector are indicated next to the line.

17.2.2 The M5-M2-P triality

It is also possible to uplift the three-charge bound state to M-theory, and argue that it is related to the local structure of DVV black-hole microstates.

The charges and dipole charges of the bound state have a clear M-theory origin. For simplicity we can rename the M-theory direction $x_{11} \equiv z$. As we explained in Section 17.1.3, the two-charge bound state of F1 strings and NS5 branes can be interpreted in M-theory as the near-brane limit of the furrow created by the backreaction of M2 branes that end on M5 branes. From the perspective of the M5 brane worldvolume theory, this furrow can be constructed similarly to the Callan-Maldacena spike describing the F1 strings terminating on D3 branes.

From the M-theory perspective, the dipole branes which form the glue of the M2-M5-P bound state are also M2 and M5 branes and momentum, oriented differently. The NS5-brane along $(y1234)$ becomes an M5 brane along the same directions, and the F1 string along (y) becomes an M2 brane along (y, z). The gluing dipole branes correspond to M5 branes along $(1234z)$ and along $(y234z)$, M2 branes along $(y1)$ and along $(1z)$, and momentum along 1 and along z. Figure 17.5 reveals this triality.

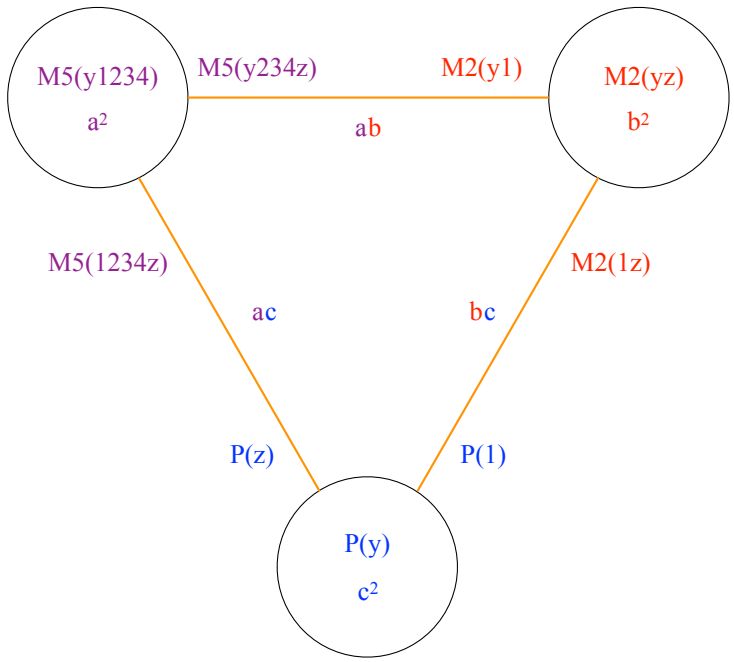

Figure 17.5: The M-theory uplift of the NS5-F1-P bound state. The nodes represent the three charges of the bound state. Every combination of two nodes and the orange line joining them corresponds to a two-charge bound state, and the dipole charges and their coefficients in the projector are indicated next to the line.

In terms of M-theory ingredients, the projector is written as:

$$\Pi_{\text{NS5-F1-P}} = \frac{1}{2}\left[1 + a\hat{P}_{\text{M5}} + b\hat{P}_{\text{M2}} + c\hat{P}_{\text{P}}\right], \tag{17.40}$$

where

$$\hat{P}_{\text{M5}} \equiv aP_{\text{M5}(y1234)} - bP_{\text{M5}(y234\,z)} + cP_{\text{M5}(1234\,z)}\,, \tag{17.41}$$
$$\hat{P}_{\text{M2}} \equiv aP_{\text{M2}(y1)} + bP_{\text{M2}(y\,z)} - cP_{\text{M2}(1\,z)}\,, \tag{17.42}$$
$$\hat{P}_{\text{P}} \equiv -aP_{\text{P}(z)} + bP_{\text{P}(1)} + cP_{\text{P}(y)}\,, \tag{17.43}$$

and the brane involutions are all of the following form:

$$P_{\text{M5}(y1234)} = \Gamma^{0y1234} \tag{17.44}$$
$$P_{\text{M2}(y1)} = \Gamma^{0y1} \tag{17.45}$$
$$P_{\text{P}(z)} = \Gamma^{0\,z}\,. \tag{17.46}$$

17.3 The Brane Content of the Super-Maze

Equations (17.41), (17.42) and (17.43), together with Figure 17.5, reveal to us the microscopic physics of the M-theory super-maze. As we explained in Section 17.1.3, to understand the local physics of the super-maze surface it is best to work in the $(y, 1, z)$ space, in which both the M5 branes and the M2 branes wrap nontrivial two-surfaces, and 1 denotes a torus direction orthogonal to the original M2 brane. One can see for example that equation (17.41) implies that at every location along the super-maze, the local M5 charge density in the $(y, 1)$ direction (proportional to the projection of the surface of the super-maze along the $(y, 1)$-plane) is equal to a times the mass density of the full configuration. We recall that the parameters a, b, c have been promoted to functions of the position on the brane bound state. One can also see that equation (17.42) implies that the local M2 charge in the direction (y, z) (again proportional to the projection of the M2 charge of the super-maze in the (y, z)-plane) is equal to b times the mass density.[9]

We can span the $(y, 1, z)$ space using orthonormal vectors (u_y, u_1, u_z). Let $u^{\perp}_{\text{M5}}$ be the unit vector orthogonal to the two-dimensional M5-brane surface in the $(y, 1, z)$ space. Let $u^{\perp}_{\text{M2}}$ be its equivalent for the M2-brane, and u_{P} the unit vector along the direction of the momentum P. Then, by choosing the orientation signs appropriately, one can show that the equations (17.41), (17.42) and (17.43) imply successively

$$a = u^{\perp}_{\text{M5}} \cdot u_z\,, \qquad b = u^{\perp}_{\text{M5}} \cdot u_1\,, \qquad c = u^{\perp}_{\text{M5}} \cdot u_y\,, \tag{17.47}$$
$$a = u^{\perp}_{\text{M2}} \cdot u_z\,, \qquad b = u^{\perp}_{\text{M2}} \cdot u_1\,, \qquad c = u^{\perp}_{\text{M2}} \cdot u_y\,, \tag{17.48}$$
$$a = u_{\text{P}} \cdot u_z\,, \qquad b = u_{\text{P}} \cdot u_1\,, \qquad c = u_{\text{P}} \cdot u_y\,. \tag{17.49}$$

[9] Strictly speaking, the value is $\pm b$, where the choice of $\pm$ depends on which one of the two unit vectors orthogonal to the M5-brane surface we choose.

Hence, these equations simply imply that:

$$u^{\perp}_{\rm M5} = u^{\perp}_{\rm M2} = u_{\rm P}\,. \tag{17.50}$$

Thus, even though the super-maze has several M5 and M2 local charges pointing in different directions, when one zooms in on any particular location one finds a tilted M5 brane with parallel M2 charge dissolved in it and orthogonal momentum, which is a configuration preserving 16 supercharges. Of course, these 16 supercharges vary as one moves to a different location of the super-maze, and only 4 of them remain unchanged - the supercharges corresponding to the F1-NS5-P system whose microstates we are constructing.

Our projector also makes it clear how the energy density of the super-maze is distributed among its constituents. Before adding momentum ($c = 0$), we have a static y-independent maze, that contains M5 and M2 branes wrapping y. If one concentrates on a single furrow in the maze, the surface can de described by an equation $z = f(x_1)$. One can then parametrize a and b by an angle, β, that depends on x_1:

$$a \;=\; \cos\beta\,, \qquad b \;=\; \sin\beta\,. \tag{17.51}$$

This angle β corresponds locally to the bending of the surface of the momentum-less maze in the (y, z) plane: $\tan\beta = f'(x_1)$.

We can now compute the energy density of the momentum-less maze from its M5- and M2-brane constituent charges. Using (17.4), one finds

$$Q^{M5}_{(y1234)} \;=\; M\cos^2\beta\,, \qquad\qquad Q^{M5}_{(y234z)} \;=\; -\,M\cos\beta\sin\beta\,, \tag{17.52}$$

$$Q^{M2}_{(y1)} \;=\; M\cos\beta\sin\beta\,, \qquad\qquad Q^{M2}_{(yz)} \;=\; M\sin^2\beta\,, \tag{17.53}$$

where M is the mass density. As usual, the square of the energy density is equal to the sum of the squares of all the charges

$$M^2 \;=\; \sum_I (Q_I)^2\,. \tag{17.54}$$

However, since the ratio of the M5 and M2 charges is the same as the angle of the furrow, the mass simplifies to the usual BPS mass of a two-charge system:

$$M \;=\; Q^{M5}_{(y1234)} + Q^{M2}_{(yz)}\,. \tag{17.55}$$

If one now adds momentum, the super-maze oscillates along y. The furrow can now be described by a generic function of two variables (see Figure 17.6.), and the bending angle, β, can also become y-dependent.

Moreover. we also need to introduce an additional "wiggling" angle, α, corresponding to the slope of the furrow waves carrying momentum along the y direction. This angle can also depend on both y and x_1. The parameters a, b and c can now be expressed in terms of these angles as

$$a = \cos\alpha\cos\beta = c_\alpha c_\beta\,, \qquad b = \cos\alpha\sin\beta = c_\alpha s_\beta\,, \qquad c = \sin\alpha = s_\alpha\,. \tag{17.56}$$

The energy density of the momentum-carrying furrow is distributed between the branes and the momentum:

$$Q^{M5}_{(y1234)} = Mc_\alpha^2 c_\beta^2\,, \qquad Q^{M5}_{(y234z)} = -Mc_\alpha^2 c_\beta s_\beta\,, \qquad Q^{M5}_{(1234z)} = Mc_\alpha s_\alpha c_\beta\,, \tag{17.57}$$

$$Q^{M2}_{(y1)} = Mc_\alpha^2 c_\beta s_\beta\,, \qquad Q^{M2}_{(yz)} = Mc_\alpha^2 s_\beta^2\,, \qquad Q^{M2}_{(1z)} = -Mc_\alpha s_\alpha s_\beta\,, \tag{17.58}$$

$$Q^{P}_{(1)} = -Mc_\alpha s_\alpha s_\beta\,, \qquad Q^{P}_{(z)} = Mc_\alpha s_\alpha c_\beta\,, \qquad Q^{P}_{(y)} = Ms_\alpha^2\,, \tag{17.59}$$

and once again, this leads to the BPS condition for the three-charge system

$$M = Q^{M5}_{(y1234)} + Q^{M2}_{(yz)} + Q^{P}_{y}\,. \tag{17.60}$$

Note that as one moves in the $(y,1)$ plane, the projection of the M5 charge in this plane remains constant. Indeed, the original five-brane wraps the $y,1$ plane, and its charge density cannot therefore depend on y or x_1. This appears to be in conflict with equation (17.57), but we have to realize that M is the mass density of the furrow in the $(y,1)$ plane, which changes as one moves along the furrow. Hence, $Q^{M5}_{(y1234)}$ is independent on α and β, but M depends on them:

$$M(y,x_1) = \frac{Q^{M5}_{(y1234)}}{\cos^2\alpha(y,x_1)\cos^2\beta(y,x_1)}\,. \tag{17.61}$$

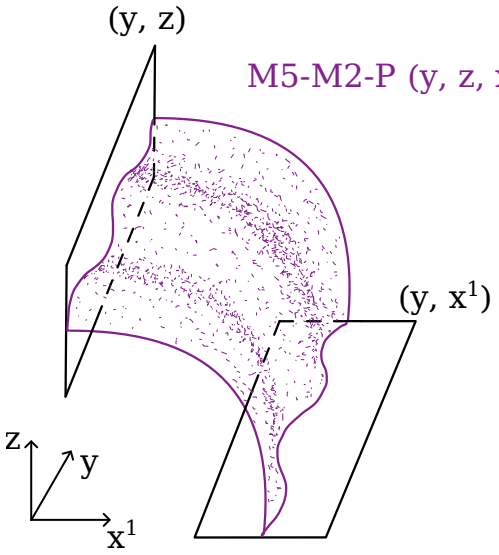

Figure 17.6: Wiggling half-furrow.

17.4 In lieu of a Conclusion: Some thoughts on Super-Maze backreaction

One key question about the super-maze we discovered is whether it gives rise to a horizonless and possibly smooth solution in the regime of parameters where the classical

black-hole solution exists. Naïvely one may argue that, since the super-maze contains N_1N_5 M2 brane strips crammed into a very small torus, its backreaction will give rise to a solution whose curvature is too large to be reliably described by supergravity. However, this intuition fails to take into account the fact that when branes backreact they can blow up the size of the transverse spacetime.

The key feature of the super-maze that makes us confident that its backreaction will be smooth and horizonless is the local enhancement of the supersymmetry to 16 supercharges. This is the smoking gun of the construction of the brane bound states that account for the entropy of the two-charge system. This is perhaps best known from the physics of supertubes [118,119]: A supertube can have arbitrary shape and, if one zooms in at a certain location along this shape, one finds a brane system that preserves 16 supersymmetries. Moreover, as one moves along the supertube these supersymmetries rotate, and only a subset of 8 of them is preserved by the full configuration. When the supertube is dualized to the D1-D5 (or F1-NS5) duality frame and its two charges correspond to D1 and D5 (or F1 and NS5) branes [52, 117], the presence of 16 supercharges locally is equivalent to the existence of a smooth horizonless supergravity solution [120]. Another examples of a two-charge brane bound states is the F1 string carrying longitudinal momentum [113], reviewed in Section 17.1. This solution has again 8 supercharges, but if one zooms in near the location of the momentum-carrying string one finds a solution with 16 supercharges. These supercharges rotate as one moves along the string profile, and only 8 of them remain invariant and are preserved by the whole configuration. A similar bound state can be made from any brane carrying longitudinal momentum.

A third, slightly less known illustration of a two-charge bound state that has 16 supercharges locally is the magnetube, which has again two charges, corresponding to an M5 brane and longitudinal momentum, which are bound together by the presence of M2 brane dipole charges [114, 115]. Finally, a fourth illustration of this phenomenon is the NS5-P bound state recently constructed in [69], where the supersymmetry is enhanced locally to 16 supercharges because of the presence of dipolar D0 and D4 charges on the NS5 worldvolume.

There also exist brane configurations that have the same charges as those of a three-charge black hole, and again have 16 supercharges locally and only 4 globally. When the brane configurations correspond to multi-center solutions [123] whose centers are fluxed D6 branes (which preserve locally 16 supercharges), the solutions uplift [124] to the smooth horizonless bubbling solutions in eleven dimensions constructed in [93, 94]. Another three-charge brane configuration that has locally 16 supercharges is the superstratum conjectured in [116], which served as inspiration for the building of superstratum supergravity solutions [18].

Note that in all these systems, in the absence of the dipolar branes providing the "glue" and in the absence of the local enhancement of the supersymmetry to 16 supercharges, one obtains singular solutions or solutions with a horizon, which do not describe microscopic degrees of freedom of these systems, but rather ensemble averages. Thus the local enhancement of the supersymmetry is the key indication that the backreaction of

the brane bound state will result in a horizonless solution that describes a pure state of the system.

It is important to remark that the local enhancement of supersymmetry and the absence of a horizon are duality-frame-invariant phenomena. Of course, in some duality frames a smooth solution can become a singular solution, but a solution with an event horizon can never be dualized to a solution without one [125] and viceversa.

One can also speculate on how the supergravity solution corresponding to a super-maze may look. In Figure 17.7 we illustrate the shape of a super-maze corresponding to two M5 branes extending along x_1 and a single fractionated M2 brane extended along z (the M-Theory direction) and smeared over three of the M5-brane worldvolume directions, x_{234}. Before the fractionation, the M2 brane does not pull on the M5 branes; this is depicted in the left panel. Once the M2 brane gets fractionated, its components start pulling on the M5 brane. However, since the M2 brane strips have been smeared along x_{234}, they end on a codimension-one surface inside the M5 branes. Therefore, the pull of a fractionated M2 brane does not give rise to a spike, but rather to a wedge.[10]

As one can see from the middle panel of Figure 17.7, when the distance between the two M5 branes is large, the configuration consists of several M5 branes wedges with dissolved M2 charge, pulled by M2 branes extended along z. However, the bent M5 branes can move freely along the z direction, and when two opposite M5 wedges become close they can transform into the brane web depicted in the right panel, which contains also un-fluxed coincident M5 branes. In general, a more complicated super-maze smeared over three of the M5-brane worldvolume directions will correspond to a brane web in the (x_1, z)-plane which has the all the three ingredients of the web in the right panel of Figure 17.7.

If the M2 branes are not smeared, the resulting maze does not have any "bare" M2 lines, but will be everywhere a fluxed M5 brane.[11] One can then ask how the supergravity solution corresponding to this M5 super-maze will look. First, the M5 branes source a magnetic four-form whose flux on a four-sphere is constant. When the M5 branes backreact, there will be a geometric transition: this four-sphere becomes large and topologically nontrivial, while the nontrivial maze surface wrapped by the M5 branes will shrink to zero size. Thus, the maze of M5 branes will transform into a maze of bubbles with fluxes.

As we have discussed in the Introduction, the existence of super-mazes and the possibility that their supergravity solution might be smooth, represents a paradigm shift for the microstate geometry programme and for the fuzzball conjecture in general. The starting point of this conjecture is the idea that collapsing matter do not form horizons in nature, but rather transition into horizonless "fuzzball" solutions of string theory. Stan-

[10] Remember that the Callan-Maldacena spike corresponds to a string ending on a codimension-three defect inside the D3 brane, and the profile of the pulled D3 brane is similar to the harmonic function in three dimensions, $1/r$. Here, the M2 branes end on a codimension-one defect, so the profile of the pulled M5 brane has the shape of the harmonic function in one dimension, $|x_1|$, and looks like a wedge.

[11] Even when the M2 branes are smeared, one can argue that because the distance between the M5 branes on the M-theory circle is small, the maze components will be mostly fluxed and unfluxed M5 branes.

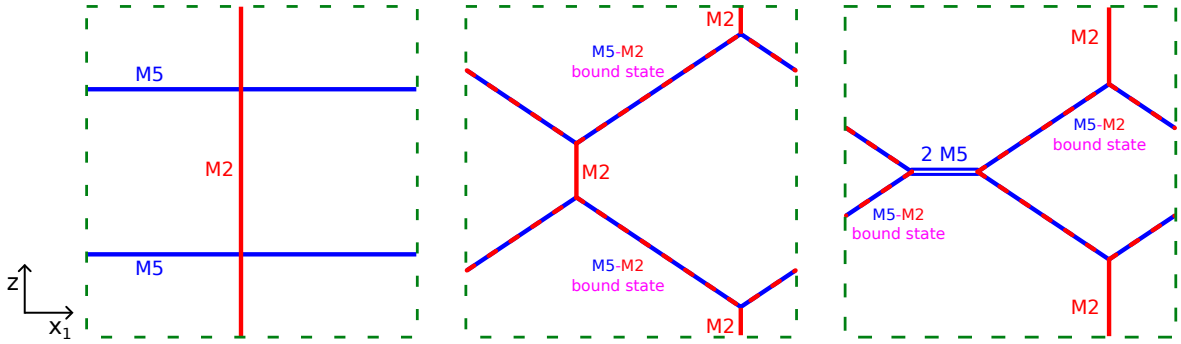

Figure 17.7: A super-maze made of 2 M5 branes and a single M2 brane which is smeared along three of the M5 brane worldvolume directions. Before the fractionation the M2 brane does not pull on the M5 branes, and can be freely taken away. After the fractionation (middle panel), each strip of the M2 branes deforms the M5 brane in its vicinity. As the branes move, the web depicted in the middle panel can also transform in the web depicted in the right panel, which has regions of coincident un-fluxed M5 branes.

dard black holes are then seen as average descriptions of the space of microstates that the stringy fuzzball matter can reach. One also expects on general grounds that some of these fuzzball solutions will have a classical limit, and will be describable purely using low-energy supergravity, as microstate geometries.

Despite the extraordinary success of the microstate geometry programme, the entropy of the solutions constructed so far, of order $\sqrt{N_1 N_5} N_P^{1/4}$ is parametrically smaller than the entropy of the three-charge black hole, $\sqrt{N_1 N_5 N_P}$. Furthermore, all the solutions that have been constructed break the spacetime spherical symmetry of the black-hole horizon, while we expect $\sqrt{5/6}$ of the black hole entropy to come from configurations that do not break this symmetry [112].[12]

The super-maze promises to solve both these problems at the same time. On one hand, we have constructed the super-maze using the types of "glue" that preserve the rotational invariance of the black hole. Furthermore, the DVV microstates that we have argued to backreact into super-maze configuration correspond to momentum carriers that are purely bosonic. Hence, we expect the super-maze and its corresponding supergravity solutions to have an entropy of order $2\pi\sqrt{\frac{4}{6} N_1 N_5 N_P}$.[13] Furthermore, since two of the fermionic zero modes also preserve the rotational symmetry of the black-hole horizon, and the super-maze is the most general brane bound state with black-hole charges that preserves this symmetry, it is possible that the super-maze could even have an entropy of order $2\pi\sqrt{\frac{5}{6} N_1 N_5 N_P}$.

Our construction also allows us to speculate how we may try to capture the remaining part of the black-hole entropy, which comes from fermion momentum carriers that break

[12] For other extremal black holes there are arguments that most of the entropy comes from such microstates [126].

[13] See also [127], expecting that disentangled microstates [128] – and therefore microstates without smooth horizons – to account for at least a finite fraction of the black-hole entropy.

the rotational symmetry of the black-hole horizon [112]: Instead of using the super-maze glue, we could could try to use the other types of glue, and construct generalizations of the super-maze that break this rotational symmetry.

It would be very interesting to construct the fully backreacted super-maze solutions, and to understand how this entropy is realized in supergravity. It would be also interesting to apply the "making bound states with glue" philosophy we used in this chapter to reveal the microscopic structure of black holes in other duality frames, where microstate counting has not been done.

Chapter 18

Themelia: the irreducible microstructure of black holes

This Chapter reviews the work of [44].

Whether you describe it in General Relativity or think of it as a strongly-coupled quantum object, a black hole must necessarily reduce matter to its most fundamental constituents. From the perspective of string theory, this is usually interpreted as meaning strings and branes, but we will argue that the full range of fundamental constituents must include more general species of objects that we will call *themelia*. A themelion is defined to be any object in string theory that *locally preserves* 16 supercharges. This certainly includes fundamental strings and branes, but a themelion can carry multiple charges and preserve less supersymmetry when taken as a whole. A themelion will typically have varying charge densities along a non-trivial profile, but the defining idea is that when one "zooms in" on a small segment of the themelion, the localized part preserves sixteen supersymmetries and those supersymmetries will generically depend on their location on the themelion.

Our purpose here is not only to characterize some large families of themelia, but also to show that they play the central role in the description of black-hole microstructure, and that they are necessarily the irreducible constituents of a supersymmetric fuzzball. As we will describe, themelia not only include all known supersymmetric microstate geometries, but also greatly extend their range. Indeed, a central result of this chapter will be to exhibit themelia that embed the microstate geometries known as superstrata [18, 20, 21] into highly fractionated brane configurations that include the super-maze [43].

The fuzzball paradigm [4, 12] seeks a gravitational and quantum description of black holes, and their microstructure, in terms of horizonless objects in string theory. The idea is that, because individual microstates have no entropy, they cannot have a horizon, and that horizons only arise through ensemble averaging. Fuzzballs are supposed to represent a new phase that emerges when matter is compressed to black-hole densities, and this new phase prevents the formation of a horizon or singularity.

The challenge has been to formulate fuzzballs more precisely [129] and this has been done largely through the construction of huge families of examples: In particular, mi-

crostate geometries are realizations of the fuzzball paradigm in terms of smooth solutions to supergravity. What is perhaps most startling about this program is the extent to which it can be realized. (For recent reviews, see [12,130].) This extensive body of work has also led to a much deeper understanding of the new phase of matter that underlies fuzzballs, and hence our proposal that their fundamental constituents should be themelia.

Fundamental constituents must themselves be horizonless. But this is not sufficient: there are "horizonless" string configurations, like the unadorned D1-D5 solution, that still have microstructure. While the classical horizon of such an object has vanishing area, it can be argued to have a "Planck-scale horizon" that accounts for the entropy of its microstructure [9]. On the other hand, the sixteen supersymmetries of the themelion not only preclude it from having a horizon, even at the Planck scale, but also makes it a fundamental bound state, an indivisible "atomic object" of string theory – hence the building block of fuzzballs.

Objects with 16 supersymmetries can always be dualized to a system consisting of a single species of brane, such as a stack of F1's, or the empty space of a KKM. A generic themelion is, however, highly non-trivial: It only has 16 supersymmetries *locally*, and so the "trivializing" duality transformation depends on the location on the themelion profile. In any fixed duality frame, a themelion can carry a huge range of charges that *vary* with location. Some of these will average to zero over the themelion, and some will average to non-zero values. We will refer to these as *dipolar* and *global* charges respectively. The global charges determine the overall supersymmetry preserved by the themelion.

The important point about themelia is that, individually, each one has essentially no microstructure and, upon dualizations, can be characterized locally using string theory (as an F1) or geometry (as a KKM). However, globally, themelia can have huge moduli spaces, expressed in terms of shapes and charge densities, and so they can encode a vast number of microstates within their configuration spaces. Conversely, because of the 16 supersymmetries, the moduli space of a themelion cannot *ipso facto* contain any black holes, or give rise to horizons.

Superstrata were originally conjectured to exist [116] entirely based on the underlying principle of themelia: namely, 16 supersymmetries locally. Five years later, large families of superstratum supergravity solutions were explicitly constructed [18, 20, 21] but their connection with the themelion of [116] was not clear.

In this chapter we exhibit the themelion structure of the superstratum solution, and show that the supergravity constraints imposed by smoothness are equivalent to requiring that themelia have 16 local supercharges. We also reveal a similar structure in the recently constructed "vector superstrata" [131].

In addition to superstrata, one should recall that there is another huge family of smooth horizonless microstate geometries: the bubbling solutions constructed from ambipolar Gibbons-Hawking (GH) geometries [93, 94, 97]. Upon reduction to 10 dimensions along the GH fiber, one obtains a multi-center solution [123] where each center has 16 supercharges [124] (and hence is a themelion).

Based on our observations, we conjecture a relation between bound states of themelia

and smooth horizonless supergravity solutions:

The Themelion Conjecture:
All smooth horizonless solutions come from bound states of themelia with KKM charge. All bound states of such themelia give rise to a smooth supergravity solution.

As we remarked above, each themelion can have a large moduli space. Furthermore, combining different themelia can lead to an enhancement of the moduli space. As we will show, the superstratum solution is a combination of two themelia, each of which involves a function of one variable and yet, the generic superstratum solution is expected to be parametrized by arbitrary functions of three variables [25]. Therefore, our conjecture does not imply that a choice of component themelia leads to a unique smooth horizonless solution.

18.1 Themelia

To pin down the structure of a particular themelion, one must first specify its global charges, and the amount of supersymmetry it will preserve overall. One then chooses dipolar charges as "glue" that will bind the global object into a bound state with 16 supersymmetries locally [43]. There are typically multiple choices for such glue and, as we will see, one can often combine different types of glue to create an even larger themelion moduli space. The choice of these dipole charges is also motivated by the underlying physics of the themelion.

The construction, of course, depends on the duality frame and the charges we want the themelion to carry. Here we will work exclusively in the Type IIA/M-theory frame and focus on themelia that have the F1, NS5 and P charges of a supersymmetric black hole. We can uplift everything to M-theory, where the supersymmetries, $\mathcal{Q}$, are 32-component spinors and the themelion building blocks are M2 and M5 branes, momentum, P, and KKM charge. The supersymmetries of the themelion are then defined by projectors involving gamma matrices.

$$\Pi\mathcal{Q} \;=\; 0, \qquad \Pi = \frac{1}{2}\,(1 \;+\; P), \tag{18.1}$$

where the matrices, P, are given by [116]:

$$\begin{aligned} &P_{\mathrm{M2}(12)} = \Gamma^{012}\,, \qquad P_{\mathrm{M5}(12345)} = \Gamma^{012345} \\ &P_{\mathrm{P}(1)} = \Gamma^{01}\,, \quad P_{\mathrm{KKM}(123456;7)} = \Gamma^{0123456} = \Gamma^{789\,10}\,. \end{aligned}$$

Here the indices indicate the directions along which the branes extend. For the KKM the last entry denotes the "special direction" of the fibration.

We will also focus on the $\mathbb{T}^4$ compactification of IIA supergravity to six dimensions and will denote the M-theory circle by z and the torus directions as $1, 2, 3, 4$. We will also introduce two other circles: an $S^1(y)$ corresponding to the common direction of the F1 strings and NS5 branes that give global charges, and a "space-time" ψ-circle transverse to

the $\mathbb{T}^4 \times S^1(y)$. If the ψ direction is non-compact then charges corresponding to branes wrapping this direction are necessarily dipolar. We will also find it useful to use the standard IIA nomenclature: NS5, F1, D2 , D4 and D6 to encode the way in which the M-theory objects wrap the z-circle.

An archetypical example of the relation between themelia and supergravity solution comes from the Lunin-Mathur 8-supercharge solution [117]. This is a smooth horizonless solution, which can be thought of as a supertube [118] with F1(y) and NS5(1234y) charges and a KKM(1234$\psi z; y$) dipole charge. The global supersymmetries are defined by the vectors, ξ, satisfying:

$$\frac{1}{2}(1 \, + \, \Gamma^{0yz})\,\xi \;=\; 0\,, \quad \frac{1}{2}(1 \, + \, \Gamma^{01234y})\,\xi \;=\; 0\,. \tag{18.2}$$

This solution is made of two themelia. The first themelion is at the "supertube locus" and has F1 and NS5 charges, as well as a glue coming from the angular momentum P(ψ) along the supertube direction, ψ, and the KKM(1234$\psi z; y$). Its projector has [116]:

$$P \;=\; \lambda_1\Gamma^{0yz} \;+\; \lambda_2\Gamma^{01234y} \;+\; \lambda_3\Gamma^{0\psi} \;+\; \lambda_4\Gamma^{01234\psi z}\,. \tag{18.3}$$

If one takes $\lambda_1 = \cos^2\phi$, $\lambda_2 = \sin^2\phi$ and $\lambda_3 = -\lambda_4 = \sin\phi\cos\phi$, then one has:

$$P^2 \;=\; 1\,, \qquad \Pi\,\xi \;=\; \frac{1}{2}(1+P)\,\xi \;=\; 0\,. \tag{18.4}$$

The identity $\Pi^2 = \Pi$ means that Π only has eigenvalues 0 or 1 and, combined with the fact that the products of gamma matrices are traceless, it means that Π must have sixteen null vectors, preserving 16 supersymmetries. However eight of those supersymmetries depend upon the parameter, ϕ, and eight are independent of ϕ and are determined by the global F1 and NS5 charges as in (18.2).

The second themelion is a bit less obvious when the supertube is in $\mathbb{R}^4$, but can be seen easily if one embeds the Lunin-Mathur geometry in Taub-NUT [132, 133]: The "center-of-space" themelion is a KKM wrapping the ($y1234z$) directions and with a special direction ψ. This reflects a more general principle: to reveal the themelion sources of a solution one should write it as a fibration over a spatial $\mathbb{R}^3$. The themelia are located where the fibers degenerate.

Supergravity superstrata of [18, 20, 21] are built by adding momentum waves along y to a generalized supertube solution. These momentum waves cannot be sourced on the themelion at the supertube locus, where the y-circle degenerates. Instead, they are sourced at the center of space, promoting the simple KKM themelion to a much more complicated momentum-carrying themelion.

To recast the original supergravity superstrata [18, 20, 21] in our IIA/M-theory frame, we perform an S-duality and a T-duality along one direction of the $\mathbb{T}^4$, which we can choose to be x_1. By writing the superstratum solution as circle fibrations over an $\mathbb{R}^3$ base, one can easily read off all the themelion charges from the singularities in the fluxes and metric functions. In particular, there are warp factors that diverge at the supertube

location. These correspond to the global F1 (M2(yz)) and NS5 (M5($y1234$)) charges, and equal amounts of dipolar M2($1y$) and M5($z234y$) charges. At the center of space there are also singularities corresponding to the same set of branes wrapped on the ψ direction: M2(ψz), M5($\psi 1234$) and equal amounts of M2($\psi 1$) and M5($\psi 234z$). These branes are dipolar. There is also the KKM with special direction ψ at the center of space.

In this chapter, we will focus on three-charge themelia (with four global supercharges) carrying the charges F1(y), NS5($1234y$) and P(y) in Type IIA/M-theory. The global supersymmetries are given by:

$$\begin{aligned} &\frac{1}{2}(1 + \Gamma^{0yz})\,\xi = 0\,, \quad \frac{1}{2}(1 + \Gamma^{01234y})\,\xi = 0\,, \\ &\frac{1}{2}(1 + \Gamma^{0y})\,\xi = 0\,. \end{aligned} \tag{18.5}$$

The most general themelion projector with these charges and the dipole charges corresponding to the superstrata considered above is:

$$\begin{aligned} P = &(\alpha_1\Gamma^{0yz} + \alpha_2\Gamma^{0y1234} + \alpha_3\Gamma^{0y} + \alpha_4\Gamma^{0y1234z}) \\ &+ (\alpha_5\Gamma^{0\psi z} + \alpha_6\Gamma^{0\psi 1234} + \alpha_7\Gamma^{0\psi} + \alpha_8\Gamma^{0\psi 1234z}) \\ &+ (\alpha_9\Gamma^{0y1} + \alpha_{10}\Gamma^{0y234z}) + (\alpha_{11}\Gamma^{0\psi 1} + \alpha_{12}\Gamma^{0\psi 234z})\,, \end{aligned} \tag{18.6}$$

where the α_j can be interpreted as local charge densities divided by the mass density.

The global supercharge condition (18.5) leads to the following linear constraints:

$$\alpha_1 + \alpha_2 + \alpha_3 + \alpha_4 = 1\,, \tag{18.7}$$

$$\alpha_5 + \alpha_6 + \alpha_7 + \alpha_8 = 0\,, \tag{18.8}$$

$$\alpha_{10} = -\alpha_9\,, \quad \alpha_{11} = -\alpha_{12}\,, \tag{18.9}$$

and the projector condition $P^2 = 1$ in (18.4), leads to several quadratic conditions, which include, for example:

$$(\alpha_1\alpha_2 + \alpha_3\alpha_4 - \alpha_9^2) + (\alpha_5\alpha_6 + \alpha_7\alpha_8 - \alpha_{11}^2) = 0\,. \tag{18.10}$$

The complete solution to the *themelion constraints*, obtained using (18.6) in equations (18.4) and (18.5) is given by (F.1) and (F.2) with $\theta_2 = \frac{\pi}{2}$, $\varphi_2 = 0$.

Our first result is that: *All existing microstate geometries - both bubbling solutions and superstrata - are bound states of multiple themelia defined by* (18.6).

We find that all the themelion constraints have counterparts in the supergravity solutions. However, the relation is subtle. First, the themelion analysis is done for a non-backreacted brane probe in flat space. Thus, to link the supergravity charges to the α_i we have to arrange that themelion's environment be that of empty space: in particular one must perform large gauge transformations to eliminate all the Wilson lines along the themelion. Secondly, the themelion wraps several compact directions, whose radii affect the charge densities and hence the α_i. Since these radii typically vary across spacetime, some of the themelion constraints impose conditions on the location of the themelion itself.

Object	Coefficient	
F1(y)	α_1	x_1
NS5(y1234)	α_2	y_1
P(y)	α_3	z_1
KKm(y1234;ψ)	α_4	
D2(y1)	α_9	u_1
D4(y234)	$\alpha_{10} = -\alpha_9$	
D0	α_{13}	v_1
D4(1234)	$\alpha_{14} = -\alpha_{13}$	
F1(1)	α_{17}	w_1
P(1)	$\alpha_{18} = -\alpha_{17}$	

Object	Coefficient	
F1(ψ)	α_5	x_2
NS5(ψ1234)	α_6	y_2
P(ψ)	α_7	z_2
KKm(ψ1234;y)	α_8	
D2(ψ1)	α_{11}	u_2
D4(ψ234)	$\alpha_{12} = -\alpha_{11}$	
D2(yψ)	α_{15}	v_2
D6(yψ1234)	$\alpha_{16} = -\alpha_{15}$	
NS5(yψ234)	α_{19}	w_2
KKm(yψ234; 1)	$\alpha_{20} = -\alpha_{19}$	

Table 18.1: The Type IIA constituents and parametrization of the most general themelion with $\mathbb{T}^3$ invariance.

The simplest themelion constraint to interpret is (18.7), which reflects the fact that the mass density of the themelion is the sum of its global charge densities: $M = Q_1 + Q_2 + Q_3 + Q_4$. The parameters in the second constraint, (18.8), depend on distinct powers or the radius of the ψ-circle, and so this determines the possible locations of the themelion. In particular, for the bubbling solutions of [93, 94, 97], this constraint is equivalent to the bubble equations [1]. The last linear equations (18.9) reflect the fact that, in the six-dimensional supergravity theories used to build superstrata and bubbling solutions, the tensor fields corresponding to $\alpha_{9,10,11,12}$ must be anti-self dual.

For bubbling solutions the quadratic constraints, like (18.10), correspond to smoothness conditions, giving exactly the quadratic constraints on the sources of harmonic functions needed to construct smooth horizonless solutions of [93, 94, 97].

As we noted earlier, a superstratum is made of two themelia: one at the supertube locus and one at the center of space. Using the correspondence between parameters in branes in Table 18.1, one can see that the supertube themelion has $\alpha_{3,4,5,6,11,12} = 0$ and $\alpha_7 + \alpha_8 = \alpha_9 + \alpha_{10} = 0$. The simplest way to identify the parameters of the center-of-space themelion is to perform a "spectral inversion," $\psi \leftrightarrow y$, [134] [2] and then one sees that this themelion has $\alpha_{1,2,7,8,9,10} = 0$ and $\alpha_{11} + \alpha_{12} = \alpha_3 + \alpha_4 = 0$.

Remembering that the supertube themelion has charge densities that depend on ψ, and the center-of-space themelion has charge densities that depend on y one sees that (18.10) imposes two independent constraints on these densities. Amazingly, these are exactly the coiffuring constraints [21], which were necessary to construct smooth supergravity solutions.

[1] A similar relation between bubble equations and probe-brane constraints has been found for supertubes probing bubbling solutions [120]

[2] We note that spectral inversion is inconsistent with (18.7) and (18.8). Consistency can be restored by performing a large gauge transformation in supergravity to eliminate Wilson lines.

18.2 The hyperstratum

The themelia that enter in the construction of the superstrata actually belong to a much larger moduli space of themelia. Indeed, the Type IIB superstratum only had fields that preserve the $\mathbb{T}^4$ invariance, but when we dualize it to the Type IIA/M-Theory duality frame we use in this Chapter, it only has a $\mathbb{T}^3$ invariance, along the directions 234. This suggests one should consider a more general themelion which preserves this $\mathbb{T}^3$ invariance and has branes that can wrap $1, y, z$ and ψ. This themelion can have 20 possible species of branes:

$$\mathrm{M2}(0ab)\,,\quad \mathrm{M5}(0234ab)\,,\quad \mathrm{P}(a)\,,\quad \mathrm{KKM}(0234abc)\,, \tag{18.11}$$

where $a, b, c \in \{1, y, z, \psi\}$. The complete set of species is described in the IIA nomenclature in Table 18.1.

The projector is now constructed using $\hat{P} = P + P'$ where P is given by (18.6) and

$$\begin{aligned} P' = {} & \alpha_{13}\Gamma^{0z} + \alpha_{14}\Gamma^{01234z} + \alpha_{15}\Gamma^{0y\psi} + \alpha_{16}\Gamma^{0y\psi1234} \\ & + \alpha_{17}\Gamma^{01z} + \alpha_{18}\Gamma^{01} + \alpha_{19}\Gamma^{0y\psi234} + \alpha_{20}\Gamma^{0y\psi234z}\,. \end{aligned} \tag{18.12}$$

We find that the null-space condition (18.5) now imposes eight linear constraints on the α_j, while the projection condition yields another 15 quadratic constraints. This is a hugely overdetermined system, and if we first use the linear constraints, we can re-parametrize the system in terms of three vectors in $\mathbb{C}^3$, defined by:

$$\begin{aligned} \vec{p}_1 &\equiv (u_1 + iu_2\,, -(w_1 - iw_2)\,, x_1 + ix_2)\,, \\ \vec{p}_2 &\equiv (-i(v_1 + iv_2)\,, -i(y_1 - iy_2)\,, -i(w_1 - iw_2))\,, \\ \vec{p}_3 &\equiv (-(z_1 + iz_2)\,, -(v_1 + iv_2)\,, u_1 + iu_2)\,. \end{aligned} \tag{18.13}$$

where $(u_1, \ldots, z_2)$ are real parameters. Note that each vector p_i has an entry in common with both other vectors and so there are twelve independent real parameters and their relationship with the α_j may be found in (F.1). The projection condition, $\hat{P}^2 = \hat{P}$, is equivalent to the statement that the $\vec{p}_j$ are orthonormal in $\mathbb{C}^3$. This means that one can then use $U(3)$ to rotate the $\vec{p}_j$ to a simple canonical form:

$$\vec{p}_1{}' \equiv (0\,, 0\,, 1)\,,\ \vec{p}_2{}' \equiv (0\,, \mp i\,, 0)\,,\ \vec{p}_3{}' \equiv (\mp 1\,, 0\,, 0)\,. \tag{18.14}$$

Note that this basis corresponds to $x_1 = 1$, $y_1 = z_1 = \pm 1$, with all the other parameters set to zero. From (F.1) one sees that this themelion corresponds to $\alpha_1 = 1$ (for $+$), or $\alpha_4 = 1$ (for $-$) with all the other α_j vanishing. Thus a $U(3)$ U-duality rotation can *locally* map this themelion onto a stack of F1 strings or a stack of coincident KKM's.

Using the U(3) one can parametrize the most general themelion, remembering that the rotation must be restricted by the constraints on interrelated components of the $\vec{p}_i$ in (18.13). The result is a six parameter family, (F.2), given by the angles, $\theta_1, \theta_2, \varphi_j$, $j = 1, 2, 3, 4$. As noted earlier, the projector of the supertube-locus themelion of the superstratum solution, based on (18.6), is given by $v_j = w_j = 0$, or $\theta_2 = \frac{\pi}{2}$ and $\varphi_2 = 0$.

It is not hard to see that our general themelion also include the themelia that enter the construction of the vector superstratum of [131] of which a subset can be built using only NS-NS fields. The "supertube-locus" themelion of these NS-NS vector superstratum is obtained by taking $u_j = v_j = 0$, or $\theta_2 = 0$.

To obtain a themelion with no components in the space-time (ψ) directions, a glance at Table 18.1 reveals that one must remove all the constituents in the second column, and hence all the second components must vanish. This is achieved by setting all the φ-phases in (F.2) to zero. This leaves a themelion with:

$$\begin{aligned} P =&(\beta_1\,\Gamma^{0yz} + \beta_2\,\Gamma^{01234y} + \beta_3\,\Gamma^{0y}) + \beta_4\,(\Gamma^{0z} - \Gamma^{01234z}) \\ &+ \beta_5\,(\Gamma^{01} - \Gamma^{01z}) + \beta_6\,(\Gamma^{01y} + \Gamma^{0234yz})\,. \end{aligned}$$

and

$$\begin{aligned} &\beta_1 = \cos^2\frac{1}{2}\theta_1\,,\ \ \beta_2 = \sin^2\frac{1}{2}\theta_1\sin^2\theta_2\,,\ \ \beta_3 = \sin^2\frac{1}{2}\theta_1\cos^2\theta_2\,, \\ &\beta_4 = \sin^2\frac{1}{2}\theta_1\sin\theta_2\cos\theta_2\,,\ \ \beta_5 + i\beta_6 = \frac{1}{2}\sin\theta_1\,e^{i\theta_2}\,. \end{aligned}$$

Amazingly, this is the projector of the super-maze [43]. Hence, the class of themelia we obtain from $\hat{P}$ contains the themelia that govern both the original and vector superstrata, as well as the super-maze themelion. Based on the Themelion Conjecture, we expect there to be supergravity solutions made of multiple generalized themelia, which we can call *hyperstrata*. These will contain all the existing superstrata and super-mazes. Since the momentum charge is carried by different excitations in the superstrata and the super-maze, we expect the *hyperstrata* to have a larger entropy than either subclass.

Moreover, it was argued in [43] that, because the super-maze captures brane fractionation, its entropy is expected to match that of the rotationally-invariant microstates of the black hole, $2\pi\sqrt{\frac{5}{6}Q_1Q_5Q_P}$. The *hyperstratum* will capture these microstates as well those that break the spacetime rotational invariance of the black-hole horizon. Given that the hyperstratum captures fractionation and restores democracy between the y-circle and a generic torus direction, we expect it to match the full black-hole entropy. It would be exciting to construct some *hyperstratum* solutions, to see whether this intuition is realized.

By breaking the torus invariance, we have found themelia that capture fractionated branes, and perhaps the full black-hole entropy. It is thus natural ask how the phase space of themelia will expand if we relax the $\mathbb{T}^3$ invariance imposed here and allow all possible branes wrapping the compactified dimensions. Given that the generic super-maze breaks this invariance, we suspect that relaxing the $\mathbb{T}^3$ invariance will lead to a phase space that is a combination of all superstrata and generic supermazes.

Armed with our knowledge of themelia and hyperstrata, we return to the resolution of a seeming paradox of the original superstratum: its moduli space appears to have a degenerate limit to a BTZ black hole with finite horizon area [20, 21], and yet a themelion cannot have a horizon. This degenerate limit arises when one forces the two themelia of the superstratum to coincide. One of these themelia has only ψ fluctuations and a KKM that shrinks y, while the other one has only y fluctuations and a KKM that shrinks ψ.

Forcing these two themelia to coincide turns off both the ψ and y fluctuations, and either requires one to set the momentum charge to zero, or results in a configuration that is not a themelion.

However, we have seen that the themelia that give rise to the superstratum are part of a much larger family of themelia that can fluctuate not only along ψ and y, but also along z and the torus directions. The hyperstratum is built from these more generic themelia, and the coincidence limit is no longer degenerate: the momentum charge can be carried by fluctuations along z and the torus, and the resulting configuration will be another horizonless themelion, the super-maze. The presence of a black hole in the phase space of superstratum solutions is an artifact of objects made from enforcing $\mathbb{T}^4$ invariance and *smearing* the themelia. This illustrates, once again, the fuzzball precept: horizons only appear because of ensemble averaging.

Appendices

Appendix A

General solutions of the single-mode BPS equations

Here we explicitly present the general solutions to the fields that remain undetermined at the end of Section 11.2.3. These can be obtained from (10.51), (10.54) and (11.17) with the already derived solutions for λ_1, μ_1, μ_2, k and Ω_1. The equations imply that Ω_1 is constant, and we assume here that we are in a gauge where

$$\Omega_1 \equiv 1\,. \tag{A.1}$$

$$\nu = \sqrt{\frac{\sigma}{1-\xi^2}\left(1 - \frac{\left(\xi^{q_2}(1-\gamma_1\,\xi^{2\,q_1}) + \beta\,\xi^{q_1}(1-\gamma_2\,\xi^{2\,q_2})\right)^2}{\left(\xi^{q_2}(1-\gamma_1\,\xi^{2\,q_1}) - \beta\,\xi^{q_1}(1-\gamma_2\,\xi^{2\,q_2})\right)^2}\right)}, \tag{A.2}$$

$$\begin{aligned}\Phi_1 = \frac{1}{2}\Bigg(&\frac{c_5}{1-\gamma_1\,\xi^{2\,q_1}} - \frac{c_4}{1-\gamma_2\,\xi^{2\,q_2}} + \frac{(1+\gamma_1\,\xi^{2\,q_1})}{2(1-\gamma_1\,\xi^{2\,q_1})}\big((c_5-2)q_1\,\log\xi + c_7\big)\\ &-\frac{(1+\gamma_2\,\xi^{2\,q_2})}{2(1-\gamma_2\,\xi^{\,2\,q_2})}\big((c_4+2)q_2\,\log\xi + c_6\big) - \frac{\sigma}{2}\Bigg)^{-1},\end{aligned} \tag{A.3}$$

$$\begin{aligned}\Phi_2 = \frac{1}{2}\Bigg(1 - \Bigg[&\frac{\sigma\big(\xi^{q_2}(1-\gamma_1\,\xi^{2\,q_1}) + \beta\,\xi^{q_1}(1-\gamma_2\,\xi^{2\,q_2})\big)}{2\big(\xi^{q_2}(1-\gamma_1\xi^{2\,q_1}) - \beta\,\xi^{q_1}(1-\gamma_2\,\xi^{2\,q_2})\big)} - \frac{c_5}{1-\gamma_1\,\xi^{2\,q_1}} - \frac{c_4}{1-\gamma_2\,\xi^{2\,q_2}}\\ &-\frac{(1+\gamma_1\,\xi^{2\,q_1})}{2(1-\gamma_1\,\xi^{2\,q_1})}\big((c_5-2)q_1\,\log\xi + c_7\big) - \frac{(1+\gamma_2\,\xi^{2\,q_2})}{2(1-\gamma_2\,\xi^{\,2\,q_2})}\big((c_4+2)q_2\,\log\xi + c_6\big)\Bigg]^{-1}\Bigg),\end{aligned} \tag{A.4}$$

$$\begin{aligned}\Psi_1 = \frac{1}{4}\Big(q_2 - \frac{2\,q_2}{1-\gamma_2\,\xi^{2\,q_2}} - q_1 - \frac{2\,q_1}{1-\gamma_1\,\xi^{2\,q_1}}\Big) - \Bigg[&\big((c_4+2)\,q_2\,\log\xi + c_4 + c_6\big)\frac{q_2\,\gamma_2\,\xi^{2\,q_2}}{(1-\gamma_2\,\xi^{2\,q_2})^2}\\ +\frac{1}{2}\frac{c_4\,q_2}{1-\gamma_2\,\xi^{2\,q_2}} + \big((c_5-2)\,q_1\,\log\xi + c_5 + c_7\big)&\frac{q_1\,\gamma_1\,\xi^{2\,q_1}}{(1-\gamma_1\,\xi^{2\,q_1})^2} + \frac{1}{2}\,\frac{c_5\,q_1}{1-\gamma_1\,\xi^{2\,q_1}} + c_8\Bigg]\times\\ \times\frac{1}{2}\Bigg(&\frac{c_5}{1-\gamma_1\,\xi^{2\,q_1}} - \frac{c_4}{1-\gamma_2\,\xi^{2\,q_2}} + \frac{(1+\gamma_1\,\xi^{2\,q_1})}{2(1-\gamma_1\,\xi^{2\,q_1})}\big((c_5-2)q_1\,\log\xi + c_7\big)\\ &-\frac{(1+\gamma_2\,\xi^{2\,q_2})}{2(1-\gamma_2\,\xi^{\,2\,q_2})}\big((c_4+2)q_2\,\log\xi + c_6\big) - \frac{\sigma}{2}\Bigg)^{-1},\end{aligned} \tag{A.5}$$

$$\Psi_2 = -\frac{1}{2} + \frac{q_1+q_2}{4} + \frac{q_1}{4}\Big[\frac{2\,\xi^{2\,q_2}(1-\gamma_1^2\,\xi^{4\,q_1})}{\xi^{2\,q_2}(1-\gamma_1\,\xi^{2\,q_1})^2-\beta^2\,\xi^{2\,q_1}(1-\gamma_2\,\xi^{2\,q_2})^2} + \frac{2}{1-\gamma_1\,\xi^{2\,q_1}} - 4\Big]$$
$$+\frac{q_2}{4}\Big[\frac{2}{1-\gamma_2\,\xi^{2\,q_2}} - \frac{2\,\beta^2\,\xi^{2\,q_1}(1-\gamma_2^2\,\xi^{4\,q_2})}{\xi^{2\,q_2}(1-\gamma_1\,\xi^{2\,q_1})^2-\beta^2\xi^{2\,q_1}(1-\gamma_2\,\xi^{2\,q_2})^2} - 4\Big]$$
$$+\frac{\gamma_2\,\xi^{2\,q_2}(2\,\gamma_1(q_1-q_2)(q_1+q_2)^2\xi^{2\,q_1}+\gamma_1^2\,q_2^2(2\,q_1+q_2)\,\xi^{4\,q_1}+q_2^3)-\gamma_1\,q_1^2\,\xi^{2\,q_1}(q_1+\gamma_2^2\,\xi^{4\,q_2}(q_1+2\,q_2))}{2\,\gamma_2\,q_2^2\,\xi^{2\,q_2}(1-\gamma_1\,\xi^{2\,q_1})^2-2\,\gamma_1\,q_1^2\xi^{2\,q_1}(1-\gamma_2\,\xi^{2\,q_2})^2}$$
$$+\frac{1}{2}\Big[\big((c_4+2)\,q_2\,\log\xi+c_4+c_6\big)\frac{q_2\,\gamma_2\,\xi^{2\,q_2}}{(1-\gamma_2\,\xi^{2\,q_2})^2} + \frac{1}{2}\frac{c_4\,q_2}{1-\gamma_2\,\xi^{2\,q_2}} + \frac{1}{2}\,\frac{c_5\,q_1}{1-\gamma_1\,\xi^{2\,q_1}} + c_8$$
$$+\big((c_5-2)\,q_1\,\log\xi+c_5+c_7\big)\frac{q_1\,\gamma_1\,\xi^{2\,q_1}}{(1-\gamma_1\,\xi^{2\,q_1})^2}\Big]\times\Big[\frac{\sigma\big(\xi^{q_2}(1-\gamma_1\,\xi^{2\,q_1})+\beta\,\xi^{q_1}(1-\gamma_2\,\xi^{2\,q_2})\big)}{2\big(\xi^{q_2}(1-\gamma_1\xi^{2\,q_1})-\beta\,\xi^{q_1}(1-\gamma_2\,\xi^{2\,q_2})\big)} - \frac{c_5}{1-\gamma_1\,\xi^{2\,q_1}}$$
$$-\frac{c_4}{1-\gamma_2\,\xi^{2\,q_2}} - \frac{(1+\gamma_1\,\xi^{2\,q_1})}{2(1-\gamma_1\,\xi^{2\,q_1})}\big((c_5-2)q_1\,\log\xi+c_7\big) - \frac{(1+\gamma_2\,\xi^{2\,q_2})}{2(1-\gamma_2\,\xi^{\,2\,q_2})}\big((c_4+2)q_2\,\log\xi+c_6\big)\Big]^{-1}, \tag{A.6}$$

$$\Omega_0 = \Big[\frac{(1-\xi^2)^2\big(\gamma_2\,q_2^2\,\xi^{2\,q_2}(1-\gamma_1\xi^{2\,q_1})^2-\gamma_1\,q_1^2\,\xi^{2\,q_1}(1-\gamma_2\,\xi^{2\,q_2})^2\big)}{4\,\xi^2(1-\gamma_1\,\xi^{2\,q_1})^2(1-\gamma_2\,\xi^{2\,q_2})^2}\times$$
$$\times\Big(\frac{2\,c_5}{1-\gamma_1\,\xi^{2\,q_1}} - \frac{2\,c_4}{1-\gamma_2\,\xi^{2\,q_2}} - \sigma + \frac{(1+\gamma_1\,\xi^{2q_1})}{1-\gamma_1\,\xi^{2\,q_1}}\big((c_5-2)q_1\,\log\xi+c_7\big)$$
$$-\frac{(1+\gamma_2\,\xi^{2\,q_2})}{1-\gamma_2\,\xi^{2\,q_2}}\big((c_4+2)q_2\,\log\xi+c_6\big)\Big)\times\Big(-\frac{2\,c_5}{1-\gamma_1\,\xi^{2\,q_1}} - \frac{2\,c_4}{1-\gamma_2\,\xi^{2\,q_2}}$$
$$-\frac{(1+\gamma_1\,\xi^{2q_1})}{1-\gamma_1\,\xi^{2\,q_1}}\big((c_5-2)q_1\,\log\xi+c_7\big) - \frac{(1+\gamma_2\,\xi^{2\,q_2})}{1-\gamma_2\,\xi^{2\,q_2}}\big((c_4+2)q_2\,\log\xi+c_6\big)$$
$$+\frac{\sigma\big(\xi^{q_2}(1-\gamma_1\,\xi^{2\,q_1})+\beta\,\xi^{q_1}(1-\gamma_2\,\xi^{2\,q_2})\big)}{\xi^{q_2}(1-\gamma_1\,\xi^{2\,q_1})-\beta\,\xi^{q_1}(1-\gamma_2\,\xi^{2\,q_2})}\Big)\Big]^{1/2}. \tag{A.7}$$

Appendix B

Reduced equations on special locus

The definition of the special locus in supergravity is introduced in Section 12.2.3, and its consequences in the double-mode truncation are explored in Section 12.3.2. In this Appendix we derive the consequences of these properties on the equations of motion. For completeness, we will restate the relations characterizing it, namely:

$$\begin{aligned} \mu_{1,2} = \lambda_{1,2} &= \frac{1}{2}\log\Big(1 - \frac{1-\xi^2}{2}\nu_{1,2}^2\Big), \\ m_5 &= -\frac{1}{2}(1-\xi^2)\,\nu_1\,\nu_2, \quad m_6 = 0, \end{aligned} \tag{B.1}$$

The matrix m, (9.28), is thus given by

$$m \;=\; \begin{pmatrix} 1-\frac{1}{2}(1-\xi^2)\,\nu_1^2 & 0 & -\frac{1}{2}(1-\xi^2)\,\nu_1\,\nu_2 & 0 \\ 0 & 1 & 0 & 0 \\ -\frac{1}{2}(1-\xi^2)\,\nu_1\,\nu_2 & 0 & 1-\frac{1}{2}(1-\xi^2)\,\nu_2^2 & 0 \\ 0 & 0 & 0 & 1 \end{pmatrix}, \tag{B.2}$$

with only one non-trivial eigenvalue, given by

$$m_0 = 1 - \frac{1}{2}\,\chi_I\chi_I = 1 - \frac{1}{2}(1-\xi^2)\big(\nu_1^2+\nu_2^2\big)\,. \tag{B.3}$$

Moreover, χ is a null vector of $\widetilde{F}$

$$\widetilde{F}_{\mu\nu}{}^{IJ}\,\chi_J \;=\; 0\,, \tag{B.4}$$

which results in the following algebraic relation between the gauge fields

$$\Phi_4\,\Psi_2 + \Phi_3\,\Psi_1 - \Phi_1\,\Psi_3 - \Phi_2\,\Psi_4 = 0. \tag{B.5}$$

Substituting the relations above in the equations of motion leads to a reduced set of "almost BPS" equations. The procedure is tedious, so we will only present the final results. It will prove convenient to define the following complex vectors:

$$\mathcal{V}^F \;=\; \begin{pmatrix} F_1 + iF_4 \\ 0 \\ -F_3 + iF_2 \\ 0 \end{pmatrix}, \qquad \mathcal{V}^\Phi \;=\; \begin{pmatrix} \Phi_1 + i\Phi_4 \\ 0 \\ -\Phi_3 + i\Phi_2 \\ 0 \end{pmatrix}. \tag{B.6}$$

where the functions F_j have been defined in (10.59). We will also define

$$\Lambda = 2\,m_0 = 2 - (1-\xi^2)\big(\nu_1^2 + \nu_2^2\big)\,. \tag{B.7}$$

The gauge fields all satisfy first-order linear ODEs:

$$\xi\partial_\xi(\Phi_1 + i\Phi_4) = \frac{\sqrt{1-\xi^2}\,\nu_2}{\Lambda}\,\Omega_1(i\chi_I)\mathcal{V}_I^F, \qquad \xi\partial_\xi(\Phi_3 - i\Phi_2) = \frac{\sqrt{1-\xi^2}\,\nu_1}{\Lambda}\,\Omega_1(i\chi_I)\mathcal{V}_I^F,$$

$$\xi\partial_\xi(\Psi_1 + i\Psi_4) = \frac{\sqrt{1-\xi^2}\,\nu_2}{\Lambda}\,\Omega_1(i\chi_I)\bigg(\frac{k}{1-\xi^2}\mathcal{V}_I^F + H_0\mathcal{V}_I^\Phi\bigg),$$

$$\xi\partial_\xi(\Psi_3 - i\Psi_2) = \frac{\sqrt{1-\xi^2}\,\nu_1}{\Lambda}\,\Omega_1(i\chi_I)\bigg(\frac{k}{1-\xi^2}\mathcal{V}_I^F + H_0\mathcal{V}_I^\Phi\bigg).$$

The above equations also imply:

$$\begin{aligned} &\nu_1\,\Phi_1' - \nu_2\,\Phi_3' = 0, \qquad &&\nu_2\,\Phi_2' + \nu_1\,\Phi_4' = 0,\\ &\nu_1\,\Psi_1' - \nu_2\,\Psi_3' = 0, \qquad &&\nu_2\,\Psi_2' + \nu_1\,\Psi_4' = 0. \end{aligned} \tag{B.8}$$

The equation for k is also first-order and linear:

$$\Omega_1\,\xi\partial_\xi\bigg(\frac{k}{1-\xi^2}\bigg) + 8\big(\Phi_1\,\Phi_2 + \Phi_3\,\Phi_4 - \kappa\big)H_0 = 0, \tag{B.9}$$

where κ is a constant of integration, that can be determined order by order in the perturbative expansion using the regularity constraints. One can also derive a first-order equation for H_0, and through it the metric fields Ω_0 and Ω_1:

$$\Omega_1\,\xi\partial_\xi\log(H_0) - 8\big(\Phi_1\,F_2 + \Phi_2\,F_1 + \Phi_3\,F_4 + \Phi_4\,F_3\big) - 16\kappa\frac{k}{1-\xi^2} + \varpi = 0, \tag{B.10}$$

where ϖ is another constant of integration. The metric sector of the equations does not fully reduce to first-order, hence one has to complement (B.10) with the second-order equation of motion for Ω_1:

$$2\,\frac{\xi\partial_\xi(\xi\partial_\xi\Omega_1)}{\Omega_1 H_0} \;-\; 2\,\frac{\Lambda+2}{\Lambda}\,\Omega_1^2 \;+\; H_0^{-2}\bigg(\xi\partial_\xi\frac{k}{1-\xi^2}\bigg)^2 - \frac{8}{\Lambda}\big|\chi_I\mathcal{V}_I^\Phi\big|^2 = 0. \tag{B.11}$$

Finally, we need equations for $\nu_{1,2}$. One can derive a Wronskian type of constraint for them:

$$\frac{\xi(1-\xi^2)\Omega_1}{\Lambda}\big(\nu_2\,\nu_1' - \nu_1\,\nu_2'\big) = 4\,\big(\Phi_4\,\Psi_1 - \Phi_1\,\Psi_4 + \Phi_3\,\Psi_2 - \Phi_2\,\Psi_3\big), \tag{B.12}$$

which is to be supplemented by one second-order differential equation from the equations of motion of ν_1 and ν_2, that we can write in terms of the eigenvalue Λ:

$$\xi\partial_\xi(\xi\partial_\xi\Lambda) + \frac{3\Lambda-4}{2\Lambda(2-\Lambda)}(\xi\partial_\xi\Lambda)^2 + (\xi\partial_\xi\log\Omega_1)(\xi\partial_\xi\Lambda) - 8\,\big|\chi_I\mathcal{V}_I^F\big|^2 + 8H_0\,\big|\chi_I\mathcal{V}_I^\Phi\big|^2 \tag{B.13}$$

$$+\,32\frac{\Lambda^2}{(2-\Lambda)\Omega_1^2}(\Phi_1\Psi_4 + \Phi_2\Psi_3 - \Phi_3\Psi_2 - \Phi_4\Psi_1)^2 + 2(2-\Lambda)\Omega_1^2 H_0 \;=\; 0\,, \tag{B.14}$$

Appendix C

Uplift to six dimensions

The solutions of the three-dimensional gauged supergravity can be uplifted to type IIB supergravity compactified on a four-dimensional compact space $\mathcal{M}$, which can be either $\mathbb{T}^4$ or $K3$. The latter is the appropriate framework to interpret the solutions as bound states of D1 and D5 branes and to perform the holographic analysis. The compact space $\mathcal{M}$ plays a trivial role in our solutions and one can conveniently focus on the remaining six-dimensional directions, which we describe, following [36, 53, 135], by the 6D Einstein metric ds_6^2, the three-forms $G^{(I)}$ and the scalars $\phi^{(mr)}$. In our solutions the only non-trivial fields sit in the gravity multiplet, which contains the three-form $G^{(5)}$, and two tensor multiplets, which add two more three-forms, $G^{(6)}$, $G^{(7)}$, and two scalars, $\phi^{(56)}$, $\phi^{(57)}$. From the ten-dimensional perspective the non-trivial fields are: the RR forms, C_0, C_2, C_4, the NSNS two-form, B_2, the dilaton, Φ, and the volume of $\mathcal{M}$, V_4; since the RR four-form has only a component along $\mathcal{M}$, plus the 6D component needed for self-duality, we will simply denote by C_4 the scalar giving its $\mathcal{M}$-component; we will also denote by C_6 the two-form in 6D obtained by reducing on $\mathcal{M}$ the six-form dual to C_2. The four scalars, ϕ, V_4, C_0, C_4, are related by

$$C_4 = \frac{e^{2\Phi} C_0}{e^{2\Phi} C_0^2 + 1}\,, \quad V_4^2 = \frac{e^{2\Phi}}{e^{2\Phi} C_0^2 + 1}\,. \tag{C.1}$$

The relation between the 10D and 6D quantities is

$$\phi^{(56)} = \frac{1}{2}\left[\sqrt{\frac{Q_5}{Q_1}\frac{C_4}{C_0}} - \sqrt{\frac{Q_1}{Q_5}\frac{C_0}{C_4}}\right], \quad \phi^{(57)} = \sqrt{C_0 C_4}\,, \tag{C.2}$$

$$G^{(5)} = \frac{Q_1 G^{(1)} + Q_5 G^{(2)}}{2Q_1 Q_5}\,, \quad G^{(6)} = \frac{Q_1 G^{(1)} - Q_5 G^{(2)}}{2Q_1 Q_5}\,, \quad G^{(7)} = -\frac{G^{(4)}}{\sqrt{Q_1 Q_5}}\,, \tag{C.3}$$

with

$$G^{(1)} = \frac{1}{2} dC_2\,, \quad G^{(2)} = \frac{1}{2} dC_6\,, \quad G^{(4)} = -\frac{1}{2} dB_2\,; \tag{C.4}$$

Q_1 and Q_5 are the D1 and D5 supergravity charges that determine the magnetic (S^3) components of the three-forms at infinity: $G^{(1)}|_{S^3} \to Q_5$, $G^{(2)}|_{S^3} \to Q_1$.

The general uplift formulas were given in [27]: we would like to make these formulas explicit for the Q-ball truncations introduced in Chapter 9; we will work in the axial gauge specified by the functions in (9.32). It is convenient to define

$$\Gamma_i = e^{\lambda_i}\cos^2\varphi_i + e^{-\lambda_i}\sin^2\varphi_i \quad (i=1,2)\,, \tag{C.5}$$

$$\Delta = e^{\mu_1}\Gamma_1\sin^2\theta + e^{\mu_2}\Gamma_2\cos^2\theta + 2\left(m_5\cos\varphi_1\cos\varphi_2 + m_6\sin\varphi_1\sin\varphi_2\right)\sin\theta\cos\theta\,, \tag{C.6}$$

$$\det(m) = (e^{\mu_1+\mu_2} - e^{-\lambda_1-\lambda_2}m_5^2)(e^{\mu_1+\mu_2} - e^{\lambda_1+\lambda_2}m_6^2)\,, \tag{C.7}$$

$$X = \sqrt{1-\xi^2}\left(\nu_1\cos\varphi_1\sin\theta + \nu_2\cos\varphi_2\cos\theta\right). \tag{C.8}$$

Then the 6D Einstein metric is

$$ds_6^2 = (\det(m))^{-1/2}\,\Delta^{1/2}\,ds_3^2 + R_{AdS}^2\,(\det(m))^{1/2}\,\Delta^{-1/2}\left(G_{\alpha\beta}\,\mathcal{D}y^\alpha\,\mathcal{D}y^\beta\right)\,, \tag{C.9}$$

where ds_3^2 is defined in (7.18), the components of the S^3 metric are

$$\begin{aligned} G_{\theta\theta} &= e^{\mu_2}\left[\frac{e^{-\lambda_1}\cos^2\varphi_1}{e^{\mu_1+\mu_2}-e^{-\lambda_1-\lambda_2}m_5^2} + \frac{e^{\lambda_1}\sin^2\varphi_1}{e^{\mu_1+\mu_2}-e^{\lambda_1+\lambda_2}m_6^2}\right]\cos^2\theta \\ &+ e^{\mu_1}\left[\frac{e^{-\lambda_2}\cos^2\varphi_2}{e^{\mu_1+\mu_2}-e^{-\lambda_1-\lambda_2}m_5^2} + \frac{e^{\lambda_2}\sin^2\varphi_2}{e^{\mu_1+\mu_2}-e^{\lambda_1+\lambda_2}m_6^2}\right]\sin^2\theta \\ &+ 2\left[\frac{e^{-\lambda_1-\lambda_2}\,m_5\cos\varphi_1\cos\varphi_2}{e^{\mu_1+\mu_2}-e^{-\lambda_1-\lambda_2}m_5^2} + \frac{e^{\lambda_1+\lambda_2}\,m_6\sin\varphi_1\sin\varphi_2}{e^{\mu_1+\mu_2}-e^{\lambda_1+\lambda_2}m_6^2}\right]\sin\theta\cos\theta\,, \end{aligned} \tag{C.10a}$$

$$G_{\varphi_1\varphi_1} = e^{\mu_2}\left[\frac{e^{-\lambda_1}\sin^2\varphi_1}{e^{\mu_1+\mu_2}-e^{-\lambda_1-\lambda_2}m_5^2} + \frac{e^{\lambda_1}\cos^2\varphi_1}{e^{\mu_1+\mu_2}-e^{\lambda_1+\lambda_2}m_6^2}\right]\sin^2\theta\,, \tag{C.10b}$$

$$G_{\varphi_2\varphi_2} = e^{\mu_1}\left[\frac{e^{-\lambda_2}\sin^2\varphi_2}{e^{\mu_1+\mu_2}-e^{-\lambda_1-\lambda_2}m_5^2} + \frac{e^{\lambda_2}\cos^2\varphi_2}{e^{\mu_1+\mu_2}-e^{\lambda_1+\lambda_2}m_6^2}\right]\cos^2\theta\,, \tag{C.10c}$$

$$\begin{aligned} G_{\theta\varphi_1} &= e^{\mu_2}\left[-\frac{e^{-\lambda_1}}{e^{\mu_1+\mu_2}-e^{-\lambda_1-\lambda_2}m_5^2} + \frac{e^{\lambda_1}}{e^{\mu_1+\mu_2}-e^{\lambda_1+\lambda_2}m_6^2}\right]\sin\varphi_1\cos\varphi_1\sin\theta\cos\theta \\ &+ \left[-\frac{e^{-\lambda_1-\lambda_2}\,m_5\sin\varphi_1\cos\varphi_2}{e^{\mu_1+\mu_2}-e^{-\lambda_1-\lambda_2}m_5^2} + \frac{e^{\lambda_1+\lambda_2}\,m_6\cos\varphi_1\sin\varphi_2}{e^{\mu_1+\mu_2}-e^{\lambda_1+\lambda_2}m_6^2}\right]\sin^2\theta\,, \end{aligned} \tag{C.10d}$$

$$\begin{aligned} G_{\theta\varphi_2} &= e^{\mu_1}\left[\frac{e^{-\lambda_2}}{e^{\mu_1+\mu_2}-e^{-\lambda_1-\lambda_2}m_5^2} - \frac{e^{\lambda_2}}{e^{\mu_1+\mu_2}-e^{\lambda_1+\lambda_2}m_6^2}\right]\sin\varphi_2\cos\varphi_2\sin\theta\cos\theta \\ &+ \left[\frac{e^{-\lambda_1-\lambda_2}\,m_5\cos\varphi_1\sin\varphi_2}{e^{\mu_1+\mu_2}-e^{-\lambda_1-\lambda_2}m_5^2} - \frac{e^{\lambda_1+\lambda_2}\,m_6\sin\varphi_1\cos\varphi_2}{e^{\mu_1+\mu_2}-e^{\lambda_1+\lambda_2}m_6^2}\right]\sin^2\theta\,, \end{aligned} \tag{C.10e}$$

$$G_{\varphi_1\varphi_2} = -\left[\frac{e^{-\lambda_1-\lambda_2}m_5\,\sin\varphi_1\sin\varphi_2}{e^{\mu_1+\mu_2}-e^{-\lambda_1-\lambda_2}m_5^2} + \frac{e^{\lambda_1+\lambda_2}m_6\,\cos\varphi_1\cos\varphi_2}{e^{\mu_1+\mu_2}-e^{\lambda_1+\lambda_2}m_6^2}\right]\sin\theta\cos\theta\,, \tag{C.10f}$$

and the S^3 one-forms are

$$\mathcal{D}y^\alpha = dy^\alpha - K^\alpha_{IJ}\,\tilde{A}^{IJ}\,, \tag{C.11}$$

with $K^\alpha_{IJ} = -K^\alpha_{IJ}$ the S^3 Killing vectors

$$
\begin{aligned}
K_{12} &= \frac{\partial}{\partial\varphi_1}\,,\ K_{34} = \frac{\partial}{\partial\varphi_2}\,,\\
K_{13} &= \cos\varphi_1\cos\varphi_2\,\frac{\partial}{\partial\theta} - \sin\varphi_1\cos\varphi_2\cot\theta\,\frac{\partial}{\partial\varphi_1} + \cos\varphi_1\sin\varphi_2\tan\theta\,\frac{\partial}{\partial\varphi_2}\,,\\
K_{14} &= \cos\varphi_1\sin\varphi_2\,\frac{\partial}{\partial\theta} - \sin\varphi_1\sin\varphi_2\cot\theta\,\frac{\partial}{\partial\varphi_1} - \cos\varphi_1\cos\varphi_2\tan\theta\,\frac{\partial}{\partial\varphi_2}\,,\\
K_{23} &= \sin\varphi_1\cos\varphi_2\,\frac{\partial}{\partial\theta} + \cos\varphi_1\cos\varphi_2\cot\theta\,\frac{\partial}{\partial\varphi_1} + \sin\varphi_1\sin\varphi_2\tan\theta\,\frac{\partial}{\partial\varphi_2}\,,\\
K_{24} &= \sin\varphi_1\sin\varphi_2\,\frac{\partial}{\partial\theta} + \cos\varphi_1\sin\varphi_2\cot\theta\,\frac{\partial}{\partial\varphi_1} - \sin\varphi_1\cos\varphi_2\tan\theta\,\frac{\partial}{\partial\varphi_2}\,.
\end{aligned}
\tag{C.12}
$$

All the scalars can be reconstructed from the dilaton and axion, which are given by

$$
e^{2\Phi} = \frac{Q_1}{4Q_5}\,\frac{(X^2+2\Delta)^2}{\Delta} \quad,\quad C_0 = \sqrt{\frac{2Q_5}{Q_1}}\,\frac{X}{X^2+2\Delta}\,. \tag{C.13}
$$

Formulas for the three-forms are considerably more cumbersome. We will only give the results that are used in the holographic computation, i.e. the components, $G^{(I)}|_{S^3}$, of the three-forms along the S^3 (divided by the volume of the round S^3) for the restricted ansatz with $\mu_2 = \lambda_2 = \nu_2 = m_5 = m_6 = \Phi_3 = \Psi_3 = \Phi_4 = \Psi_4 = 0$:

$$
G^{(1)}|_{S^3} = \frac{Q_5\,e^{\mu_1}}{\Delta}\left[\frac{e^{\lambda_1}+e^{-\lambda_1}}{2} - \frac{e^{\mu_1}(e^{2\lambda_1}\cos^2\varphi_1 + e^{-2\lambda_1}\sin^2\varphi_1) - e^{\mu_2}\Gamma_1}{\Delta}\sin^2\theta\right]\,, \tag{C.14a}
$$

$$
\begin{aligned}
G^{(2)}|_{S^3} = Q_1 - \frac{Q_1}{2}(1-\xi^2)\nu_1^2\Big[&e^{\mu_2}\left(\frac{\cos 2\theta}{\Delta} - \frac{e^{\mu_1}\Gamma_1 - e^{\mu_2}}{\Delta^2}\sin^2\theta\cos^2\theta\right)\cos^2\varphi_1\\
&- \frac{1}{4}\frac{\partial}{\partial\varphi_1}\left(\frac{\sin(2\varphi_1)}{\Delta}\right)(e^{\mu_1-\lambda_1}\sin^2\theta + e^{\mu_2}\cos^2\theta)\Big]\,,
\end{aligned}
\tag{C.14b}
$$

$$
G^{(7)}|_{S^3} = X\frac{e^{\mu_1}}{2\sqrt{2}\Delta}\left[e^{-\lambda_1} - 2\frac{(e^{\mu_1}+e^{\mu_2}\Gamma_1)\sin^2\theta + e^{\mu_2}(e^{\lambda_1}+e^{-\lambda_1})\cos^2\theta)}{\Delta}\right]\,. \tag{C.14c}
$$

Appendix D

$\mathbb{Z}_2$ symmetric beta class equations for numerics

Here are the equations for the $\mathbb{Z}_2$ symmetric case of the beta class of solutions - that is, $n_1 = n_2 = n$, $\beta_1 = \beta_2 = \beta$ and $\mu_1 = \mu_2$, $\lambda_1 = \lambda_2$, $\Phi_1 = \Phi_2$ and $\Psi_1 = \Psi_2$. For numerical convenience, we have defined $k = \xi\,\kappa$. The equations follow:

$$E_{\mu_1} \equiv \xi\,(1-\xi^2)^2\,\Omega_0^2\,\Omega_1\,\partial_\xi\big(\xi\,\Omega_1\,\mu_1'\big) - 4\,e^{2\,\mu_1}(1-\xi^2)^2\,\Omega_1^2\big(\xi\,\kappa\,\Phi_1' - (1-\xi^2)\,\Psi_1'\big)^2$$
$$+4\,e^{2\,\mu_1}\,\xi^2(1-\xi^2)^2\Omega_0^2\,\Phi_1'^2 + 4\,e^{-4\,\mu_1}\xi^2\,\Omega_0^4\,\Omega_1^2\,\big(1-e^{2\,\mu_1}\big) = 0,$$

$$E_{\lambda_1} \equiv \xi\,(1-\xi^2)^2\,\Omega_1\,\partial_\xi\big(\xi\,\Omega_1\,\lambda_1'\big) - 2\,\sinh\big(2\,\lambda_1\big)\Big(4\,\Omega_1^2\,\big(\xi\,\kappa\,\Phi_1 - (1-\xi^2)\,\Psi_1\big)^2 - 4\,\xi^2\Omega_0^2\,\Phi_1^2\Big) = 0,$$

$$E_{\Phi_1} \equiv -4\,\xi^2\,\sinh\big(\lambda_1\big)^2\,\Phi_1\,\Omega_0^4\,\Omega_1 + e^{2\,\mu_1}\,\xi\,(1-\xi^2)^2\,\Omega_0^2\,\Big(-\xi\,\Phi_1'\,\Omega_1' + \Omega_1\,\big((1+2\,\xi\,\mu_1')\,\Phi_1' + \xi\,\Phi_1''\big)\Big)$$
$$-(1-\xi^2)\,\Omega_1^2\,\Big[-2\,\xi\,\Omega_0^2\,\big(\xi\,\kappa\,\Phi_1' - (1-\xi^2)\,\Psi_1'\big) + e^{2\,\mu_1}\,\Omega_1\,\big((1+\xi^2)\,\kappa + \xi\,(1-\xi^2)\,\kappa'\big)\big(\xi\,\kappa\,\Phi_1' - (1-\xi^2)\,\Psi_1'\big)\Big] = 0,$$

$$E_{\Psi_1} \equiv -\kappa\,\Omega_1^2\,\Big[-2\,\xi\,\Omega_0^2\,\big(\xi\,\kappa\,\Phi_1' - (1-\xi^2)\,\Psi_1'\big) + e^{2\,\mu_1}\,\Omega_1\,\big((1+\xi^2)\,\kappa + \xi\,(1-\xi^2)\,\kappa'\big)\big(\xi\,\kappa\,\Phi_1' - (1-\xi^2)\,\Psi_1'\big)\Big]$$
$$+e^{2\,\mu_1}\,\Omega_0\,\Phi_1'\,\Big[-\xi\,(1-\xi^2)\,\Omega_0\,\Omega_1\,(\kappa + \xi\,\kappa') + 2\,\xi\,\kappa\,\Big(\xi\,(1-\xi^2)\,\Omega_1\,\Omega_0' + \Omega_0\,\big(\Omega_1 - \xi\,(1-\xi^2)\,\Omega_1'\big)\Big)\Big]$$
$$-e^{2\,\mu_1}\,(1-\xi^2)\,\Omega_0\,\Big[\Omega_0\Big(\Psi_1'\,\big(\Omega_1\,(1+3\,\xi^2 - 2\,\xi(1-\xi^2)\,\mu_1') - \xi\,(1-\xi^2)\,\Omega_1'\big) - \xi\,(1-\xi^2)\,\Omega_1\,\Psi_1''\Big)$$
$$+2\,\xi\,(1-\xi^2)\,\Omega_1\,\Psi_1'\,\Omega_0'\Big] - 2\,\xi^2\,\Omega_0^4\,\Phi_1' - 4\,\xi\sinh\big(\lambda_1\big)^2\,\Psi_1\,\Omega_0^4\,\Omega_1 = 0,$$

$$E_{\Omega_0} \equiv 2\,\xi\,\Omega_1\Big[-\xi(1-\xi^2)^2\,\Omega_1\,\Omega_0'^2 + \Omega_0^2\big(4\,\xi\,\Omega_1 + (1-\xi^4)\,\Omega_1'\big) + (1-\xi^2)^2\,\Omega_0\big(\Omega_0'(\Omega_1 + \xi\,\Omega_1') + \xi\,\Omega_1\Omega_0''\big)\Big]$$
$$-\Omega_1^4\,\big((1+\xi^2)\kappa + \xi(1-\xi^2)\kappa'\big)^2 + 32\,\Omega_0^2\,\Omega_1^2\,\sinh\big(\lambda_1\big)^2\big(\xi\,\kappa\,\Phi_1 - (1-\xi^2)\,\Psi_1\big)^2 + 8\,(1-\xi^2)^2\xi^2\,\Omega_0^2\,e^{2\,\mu_1}\,\Phi_1'^2$$
$$+4\,e^{-4\,\mu_1}\,\xi^2\,\Omega_0^4\,\Omega_1^2\,\big(1-2\,e^{2\,\mu_1}\big) = 0,$$

$$E_{\Omega_1} \equiv -32\,\xi^2\,\sinh\big(\lambda_1\big)^2\,\Phi_1^2\,\Omega_0^4 + 4\,e^{-4\,\mu_1}\,\xi^2\,\Omega_0^4\,\Omega_1^2\,\big(1-2\,e^{2\,\mu_1}\big) + \Omega_1^4\big((1+\xi^2)\,\kappa + \xi\,(1-\xi^2)\,\kappa'\big)^2$$
$$-8\,(1-\xi^2)^2\,\Omega_1^2\,e^{2\,\mu_1}\,\big(\xi\,\kappa\,\Phi_1' - (1-\xi^2)\,\Psi_1'\big)^2 + 2\,\xi\,(1-\xi^2)^2\Omega_0^2\,\Omega_1\,\big(\Omega_1' + \xi\,\Omega_1''\big) = 0,$$

$$E_\kappa \equiv 32\,\xi\,\sinh\big(\lambda_1\big)^2\,\Phi_1\,\big(\xi\,\kappa\,\Phi_1 - (1-\xi^2)\,\Psi_1\big)\,\Omega_0^3 + 8\,\xi\,(1-\xi^2)^2\,\Omega_0\,e^{2\,\mu_1}\Phi_1'\,\big(\xi\,\kappa\,\Phi_1' - (1-\xi^2)\,\Psi_1'\big)$$
$$-(1-\xi^2)\,\Omega_1\,\Big[2\,\xi\,\Omega_1\,\big((1+\xi^2)\,\kappa + \xi\,(1-\xi^2)\,\kappa'\big)\Omega_0' + \Omega_0\big(-3\,\xi\,\big((1+\xi^2)\kappa + \xi\,(1-\xi^2)\,\kappa'\big)\,\Omega_1'$$
$$-(1-\xi^2)\,\Omega_1\,\big(-\kappa + \xi\,(\kappa' + \xi\,\kappa'')\big)\big)\Big] = 0. \tag{D.1}$$

These are the equations we integrate numerically. However, one can show that a linear combination of E_{Φ_1}, E_{Ψ_1} and E_κ reduces to a first order equation, namely:

$$\frac{(1-\xi^2)^2}{\xi}\frac{\Omega_1^3}{\Omega_0^2}\,\partial_\xi\left(\frac{\xi\,\kappa}{1-\xi^2}\right)+8\frac{e^{2\,\mu_1}\,(1-\xi^2)^2\,\Omega_1\left(\frac{\xi\,\kappa}{1-\xi^2}\,\Phi_1'-\Psi_1'\right)}{\xi\,\Omega_0^2}\Phi_1+8\,\Phi_1^2-c_\kappa=0, \quad \text{(D.2)}$$

where c_κ is a constant of integration. Equation (D.2) generalizes to the $n_1 \neq n_2$ beta class and we treat it as the equation of motion for the Ψ_1 gauge field, implying that the latter is governed by a first-order differential equation. It is not related to the 3 constraint equations. The latter reduce to a single constraint for the beta class (for general $n_{1,2}$), as the ones coming from the Maxwell equations are automatically satisfied. Only the Einstein constraint remains non-trivial and we omit it here, as it is rather cumbersome. We use it to monitor the convergence of our numerics.

Appendix E

Projectors and involutions for branes

In this Appendix we list the involutions associated to common brane type. In Type II string theory, they are:

$$\begin{aligned}
P_{\mathrm{P}} &= \Gamma^{01}\,, & P_{\mathrm{F1}} &= \Gamma^{01}\sigma_3\,, \\
P^{\mathrm{IIA}}_{\mathrm{NS5}} &= \Gamma^{012345}\,, & P^{\mathrm{IIB}}_{\mathrm{NS5}} &= \Gamma^{012345}\sigma_3\,, \\
P^{\mathrm{IIA}}_{\mathrm{KKM}(12345;6)} &= \Gamma^{012345}\sigma_3\,, & P^{\mathrm{IIB}}_{\mathrm{KKM}(12345;6)} &= \Gamma^{012345}\,, \\
P_{\mathrm{D0}} = \Gamma^{0} i\sigma_2\,, \quad P_{\mathrm{D2}} &= \Gamma^{012}\sigma_1\,, & P_{\mathrm{D4}} &= \Gamma^{01234} i\sigma_2\,, \quad P_{\mathrm{D6}} = \Gamma^{0123456}\sigma_1\,, \\
P_{\mathrm{D1}} = \Gamma^{01}\sigma_1\,, \quad P_{\mathrm{D3}} &= \Gamma^{0123} i\sigma_2\,, & P_{\mathrm{D5}} &= \Gamma^{012345}\sigma_1\,.
\end{aligned} \tag{E.1}$$

The projectors in M-theory are given by:

$$P_{\mathrm{P}} = \Gamma^{01}\,, \qquad P_{\mathrm{M2}} = \Gamma^{012}\,, \qquad P_{\mathrm{M5}} = \Gamma^{012345}\,, \qquad P^{\mathrm{IIB}}_{\mathrm{KKm}} = \Gamma^{0123456}\,. \tag{E.2}$$

Appendix F

Parametrizing the themelia

In the interest of efficiency we parametrize the most general themelion considered in this manuscript, which should be the building block of hyperstrata, via:

$$\begin{aligned}
\alpha_1 &= \frac{1}{4}\,(1+x_1+y_1+z_1)\,,\ \alpha_2 = \frac{1}{4}\,(1-x_1+y_1-z_1)\,,\\
\alpha_3 &= \frac{1}{4}\,(1-x_1-y_1+z_1)\,,\ \alpha_4 = \frac{1}{4}\,(1+x_1-y_1-z_1)\,,\\
\alpha_5 &= \frac{1}{4}\,(x_2+y_2+z_2)\,,\ \alpha_6 = \frac{1}{4}\,(-x_2+y_2-z_2)\,,\\
\alpha_7 &= \frac{1}{4}\,(-x_2-y_2+z_2)\,,\ \alpha_8 = \frac{1}{4}\,(x_2-y_2-z_2)\,,\\
\alpha_9 &= \alpha_{10} = \frac{1}{2}\,u_1\,,\ \alpha_{11} = \alpha_{12} = \frac{1}{2}\,u_2\,,\ \alpha_{13} = -\alpha_{14} = \frac{1}{2}\,v_1\,,\\
\alpha_{15} &= -\alpha_{16} = \frac{1}{2}\,v_2, \alpha_{17} = -\alpha_{18} = \frac{1}{2}\,w_1, \alpha_{19} = -\alpha_{20} = \frac{1}{2}\,w_2.
\end{aligned} \tag{F.1}$$

and the solution to the projection conditions is:

$$\begin{aligned}
&u_1 + iu_2 = s_1 s_2\, e^{i\varphi_1}\,,\\
&v_1 + iv_2 = s_2 c_2\, e^{i(\varphi_1-\varphi_2-\varphi_3)}(e^{-2i\varphi_4} - c_1)\,,\\
&w_1 + iw_2 = s_1 c_2\, e^{i\varphi_2}\,, \quad x_1 + ix_2 = c_1 e^{i\varphi_3}\,,\\
&y_1 + iy_2 = e^{i(2\varphi_2+\varphi_3)}\,(c_1 c_2^2 + s_2^2\, e^{-2i\varphi_4})\,,\\
&z_1 + iz_2 = e^{i(2\varphi_1-\varphi_3)}\,(c_2^2\, e^{2i\varphi_4} + c_1 s_2^2)\,,
\end{aligned} \tag{F.2}$$

where $c_j \equiv \cos\theta_j$ and $s_j \equiv \sin\theta_j$. The quadratic terms appear because some $U(3)$ rotation angles must be fixed in terms of others to preserve the relationships between the components, (18.13) of the $\vec{p}_j$.

Bibliography

[1] I. Bena, S. El-Showk, and B. Vercnocke, "Black Holes in String Theory," *Springer Proc.Phys.* **144** (2013) 59–178.

[2] **LIGO Scientific, Virgo** Collaboration, B. P. Abbott *et al.*, "Observation of Gravitational Waves from a Binary Black Hole Merger," *Phys. Rev. Lett.* **116** no. 6, (2016) 061102, arXiv:1602.03837 [gr-qc].

[3] **Event Horizon Telescope** Collaboration, K. Akiyama *et al.*, "First M87 Event Horizon Telescope Results. I. The Shadow of the Supermassive Black Hole," *Astrophys. J.* **875** no. 1, (2019) L1, arXiv:1906.11238 [astro-ph.GA].

[4] S. D. Mathur, "The information paradox: A pedagogical introduction," *Class. Quant. Grav.* **26** (2009) 224001, arXiv:0909.1038 [hep-th].

[5] R. Penrose, "Gravitational collapse: The role of general relativity," *Riv. Nuovo Cim.* **1** (1969) 252–276.

[6] S. D. Mathur, "The fuzzball proposal for black holes: An elementary review," *Fortsch. Phys.* **53** (2005) 793–827, arXiv:hep-th/0502050.

[7] J. Polchinski and M. J. Strassler, "The String dual of a confining four-dimensional gauge theory," arXiv:hep-th/0003136 [hep-th].

[8] S. D. Mathur, "Fuzzballs and the information paradox: A Summary and conjectures," arXiv:0810.4525 [hep-th].

[9] A. Sen, "Extremal black holes and elementary string states," *Mod. Phys. Lett.* **A10** (1995) 2081–2094, arXiv:hep-th/9504147.

[10] A. Strominger and C. Vafa, "Microscopic Origin of the Bekenstein-Hawking Entropy," *Phys. Lett.* **B379** (1996) 99–104, arXiv:hep-th/9601029.

[11] N. P. Warner, "Lectures on Microstate Geometries," arXiv:1912.13108 [hep-th].

[12] I. Bena, E. J. Martinec, S. D. Mathur, and N. P. Warner, "Fuzzballs and Microstate Geometries: Black-Hole Structure in String Theory," arXiv:2204.13113 [hep-th].

[13] P. Heidmann, *Black-Hole Microstates in String Theory: Black is the Color but Smooth are the Geometries?* PhD thesis, Orsay, 2019.

[14] B. Cabrera Palmer and D. Marolf, "Counting supertubes," *JHEP* **06** (2004) 028, arXiv:hep-th/0403025.

[15] D. Bak, Y. Hyakutake, and N. Ohta, "Phase moduli space of supertubes," *Nucl. Phys.* **B696** (2004) 251–262, arXiv:hep-th/0404104.

[16] D. Bak, Y. Hyakutake, S. Kim, and N. Ohta, "A geometric look on the microstates of supertubes," *Nucl. Phys.* **B712** (2005) 115–138, arXiv:hep-th/0407253.

[17] V. S. Rychkov, "D1-D5 black hole microstate counting from supergravity," *JHEP* **01** (2006) 063, arXiv:hep-th/0512053.

[18] I. Bena, S. Giusto, R. Russo, M. Shigemori, and N. P. Warner, "Habemus Superstratum! A constructive proof of the existence of superstrata," *JHEP* **05** (2015) 110, arXiv:1503.01463 [hep-th].

[19] I. Bena, E. Martinec, D. Turton, and N. P. Warner, "Momentum Fractionation on Superstrata," *JHEP* **05** (2016) 064, arXiv:1601.05805 [hep-th].

[20] I. Bena, S. Giusto, E. J. Martinec, R. Russo, M. Shigemori, D. Turton, and N. P. Warner, "Asymptotically-flat supergravity solutions deep inside the black-hole regime," *JHEP* **02** (2018) 014, arXiv:1711.10474 [hep-th].

[21] I. Bena, S. Giusto, E. J. Martinec, R. Russo, M. Shigemori, D. Turton, and N. P. Warner, "Smooth horizonless geometries deep inside the black-hole regime," *Phys. Rev. Lett.* **117** no. 20, (2016) 201601, arXiv:1607.03908 [hep-th].

[22] I. Bena, E. Martinec, D. Turton, and N. P. Warner, "M-theory Superstrata and the MSW String," *JHEP* **06** (2017) 137, arXiv:1703.10171 [hep-th].

[23] I. Bena, E. J. Martinec, R. Walker, and N. P. Warner, "Early Scrambling and Capped BTZ Geometries," *JHEP* **04** (2019) 126, arXiv:1812.05110 [hep-th].

[24] N. Čeplak, R. Russo, and M. Shigemori, "Supercharging Superstrata," *JHEP* **03** (2019) 095, arXiv:1812.08761 [hep-th].

[25] P. Heidmann and N. P. Warner, "Superstratum Symbiosis," *JHEP* **09** (2019) 059, arXiv:1903.07631 [hep-th].

[26] P. Heidmann, D. R. Mayerson, R. Walker, and N. P. Warner, "Holomorphic Waves of Black Hole Microstructure," *JHEP* **02** (2020) 192, arXiv:1910.10714 [hep-th].

[27] D. R. Mayerson, R. A. Walker, and N. P. Warner, "Microstate Geometries from Gauged Supergravity in Three Dimensions," *JHEP* **10** (2020) 030, arXiv:2004.13031 [hep-th].

[28] M. Shigemori, "Superstrata," *Gen. Rel. Grav.* **52** no. 5, (2020) 51, arXiv:2002.01592 [hep-th].

[29] I. Bena, F. Eperon, P. Heidmann, and N. P. Warner, "The Great Escape: Tunneling out of Microstate Geometries," *JHEP* **04** (2021) 112, arXiv:2005.11323 [hep-th].

[30] S. Giusto, M. R. R. Hughes, and R. Russo, "The Regge limit of AdS_3 holographic correlators," *JHEP* **11** (2020) 018, arXiv:2007.12118 [hep-th].

[31] S. Giusto, E. Moscato, and R. Russo, "AdS_3 holography for 1/4 and 1/8 BPS geometries," *JHEP* **11** (2015) 004, arXiv:1507.00945 [hep-th].

[32] A. Bombini, A. Galliani, S. Giusto, E. Moscato, and R. Russo, "Unitary 4-point correlators from classical geometries," *Eur. Phys. J.* **C78** no. 1, (2018) 8, arXiv:1710.06820 [hep-th].

[33] S. Giusto, S. Rawash, and D. Turton, "Ads_3 holography at dimension two," *JHEP* **07** (2019) 171, arXiv:1904.12880 [hep-th].

[34] J. Garcia i Tormo and M. Taylor, "One point functions for black hole microstates," *Gen. Rel. Grav.* **51** no. 7, (2019) 89, arXiv:1904.10200 [hep-th].

[35] I. Bena, P. Heidmann, R. Monten, and N. P. Warner, "Thermal Decay without Information Loss in Horizonless Microstate Geometries," arXiv:1905.05194 [hep-th].

[36] S. Rawash and D. Turton, "Supercharged AdS_3 Holography," *JHEP* **07** (2021) 178, arXiv:2105.13046 [hep-th].

[37] A. Houppe and N. P. Warner, "Supersymmetry and Superstrata in Three Dimensions," arXiv:2012.07850 [hep-th].

[38] B. Ganchev, A. Houppe, and N. P. Warner, "Q-balls meet fuzzballs: non-BPS microstate geometries," *JHEP* **11** (2021) 028, arXiv:2107.09677 [hep-th].

[39] B. Ganchev, S. Giusto, A. Houppe, and R. Russo, "AdS_3 holography for non-BPS geometries," *Eur. Phys. J. C* **82** no. 3, (2022) 217, arXiv:2112.03287 [hep-th].

[40] B. Ganchev, A. Houppe, and N. P. Warner, "New superstrata from three-dimensional supergravity," *JHEP* **04** (2022) 065, arXiv:2110.02961 [hep-th].

[41] B. Ganchev, A. Houppe, and N. P. Warner, "Elliptical and Purely NS Superstrata," arXiv:2207.04060 [hep-th].

[42] B. Ganchev, S. Giusto, A. Houppe, R. Russo, and N. P. Warner, "Microstrata." work in progress, unpublished.

[43] I. Bena, S. D. Hampton, A. Houppe, Y. Li, and D. Toulikas, "The (amazing) super-maze," *JHEP* **03** (2023) 237, arXiv:2211.14326 [hep-th].

[44] I. Bena, N. Čeplak, S. D. Hampton, A. Houppe, D. Toulikas, and N. P. Warner, "Themelia: the irreducible microstructure of black holes," arXiv:2212.06158 [hep-th].

[45] S. W. Hawking, "Particle Creation by Black Holes," *Commun. Math. Phys.* **43** (1975) 199–220. [Erratum: Commun.Math.Phys. 46, 206 (1976)].

[46] C. G. Callan and J. M. Maldacena, "D-brane Approach to Black Hole Quantum Mechanics," *Nucl. Phys.* **B472** (1996) 591–610, arXiv:hep-th/9602043.

[47] J. M. Maldacena and L. Susskind, "D-branes and Fat Black Holes," *Nucl. Phys.* **B475** (1996) 679–690, arXiv:hep-th/9604042.

[48] S. G. Avery, "Using the D1D5 CFT to Understand Black Holes," arXiv:1012.0072 [hep-th].

[49] J. B. Gutowski, D. Martelli, and H. S. Reall, "All supersymmetric solutions of minimal supergravity in six dimensions," *Class. Quant. Grav.* **20** (2003) 5049–5078, arXiv:hep-th/0306235.

[50] I. Bena, S. Giusto, M. Shigemori, and N. P. Warner, "Supersymmetric Solutions in Six Dimensions: A Linear Structure," *JHEP* **1203** (2012) 084, arXiv:1110.2781 [hep-th].

[51] S. Giusto, L. Martucci, M. Petrini, and R. Russo, "6D microstate geometries from 10D structures," *Nucl.Phys.* **B876** (2013) 509–555, arXiv:1306.1745 [hep-th].

[52] O. Lunin, J. M. Maldacena, and L. Maoz, "Gravity solutions for the D1-D5 system with angular momentum," arXiv:hep-th/0212210.

[53] I. Kanitscheider, K. Skenderis, and M. Taylor, "Fuzzballs with internal excitations," *JHEP* **06** (2007) 056, arXiv:0704.0690 [hep-th].

[54] I. Kanitscheider, K. Skenderis, and M. Taylor, "Holographic anatomy of fuzzballs," *JHEP* **04** (2007) 023, arXiv:hep-th/0611171.

[55] N. S. Deger, A. Kaya, E. Sezgin, and P. Sundell, "Matter coupled AdS(3) supergravities and their black strings," *Nucl. Phys. B* **573** (2000) 275–290, arXiv:hep-th/9908089.

[56] H. Nicolai and H. Samtleben, "N=8 matter coupled AdS(3) supergravities," *Phys. Lett.* **B514** (2001) 165–172, arXiv:hep-th/0106153 [hep-th].

[57] N. S. Deger, H. Samtleben, O. Sarıoğlu, and D. Van den Bleeken, "A supersymmetric reduction on the three-sphere," *Nucl. Phys.* **B890** (2014) 350–362, arXiv:1410.7168 [hep-th].

[58] H. Samtleben and O. Sarıoğlu, "Consistent S^3 reductions of six-dimensional supergravity," *Phys. Rev.* **D100** no. 8, (2019) 086002, arXiv:1907.08413 [hep-th].

[59] H. Nicolai and H. Samtleben, "Compact and noncompact gauged maximal supergravities in three-dimensions," *JHEP* **04** (2001) 022, arXiv:hep-th/0103032.

[60] H. Nicolai and H. Samtleben, "Kaluza-Klein supergravity on AdS(3) x S**3," *JHEP* **09** (2003) 036, arXiv:hep-th/0306202 [hep-th].

[61] N. Marcus and J. H. Schwarz, "Three-Dimensional Supergravity Theories," *Nucl. Phys. B* **228** (1983) 145.

[62] I. Bena and N. P. Warner, "One ring to rule them all ... and in the darkness bind them?," *Adv. Theor. Math. Phys.* **9** (2005) 667–701, arXiv:hep-th/0408106.

[63] G. W. Gibbons and S. W. Hawking, "Gravitational Multi - Instantons," *Phys. Lett. B* **78** (1978) 430.

[64] V. Balasubramanian, J. de Boer, E. Keski-Vakkuri, and S. F. Ross, "Supersymmetric conical defects: Towards a string theoretic description of black hole formation," *Phys. Rev.* **D64** (2001) 064011, arXiv:hep-th/0011217.

[65] J. M. Maldacena and L. Maoz, "De-singularization by rotation," *JHEP* **12** (2002) 055, arXiv:hep-th/0012025.

[66] S. D. Mathur, "Gravity on AdS(3) and flat connections in the boundary CFT," arXiv:hep-th/0101118.

[67] O. Lunin, "Adding momentum to D1-D5 system," *JHEP* **04** (2004) 054, arXiv:hep-th/0404006.

[68] I. Bena, N. Bobev, and N. P. Warner, "Spectral Flow, and the Spectrum of Multi-Center Solutions," *Phys. Rev.* **D77** (2008) 125025, arXiv:0803.1203 [hep-th].

[69] I. Bena, N. Ceplak, S. Hampton, Y. Li, D. Toulikas, and N. P. Warner, "Resolving Black-Hole Microstructure with New Momentum Carriers," arXiv:2202.08844 [hep-th].

[70] K. Goldstein and S. Katmadas, "Almost BPS black holes," *JHEP* **05** (2009) 058, arXiv:0812.4183 [hep-th].

[71] I. Bena, G. Dall'Agata, S. Giusto, C. Ruef, and N. P. Warner, "Non-BPS Black Rings and Black Holes in Taub-NUT," *JHEP* **06** (2009) 015, arXiv:0902.4526 [hep-th].

[72] I. Bena, S. Giusto, C. Ruef, and N. P. Warner, "Multi-Center non-BPS Black Holes - the Solution," *JHEP* **11** (2009) 032, arXiv:0908.2121 [hep-th].

[73] N. Bobev and C. Ruef, "The Nuts and Bolts of Einstein-Maxwell Solutions," *JHEP* **01** (2010) 124, arXiv:0912.0010 [hep-th].

[74] I. Bena, S. Giusto, C. Ruef, and N. P. Warner, "A (Running) Bolt for New Reasons," *JHEP* **11** (2009) 089, arXiv:0909.2559 [hep-th].

[75] I. Bena, S. Giusto, C. Ruef, and N. P. Warner, "Supergravity Solutions from Floating Branes," *JHEP* **03** (2010) 047, arXiv:0910.1860 [hep-th].

[76] I. Bena, C. Ruef, and N. P. Warner, "Imaginary Soaring Branes: A Hidden Feature of Non-Extremal Solutions," *JHEP* **1205** (2012) 143, arXiv:1105.6255 [hep-th].

[77] O. Vasilakis and N. P. Warner, "Mind the Gap: Supersymmetry Breaking in Scaling, Microstate Geometries," *JHEP* **1110** (2011) 006, arXiv:1104.2641 [hep-th].

[78] C. M. Bender and S. A. Orszag, *Advanced Mathematical Methods for Scientists and Engineers I*. International series in pure and applied mathematics. springer ed., 1999. https://link.springer.com/book/10.1007/978-1-4757-3069-2.

[79] M. Taylor, "Matching of correlators in AdS(3) / CFT(2)," *JHEP* **06** (2008) 010, arXiv:0709.1838 [hep-th].

[80] S. Deger, A. Kaya, E. Sezgin, and P. Sundell, "Spectrum of D = 6, N = 4b supergravity on AdS(3) x S(3)," *Nucl. Phys.* **B536** (1998) 110–140, arXiv:hep-th/9804166.

[81] K. Skenderis and M. Taylor, "Fuzzball solutions and D1-D5 microstates," *Phys. Rev. Lett.* **98** (2007) 071601, arXiv:hep-th/0609154.

[82] N. Ceplak, S. Giusto, M. R. R. Hughes, and R. Russo, "Holographic correlators with multi-particle states," *JHEP* **09** (2021) 204, arXiv:2105.04670 [hep-th].

[83] S. de Haro, S. N. Solodukhin, and K. Skenderis, "Holographic reconstruction of space-time and renormalization in the AdS / CFT correspondence," *Commun.Math.Phys.* **217** (2001) 595–622, arXiv:hep-th/0002230 [hep-th].

[84] M. Baggio, J. de Boer, and K. Papadodimas, "A non-renormalization theorem for chiral primary 3-point functions," *JHEP* **07** (2012) 137, arXiv:1203.1036 [hep-th].

[85] E. D'Hoker, D. Z. Freedman, S. D. Mathur, A. Matusis, and L. Rastelli, "Extremal correlators in the AdS / CFT correspondence," arXiv:hep-th/9908160.

[86] G. Arutyunov and S. Frolov, "On the correspondence between gravity fields and CFT operators," *JHEP* **04** (2000) 017, arXiv:hep-th/0003038.

[87] F. Aprile, J. M. Drummond, P. Heslop, H. Paul, F. Sanfilippo, M. Santagata, and A. Stewart, "Single particle operators and their correlators in free $\mathcal{N} = 4$ SYM," *JHEP* **11** (2020) 072, arXiv:2007.09395 [hep-th].

[88] J. Hansen and P. Kraus, "Generating charge from diffeomorphisms," *JHEP* **0612** (2006) 009, arXiv:hep-th/0606230 [hep-th].

[89] O. J. C. Dias, J. E. Santos, and B. Way, "Numerical Methods for Finding Stationary Gravitational Solutions," *Class. Quant. Grav.* **33** no. 13, (2016) 133001, arXiv:1510.02804 [hep-th].

[90] J. M. Maldacena, "Black holes in string theory," arXiv:hep-th/9607235.

[91] R. Dijkgraaf, E. P. Verlinde, and H. L. Verlinde, "BPS spectrum of the five-brane and black hole entropy," *Nucl. Phys. B* **486** (1997) 77–88, arXiv:hep-th/9603126.

[92] S. Giusto and S. D. Mathur, "Geometry of D1-D5-P bound states," *Nucl. Phys.* **B729** (2005) 203–220, arXiv:hep-th/0409067.

[93] I. Bena and N. P. Warner, "Bubbling supertubes and foaming black holes," *Phys. Rev.* **D74** (2006) 066001, arXiv:hep-th/0505166.

[94] P. Berglund, E. G. Gimon, and T. S. Levi, "Supergravity microstates for BPS black holes and black rings," *JHEP* **0606** (2006) 007, arXiv:hep-th/0505167 [hep-th].

[95] I. Bena, C.-W. Wang, and N. P. Warner, "The foaming three-charge black hole," *Phys. Rev.* **D75** (2007) 124026, arXiv:hep-th/0604110.

[96] I. Bena, C.-W. Wang, and N. P. Warner, "Mergers and Typical Black Hole Microstates," *JHEP* **11** (2006) 042, arXiv:hep-th/0608217.

[97] I. Bena and N. P. Warner, "Black holes, black rings and their microstates," *Lect. Notes Phys.* **755** (2008) 1–92, arXiv:hep-th/0701216.

[98] I. Bena, C.-W. Wang, and N. P. Warner, "Plumbing the Abyss: Black Ring Microstates," *JHEP* **07** (2008) 019, arXiv:0706.3786 [hep-th].

[99] I. Bena, N. Bobev, S. Giusto, C. Ruef, and N. P. Warner, "An Infinite-Dimensional Family of Black-Hole Microstate Geometries," *JHEP* **1103** (2011) 022, arXiv:1006.3497 [hep-th].

[100] I. Bena, A. Houppe, and N. P. Warner, "Delaying the Inevitable: Tidal Disruption in Microstate Geometries," *JHEP* **02** (2021) 103, arXiv:2006.13939 [hep-th].

[101] M. Bianchi, J. F. Morales, and L. Pieri, "Stringy origin of 4d black hole microstates," *JHEP* **06** (2016) 003, arXiv:1603.05169 [hep-th].

[102] M. Bianchi, J. F. Morales, L. Pieri, and N. Zinnato, "More on microstate geometries of 4d black holes," *JHEP* **05** (2017) 147, arXiv:1701.05520 [hep-th].

[103] P. Heidmann, "Four-center bubbled BPS solutions with a Gibbons-Hawking base," *JHEP* **10** (2017) 009, arXiv:1703.10095 [hep-th].

[104] I. Bena, P. Heidmann, and P. F. Ramirez, "A systematic construction of microstate geometries with low angular momentum," *JHEP* **10** (2017) 217, arXiv:1709.02812 [hep-th].

[105] J. Avila, P. F. Ramirez, and A. Ruiperez, "One Thousand and One Bubbles," *JHEP* **01** (2018) 041, arXiv:1709.03985 [hep-th].

[106] A. Tyukov, R. Walker, and N. P. Warner, "The Structure of BPS Equations for Ambi-polar Microstate Geometries," *Class. Quant. Grav.* **36** no. 1, (2019) 015021, arXiv:1807.06596 [hep-th].

[107] M. Shigemori, "Counting Superstrata," arXiv:1907.03878 [hep-th].

[108] D. R. Mayerson and M. Shigemori, "Counting D1-D5-P microstates in supergravity," *SciPost Phys.* **10** no. 1, (2021) 018, arXiv:2010.04172 [hep-th].

[109] N. Seiberg, "New theories in six-dimensions and matrix description of M theory on T**5 and T**5 / Z(2)," *Phys. Lett.* **B408** (1997) 98–104, arXiv:hep-th/9705221 [hep-th].

[110] D. Kutasov, "Introduction to little string theory," *ICTP Lect. Notes Ser.* **7** (2002) 165–209.

[111] C. G. Callan and J. M. Maldacena, "Brane death and dynamics from the Born-Infeld action," *Nucl. Phys. B* **513** (1998) 198–212, arXiv:hep-th/9708147.

[112] I. Bena, M. Shigemori, and N. P. Warner, "Black-Hole Entropy from Supergravity Superstrata States," *JHEP* **1410** (2014) 140, arXiv:1406.4506 [hep-th].

[113] A. Dabholkar, J. P. Gauntlett, J. A. Harvey, and D. Waldram, "Strings as Solitons & Black Holes as Strings," *Nucl. Phys.* **B474** (1996) 85–121, arXiv:hep-th/9511053.

[114] S. D. Mathur and D. Turton, "Oscillating supertubes and neutral rotating black hole microstates," *JHEP* **04** (2014) 072, arXiv:1310.1354 [hep-th].

[115] I. Bena, S. F. Ross, and N. P. Warner, "On the Oscillation of Species," *JHEP* **1409** (2014) 113, arXiv:1312.3635 [hep-th].

[116] I. Bena, J. de Boer, M. Shigemori, and N. P. Warner, "Double, Double Supertube Bubble," *JHEP* **10** (2011) 116, arXiv:1107.2650 [hep-th].

[117] O. Lunin and S. D. Mathur, "Metric of the multiply wound rotating string," *Nucl. Phys.* **B610** (2001) 49–76, arXiv:hep-th/0105136.

[118] D. Mateos and P. K. Townsend, "Supertubes," *Phys. Rev. Lett.* **87** (2001) 011602, arXiv:hep-th/0103030.

[119] R. Emparan, D. Mateos, and P. K. Townsend, "Supergravity supertubes," *JHEP* **07** (2001) 011, arXiv:hep-th/0106012.

[120] I. Bena, N. Bobev, C. Ruef, and N. P. Warner, "Supertubes in Bubbling Backgrounds: Born-Infeld Meets Supergravity," *JHEP* **07** (2009) 106, arXiv:0812.2942 [hep-th].

[121] N. R. Constable, R. C. Myers, and O. Tafjord, "The Noncommutative bion core," *Phys. Rev. D* **61** (2000) 106009, arXiv:hep-th/9911136.

[122] I. Bena, J. Blåbäck, R. Minasian, and R. Savelli, "There and back again: A T-brane's tale," *JHEP* **11** (2016) 179, arXiv:1608.01221 [hep-th].

[123] B. Bates and F. Denef, "Exact solutions for supersymmetric stationary black hole composites," *JHEP* **1111** (2011) 127, arXiv:hep-th/0304094 [hep-th].

[124] V. Balasubramanian, E. G. Gimon, and T. S. Levi, "Four Dimensional Black Hole Microstates: From D-branes to Spacetime Foam," *JHEP* **0801** (2008) 056, arXiv:hep-th/0606118 [hep-th].

[125] G. T. Horowitz and D. L. Welch, "Duality invariance of the Hawking temperature and entropy," *Phys. Rev. D* **49** (1994) 590–594, arXiv:hep-th/9308077.

[126] H. W. Lin, J. Maldacena, L. Rozenberg, and J. Shan, "Holography for people with no time," arXiv:2207.00407 [hep-th].

[127] Z. Wei and Y. Yoneta, "Counting atypical black hole microstates from entanglement wedges," arXiv:2211.11787 [hep-th].

[128] P. Hayden and G. Penington, "Black hole microstates vs. the additivity conjectures," arXiv:2012.07861 [hep-th].

[129] I. Bena and N. P. Warner, "Resolving the Structure of Black Holes: Philosophizing with a Hammer," arXiv:1311.4538 [hep-th].

[130] I. Bena, E. J. Martinec, S. D. Mathur, and N. P. Warner, "Snowmass White Paper: Micro- and Macro-Structure of Black Holes," arXiv:2203.04981 [hep-th].

[131] N. Ceplak, "Vector Superstrata," 2022, to appear.

[132] I. Bena and P. Kraus, "Microstates of the D1-D5-KK system," *Phys. Rev.* **D72** (2005) 025007, arXiv:hep-th/0503053.

[133] I. Bena, P. Kraus, and N. P. Warner, "Black rings in Taub-NUT," *Phys. Rev.* **D72** (2005) 084019, arXiv:hep-th/0504142.

[134] B. E. Niehoff and N. P. Warner, "Doubly-Fluctuating BPS Solutions in Six Dimensions," *JHEP* **1310** (2013) 137, arXiv:1303.5449 [hep-th].

[135] L. J. Romans, "Selfduality for Interacting Fields: Covariant Field Equations for Six-dimensional Chiral Supergravities," *Nucl. Phys.* **B276** (1986) 71.